POLITECNICO DI MILANO

Scuola di Ingegneria Civile, Ambientale e Territoriale

Corso di Laurea Magistrale in Ingegneria per l'Ambiente e il Territorio

Orientamento Difesa del Suolo e Prevenzione dai Rischi Naturali

Interpretation of Borehole Heat Exchangers Thermal Response Tests under groundwater influence: analysis of three case studies

Relatore: prof.ssa Adriana Angelotti

Correlatore: dott. Andrea Zille

Elaborato di Laurea Magistrale di:

Franco Lý

matricola 802021

A.A. 2014/2015

Homo faber fortunae suae.

- Appio Claudio Cieco -

Franco Lý

Interpretation of Borehole Heat Exchangers Thermal Response Tests
under groundwater influence: analysis of three case studies

Abstract

The design of low-temperature geothermal systems requires the knowledge of the thermal properties of the subsurface and the boreholes, in particular an effective ground thermal conductivity λ_{eff} and the so-called borehole thermal resistance R_b.

As it is hardly possible to obtain sufficiently accurate values of these parameters from geological or soil-profile information, *Thermal Response Tests* (TRTs) have been developed to provide measurements in situ.

The standard TRT evaluation is commonly based on the *Kelvin Infinite Line Source* (ILS) theory, but it presents several shortcomings. The main limitation is the assumption of a pure conductive heat exchange. In presence of significant aquifers, it does not consider the effects of groundwater flow and simplifies all possible heat transfer processes of the subsurface as purely conductive transport with an effective thermal conductivity.

The main purpose of this master thesis is to verify the applicability of the *Moving Line Source* (MLS) theory to interpret ground-water influenced TRTs of vertical borehole heat exchangers (BHEs) as very recently proposed by (Wagner V. a., 2013). This alternative approach consists in a three variable parameters estimation procedure, which takes into consideration the simultaneous heat transport by advection and conduction.

A script in MATLAB of the MLS solution is ad hoc implemented and tested for three case studies in order to estimate more suitable parameters for a detailed simulation of effective heat transport in the subsurface. In addition, a time criterion for data significativity is proposed for the MLS approach to disregard data related to initial times, when heat transfer basically involves the borehole volume.

In general, the parameters estimation returned multiple solutions, confirming the findings of (Wagner V. a., 2013), that a TRT evaluation based on MLS equation is an ill-posed problem, where solutions to the inverse problem are non-unique.

However, the procedure led to optimal results for Claviere case study: the interpretation required a careful analysis based on solutions RMSE comparison and physical remarks to discriminate among them. The *best fit* solution corresponds to $\lambda = 2,77 \ W/(m \cdot K)$, $v = 7,6E\text{-}05 \ m/s$ and $R_b = 0,100 \ m \cdot K/W$, representing a valid set of parameters in agreement with the specific site characteristics.

On the other hand, MLS approach turned to be not straightforward both for Lodi and Trento TRTs. In each of those case studies two main solutions were obtained, of which the

evaluation cannot be performed unless additional tests are performed and results compared to validate MLS analysis.

As final remarks of this study, we recommend MLS as a suitable alternative for TRT analysis if λ_{eff} value cannot be estimated by ILS approach, and to perform longer tests, if the presence of aquifers is detected, in order to evaluate the convergence of λ_{eff} by means of a step by step interpretation.

Further efforts are necessary to understand how fit solutions depend on initial guess parameters and how to discriminate among multiple solutions found, especially in case where advection and conduction in the ground are competitive.

Franco Lý

*Interpretation of Borehole Heat Exchangers Thermal Response Tests
under groundwater influence: analysis of three case studies*

Estratto

La corretta progettazione di impianti geotermici a bassa temperatura richiede la conoscenza delle proprietà termiche del sottosuolo e dei pozzi, nello specifico una conducibilità termica efficace del terreno λ_{eff} e la resistenza termica del pozzo R_b.

Dato che difficilmente è possibile dedurre dei valori accurati di questi parametri da informazioni geologiche o dal profilo stratigrafico del terreno, è stato allora sviluppato il *Test di Risposta Termica* (TRT) per fornire misurazioni in situ.

Il metodo standard per l'interpretazione dei dati di un TRT è in genere basato sul modello analitico della *Sorgente Lineare Infinita* (ILS), il quale presenta tuttavia diversi limiti. Il principale difetto è l'ipotesi di uno scambio termico per sola conduzione. Infatti, in presenza di importanti acquiferi, il modello non considera gli effetti del flusso d'acqua sotterraneo e semplifica tutti i possibili processi di scambio termico del sottosuolo con un trasporto puramente conduttivo per mezzo di un parametro equivalente λ_{eff}.

L'obiettivo principale di questa tesi magistrale è quello di verificare l'applicabilità della teoria della *Sorgente Lineare in Movimento* (MLS) per interpretare TRT influenzati dalle acque sotterranee come recentemente proposto da (Wagner V. a., 2013). Questo metodo alternativo consiste in una procedura di stima a tre parametri variabili, che tiene conto di uno scambio termico simultaneo tramite avvezione e conduzione.

Uno script della soluzione MLS è stato implementato ad hoc in MATLAB ed è stato testato per i tre casi studio al fine di ottenere la stima di parametri più adeguati a rappresentare l'effettivo trasporto di calore nel terreno. Inoltre, è stato proposto un criterio temporale per la significatività dei dati relativo al metodo della MLS, in modo da scartare i dati relativi a tempi iniziali, quando lo scambio termico interessa il volume della sonda geotermica.

In generale, il processo di stima ha generato soluzioni multiple, confermando le scoperte di (Wagner V. a., 2013), ovvero che la valutazione di un TRT basato sul metodo della MLS è un problema mal posto, la cui soluzione non è unica.

Ciononostante, il metodo ha condotto ad ottimi risultati per il caso studio di Claviere: l'interpretazione ha richiesto un'attenta analisi basata sul confronto degli RMSE delle soluzioni e su osservazioni fisiche per discriminare le soluzioni. La soluzione *best fit* corrisponde a λ = *2,77 W/(m·K)*, *v* = *7,6E-05 m/s* e R_b = *0,100 m·K/W*, la quale rappresenta un valido set di parametri in accordo con le caratteristiche sito specifiche del caso studio.

Franco Lý

*Interpretation of Borehole Heat Exchangers Thermal Response Tests
under groundwater influence: analysis of three case studies*

D'altra parte, il metodo della MLS è risultato non essere di facile valutazione per entrambi i TRT di Lodi e Trento. In ciascuno di quei casi studio, due soluzioni principali sono state ottenute, delle quali il discernimento non è possibile a meno di ulteriori test con cui confrontarsi per validare l'analisi MLS.

Come osservazione finale di questa indagine, raccomandiamo il metodo della MLS come valida alternativa per la analisi dei dati di TRT nel caso λ_{eff} non possa essere stimata tramite metodo della ILS, e di eseguire *Test di Risposta Termica* più lunghi qualora sia localizzata la presenza di acquiferi, al fine di esaminare la convergenza di λ_{eff} per mezzo di una interpretazione step by step.

Ulteriori studi sono necessari per comprendere come le soluzioni dei fit dipendano dai parametri iniziali e come discriminare tra le soluzioni multiple ottenute, specialmente in casi dove i fenomeni di avvezione e conduzione nel terreno sono comparabili.

Franco Lý

*Interpretation of Borehole Heat Exchangers Thermal Response Tests
under groundwater influence: analysis of three case studies*

Acknowledgements

First of all, I would like to express my full gratitude to Professor Adriana Angelotti for the great opportunity to do my Master Thesis in collaboration with the Department of Energy and for her assistance and interest to my activities during the whole period.

Thanks a lot to Andrea Zille, which partnership was precious more than ever. His field experience and enthusiasm in research encouraged me along all the project.

Many thanks to Matteo Antelmi for his immediate availability in cooperating in a second stage of the thesis despite several commitments. He proved to be a skillful researcher, especially in numerical modeling.

I am very grateful to all my friends, both here in Italy and around the world. I want to thank Chiara Buratti, Lorenzo De Lucia, Stefano Gelmini and Valentina Bolis for their friendship and for the daily support. I want to cite Jorge Gonzalez and Paula Breslin for their kindness in reviewing my dissertation.

Special thanks to my last year university mates, Giordana Brognoli and Riccardo Borutti, with them also the harder project was a joke.

Thanks also to all my climbing fellows, this recent passion taught me to face hard situations with calm and cold blood.

In the end, I would like to express my total appreciation to my parents and my brother, they always drove me through every problem and sustained me to work hard. The sacrifices that they have done make all this possible.

➢ Adriana Angelotti - Environmental Technical Physics, Assistant Professor (Department of Energy; Politecnico of Milano)
➢ Andrea Zille - PhD Geothermal Energy Consultant (ELCO Italia)
➢ Matteo Antelmi - PhD Candidate (Department of Civil and Environmental Engineering; Politecnico of Milano)

Table of Contents

Franco Lý

Interpretation of Borehole Heat Exchangers Thermal Response Tests under groundwater influence: analysis of three case studies

Franco Lý

Interpretation of Borehole Heat Exchangers Thermal Response Tests
under groundwater influence: analysis of three case studies

Franco Lý

*Interpretation of Borehole Heat Exchangers Thermal Response Tests
under groundwater influence: analysis of three case studies*

14

Franco Lý

Interpretation of Borehole Heat Exchangers Thermal Response Tests
under groundwater influence: analysis of three case studies

List of Figures

Franco Lý

Interpretation of Borehole Heat Exchangers Thermal Response Tests
under groundwater influence: analysis of three case studies

Franco Lý

Interpretation of Borehole Heat Exchangers Thermal Response Tests
under groundwater influence: analysis of three case studies

Franco Lý

Interpretation of Borehole Heat Exchangers Thermal Response Tests
under groundwater influence: analysis of three case studies

Franco Lý

Interpretation of Borehole Heat Exchangers Thermal Response Tests
under groundwater influence: analysis of three case studies

List of Tables

Franco Lý

Interpretation of Borehole Heat Exchangers Thermal Response Tests
under groundwater influence: analysis of three case studies

Franco Lý

Interpretation of Borehole Heat Exchangers Thermal Response Tests
under groundwater influence: analysis of three case studies

Introduction and Aim of Thesis

The work presented in this master thesis is carried out as the result of a study which involved the collaboration between the department of Energy, the department of Civil and Environmental Engineering and ELCO Italia.

The aim of this master thesis is to explore an alternative analytical approach to interpret ground-water influenced thermal response tests of vertical borehole heat exchangers, in order to obtain the necessary thermo-physical parameters to properly design low-temperature geothermal plants.

The dissertation hereafter presented, is carried out under the guidance of professor Adriana Angelotti (Department of Energy, Politecnico of Milano) who also supplied me raw data of Lodi case study. While raw data of Claviere and Trento case studies were kindly provided by PhD geothermal energy consultant Andrea Zille (ELCO Italia). The main part of this thesis consists in applying standard and experimental analytical solutions to interpret data of TRT under groundwater influence.

Secondly, the interest focuses on heat exchange simulations of Lodi TRT by numerical modeling in MODFLOW as the natural development of Marocchi's thesis (Marocchi, 2015) with the collaboration of a researcher, Matteo Antelmi (Department of Civil and Environmental Engineering, Politecnico of Milano).

The main work of this thesis was accomplished between February and September 2015. The dissertation is so organized:

- Chapter 1
  General Background

- Chapter 2
  Thermal Response Test

- Chapter 3-4-5
  TRT Analysis of Three Case Studies

- Chapter 6
  Conclusions

- Chapter 7
  Appendices and Attachments

Franco Lý

Interpretation of Borehole Heat Exchangers Thermal Response Tests under groundwater influence: analysis of three case studies

1 General Backgrounds

1.1 Foreword

This chapter tries to provide an introduction about the sources of geothermal energy and its possible applications on electricity production and space heating. The main interest is on shallow geothermal sources, where a ground source heat pump (GSHP) can be coupled to exploit heat exchange with the ground to obtain a warm fluid at mild temperatures (until *40°C*); these systems are especially employed to warm up small-medium size dwellings.

Since in this experimental work, estimated parameters from interpretation of TRTs are obtained to calculate the required length of vertical BHEs in a given application, which is the main cost associated to a GSHP system; it seems opportune to provide an introduction to the main concepts of heat engines and heat pumps, especially coupled to the ground.

In addition, because three groundwater influenced TRTs are analyzed, a brief description of main hydro-geological phenomena and hydraulic properties of the aquifers is provided in order to have a general understanding of hydro-geological processes that can affect heat transport mechanisms in the subsurface in presence of groundwater flow.

Therefore the aim of this chapter is to deal with three main topics:

1. The first part gives a background on geothermal resources and their application, focusing on shallow geothermal sources which are fundamental to low-temperature geothermal plants.

2. The second part concerns the principles of thermodynamics and fundamental concepts that are necessary to differentiate heat engines (direct cycle - high temperature geothermal system) from heat pumps/refrigerators (inverse cycle, heat pump or refrigeration cycle - low-temperature geothermal system); this overview is to support the comprehension of the operation of a reversible heat pump of a low-temperature geothermal plant.

3. The last part deals with basic notions of hydrogeology and hydraulic properties of aquifers. To conclude the chapter, the final section describes main heat transfer mechanisms in an aquifer defining the energy equation for porous media with water advection.

Franco Lý

Interpretation of Borehole Heat Exchangers Thermal Response Tests
under groundwater influence: analysis of three case studies

1.2   Low-Temperature Geothermal Plant

Geothermal energy is defined as a kind of energy linked to endogenic heat of the Earth; phenomena like volcanoes, geysers, fumaroles and hot spring are the evident demonstrations of the presence of stored heat in the earth's crust.

Such heat originates firstly from the decay of radioactive isotopes, especially present in the mantle (in prevalence Uranium 238, Uranium 235, Thorium 232 and Potassium 40) and secondly from the heat spread by the core of the planet, which is irregularly distributed within the earth's crust, due to the heterogeneity of this stratum and according to the circulation movements of the fluid at different temperatures (magmatic, thermal and meteoric fluids).
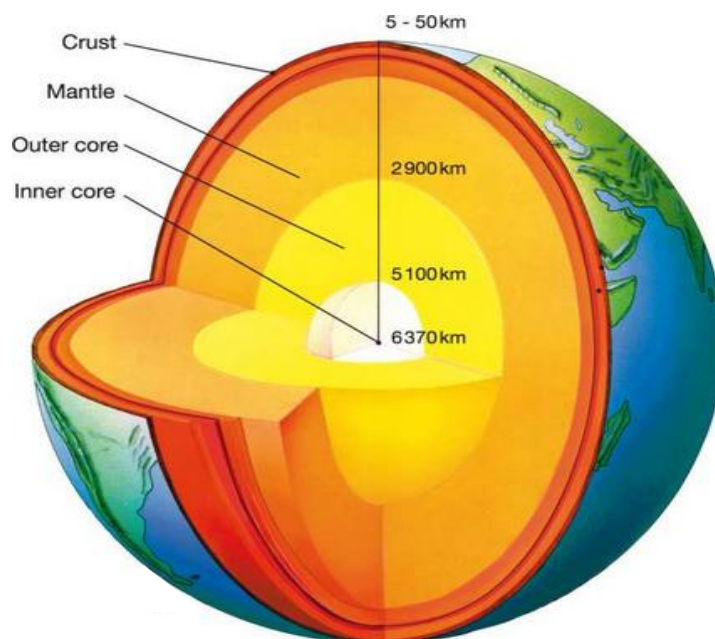
Figure 1-1 - Earth cross section (source www.diercke.com).

As illustrated in Figure 1-1, earth's crust is about *33 km* thick; deep perforations, which manage to reach a maximum depth of *11 km*, and in the majority of the cases oriented to research hydrocarbons, have permitted to observe a temperature increase with depth of about *2,5÷3°C* every *100 meters* (geothermal gradient). However, it is necessary to assert that in some regions these values move away remarkably from the average: in area characterized by the presence of sediments recently originated in geological terms, the geothermal gradient can even be inferior to *1°C /100 m*; vice versa, in some areas defined

geothermal, the gradient can result to be *9-12°C* every *100 meters* and in some cases even *30°C /100m* (Delmastro, 2011).

The calculation of the mean geothermal flux that reaches the surface and wastes in the space leads to a value of about *0,03 W/m²*. Assuming at first approximation the Earth as a spherical surface with radius *6370 km*, it results a constant flux of *31000 billions of Watt*.
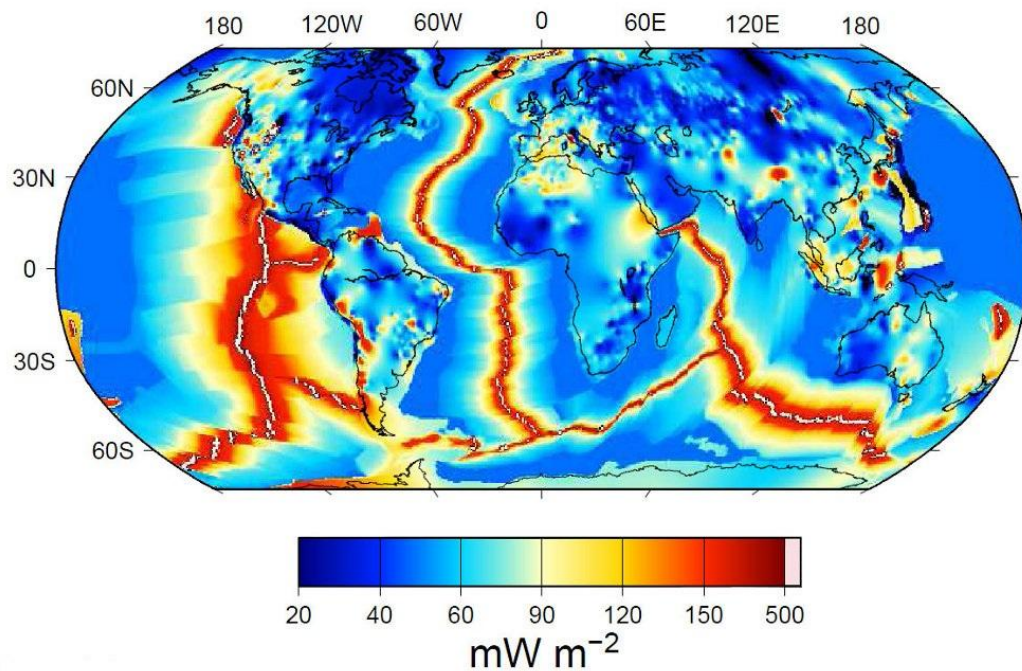
Figure 1-2 - Earth geothermal flux (source: wattsupwiththat.com).

The main problem related to the exploitation of this resource is the fact that this energy comes to the surface at a temperature practically identical to the ambient temperature: therefore it is necessary to extract it in depth, where the thermal level is generally more elevated and thus usable by means of heat engines.

This energy is completely renewable and with nil environmental impact, independently from the use, the considered geothermal energy, already dispersed by the Earth, is transferred, channeled and exploited until given back to the environment in the same way as it would be wasted by the ground.

Geothermal energy can be classified in two typologies based on the thermodynamic features of the fluids and purpose sectors:

− *High-temperature*, relative to the production of electricity and to industrial use - fluid with temperature higher than *150°C*

− *Medium and Low-temperature*, relative to a direct use in civil, agricultural and industrial fields - fluid with temperature in a range of *100-150°C* and inferior to *100°C* respectively.

Figure 1-3 - a) Hellisheidi Geothermal power plant, Iceland; b) Rijksmuseum heated up by low-temperature geothermal system, Netherlands.

The production temperature depends obviously on the local geothermal gradient and extraction depth. Concerning the depth, it is possible to distinguish low-temperature geothermal sources in:

− *Shallow geothermal source* (within *1000 m*, *12÷45°C*) for applications with vertical borehole heat exchangers (BHEs) that exploits heat exchange with the ground to obtain a warm fluid at moderate temperatures (until *40°C*) by means of ground source heat pump (GSHP). These systems are especially employed to warm up small and medium size dwellings;

− *Deep geothermal source* (beyond *1000 m*, above *45°C*) for applications with deep BHE, even to *2500 m*, that allows to attain fluids at high temperature for direct usage, or with heat pump or with a supporting boiler. Such applications turns out to be suitable for large residences and/or for district heating;

− *Hot spring source* (within few hundreds of meters, until *100°C*) for direct use or with heat pumps for small size users and in some cases for district heating - fostered by hot wells, hot springs, geothermal exchangers.

Low-temperature geothermal sector includes both deposits of water with temperature inferior to *100°C*, usable especially for direct purpose (space heating of dwellings, greenhouses, industrial plants) and even all the systems that, by heat exchange with the subsurface, extract endogenous heat at various thermal level and permit to heat water to temperature inferior to *100°C*.

Field experiments for low-temperature geothermal systems sizing are applied on vertical borehole heat exchangers involving typically shallow geological layers where three ground zones (Figure 1-4) can be distinguished in:

− A shallow zone reaching a depth of about *0-15 m*, where the ground temperature distribution depends mainly on seasonal cycle of weather conditions;
− A constant-temperature zone below a depth of about *15-30 m*, where the ground temperature remains relatively constant and is close to the average ambient temperature;
− A deep zone below *30 m*, where the temperature increases linearly with depth.
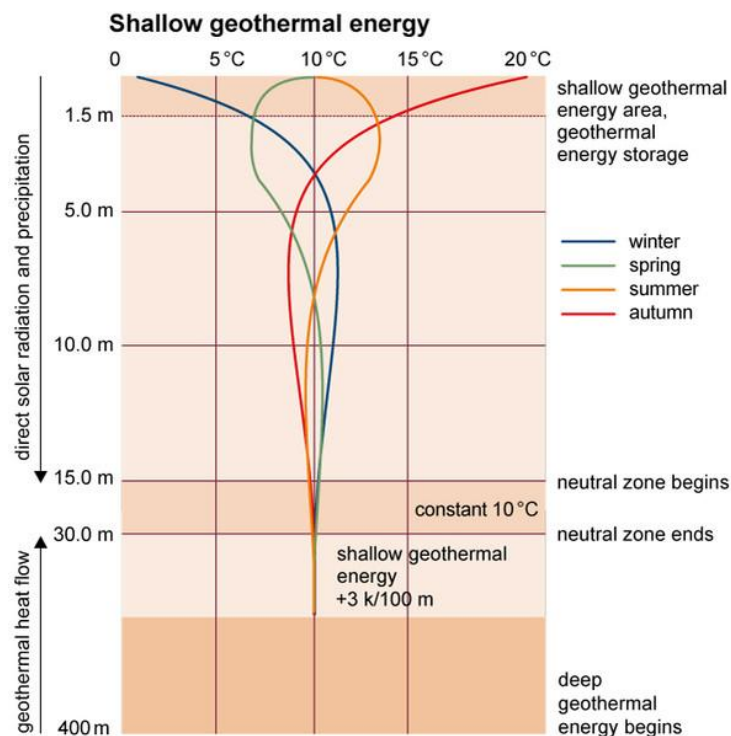
Figure 1-4 - Typical ground temperature profile in different seasons, considering only conductive heat transfer and atmospheric influence (source: www.solarpraxis.de).

1.3 Thermodynamic Cycles

A heat engine to work does always need two reservoirs at different temperatures: the second principle of the thermodynamics states in fact, that it is not possible to achieve a transformation, which unique result is to convert completely the heat extracted by a sink into work.

A heat pump has an inverse behavior in respect to the heat engine, the direction of heat fluxes are all inverted. This difference can be intuitively distinguished by the work, incoming or out coming the system. A reservoir is defined as *source* if the heat is exiting from it and as heat *sink* if the heat is incoming.

A heat engine, permitting the spontaneous transfer of heat from a hot reservoir *source* at temperature T_1 to a cold reservoir *sink* with temperature $T_2 < T_1$, has the capability to generate work. It carries out per definition a direct cycle. Concerning a single cycle, the engine extract heat Q_1 from the hot reservoir *source* and supply a work $W = |Q_1| - |Q_2|$. Thus a heat Q_2 is transferred to the cold reservoir *sink.*
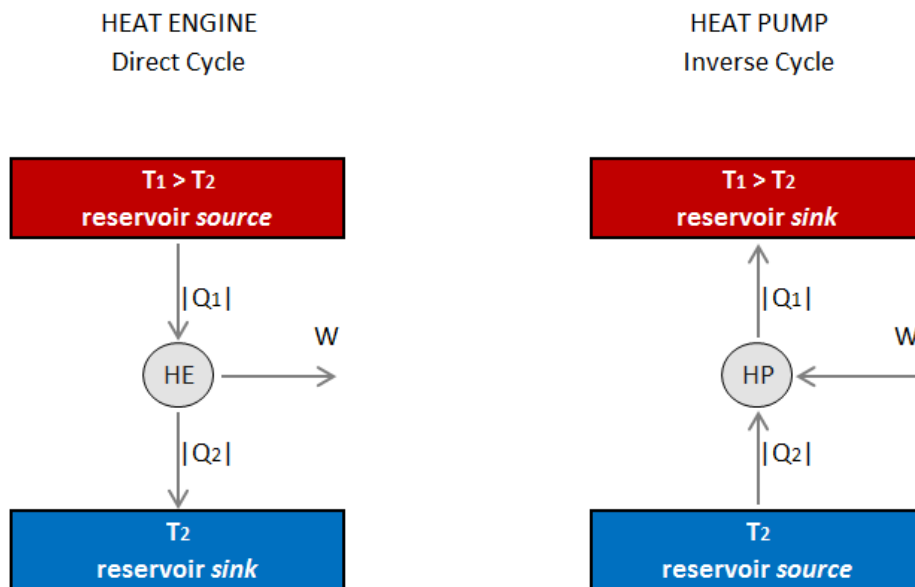
Figure 1-5 - Direct and inverse thermal cycle for heat engine and heat pump.

The cycle is inverse when it permits the heat transfer (not spontaneous) from a cold reservoir source to a warm reservoir sink by means of external work. Concerning a single cycle, the heat pump/refrigerator extracts heat Q_2 from the reservoir *source* thanks to a work $W = |Q_1| - |Q_2|$. Hence, a heat Q_1 is transferred to reservoir *sink.*

Franco Lý

*Interpretation of Borehole Heat Exchangers Thermal Response Tests
under groundwater influence: analysis of three case studies*

1.3.1 Heat Engine - Direct Cycle

Referring to Figure 1-5, the efficiency of a heat engine is defined as the ratio between obtained work and heat extracted from the hot reservoir:

$$\eta = \frac{|W|}{|Q_1|} = \frac{|Q_1| + |Q_2|}{|Q_1|} = 1 - \frac{|Q_2|}{|Q_1|} < 1 \qquad \textbf{Eq. 1.1}$$

It can be demonstrated by Carnot's theorem that the maximum possible efficiency for a heat engine operating between two reservoirs, independently from the type of engine and fluid is equal to:

$$\eta_{carnot} = \frac{|T_1| + |T_2|}{|T_1|} = 1 - \frac{|T_2|}{|T_1|} \qquad \textbf{Eq. 1.2}$$

$$\eta < \eta_{carnot} < 1$$

Where T_1 is the temperature of the hot reservoir *source* and T_2 is the temperature of the cold reservoir *sink* expressed in *K*. Carnot's heat engines can never reach a unit efficiency. Indeed, because T_2 is superiorly limited to the *source* temperature and T_1 is inferiorly limited by the environment temperature, the transformation has necessarily efficiencies far from unit. In addition, back to real efficiency, heat dissipation external to the engine and resistances to energy transfer from a material to another reduce even more the ideal efficiency of the system.

In the context of electricity generation with high temperature geothermics, a heat engine with direct cycle idealizes a heat extraction plant from geothermal reservoir, typically at high temperatures in order to make a operating fluid evaporate and subsequently obtain electricity by means of a turbine. Exiting from the turbine, the steam re-condensates to be ready to receive new heat from the geothermal source if the cycle is closed.
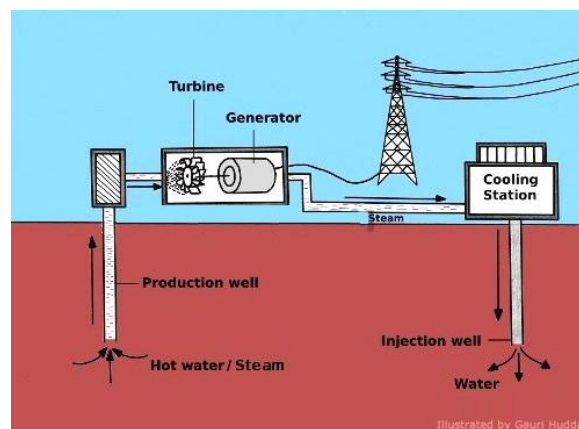
Figure 1-6 - Scheme of an electricity generation plant with geothermal source.

Franco Lý

*Interpretation of Borehole Heat Exchangers Thermal Response Tests
under groundwater influence: analysis of three case studies*

1.3.2   Heat Pump - Inverse Cycle

As previously introduced, a heat pump is the engine that allows to execute the transfer of heat from a cold body to a warm body; the employed energy for its functioning can be of electrical, mechanical or thermal origins. As any other engine, it works according to thermodynamic cycle that is analogous to the cycle of a chiller and therefore it is called refrigeration cycle (or inverse cycle).

For a heat pump in cooling mode, the coefficient of performance (*COP*) is defined as the ratio between the heat extracted from the reservoir to be cooled down and the necessary work to obtain this performance:

$$COP_{cooling} = \frac{|Q_2|}{|W|}$$

Eq. 1.3

While the *COP* of a heat pump in heating mode is defined as the ratio between the heat supplied to the reservoir to be warmed and the necessary work:

$$COP_{heating} = \frac{|Q_1|}{|W|}$$

Eq. 1.4

Referring to Figure 1-5, it can be demonstrated by Carnot's theorem that the *COPs* of a heat pump are superiorly limited by reservoirs temperatures, that is:

$$COP_{cooling} = \frac{|T_2|}{|T_1| - |T_2|}$$

Eq. 1.5

$$COP_{heating} = \frac{|T_1|}{|T_1| - |T_2|}$$

Eq. 1.6

Where T_1 is the temperature of the hot reservoir *sink* and T_2 is the temperature of the cold reservoir *source* (Figure 1-5)*.*

According to Carnot's theorem, if temperatures T_1 and T_2 get closer, the *COP* improves.

For instance, in winter the electrical consumption of the heat pump increases, if the climatic conditions become more frigid because the larger differences of temperature between the ground and the building to be warmed up reduces the *COP*.

In the same way in summer the electrical consumption augments if the temperature of the building to be cooled down is much higher than the ground. Based on this important consideration, it is convenient to have a thermal source which temperature fluctuations in time are restrained: the aquifer.

Franco Lý

*Interpretation of Borehole Heat Exchangers Thermal Response Tests
under groundwater influence: analysis of three case studies*

To maintain the beneficial effect of a heat pump it is necessary to supply continuously work. The possibility of forcing the heat flux from a *source* to a *sink* occurs exploiting the specific properties of refrigerant fluids that undergo thermo-dynamical transformations. In particular, in a heat pump, work is applied to power a mechanical or electrical compressor that drives a fluid compression-expansion cycle. The refrigerant fluid absorbs heat from the outside environment in a heat exchanger called *evaporator* and volatilizes. This warm refrigerant gas is then compressed and the temperature rise to maybe *60-70°C*. The hot gas releases its heat to a space-heating system in another heat exchanger called *condenser*. The now liquid refrigerant finally passes through an expansion valve and cools down, ready to start the cycle. A ground source heat pump is simply a heat pump that is coupled to the ground or groundwater (Banks, 2009). (Note that the configuration of the heat pump can also be reversed to provide space cooling, by coupling the evaporator to the building and the condenser to the ground).

There can be different classifications based on thermodynamic industrial cycles and adopted fluid.

Classification for type of thermodynamic cycle
- Steam Cycle
- Transcritical Cycle
- Gas Power Cycle

Classification for the exchange on the external environment side
- Water
- Air
- Brine
- Direct exchange with the ground (without heat carrier fluid)

Concerning to the field of machineries generally used in geothermal applications, it can be noticed that the majority of the market is represented by electrical heat pump (reversible and not reversible). The frequently used refrigerants are essentially four: R22 (abandon in progress caused by ozone impact), R134a, R407C (abandon in progress for technological and marketing reasons) and R410A (Delmastro, 2011). In all this four cases the machineries work with a steam cycle.

Few industrial products are of different types for geothermal use: some absorption heat pumps, even more rare endothermic, carbon dioxide and direct evaporation engines. Many systems use also propane as a refrigerant. In this case the industrialization is related to the risk of explosion of the propane, while there are no difficulties linked to the refrigerating circuit since the material in use are standard.

Among the most diffused electrical heat pump with steam cycle (both geothermal applications and air engine) further categories are discernible.

Classification for type of compressor
- Water
- Air
- Brine
- Direct exchange with the ground (without heat carrier fluid)

Classification for exchange on the user side
- Water (hydronic system)
- Air (roof-top system)

For heat pumps with heat exchanger not by air, the classification proposed by(ASHRAE, 2007) is based on the typology of the adopted source.

Classification ASHRAE

- SWHP (Surface Water Heat Pump): is a heat pump which uses shallow water as sink. They are defined direct if they extract water from streams. They are indirect if water are used to skim the exchanger;

- GWHP (Ground Water Heat Pump): they exploited thermal source is ground-water from aquifer that is extracted and re-injected in the same aquifer otherwise in a shallow water stream;

- GCHP (Ground-Coupled Heat Pump): they exploit the heat of the ground through borehole heat exchangers. They are also called *GSHP* (Ground-Source Heat Pump).
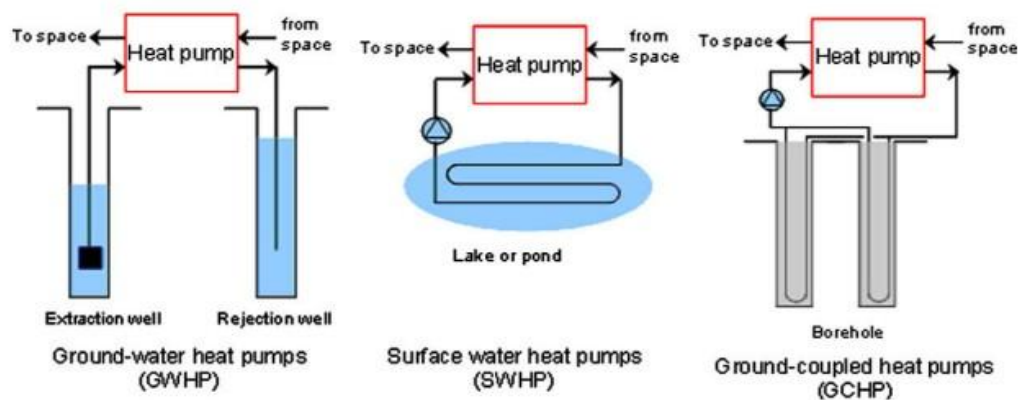
Figure 1-7 - ASHRAE classification of GSHPs.

Franco Lý

Interpretation of Borehole Heat Exchangers Thermal Response Tests
under groundwater influence: analysis of three case studies

1.4 Ground-Source Heat Pump

Ground-source heat pumps (GSHPs) are space heating and cooling plants which exploit the soil as a thermal source or sink, through the circulation of a heat carrier fluid in a closed pipe loop. Vertical pipe loops are installed in boreholes and used as heat exchangers, which reach commonly depths of *50-200 m*. Large thermal inertia of soil reduces greatly seasonal variation of the air temperature guaranteeing a stable source of heat for the system. GHSP have a great potential for energy, cost and CO_2 emission saving (Curtis, 2005). In fact, GHSP in place of methane furnaces allows the CO_2 emissions to be reduced by up to *84%* (Saner, 2010). From the economic point of view, the geothermal heat pumps lead to a considerable reduction of maintenance costs and although their installation is more expensive than the other heating and cooling plants, the payback periods proved to be reasonable (Casasso, 2014). Thermal exploitation of the soil induces a gradual temperature drift, an accurate heat transport modeling of soil and aquifer systems is essential for a correct design of GSHPs.
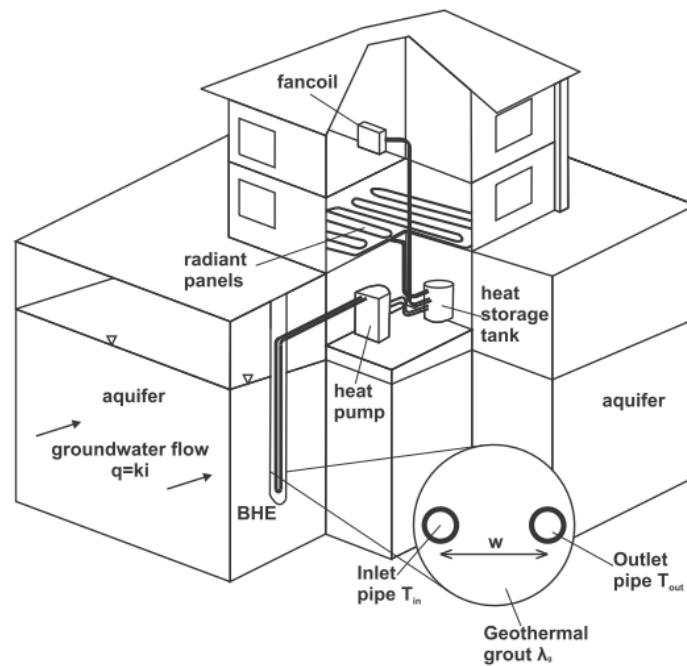
Figure 1-8 - Scheme of a ground source heat pump (GSHP) (Casasso, 2014).

The borehole heat exchanger (BHE) exchanges heat between the surrounding soil and the heat pump. A thermal storage tank helps to diminish the frequency of start-up and stop of the heat pump. Radiant panels and fan coils are the most spread heating terminals for GSHPs. If present, groundwater flow enhances the heat transport around the BHE, permitting to achieve better energy performances.

Franco Lý

Interpretation of Borehole Heat Exchangers Thermal Response Tests
under groundwater influence: analysis of three case studies

1.5 Borehole Heat Exchanger

Borehole completion is a key design factor for low-temperature GSHP systems. The way it is done controls the thermal performance of the borehole, i.e., how much heat transfer the borehole can accomplish. Boreholes must be constructed according to local regulations. Borehole diameter is an engineering matter determined by heat transfer issues and the construction equipment available for drilling the vertical borehole. The heating and cooling industry and regulators should recognize no single solution is best for all geological and hydrological settings.

A good practice before starting the operations is to arrange the tracks for the access of the borehole driller. Also electrical and hydraulic connections have to be organized to be of service for operations. Eventually, the tanks for collecting drilling mud are pre-emptively prepared.

The drillings are executed in order to avoid pollutants contamination of the subsurface. In particular, oil leakages from the driller have to be absolutely avoided. Cooling fluids like air, water or drilling mud can be used such that they do not cause chemical or biological changes in the subsurface. The perforation is performed with a technique chosen by the drilling company so as to optimize site operation, and usually with borehole diameters of *127 mm* or *154 mm*. In cases where it is necessary to guarantee the stability of the well and reduce the dispersion of cooling liquids, it is possible to use borehole casing until opportune depths. The verticality of the borehole has to be kept by means of the level and adjusting the velocity of the perforation according to the geological condition of each layer(Delmastro, 2011).

The special connections at the base of the vertical pipe loop are usually in HDPE PE100 PN16 and welded in the factory to the pipes which constitute the remaining part of the closed loop. They must have a little well for containing eventual solid parts fallen inside the BHE and have a curve-shape profile to reduce head losses at minimum. The U-connection needs to have a specific coupling for the deadweight, guaranteed until *100 kg*. The pipes arrive to the construction site already assembled and protected by nylon. It is useful to control the length before the installation.

The filling material of the borehole is usually a premixed grout. This material has to be studied for geothermal applications with enhanced thermal conductivity, resistance to freezing, permeability < *10^{-8} m/s*, suspension viscosity (*Marsch* number with spout diameter *8 mm*) < *20 s*, temperature variation along the maturation < *15°C* and no volume variation during grout hardening (Delmastro, 2011).

Franco Lý

*Interpretation of Borehole Heat Exchangers Thermal Response Tests
under groundwater influence: analysis of three case studies*

The pipes have to be handled with attention to avoid mechanical damages. In order to facilitate the installation of the pipes, they have to be filled with water before their application. During the insertion in the borehole, the pipes do not have to experience to pressure higher than nominal pressure, both internally and externally. The application of the pipes has to occur immediately after the end of the perforation and subsequently the borehole has to be grouted. It should be avoided that the pipes remain in the borehole without cementation for more than few hours. The insertion of the pipes in the borehole has to be assisted by a winder and a roller conveyor. In case of damage during the process, it has to be extracted and substituted. The pipes have to be accompanied in the borehole, avoiding speeds such that can generate mechanical damages to the pipe walls or to the base of the pipe in case of sudden stop (Delmastro, 2011).

The insertion of the injection pipe has to occur simultaneously with the pipes for the heat carrier fluid. The injection pipe has to reach the bottom of the borehole and it cannot present lateral windows: the premixed grout has to fill the borehole from the bottom to the top. The injection pipe will be left inside the borehole. Before, during and/or immediately after the cementation the pressure test has to be performed on the closed loop. The test must verify that there are no macroscopic losses and therefore it is permitted a modest head loss.

In filling the volume between pipe and borehole it is fundamental to guarantee a good thermal coupling between the vertical closed loop and the ground; and avoid the possibility that the deep aquifers can be contaminated from the surface. The grout injection has to start from the bottom, such that the mortar, going up, fills all the cavities. The process can be considered complete when the grout reaches the surface of the borehole. In case the level of grouting falls down, it can be reintegrated from the bottom if the hardening is not at an advanced phase, otherwise from the top with another injection pipe that can be recuperated. When the cementation is completed, the vertical closed loop is washed by water. Then a visual checking is recommended (Delmastro, 2011).

After two weeks the final pressure test is performed. Because the visco-plastic strain of the pipe can require some days and assume important values, it is necessary to recharge periodically the loop at the test pressure. The pressure must be stable for a duration of at least two hours. Then, the flow test can be performed. It consists in verifying the characteristic curve of each single U-loop. A differential pressure transducer and a flow-meter are used, with circulating pump set at variable velocity (three velocity values) and discharge similar to the project one. The maximum variation can be *5%* from nominal value.

1.6 Hydraulic Properties of an Aquifer

Along the hydro-geological cycle, a portion of the rainfall percolates through the soil to reach the water table to become groundwater. This volume of water defines the available quantity of groundwater available for long-term water-supply development.

Groundwater usually flows through saturated rock under the influence of a hydraulic gradient which, in unconfined aquifers, is the water table. Rocks which both contain groundwater and allow water to flow through them in significant quantities are termed *aquifers*. The critical part of this definition is that the rock allows a significant flow of water, rather than just containing it. This is because some rocks, such as clays, have relatively high water content although water is unable to flow through them easily. Other rocks may not be saturated but still have the property to permit water to flow, and therefore should be regarded in the same light as an aquifer.

Unless groundwater is removed by pumping from wells, it will flow through an aquifer towards natural discharge points, which comprise springs, seepages into stream and rivers, and discharge directly into the sea. The property of an aquifer which allows fluids to flow through it is termed *permeability*, and this is controlled by geological factors. Properties of the fluid are also important, and water permeability is often called *hydraulic conductivity*. Hydrogeologists often think of hydraulic conductivity on a field scale in terms of an aquifer's *transmissivity*, which is the hydraulic conductivity multiplied by the effective saturated thickness of the aquifer (Brassington, 1998).

In both sedimentary rocks and unconsolidated sediments, groundwater is contained in and moves through the pore spaces between individual grains. Fissure systems in solid rocks can significantly increase the hydraulic conductivity of the rock mass. Indeed, in crystalline aquifers of all types, most groundwater flow takes place through fissures and very little, if any, moves through the body of the rock itself. Some geological materials do not transmit groundwater at significant rates, while others only permit small quantities to flow through them. Such materials are termed *aquicludes* and *aquitards* respectively, and although they do not transmit much water, they play a major role in controlling the movement of water through aquifers. Very few natural materials are completely uniform and most contain aquiclude and aquitard materials (Brassington, 1998). Figure 1-9 shows how the presence of an aquiclude, such as clay, can give rise to springs and may support perched water table above the main water table in an aquifer.

Franco Lý

*Interpretation of Borehole Heat Exchangers Thermal Response Tests
under groundwater influence: analysis of three case studies*
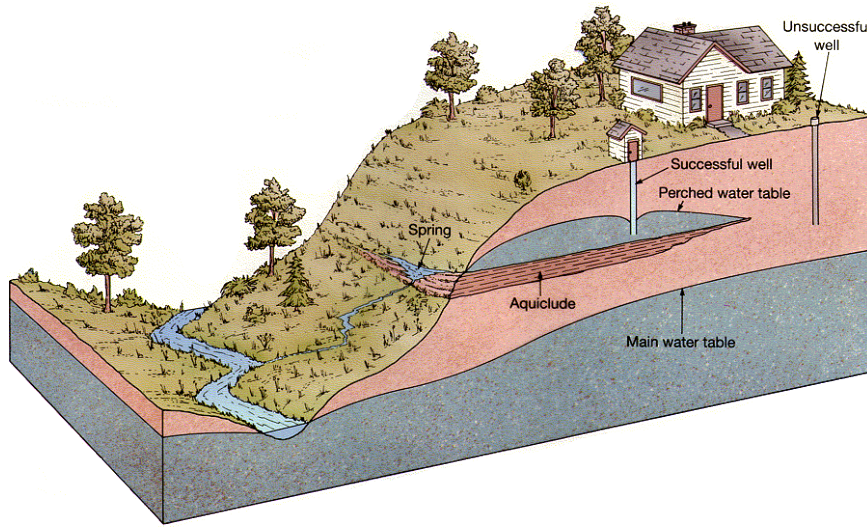
Figure 1-9 - Perched water table above the main water table originated by the presence of an aquiclude (http://geophysics.ou.edu)

When an aquifer is overlain by impermeable rocks, the pressure of the groundwater body can be such that the level of water in wells would rise above the base of the overlying rock (i.e. the top of the aquifer). In such instance the aquifer is said to be *confined*. Sometimes this pressure may be sufficiently great so that the water will rise above the ground surface and flow from wells and boreholes without pumping. This condition is termed artesian flow and both the aquifer and the wells which tap it are said to be *artesian* (Figure 1-10). A groundwater system, thus consists of rainfall recharge percolating into the ground, reaching the water table, and flowing through rocks of varying permeabilities towards natural discharge points. The rate at which water flows through the system depends upon the rainfall, evaporation, permeability and many other factors (Brassington, 1998).
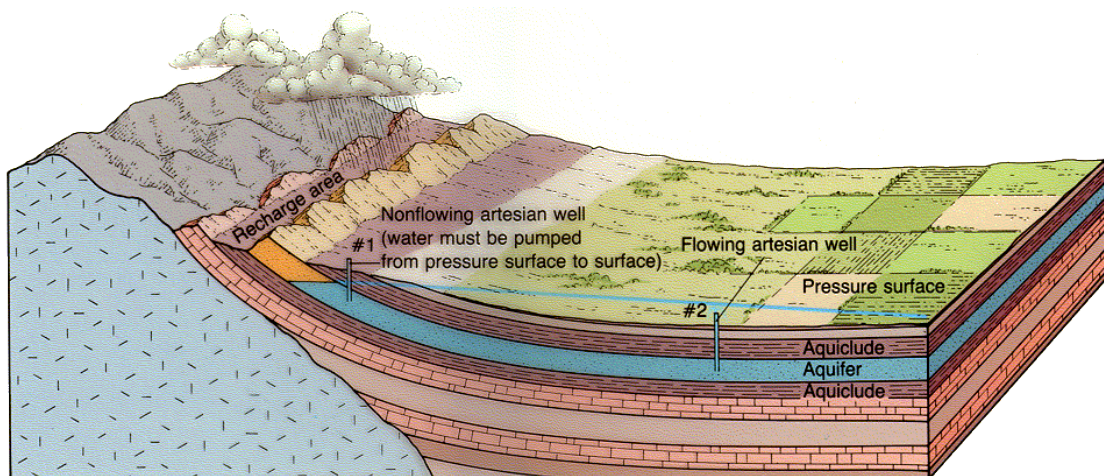
Figure 1-10 - Artesian system: confined groundwater; piezometric surface lies above water table (http://geophysics.ou.edu)

Groundwater flows through an aquifer when the water levels within it are at different elevations. The difference in groundwater levels between two or more places is called *head loss* and is usually expressed in meters. The slope of the water table is called *hydraulic gradient i*, and is the dimensionless ratio of head to distance.

$$i = \frac{\Delta h}{l}$$ **Eq. 1.7**
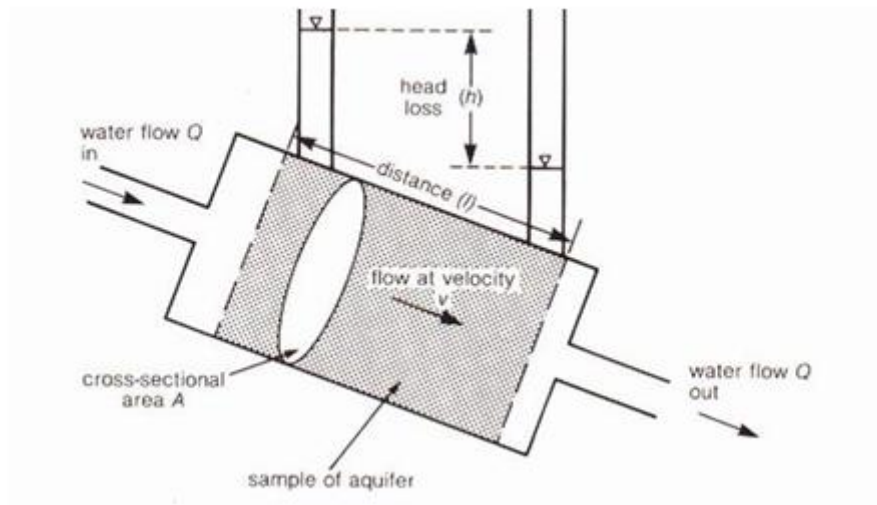
Figure 1-11 - Diagram representation of Darcy's experiment showing that the velocity *v* of water flowing through a porous medium is equal to the hydraulic gradient *i*, times a constant *k* permeability.

The equation which relates the groundwater-flow rate Q to the cross-sectional area of the aquifer *A* and the hydraulic gradient *i* is known as Darcy's law and has the following form:

$$Q = -K \cdot A \cdot i$$ **Eq. 1.8**

The negative sign is for mathematical correctness and indicates that the flow of water is in the direction of decreasing head. However, from a practical point of view the negative sign may be ignored. In the equation, *K* is the *hydraulic conductivity*, which is defined as the volume of water that will flow through a unit cross-sectional area of the aquifer in unit time, under a unit hydraulic gradient and at a specified temperature. The usual units of hydraulic conductivity are meters per day (*m/day*). Hydraulic conductivity is also expressed in meters per second (*m/s*). Darcy's equation can also be written as:

$$v = \frac{Q}{A} = -K \cdot i$$ **Eq. 1.9**

In **Eq. 1.9** *v* is the apparent velocity of the water flow which is also known as the *Darcy velocity* or groundwater flow. The equation assumes that the flow takes place over the cross-sectional area of the aquifer without regard for the relative proportion of the solid parts to the pore spaces. In reality the flow is restricted to the pore space, so the actual velocity is much greater than the Darcy velocity. The average actual velocity is defined as:

$$V_a = \frac{Q}{\phi_e \cdot A}$$
          Eq. 1.10

where ϕ_e is the effective porosity of the aquifer.

Permeability depends on the properties of the aquifer which allow water to flow through it, and also on the density and viscosity of the water. These properties of water are affected by a number of conditions. For example, the density increases with greater concentrations of dissolved minerals. However, the most important factor is temperature, because relatively small changes alter the viscosity of the water by significant amounts. An increase in water temperature from 5°C to about 30°C will double the hydraulic conductivity. According to Darcy's law this will double the velocity at which groundwater flows. As the temperature of groundwater remain constant through the year in deep aquifers, these changes are not normally a problem, except in some shallow aquifers in areas of climate extremes or in situations involving waste water and industrial effluent (Brassington, 1998).

The amount of water held in a rock depends upon its *porosity*. This is the proportion of the volume of rock which consists of pores, and is usually expressed as a percentage of the total rock mass. The principal factors which control porosity are grain size and shape, the degree of sorting, the extent of chemical cementation and the amount of fracturing. Figure 1-12 shows how porosity varies with grain shape and the degree of sorting in unconsolidated sediments. Those sediments which have been ideally sorted and have rounded grains of uniform size are the most porous. Porosity decreases as the angularity of the grain increases, because grains pack together more closely. Similarly, as the degree of sorting is reduced. The amount of interconnected pore space which is available for fluid flow is termed the effective porosity and is also expressed as a percentage of the rock mass.
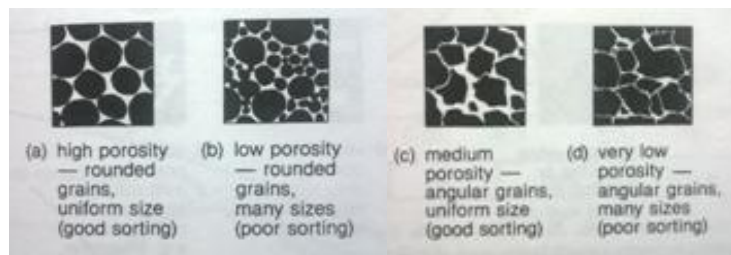
Figure 1-12 - Porosity in unconsolidated sediments varies with degree of sorting and with the shape of grains.

Franco Lý

*Interpretation of Borehole Heat Exchangers Thermal Response Tests
under groundwater influence: analysis of three case studies*

In consolidated rock, porosity tends to be lower than in unconsolidated sediments, because part of the pore space is taken up with cement. Some rocks with relatively high porosity values may be poor transmitters of water because the individual pores are not interconnected. Figure 1-13 illustrates some of the aspects of porosity development in consolidated rocks. Porosity which has developed after the rocks have formed is termed *secondary porosity* to distinguish it from intergranular or primary porosity. It typically results from two causes. Fracture porosity is caused by cracks in the rock associated with joints, bedding plane fissures, tectonic joints and faulting. Secondary porosity also results from solution of the aquifer rock itself, which is common in limestones.
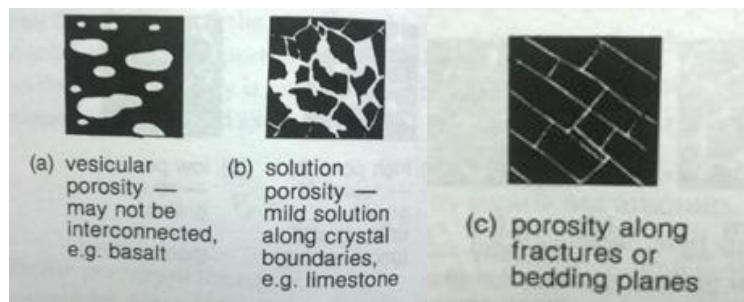
Figure 1-13 - Porosity in consolidated rocks. Note that example (c) shows bedding planes rather than individual grains, so covers much larger mass of rock than Figure 1-12.

Basically, porosity does not provide a direct measure of the amount of water that will drain out of the aquifer because some water will remain in the rock, retained around individual grains by surface-tension forces. Such water defines the specific retention. The volume of water which will drain from the aquifer is termed the specific yield, and is a measure of how much water will flow from and aquifer under the influence of gravity. For further details on specific yield and specific storage (Marocchi, 2015) is suggested to be consulted.

Table 1 - Indicative value of porosity for a range of geological materials.

Material	Porosity (%)	Material	Porosity (%)
Coarse gravel	28	Loess	49
Medium gravel	32	Peat	92
Fine gravel	34	Schist	38
Coarse sand	39	Siltstone	35
Medium sand	39	Claystone	43
Fine sand	43	Shale	6
Salt	46	Till - mainly sand	31
Fine-grained sandstone	33	Till - mainly silt	34
Clay	42	Tuff	41
Medium-grained sandstone	37	Basalt	17
Limestone	30	Gabbro (weathered)	43
Dolomite	26	Granite (weathered)	45
Dune sand	45		

Franco Lý

Interpretation of Borehole Heat Exchangers Thermal Response Tests under groundwater influence: analysis of three case studies

1.7 Heat Transfer in an Aquifer

For common low-temperature geothermal plants, the boreholes may penetrate several geologic strata. The ability of the vertical borehole exchanger to exchange heat with the ground depends on local geology, hydrogeology and other conditions that impact the feasibility and economics of the GSHP systems. Thus, heat transfer between a BHE and its surrounding soil/rock results rather complicated and difficult to model for the purpose of sizing the exchanger or energy analysis of the system. Besides the structural and geometrical configuration of the exchanger, a lot of factors influence the exchanger performance, such as the ground temperature distribution, soil moisture content and its thermal properties, groundwater movement and possible freezing and thawing in soil. The heat dissipation from the pipes in boreholes to far-field ground is a transient process involving a large domain and complicated geometry (Diao, 2004).

The presence of groundwater makes the heat transfer process even more intricate. Water movement in actual "streams" in underground channels is rare and confined to specific geological situations. The subsurface, however, generally has porosity (voids and fractures). The water table is the dividing line between ground with some air in the pores and ground that is saturated with water. Below that level, water is held and moves between the grains of geologic formations in response to hydraulic gradients (**Eq. 1.7**). Rates of lateral groundwater flow vary, ranging from meter per year to meters per day according to local geologic and hydraulic conditions. High flow rates will generally be associated with specific strata types, particularly very coarse gravels or sands. Hence, the heat dissipation in aquifers may be regarded as a coupled process of heat conduction through the solid matrix and water in its pores and heat advection by moving groundwater (Diao, 2004).

In general groundwater flow is considered as beneficial to the thermal performance of BHEs since it has a moderating effect on borehole temperature in both heating and cooling modes. A moderate groundwater advection is expected to make notable difference in alleviating the possible buildup around the borehole over time. As a result, it is desirable to account for groundwater flow in heat transfer model to avoid over-sizing of the ground heat exchangers. In this master thesis, a particular attention is concerned about combined heat transfer of conduction and advection in the vertical BHE surrounded by an aquifer. A possible analytical solution to this problem is termed Moving Line Source model and is extensively treated in section 2.6.

As previously mentioned, heat transfer in BHEs is complicated and dependent of multiple factors, some of which are hard to grasp accurately in engineering practice. It is inevitable to make assumptions and simplifications in the study so the impacts of certain factors can be highlighted and analyzed in detail. In this work the ground around the boreholes is

Franco Lý

Interpretation of Borehole Heat Exchangers Thermal Response Tests
under groundwater influence: analysis of three case studies

assumed to be a homogeneous porous medium saturated by groundwater. Liquid flow in a porous medium is described by Darcy's law (**Eq. 1.9**). The volumetric flow rate per unit of cross-sectional area, i.e. Darcy velocity *v*, is equal to the average linear velocity of the liquid over the cross-section.

Heat is transported through a saturated porous medium in a combined mechanism: by conduction through its solid matrix and liquid in its pores as well as convection of moving liquid. By applying the law of conservation of energy to a control volume, an equation for heat transfer in saturated porous medium can be expressed as (Diao, 2004):

$$C_m \frac{\partial T}{\partial \tau} + \rho_w \, c_w \, \vec{v} \cdot \nabla T = \nabla \cdot (\lambda_m \nabla T)$$

Eq. 1.11

where λ_m denotes the effective thermal conductivity of the porous medium; $C_m = \rho c$ is the volumetric specific heat of the porous medium, including both the solid matrix and water in its pores, and $\rho_w c_w$ the volumetric specific heat of water. Note in **Eq. 1.11** that heat is stored and conducted through both the water and soil matrix, but only water takes part in convection of heat here. The average groundwater velocity $\vec{v}$ over a cross section of the medium may be determined by the hydraulic head distribution according to the Darcy's law if the hydraulic conductivity of the medium is known.

The volumetric thermal capacity C_m and effective thermal conductivity λ_m of the porous medium are weighted averages of those of the saturated water and solid matrix, and can be usually determined on basis of its porosity as:

$$C_m = \rho_s \cdot c_s \cdot (1 - \phi) + \rho_w \cdot c_w \cdot \phi$$

Eq. 1.12

$$\lambda_m = \lambda_s \cdot (1 - \phi) + \lambda_w \cdot \phi$$

Eq. 1.13

where:

- ϕ is the porosity [/]
- ρ_s is the solid matrix density [kg/m^3]
- ρ_w is the water density [kg/m^3]
- λ_s is the solid matrix thermal conductivity [$W/(m \cdot K)$]
- λ_w is the water thermal conductivity [$W/(m \cdot K)$]
- c_s is the solid matrix specific heat [$J/(kg \cdot K)$]
- c_w is the water specific heat [$J/(kg \cdot K)$]

Following the Eskilson's model, a further approximation is accepted that the groundwater velocity is uniform in whole domain concerned and parallel to the ground surface (Diao, 2004). The term "advection" is often used to describe such a flow. Define the velocity u is in the direction of the *x*-coordinate. Then, on the assumption of constant thermal properties **Eq. 1.11** reduces to:

$$\frac{\partial T}{\partial \tau} + U \frac{\partial T}{\partial x} = a\, \nabla^2 T$$

Eq. 1.14

where $U = u\rho_w c_w /(\rho c)$, and the effective thermal diffusivity $a = \lambda/(\rho c)$. And for the steady-state situations, the heat transfer is further simplified to:

$$U \frac{\partial T}{\partial x} = a\, \nabla^2 T$$

Eq. 1.15

Table 2 illustrates typical values of hydraulic and thermal properties of soils and rocks.

Table 2 - Typical values of hydraulic and thermal properties of soils and rocks extracted from (Diao, 2004).

Medium	K [m/s]	$u*$ [m/s (m/year)]	$\lambda**$ [W/mK]	ρc [J/m3·K]	a [m2/s]
Gravel	3,0E-03	3,0E-05	0,98	1,4E+06	7,0E-07
Sand	7,3E-05	7,3E-07	1,02	1,4E+06	7,3E-07
Sand	6,3E-06	6,3E-08	1,03	1,4E+06	7,4E-07
Silt	1,4E-07	1,4E-09	2,07	2,85E+06	7,3E-07
Clay	2,2E-10	2,2E-12	1,25	3,3E+06	3,8E-07
Limestone, dolomite	7,7E-08	7,7E-10	2,46	1,34E+07	1,8E-07
Karst limestone	1,0E-04	1,0E-06	3,50	1,34E+07	2,6E-07
Sandstone	4,2E-08	4,2E-10	4,50	3,56E+06	1,3E-06
Shale	1,4E-11	1,4E-13	2,53	3,94E+06	6,4E-07
Fractured igneous and metamorphic	1,5E-06	1,5E-08	4,61	2,2E+06	2,1E-06
Unfractured igneous and metamorphic	2,4E-12	2,4E-14	4,59	2,2E+06	2,1E-06

*Based on an assumed hydraulic gradient of 0,01 m/m.

**Saturated with water.

Franco Lý

Interpretation of Borehole Heat Exchangers Thermal Response Tests
under groundwater influence: analysis of three case studies

2 Thermal Response Test

2.1 Foreword

The design of GSHP systems requires the knowledge of the thermal properties of the subsurface and the boreholes, in particular an effective ground thermal conductivity λ_{eff} and the so-called borehole thermal resistance R_b. As it is hardly possible to obtain sufficiently accurate values of these parameters from geological or soil-profile information, Thermal Response Tests (TRTs) have been developed that provide measurements in situ.

In the conventional TRTs which scheme is described in Figure 2-2, a heat carrier fluid flowing in a vertical borehole heat exchanger is heated under constant heat injection rate by means of an electric resistance and the resulting fluid temperature perturbation is monitored in time. The observed water temperature evolution is fitted with a proper mathematical model and the above mentioned ground and heat exchanger parameters are inferred.

The aim of this chapter is to deal with three main topics:

1. Purpose of a Thermal Response Test

2. Field test methodology

3. Analytical solutions theory and their implementation

2.2 Purpose of the Test

As already mentioned, it is very important for an accurate borehole heat exchanger design to know the effective ground thermal conductivity and the vertical borehole thermal resistance.

The so called borehole thermal resistance R_b is defined as:

$$R_b = \frac{T_{fm} - T_{bw}}{q}$$ **Eq. 2.1**

where:

- T_{fm} is the mean heat carrier fluid temperature [$°C$]

- T_{bw} is the borehole wall temperature [$°C$]

- q is the heat transfer rate for unit length [W/m]
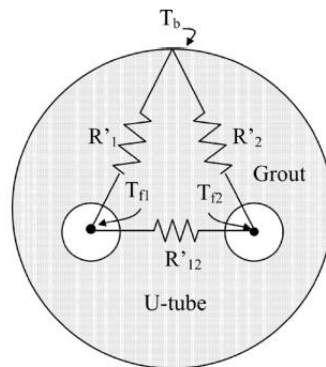
Figure 2-1 - Equivalent borehole thermal resistance circuit for a single U-pipe closed-loop (Lamarche, 2010).

R_b can be calculated based on an equivalent thermal circuit such as in Figure 2-1 or by means of a numerical heat transfer simulation. In literature several expressions are proposed for the evaluation of the unit length borehole resistance and implemented in software like DST, EED and GLHEPRO 4.0.

If for small size plants R_b values estimated from the exchanger characteristics and ground thermal conductivity λ values from literature tables such as Table 2 may be accepted, this is not recommended for remarkable size plants. For these plants, with thermal power greater than *30-50 kW* and a significant number of exchangers, it becomes necessary to perform a TRT (Delmastro, 2011). Under these values the cost incidence is such to advise the use of more elevated safety factors in planning. Indeed the measurement campaign does not

payback the large expenses for drilling. In Lombardy Region the TRT is actually mandatory for geothermal plants with thermal power greater than 50 *kW* (Regolamento Regionale 15/02/10 n.7).

The test is often performed ongoing if not even during executive planning: the BHEs field is modified before that the plant is completed and thus with cost and time optimization (reducing the number of BHEs and drilling startups).
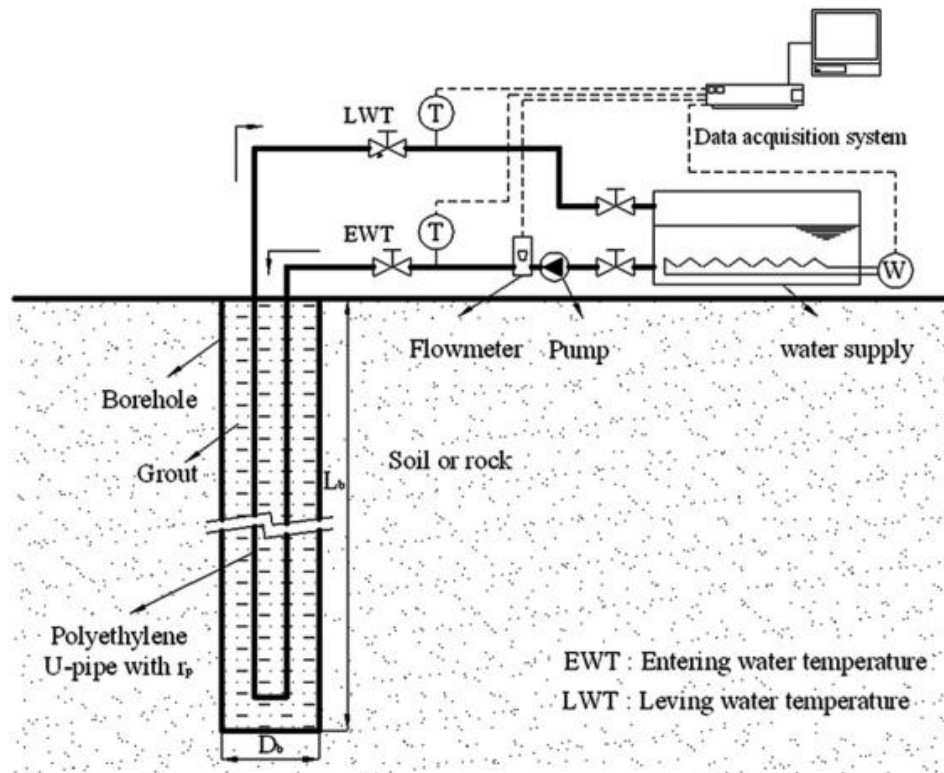
Figure 2-2 - Scheme of TRT equipment.

The test affects borehole heat exchanger one at a time and must be run when the horizontal pipe connections are not set down yet. It is directly performed in situ with a specific mobile apparatus (further details in section 2.3).

Throughout the test, it is necessary to know the heat carrier fluid properties (in particular thermal mass capacity), borehole heat exchanger geometry and have some preliminary indications on the geological context, deducible during drilling activity to install the BHE.

Franco Lý

Interpretation of Borehole Heat Exchangers Thermal Response Tests
under groundwater influence: analysis of three case studies

2.3 Field Test Methodology

A TRT unit typically consists of a pump, purge valves, an electric heating element, temperature sensors, a flow-meter, and a data logger (Figure 2-2). Some units adopt a heat pump instead of an electrical resistance for testing in cooling mode, but they are not widely used. The testing units come in various sizes, ranging from that of a suitcase to a trailer. More detailed descriptions of TRT units can be found in the study by e.g. (Gehlin S. a., 2002) and several recent examples of TRT experiments and analysis have been reported (Roth, 2004), (Sanner, 2005) and etc.. Additional studies reported alternative methods for in situ measurement of the subsurface thermal conductivity, such as the estimation of properties with temperature profiling (Rohner, 2005), tests performed with heating cables (Raymond J. a., 2010), and TRTs that included temperature measurements along the borehole (Fujii, 2009).

Recent guidelines for the test procedure, found in the work by (ASHRAE, 2007), (UNI11466, 2012) and (Sanner, 2005), are briefly summarized.

Prior to starting the test, the undisturbed subsurface temperature is measured using one of the two methods. The first method consists in recording the vertical temperature profile in the ground heat exchanger. A temperature sensor at the end of a cable is lowered down the groundwater filled borehole. The cable is connected to a universal instrument, set for the sensor, on which the temperature logging is read manually (Gehlin S. E., 2003). A weight is attached to the end of the cable to pull the sensor and cable down the borehole. Meter values are marked along the cable and temperature can be read for different depths. For the second method, water is circulated in the ground heat exchanger for *10* to *20 min* without injecting heat and water temperatures are measured with the TRT unit, to allow the measured temperature to reach a constant value assumed representative of the average subsurface temperature (low sampling time are required, e.g. *10 seconds*).

The first method appears more reliable than the second one because, for the latter, heat produced by mechanical work of the pump while operating the TRT unit can be transferred to the water in the pipes and thus introduce a bias in the measured temperature (Gehlin S. E., 2003).

Air bubbles in the ground heat exchanger must be purged before starting the test to ensure that air, which reduces heat transfer, is not trapped in the system. The volumetric flow rate of water circulating in the pipe must be large enough for the flow to remain transitional to turbulent to minimize thermal resistance due to fluid advection and to be representative of flow conditions prevailing when the heat pump system is in operation (Raymond J. a., 2011).

Franco Lý

Interpretation of Borehole Heat Exchangers Thermal Response Tests under groundwater influence: analysis of three case studies

Once the background temperature has been measured and air trapped in the pipes has been purged, the test starts by injecting heat in the ground heat exchanger to disturb subsurface temperatures.

However, before executing the test it is necessary to verify that in a radius of *10 m* from the BHE there are no other perforations or activities which can disturb the ground thermal equilibrium; moreover the test has to begin with the fluid in thermal equilibrium with the ground, that is about *2 hours* of fluid circulation (UNI11466, 2012).

It is also suggested to wait until the injected grout has reached its maturity (around at least *2-3 weeks* after its application, depending on the grout mixture). A premature test involves a surrounding ground warmer than the undisturbed situation. In the case of TRT with heat injection, the results turn out to be worse than the real case as it seems that the ground dissipates less heat than it actually does, but the undisturbed ground temperature turns out to be higher: the overall result is a net underestimation of the summer performance and a dangerous overestimation of the winter performance (Delmastro, 2011).

A common practice is to isolate any pipes lying at ground surface to prevent external heat transfer between the heat exchanger and the pump motor or the atmospheric air. The extension of these segments has to reduced at the minimum. Even with insulation, external heat transfer cannot be eliminated and it is consequently preferable to measure air temperature inside and outside the unit to quantify air temperature changes. These sensors have to be shielded from solar radiation.

During the test, a steady-power supply can help minimize fluctuations in heat injection, although these fluctuations are rarely eliminated. To account for any fluctuation in heat injection and external heat transfer, (Sanner, 2005) recommends measuring the heat injection rate from the temperature differential and the water flow rate using **Eq. 2.8**.

The water density and specific heat capacity can be assumed constant for the range of temperature variations during standard TRTs. Subsequent analysis can therefore account for variable heat injection rates if measured temperatures indicate significant variations of heat injection. An analytical solution for this case will be described in section 2.5.2.

The recommended rate for a constant heat injection test is in the range of *30* to *80 W* per *meter* of borehole (UNI11466, 2012), and the heat injection rate can be averaged during the entire test period or during selected time intervals if variable heat injection rates are used. Larger values for the specific power can activate convective phenomena or modify ground characteristics leading to evaluation of non-realistic conditions. A temperature and flow rate recording interval of at most *10 minutes* is recommended during the entire test

Franco Lý

Interpretation of Borehole Heat Exchangers Thermal Response Tests under groundwater influence: analysis of three case studies

(UNI11466, 2012). In order to have a better description of the profile in the initial phase of test, a shorter sampling time is recommended (e.g. *1 minute*).

The typical duration of a constant heat injection test is between *50* and *60 hours*, but there is no prescribed guideline for the test duration. However, there are some recommendations about the minimum duration by (UNI11466, 2012) which suggests at least *72* or possibly 96 *hours*. The test duration can further be increased to measure the water temperature recovery after heat injection is stopped. In that case, water circulation is maintained in the heat exchanger once heat injection stops, and temperature is measured until it approaches the initial background temperature. The flow rate is monitored during recovery to compute the heat injection rates and to verify if external heat transfer affects temperature, such as during a circulation test used to measure the undisturbed subsurface temperature (Raymond J. a., 2011). This practice can be very useful for a better parameters estimation, in particular for the borehole thermal resistance determination. Although in this master thesis TRTs with recovery data are not treated, because these data were not collected in the considered case studies; (Raymond J. a., 2010) deals this topic in an exhaustive way.

A brief summary of the necessary requisites of the measurement system is provided (UNI11466, 2012):

- the temperature measurement accuracy has to be ±*3℃*;
- the flow rate has to be such to guarantee a temperature difference between inlet and outlet pipes comprised *3℃* and *7℃*;
- standard deviation of the supplied power has to be inferior to ±*1,5%* of the mean value and peaks inferior to ±*10%* of the mean;
- combined accuracy of the electrical device that supplies the power and the logger that records this data has to be inferior to ±*2%* of the reading;
- temperature sampling time has to be lower than the time the fluid spend to complete a whole loop of the borehole heat exchanger.

Eventually, a procedure for injection power check is provided in (UNI11466, 2012) and it will be applied for Lodi case study in section 5.3.6.

2.4 Test Analysis

The subsurface and borehole thermal properties are estimated by reproducing heat carrier fluid temperature variations observed at the pipe inlet and outlet during the test using either an analytical or a numerical solution to the heat transfer equation. The Cylindrical and Line Source models are the most commonly used analytical solutions to interpret TRT data. Both solutions describe transient heat conduction from an infinite source embedded in a conductive homogeneous medium of infinite radial extent. Such models however are not suitable for analyzing TRTs performed in heterogeneous geological conditions or in porous subsoils where advective heat transport is also expected.

This issue was already demonstrated by (Witte H. , 2001) in its studies. He established an advection-dominated aquifer by performing a TRT, while groundwater was being extracted from a well *5 m* away from the BHE. A comparison to the results of an undisturbed TRT showed an increase in λ_{eff} value by a factor of *1,38*. In saturated conditions, ground thermal conductivity estimated with heat injection is apparently not representative, and can therefore not be used directly in modeling or design studies. Test results should be evaluated with respect to convergence on an estimate of ground thermal conductivity as outlined in Figure 2-4.

In such cases, three-dimensional numerical models can be used to analyze TRTs as in (Signorelli, 2007) although the required modeling and computational effort is significant. Signorelli compared the results from a 3D finite-element numerical model FRACTure with those of a simple analytical line-source solution and tested their sensitivity to the duration of the tests. The effects of heterogeneous subsurface conditions, groundwater movement, and variable data quality are surveyed confirming the findings by Witte.

Thus, the influence of water table fluctuations, which govern groundwater flow velocities cannot be neglected in case of important aquifers. Alternatively to numerical modeling, an analytical approach based on Moving Line Source solution can be performed to account the simultaneous heat transport by advection and conduction (Wagner V. a., 2013). The recorded TRT data is fitted by a three-variable parameters estimation technique able to determine Darcy velocity *v* along with the ground thermal conductivity and borehole thermal resistance. Estimated $\lambda_{m,eff}$ by this method is not anymore an effective parameter but it represents the properties of the porous medium containing no advective portion.

The Infinite Line-Source solution is described in detail in section 2.5, together with its extension for variable heat injection rates (section 2.5.2). Further, the Moving Line Source solution (section 2.6) is described and implemented for the studied TRTs interpretation in this master thesis.

Franco Lý

Interpretation of Borehole Heat Exchangers Thermal Response Tests
under groundwater influence: analysis of three case studies

2.5 Infinite Line Source Model

The most commonly adopted procedure to analyze a TRT is based on the Kelvin Line Source theory (Gehlin S. , 2002). This approach supposes the BHE as an infinite line source in a homogeneous, isotropic and infinite medium, which injects or extracts a constant amount of energy (*q*) per unit length by conductive heat transport only.

The temporal and spatial temperature changes around the line source can be calculated as follows:

$$T_{sub}(r, t) - T_0 = \frac{q}{4\pi\lambda_{eff}} \int_{r^2/4at}^{\infty} \frac{e^{-u}}{u} du \qquad \textbf{Eq. 2.2}$$

$$= \frac{q}{4\pi\lambda_{eff}} E_1 \left[\frac{r^2}{4at}\right] \approx \frac{q}{4\pi\lambda_{eff}} \left[ln\left(\frac{4at}{r^2}\right) - \gamma\right] \qquad \textbf{Eq. 2.3}$$

where:

- T_{sub} is the subsurface temperature [*°C*]
- T_0 is the initial/undisturbed ground temperature [*°C*]
- q is the heat transfer rate for unit length [*W/m*]
- λ_{eff} is the effective thermal conductivity of the subsurface [*W/(m·K)*]
- r is the radius [*m*]
- a is the thermal diffusivity [*m²/s*]
- t is time [*s*]
- γ is Euler constant
- u is the integration variable (*r²/4at*)
- E_1 is the exponential integral

It is assumed that the system is initially at constant temperature (T_{sub} (*r, t* = 0) = T_0) and that boundaries located at an infinite distance from the heat source (*r* = ∞) always remain at constant temperature (T_{sub} (*r* = ∞, *t*) = T_0).

When using the Infinite Line Source model to interpret a TRT, it is important to exclude from the analysis the first obtained results, since they are related to the borehole filling material and not to the ground. Not knowing precisely the position of the pipes inside the borehole, it is assumed as minimum significant time the necessary time in order that the thermal wave passes through a path at least equal to the borehole wall radius (Delmastro, 2011). This is involved into the mathematical approximation in **Eq. 2.3**.

Franco Lý

*Interpretation of Borehole Heat Exchangers Thermal Response Tests
under groundwater influence: analysis of three case studies*

Exponential Integral E1
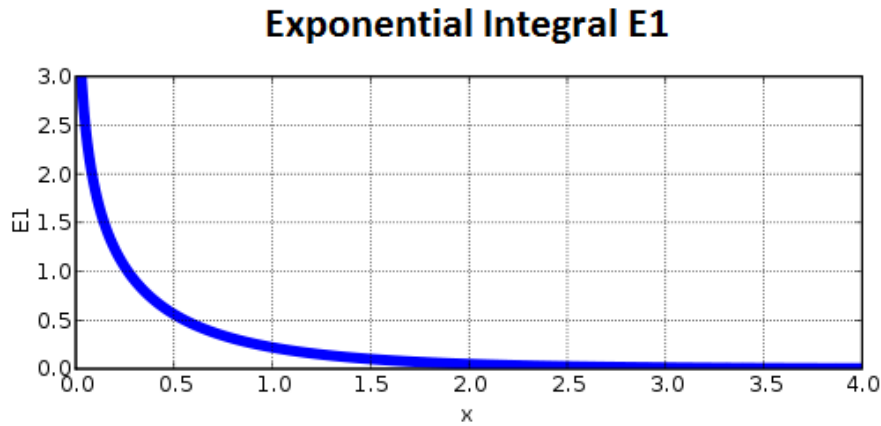
Figure 2-3 - Exponential integral function E_1

Indeed the logarithmic approximation of the exponential integral (Figure 2-3) is acceptable since it was demonstrated (Hellstrom, 1991) that the relative maximum error is less than *10%* if the following time criterion is fulfilled.

$$t \geq t_c \geq \frac{5r_{bw}^2}{a}$$

<div align="right">**Eq. 2.4**</div>

where:

- r_{bw} is the borehole wall radius [*m*]
- t_c is the characteristic time, that is the minimum time for test significativity

This error range assumes that substantial disturbances on the recorded temperature are absent and the test is properly performed. The characteristic time is initially estimated using a first guess thermal diffusivity usually inferred by literature tables such as Table 2.

The mean fluid temperature is evaluated by taking the Line Source temperature at the borehole radius and adding the effect of the thermal resistance R_b between the borehole wall and the circulating heat carrier fluid. Thus the mean fluid temperature as a function of time can be expressed:

$$T_{fm} - T_{bw} = q \cdot R_b$$

<div align="right">**Eq. 2.5**</div>

$$T_{fm}(t) = T_{bw}(t) + qR_b = \frac{q}{4\pi\lambda_{eff}} E_1\left[\frac{r_{bw}^2}{4at}\right] + T_0 + qR_b$$

<div align="right">**Eq. 2.6**</div>

$$\approx \frac{q}{4\pi\lambda_{eff}} ln(t) + q\left[R_b + \frac{1}{4\pi\lambda_{eff}}\left(ln\left(\frac{4a}{r_{bw}^2}\right) - \gamma\right)\right] + T_0$$

<div align="right">**Eq. 2.7**</div>

Franco Lý

*Interpretation of Borehole Heat Exchangers Thermal Response Tests
under groundwater influence: analysis of three case studies*

where:

− T_{fm} is the mean fluid temperature (arithmetic average between inlet and outlet temperatures) [$°C$]
− R_b is the borehole heat exchanger (BHE) thermal resistance [$m·K/W$]

In order to determine the effective thermal properties (λ_{eff} and R_b), two similar approaches are possible. The recorded TRT data are either fitted by a two variable parameters estimation technique (Roth, 2004) or by a linear regression based on the logarithmic approximation of **Eq. 2.7** (Gehlin S. , 2002),(Signorelli, 2007).

In the analysis of the case studies carried out in the present thesis (see chapter 3, 4 and 5), the approach based on the linear regression of the logarithmic approximation of **Eq. 2.7** is adopted as also suggested by (UNI11466, 2012).

The procedure to determine the effective thermal conductivity λ_{eff} and the specific BHE thermal resistance R_b, consists in the following steps:

•   calculation of the thermal power per unit length supplied by the heat carrier fluid

$$q = c_f \cdot Q \cdot (T_{in} - T_{out}) / L \qquad \textbf{Eq. 2.8}$$

 where:

− c_f is the specific heat of the fluid [$J/(°C \cdot kg)$]
− Q is the fluid mass flow rate determined by circulating pump [kg/s]
− T_{in} and T_{out} are the recorded temperature at the inlet and outlet of BHE [$°C$]
− L is the BHE overall length [m]

•   estimation of the mean heat carrier fluid temperature as function of time

$$T_{fm} = \frac{T_{in} + T_{out}}{2} \qquad \textbf{Eq. 2.9}$$

•   linear interpolation of the mean fluid temperature time series according to:

$$T_{fm} = A\, ln(t) + B \qquad \textbf{Eq. 2.10}$$

obtained by **Eq. 2.7** assuming:

$$A = \frac{q}{4 \cdot \pi \cdot \lambda_{eff}} \qquad \textbf{Eq. 2.11}$$

where A is the slope of the interpolating straight line for the temperature time series on a graph with x - axis: $ln(t)$

> y - axis: T_f

$$B = q\left[R_b + \frac{1}{4\pi\lambda_{eff}}\left(ln\left(\frac{4a}{r^2}\right) - \gamma\right)\right] + T_0 \qquad \textbf{Eq. 2.12}$$

- assessment of equivalent thermal conductivity λ_{eff} as:

$$\lambda_{eff} = \frac{q}{4 \cdot \pi \cdot A} \qquad \textbf{Eq. 2.13}$$

- calculation of the equivalent thermal diffusivity a of the ground as

$$a = \frac{\lambda_{eff}}{C} \qquad \textbf{Eq. 2.14}$$

where C is volumetric thermal capacity of the ground [$J/(m^3K)$], deductible from geological data in literature.

- determination of the undisturbed ground temperature T_0 from the measurement of the temperature reached by the heat carrier fluid at the initial circulation in the borehole heat exchanger in absence of thermal disturbance of the ground;

- assessment of the specific BHE thermal resistance R_b as

$$R_b = \frac{B - T_0}{q} - \frac{1}{4\pi\lambda_{eff}}\left[ln\left(\frac{4a}{r^2}\right) - \gamma\right] \qquad \textbf{Eq. 2.15}$$

As previously mentioned this procedure, based on the linear regression of the logarithmic approximation (**Eq. 2.7**), is valid if the time criterion i.e. **Eq. 2.4** is fulfilled. From experimental data, in the representation on log scale, it can be noticed how the linear behavior is only present for longer times, while for short period the behavior is completely non-linear.

This in an important consideration, because the evaluation of the minimum time for test significativity depends on thermal diffusivity a, which depends on ground thermal conductivity according to **Eq. 2.14**. Recalling that this last parameter can be only evaluated after the first part of the analysis, in order to estimate the characteristic time t_c (and thus the amount of data to be disregarded) it is necessary to assign a initial value for thermal diffusivity (commonly from literature table).

This introduces an inconvenient iterativity into the interpretation procedure: based on the first try thermal diffusivity, the thermal conductivity is determined which is used to calculate the thermal diffusivity of second try and so on.

2.5.1   Step by Step Test Interpretation

If the test duration is sufficiently long, it is possible to obtain a reliability index of the results by means of a step by step interpretation, that is to apply the ILS model only on a part of the dataset. In particular, the fit is performed on increasing datasets in which the initial time is selected, while the evaluation time is increased until the achievement of the complete test duration.

If the test is well executed, there are no significant fluctuations of the aquifer and the ground behavior surrounding the borehole is not heavily affected by the drillings, the effective thermal conductivity λ_{eff} and the borehole thermal resistance R_b should converge to a stable value for increasing evaluation time as demonstrated in Figure 2-4. In other cases, when the groundwater flow is significant, the estimated conductivity by means of the some approach does not converge as verified by (Witte H. , 2001) and outlined in Figure 2-5. In fact, it can be noticed that λ_{eff} increases continuously with evaluation time.
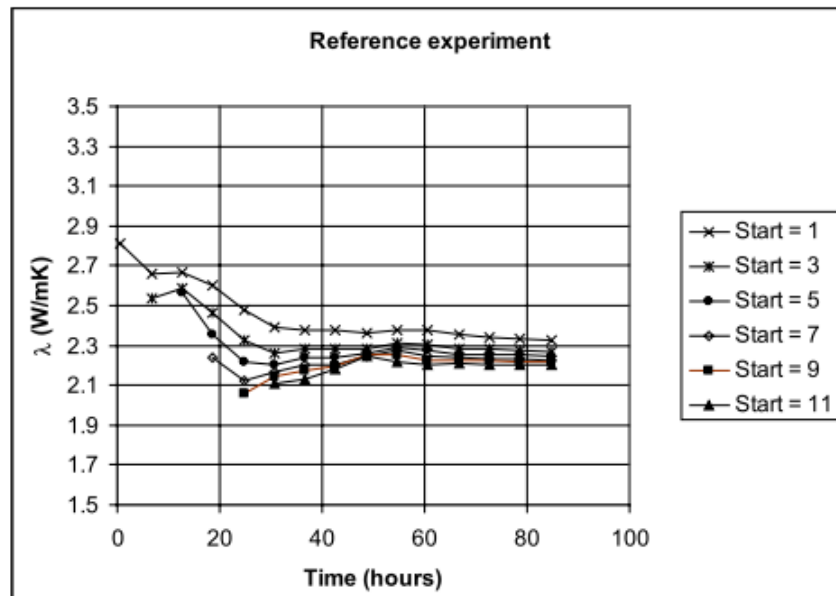
Figure 2-4 - Sensitivity graph of the estimated thermal conductivity values as a function of initial time selected and amount of data added, reference experiment.

Franco Lý

Interpretation of Borehole Heat Exchangers Thermal Response Tests under groundwater influence: analysis of three case studies
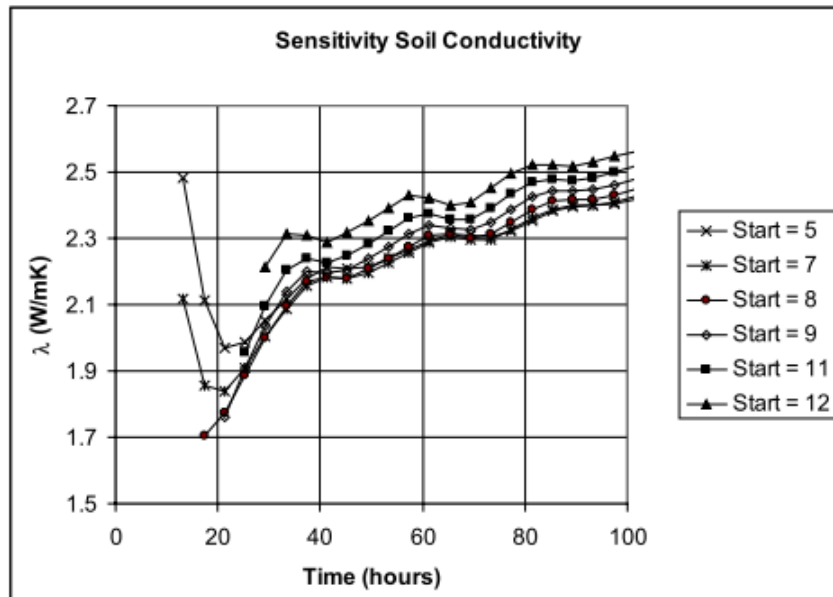
Figure 2-5 - Sensitivity graph of the estimated thermal conductivity values as a function of initial time selected and amount of data added, groundwater extraction experiment.

2.5.2 Variable Heat Injection Rates

The Line Source equation is also valid for variable heat injection rates when the superposition principle is used. The mean water temperature increment for variable heat injection rates can be written as the following convolution integral (Raymond J. a., 2011):

$$T_{fm}(t) - T_0 = \int_0^t q(\tau)G(t - \tau)d\tau \qquad \text{Eq. 2.16}$$

where the heat injection $q(\tau)$ is a continuous input function and $G(t\text{-}\tau)$ is a function that describes the impulse response determining the temperature increments at any time during a TRT that begins at time $t = 0$.

The exact expression for G depends on the analytical solution chosen. For the Line Source equation (**Eq. 2.7**), G is defined as

$$G = \frac{e^{-u}}{4\pi\lambda_{eff}(t - \tau)} \qquad \text{Eq. 2.17}$$

where:

$$u = \frac{r^2}{4\pi a(t - \tau)} \qquad \text{Eq. 2.18}$$

Franco Lý

Interpretation of Borehole Heat Exchangers Thermal Response Tests under groundwater influence: analysis of three case studies

Variable τ is replaced by u and the integral in **Eq. 2.16** becomes the exponential integral that can be expressed with E_1 when q is constant for a given period.

When heat injection can be approximated by a step function, the mean water temperature increment along the ground heat exchanger pipes is described by the sum of the contribution of step heat injection rates q_i according to:

$$T_{fm}(t) - T_0 = q(t)R_b + \sum_{i=1}^{n}(q_i - q_{i-1})\frac{E_1[u]}{4\pi\lambda_{eff}}$$

Eq. 2.19

where: $$u = \frac{r_{bw}^2}{4a(t - t_{i-1})}$$

For $q_0 = 0$ and $t_0 = 0$. The same boundary conditions and assumptions as those given for the Infinite Line Source solution with constant heat injection rates apply for **Eq. 2.19**, except that the heat injection rate now varies between steps.

The exponential integral in **Eq. 2.19** can be approximated by the following infinite Taylor series. The logarithmic approximation, i.e. the first two terms on the right hand side of **Eq. 2.20** provides an adequate approximation to the exponential integral when the time criterion is fulfilled as described for the ILS model by **Eq. 2.4**:

$$E_1[u] = \left[-\gamma - \ln(u) + \sum_{i=1}^{n}(-1)^{i+1}\frac{u^i}{i \cdot i!}\right]$$

Eq. 2.20

Therefore, similarly to **Eq. 2.7** the mean heat carrier fluid can be described according to:

$$T_{fm}(t) = q(t)R_b + \sum_{i=1}^{n}(q_i - q_{i-1})\frac{ln\left(\frac{4a(t - t_{i-1})}{r_{bw}^2}\right) - \gamma}{4\pi\lambda_{eff}} + T_0$$

Eq. 2.21

All the parameters are already dealt in **Eq. 2.3**, except for the heat injection rate per unit length q_i, which can be variable with subscript i representing a time interval for which the rate is constant.

Departure from steady-state conditions in the borehole between steps is assumed negligible because of the steady-state nature of R_b. Good correlation with measured temperature increments suggests that this assumption is valid for small variations in heat injection rate, such as those that caused external heat transfer related to atmospheric temperatures changes. The steady-state assumption does not, however, apply to early time

Franco Lý

Interpretation of Borehole Heat Exchangers Thermal Response Tests under groundwater influence: analysis of three case studies

for large variation in heat injection rate, like at the beginning of the heating and the recovery periods (Raymond J. a., 2011).

2.5.3 Analytical Solution Implementation

Differently from the ILS interpretation by linear regression (which can be performed by means of a spreadsheet program like Excel in this work), the extension with variable heat injection rates requires a more complex parameter estimation approach with numerical resolution of a convolution integral. Hence, in this thesis, a script is implemented in MATLAB, a high-level technical computing language and interactive environment for algorithm development, data visualization, data analysis, and numerical computation. An ad hoc script is developed for Lodi case study (section 5.5).

2.6 Moving Line Source Model

A TRT evaluation based on the Kelvin Infinite Line Source theory does not consider the effects of groundwater flow and simplifies all possible heat transfer processes of the subsurface as purely conductive transport with an effective thermal conductivity, λ_{eff}. Therefore it is not possible to determine the relevant heat transport parameters for advection-dominated conditions using **Eq. 2.7**.

In order to take into account the significant influence of groundwater flow, (Wagner V. a., 2013) developed in his work an analytical approach to groundwater-influenced TRTs, which provides parameters more suitable for a detailed simulation of conductive and advective heat transport in the subsurface. This extended version of the Line Source model, named Moving Line Source model (Diao, 2004), (Molina-Giraldo N. a., 2011) accounts for advection and hydrodynamic dispersion.

The temperature increase in the subsoil is calculated in Cartesian coordinates by:

$$T_{sub}(x,y,t) - T_0 = \frac{q}{4\pi C_m\sqrt{D_l D_t}} exp\left[\frac{v_{th}\cdot x}{2D_l}\right] \int_0^{v_{th}^2/4D_l} exp\left[-\left(\frac{x^2}{D_l} + \frac{y^2}{D_t}\right)\frac{v_{th}^2}{16D_l u} - u\right]\frac{du}{u} \quad \textbf{Eq. 2.22}$$

Equivalent to the approach by (Sutton, 2003), the fluid temperature of a BHE can be obtained by calculating average borehole wall temperature and by adding a qR_b term.

$$T_{fm}(t) = \frac{q}{4\pi C_m\sqrt{D_l D_t}} exp\left[\frac{v_{th} r\, cos\theta}{2D_l}\right] x \qquad\qquad \textbf{Eq. 2.23}$$

$$x \int_0^{v_{th}^2/4D_l} exp\left[-\left(\frac{(r\,cos\theta)^2}{D_l} + \frac{(r\,sen\theta)^2}{D_t}\right)\frac{v_{th}^2}{16D_l u} - u\right]\frac{du}{u} + T_0 + qR_b$$

Franco Lý

Interpretation of Borehole Heat Exchangers Thermal Response Tests under groundwater influence: analysis of three case studies

Eq. 2.22 and **Eq. 2.23** account for an effective heat transport velocity v_{th} and an effective thermal dispersion coefficient (D_l and D_t).

These parameters are determined as follows:

$$v_{th} = v_{eff} \frac{C_w}{C_m}$$

<div align="right">**Eq. 2.24**</div>

$$D_l = \frac{\lambda_{m,eff}}{C_m} + \alpha_l v_{th}$$

<div align="right">**Eq. 2.25**</div>

$$D_t = \frac{\lambda_{m,eff}}{C_m} + \alpha_t v_{th}$$

<div align="right">**Eq. 2.26**</div>

where:

- C_w is the water volumetric thermal capacity [$J/(m^3 K)$]
- C_m is the porous medium volumetric thermal capacity [$J/(m^3 K)$]
- $\lambda_{m,eff}$ is the medium thermal conductivity without advective portion [$W/(m \cdot K)$]
- v_{eff} is the obtained Darcy velocity [m/s]
- α_l is the longitudinal dispersivity [m]
- α_t is the transversal dispersivity [m]

In contrast to λ_{eff}, $\lambda_{m,eff}$ is an obtained value that only represents the properties of the porous medium and contains no advective portion. C_m or ρc is usually extracted from literature tables as Table 2 or can be evaluated by **Eq. 2.27**. The dispersivity is necessary to consider the effect of inhomogeneities of the subsurface that can affect groundwater flow. On the one hand, these are microscale inhomogeneities such as pore directions not parallel to flow direction, on the other hand also macroscale properties such as layer structures and lenses. A distinction is usually proposed between the longitudinal dispersivity (along the flow direction) and the transversal dispersivity (perpendicular to the flow direction).

Eq. 2.23 additionally accounts for advective heat transport, but it still carries some simplifying assumptions.

Similar to **Eq. 2.7** for standard TRT interpretation the effects of thermal disturbance such as from vertical heat flow along the natural vertical geothermal gradient are neglected. (Wagner V. a., 2013) demonstrated that this only introduces a minor error in standard TRT interpretation.

Franco Lý

Interpretation of Borehole Heat Exchangers Thermal Response Tests
under groundwater influence: analysis of three case studies

Disturbances from buoyancy effect are also ignored. (Hecht-Méndez, 2010) demonstrated this is a valid assumption for the simulation of common GSHP systems. Furthermore, (Gehlin S. a., 2003) reported that the termosiphon effect, which is caused by a vertical groundwater flow inside the borehole, can be neglected for properly grouted BHE.

It is important to emphasize that MLS interpretation only provides subsurface properties averaged over the total length of the BHE. Both **Eq. 2.7** and **Eq. 2.23** yield integral parameter sets to characterize the subsurface, and are not suited for resolving heterogeneous properties of the ground.

In this thesis, the parameters estimation technique that calibrates results from **Eq. 2.23** to temperature time series is performed by means of *fminsearch* function, a MATLAB ready-to-use algorithm able to find minimum of unconstrained multivariable function using derivative-free method. In particular this script uses the Nelder-Mead algorithm as explained by (Lagarias, 1998). In the next section 2.6.1, a detailed description of the MLS script is provided.

2.6.1 Script Implementation

In this present work the effects of mechanical thermal dispersion are neglected in **Eq. 2.23** in a first step as suggested in (Wagner V. a., 2013). This is considered an acceptable simplification that reduces the number of unknown parameters.

$$\alpha_l = 0$$

$$\alpha_t = 0$$

$$unknown\ parameters = \left[\, \lambda_{m,eff}, v_{eff}, R_b \,\right]$$

More details on potential errors introduced by this simplification are comprehensively discussed in (Molina-Giraldo N. a., 2011) and (Wagner V. a., 2012).

The volumetric thermal capacity and effective thermal conductivity of the ground are weighted averages of those of the saturated water and solid matrix, and can be usually determined on the basis of the porosity as:

$$C_m = \rho_s \cdot c_s \cdot (1 - \phi) + \rho_w \cdot c_w \cdot \phi \qquad \qquad \textbf{Eq. 2.27}$$

$$\lambda_m = \lambda_s \cdot (1 - \phi) + \lambda_w \cdot \phi \qquad \qquad \textbf{Eq. 2.28}$$

where:

- ϕ is the porosity [/]

- ρ_s is the solid matrix density [kg/m^3]

- ρ_w is the water density [kg/m^3]

- λ_s is the solid matrix thermal conductivity [$W/(m·K)$]

- λ_w is the water thermal conductivity [$W/(m·K)$]

- c_s is the solid matrix specific heat [$J/(kg·K)$]

- c_w is the water specific heat [$J/(kg·K)$]

The second step computes a single representative borehole wall temperature, which is necessary for the application of **Eq. 2.23**. The representative borehole wall temperature is an integral value of the entire BHE. In contrast to a conduction-system the heat propagation in an advection-dominated system is not radially symmetric. Thus, temperature at the borehole wall is not constant. To account for the asymmetric heat distribution around a BHE influenced by groundwater flow, a mean borehole wall temperature measured at eight positions is calculated according to the approach proposed by (Wagner V. a., 2013). The positions are predefined on the BHE cross section as shown in Figure 2-6.

$$\theta = \left[\frac{\pi}{4} : \frac{\pi}{4} : 2\pi\right]$$
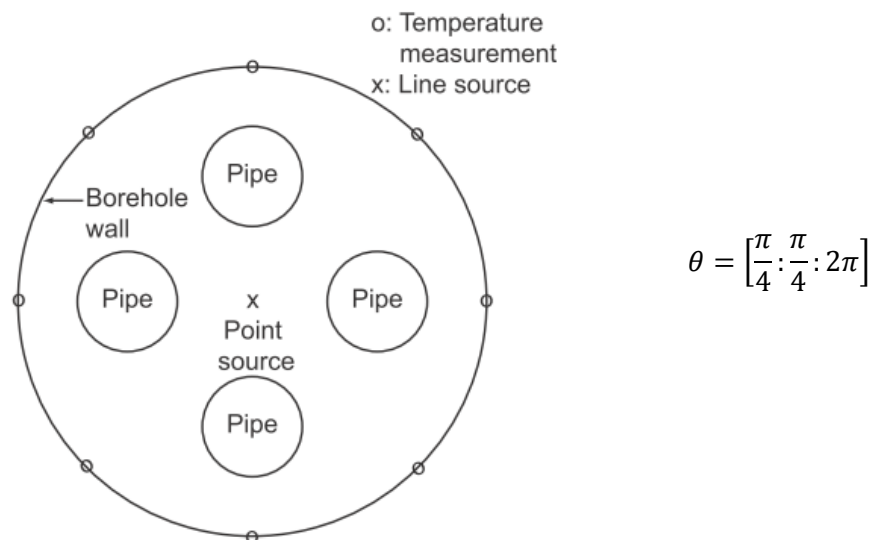
Figure 2-6 - BHE cross section with central evaluation position of the MLS equation and the temperature measurement locations at the borehole wall for the calculation of mean temperature in the case of groundwater flow (Wagner V. a., 2013).

Franco Lý

Interpretation of Borehole Heat Exchangers Thermal Response Tests
under groundwater influence: analysis of three case studies

Neglecting longitudinal and transversal dispersivity (α_l and α_t), the effective thermal dispersion coefficient (D_l and D_t) previously described in **Eq. 2.25** and **Eq. 2.26**, can now be respectively expressed as:

$$D_l = \frac{\lambda_{m,eff}}{C_m}$$

Eq. 2.29

$$D_t = \frac{\lambda_{m,eff}}{C_m}$$

Eq. 2.30

Thanks to this assumption, further simplifications can be carried on MLS equation in polar coordinates, before implementing it in MATLAB. In order to simplify mathematical expression, from now on, regarding MLS solution $\lambda_{m,eff}$ is substituted by λ, v_{eff} by v and r_{bw} by r.

While the inferior integration end is still *0*, the superior integration end (*i.e.*) of the integral function in **Eq. 2.23** is so arranged:

$$i.e. = \frac{v_{th}^2}{4D_l} = \left(v\frac{\rho_w \cdot c_w}{C_m}\right)^2 t \cdot \frac{C_m}{4\lambda} = \frac{(v \cdot \rho_w \cdot c_w)^2 \cdot t}{4\lambda \cdot C_m}$$

Eq. 2.31

The integrand of **Eq. 2.23** is then adjusted as a result of **Eq. 2.29**, **Eq. 2.30** and **Eq. 2.24**:

$$f = \frac{1}{u} \cdot exp\left[-\left(\frac{(r\,cos\theta)^2}{D_l} + \frac{(r\,sen\theta)^2}{D_t}\right)\frac{v_{th}^2}{16D_l u} - u\right]$$

$$f = \frac{1}{u} \cdot exp\left[-\left(\frac{(r\,cos\theta)^2 + (r\,sen\theta)^2}{\lambda/C_m}\right)\left(v\frac{\rho_w \cdot c_w}{C_m}\right)^2 \frac{C_m}{16\lambda \cdot u} - u\right]$$

$$f = \frac{1}{u} \cdot exp\left[-\left(\frac{(r\,cos\theta)^2 + (r\,sen\theta)^2}{\lambda}\right)\frac{(v \cdot \rho_w \cdot c_w)^2}{16\lambda \cdot u} - u\right]$$

$$f = \frac{1}{u} \cdot exp\left[-\frac{r_{bw}^2}{\lambda}\frac{(v \cdot \rho_w \cdot c_w)^2}{16\lambda \cdot u} - u\right]$$

Eq. 2.32

Hence, the expression described in **Eq. 2.32** is adopted in the script. The borehole wall temperatures located at the eight positions as described in Figure 2-6 are so reorganized and used in MATLAB:

$$T_{bw}(t) = T_0 + \frac{q}{4\pi C_m\sqrt{D_l D_t}} \cdot exp\left[\frac{v_{th} \cdot x}{2D_l}\right]\int_0^{i.e.} f \cdot du$$

Franco Lý

Interpretation of Borehole Heat Exchangers Thermal Response Tests
under groundwater influence: analysis of three case studies

$$T_{bw}(t) = T_0 + \frac{q}{4\pi C_m \sqrt{\lambda^2/C_m^2}} \cdot exp\left[\frac{v \cdot \rho_w \cdot c_w}{C_m} \cdot \frac{r_{bw}\,cos\theta}{2\lambda/C_m}\right] \int_0^{i.e.} f \cdot du$$

$$T_{bw}(t) = T_0 + \frac{q}{4\pi\lambda} \cdot exp\left[\frac{v \cdot \rho_w \cdot c_w \cdot r_{bw} \cdot cos\theta}{2\lambda}\right] \int_0^{i.e.} f \cdot du \qquad \textbf{Eq. 2.33}$$

Therefore, a single representative borehole wall temperature $\overline{T_{bw}}$ is calculated as the arithmetic mean of temperature values which are obtained from nodes located at the boundary between the subsurface and the grout material. It has to be underlined that the evaluation of the integral in **Eq. 2.33** is numerically solved for each nodes position.

The mean fluid temperature is finally determined as:

$$T_f(t) = \overline{T_{bw}}(t) + q \cdot R_b \qquad \textbf{Eq. 2.34}$$

The MLS solution is then fitted with experimental data by means of *fminsearch* function, that minimizes the Root Mean Squared Error (RMSE) between measured mean fluid temperature time series (inlet/outlet average temperature as in **Eq. 2.9**) and calculated data by **Eq. 2.34** by varying a defined set of parameters $\left[\lambda_{m,eff}, v_{eff}, R_b\right]$:

$$RMSE = \left[\sum_{i=1}^{N} \frac{\left[T_{f,MLS}(t_i) - T_{f,meas}(t_i)\right]^2}{N}\right]^{0,5} \qquad \textbf{Eq. 2.35}$$

The RMSE determines the accuracy of the fitting, and thus can be used to compare different fits. In general, when calibrating models to measurements in natural systems, the complex coupled processes involved often make it impossible that one unique set of valid parameter values can be determined (Wagner V. a., 2013).

2.6.2 Time Criterion for Data Significativity

Wagner et al. propose the adoption of the MLS theory to interpret TRT data in presence of groundwater flow (Wagner V. a., 2013), but they do not provide any time criterion, similar to Eq. 2.4 for LS, to disregard data related to initial times, when heat transfer basically involves the borehole volume. Concerning this issue, in this thesis, a method is proposed in order to identify a characteristic time t_c necessary to determine the minimum time for data validity. The borehole is thus considered as a homogeneous cylindrical volume filled of grouting material characterized by a lumped thermal capacitance and a spatially uniform temperature. Since the grouting material hydraulic conductivity is negligible, groundwater flows horizontally outside the borehole volume as depicted in Figure 2-7. It consists in a condition of forced convection for external flow, specifically a cylinder in cross flow. For further details it is suggested to refer to (Incropera, 2011). The idea is to evaluate, by means of a lumped capacity approach, the time that is necessary for the borehole volume to almost reach steady state.
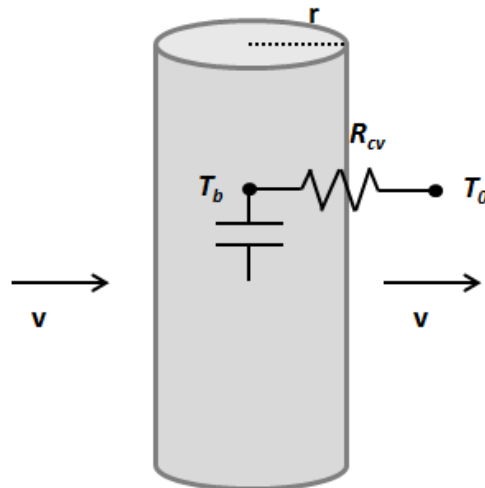
Figure 2-7 - Scheme of a borehole crossed by groundwater flow

An energy balance for the borehole volume is written, taking into account the constant heat generation inside the volume due to the U-pipe during the TRT $\dot{Q}_{in}$ and the heat losses due to convection $\dot{Q}_{out}$:

$$\frac{dU_b}{dt} = \dot{Q}_{in} - \dot{Q}_{out}$$

Eq. 2.36

where:

- U_b is the borehole volume internal energy [J]
- $\dot{Q}_{in}$ is set up by TRT conditions [J/s]

The internal energy variation can be expressed as follows:

$$\frac{dU_b}{dt} = m_b \cdot c_g \cdot \frac{dT_b}{dt}$$ **Eq. 2.37**

where:

- m_b is the borehole mass [kg]
- c_g is the filling material specific heat [$J/(°C·kg)$]
- T_b is the borehole temperature [$°C$]
- t is the time [s]

and $\dot{Q}_{out}$ is determined considering only convection heat transfer:

$$\dot{Q}_{out} = h \cdot S \cdot (T_b - T_0)$$ **Eq. 2.38**

Where h is the convection heat transfer coefficient [$W/(m^2·K)$], S is the cylindrical lateral surface of the borehole [m^2] and T_0 is the initial/undisturbed ground temperature [$°C$].

Substituting **Eq. 2.37** and **Eq. 2.38** in **Eq. 2.36**, and separating the variables the following differential equation is obtained:

$$\frac{dT_b}{-\dot{Q}_{in} + h \cdot S \cdot (T_b - T_0)} = \frac{dt}{m_b \cdot c_g}$$ **Eq. 2.39**

Eq. 2.39 can be integrated from the initial time $t = 0$ to a generic time t:

$$\int_{T_b(0)}^{T_b(t)} \frac{dT_b}{h \cdot S \cdot (T_b - T_0) - \dot{Q}_{in}} = -\frac{t}{m_b \cdot c_g}$$

Evaluating the integral on the left-hand side and assuming as initial condition $T_b(t = 0) = T_0$ the following expression is obtained:

$$ln \left[\frac{h \cdot S \cdot (T_b(t) - T_0) - \dot{Q}_{in}}{h \cdot S \cdot (T_b(t = 0) - T_0) - \dot{Q}_{in}} \right] = -\frac{t}{m_b \cdot c_g} \cdot h \cdot S$$

Franco Lý

Interpretation of Borehole Heat Exchangers Thermal Response Tests under groundwater influence: analysis of three case studies

$$ln\left[\frac{h \cdot S \cdot (T_b(t) - T_0) - \dot{Q}_{in}}{-\dot{Q}_{in}}\right] = -\frac{t}{m_b \cdot c_g} \cdot h \cdot S$$

$$h \cdot S \cdot (T_b(t) - T_0) - \dot{Q}_{in} = -\dot{Q}_{in} \cdot e^{-\frac{t}{\frac{m_b \cdot c_g}{h \cdot S}}}$$

$$T_b(t) - T_0 = \frac{\dot{Q}_{in}}{h \cdot S} \cdot \left(1 - e^{-\frac{t}{\tau_t}}\right) \qquad \textbf{Eq. 2.40}$$

Eq. 2.40 may be used to compute the temperature reached by the borehole at some time *t*.
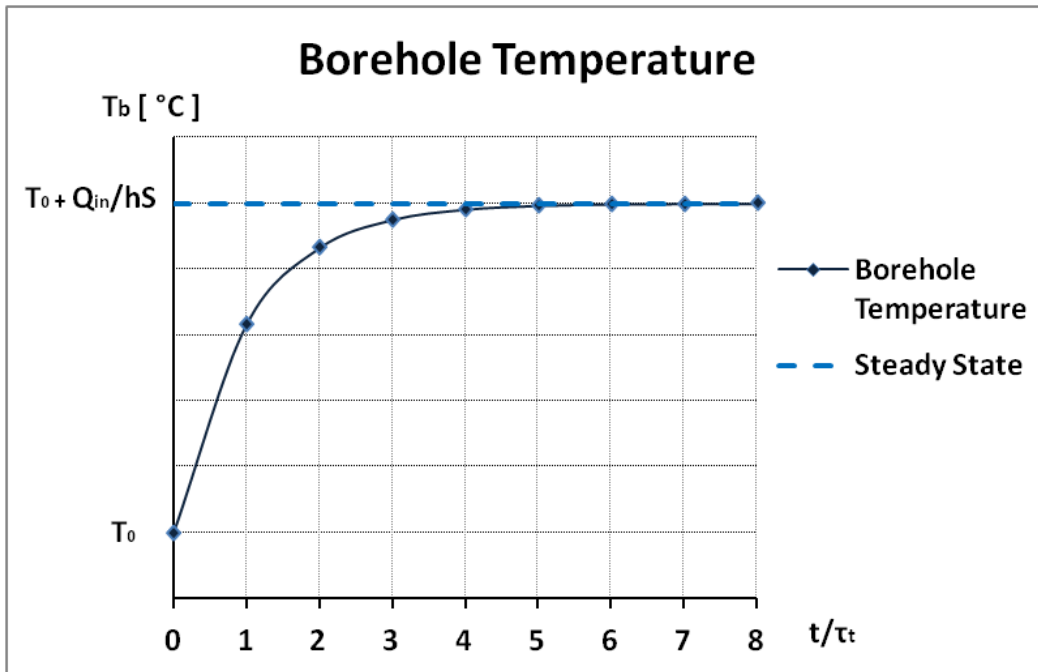
Figure 2-8 - Borehole temperature trend according to Eq. 2.40.

From the same equation τ_t is thermal time constant is interpreted as:

$$\tau_t = R_{cv} \, C_b = \left(\frac{1}{h \cdot S}\right)(m_b \cdot c_g) = \left(\frac{1}{h \cdot S}\right)(\rho_g \cdot V \cdot c_g) = \frac{\rho_g \cdot r_b \cdot c_g}{h \cdot 2} \qquad \textbf{Eq. 2.41}$$

where R_{cv} is the resistance to convection heat transfer and C_b is the lumped thermal capacitance of the borehole. Any increase in R_{cv} or C_b will cause the cylinder to respond more slowly to changes in its thermal environment. The final form of **Eq. 2.41** is obtained because the borehole mass can be expressed as $m_b = \rho_g \cdot V$ and the ratio *V/S* for cylinders (borehole) can be simplified to *r/2*.

Eventually, the characteristic time t_c is generally defined as:

$$t_c = (4 \div 5)\, \tau_t$$ **Eq. 2.42**

Assuming this range of values for the characteristic time, it is possible to guarantee the achievement of the steady state for less than *1,8 ÷ 0,7%* as it can also be noticed observing Figure 2-8.

The problem to obtain this characteristics time depends on the thermal time constant which main issue is to establish the convection heat transfer coefficient *h*, while all the other parameters are known or can be deducted.

It is then necessary to introduce the Nusselt number. This parameter is equal to the dimensionless temperature gradient at the surface, and it provides a measure of the convection heat transfer occurring at the surface.

$$Nu \equiv \frac{hL}{\lambda}$$ **Eq. 2.43**

From **Eq. 2.43** it follows that, for a prescribed geometry:

$$Nu = f(x^*, Re_L, Pr)$$ **Eq. 2.44**

The physical interpretation of the Nusselt number follows from its definition as a ratio of convection to pure conduction heat transfer. The Nusselt number is to thermal boundary layer what the friction coefficient is to the velocity boundary layer.

Eq. 2.44 implies that for a given geometry, the Nusselt number must be some universal function of *x**, *Re* and *Pr*. If these functions were known, they could be used to compute the value of *Nu* for different fluids and for different values of *v* and *L*. From knowledge of *Nu*, the local convection coefficient *h* may be found (Incropera, 2011). But since our interest is on the average heat transfer coefficient, its integration over the surface of the body, it turns to be independent to the spatial variable. Hence the functional dependence of the average Nusselt number is:

$$\overline{Nu} \equiv \frac{\overline{h}L}{\lambda} = f(Re_L, Pr)$$ **Eq. 2.45**

The choice to use the surface average coefficient is consistent, since it aims to find out the transfer rate for the entire surface, while a local coefficient is more suitable to determine the flux at a particular point on the surface. In order to establish *Nu* and deduce *h* from its functional dependence, the empirical approach is adopted. This consists in using empirical

correlation obtained from performing heat transfer measurement under controlled laboratory conditions and correlating the data in terms of appropriate dimensionless properties. Considering all the fluids, the data may be represented by an algebraic expression of the form:

$$\overline{Nu} = C \, Re_L^m \, Pr^n \qquad\qquad \textbf{Eq. 2.46}$$

In order to replicate the real conditions in Figure 2-7, the empirical correlation due to Hilpert (Incropera, 2011) is introduced:

$$\overline{Nu} \equiv \frac{\bar{h}L}{\lambda} = C \, Re_L^m \, Pr^{1/3} \qquad\qquad \textbf{Eq. 2.47}$$

which is widely used for *Pr ≥ 0,7* where the constant *C* and *m* are listed in Table 3.

Table 3 - Constants *C* and *m* of Eq. 2.47 for the circular cylinder in cross flow.

Reynolds interval		C	m
0,4	4	0,989	0,330
4	40	0,911	0,385
40	4000	0,683	0,466
4000	40000	0,193	0,618
40000	400000	0,027	0,805

The mentioned dimensionless parameters have physical interpretations that relate to the conditions in the flow, not only for boundary layers but also for other flow types. Consider the Reynolds number:

$$Re_L = \frac{\rho \cdot v \cdot L}{\mu} \qquad\qquad \textbf{Eq. 2.48}$$

where:

− ρ is the fluid density [kg/m^3]

− v is the velocity, here interpreted as the groundwater flow velocity [m/s)]

− $L = d$ characteristic dimension associated with the length scale corresponding to the maximum spatial temperature difference, for the BHE it coincides to the diameter [m]

− μ is the dynamic viscosity [$N \cdot s/m^2$]

Franco Lý

Interpretation of Borehole Heat Exchangers Thermal Response Tests
under groundwater influence: analysis of three case studies

It may be interpreted as the ratio of inertia to viscous forces in a region of characteristic dimension *L*. Inertia forces are associated with an increase in the momentum of a moving fluid.

Recalling that *Re* determines the existence of laminar or turbulent flow, for low *Re* values, viscous forces are sufficiently large to maintain laminar flow. But with increasing *Re*, viscous effect become progressively less important relative to inertia forces, and small disturbances may be amplified to a point where transition occurs (Incropera, 2011).

The Prandtl number is so defined:

$$Pr = \frac{v}{a}$$ **Eq. 2.49**

where:

- *v* is the kinematic viscosity [m^2/s], or also termed momentum diffusivity

- *a* is the thermal diffusivity [m^2/s]

The physical interpretation of the Prandtl number follows from its definition as a ratio of the momentum diffusivity to the thermal diffusivity. The Prandtl number provides a measure of the relative effectiveness of momentum and energy transport by diffusion in the velocity and the thermal boundary layers, respectively.

To resume the proposed time criterion consists in evaluating the characteristic time from the thermal time constant (**Eq. 2.41**) which depends on the convection heat transfer coefficient *h*. This parameter can be evaluated inverting average Nusselt number definition (**Eq. 2.45**). However, the average Nusselt number has a functional dependence to two dimensionless parameters (*Re* and *Pr*). For this reason an empirical correlation due to Hilpert (**Eq. 2.47**) is applied in order to estimate $\overline{Nu}$ before inverting its definition and obtain $\overline{h}$.

This method depends on a correct guess of Darcy velocity in which *Re* estimation is involved (**Eq. 2.48**). In particular an incorrect estimation of *v* of a single magnitude order can lead to wrong determination of $\overline{Nu}$ and consequently of $\overline{h}$. An initial time sensitivity analysis for the MLS analytical approach is repeatedly performed for each case study, increasing the initial time for TRT interpretation and can assist the choice of the first try Darcy velocity.

However, once the best set of valid parameters is obtained from the TRT analysis by MLS model, the goodness of the time criterion can be validated using the "obtained" Darcy

Franco Lý

Interpretation of Borehole Heat Exchangers Thermal Response Tests
under groundwater influence: analysis of three case studies

velocity. This process involves an iterativity, that can be solved along the parameters estimation for different initial time of evaluation. However, the validity of the time criterion has to be confirmed for different TRT cases and it will be demonstrated that remarkable efforts are necessary due to a large domain of possible groundwater flow (Darcy velocity can range in a large interval, from *1,0E-4* to *1,0E-13 m/s*). A good knowledge of the hydrogeology or accurate in-situ hydraulic tests can support the right choice of the groundwater flow velocity to estimate the characteristic time.

Table 4 - Characteristic time values (t$_c$ = 5τ$_t$) for typical borehole diameters.

Groundwater flow velocity [*m/s*]	Characteristic Time [*hours*]	
	L = 0,127 m	*L = 0,152 m*
1,0E-04	1,33	1,78
5,0E-05	1,74	2,33
3,0E-05	2,08	2,80
1,0E-05	2,98	4,03
8,0E-06	3,21	4,34
5,0E-06	3,75	5,07
4,0E-06	4,04	5,45
3,0E-06	/	6,00
2,0E-06	/	/

In Table 4 calculated characteristic times are provided for typical borehole diameter *d = L* in geothermal applications and for decreasing groundwater flow velocity values.

The characteristic time values are estimated considering thermophysical properties of saturated water (specific heat, dynamic viscosity, Prandtl Number and thermal conductivity) at a constant temperature of *285K* (*11,85°C*) from (Incropera, 2011).

From mixture b of Table 10 borehole filling material density and specific heat are deducted, resulting in *833 kg/m³* and *780 J/(kg·K)* respectively. This grout is a premixed employed for the filling of geothermal wells with a thermal conductivity of about *2 W/(m·K)*.

Relatively low values of groundwater flow velocity generate *Re$_L$* inferior to *0,4* using the expression in **Eq. 2.48**. This *Re$_L$* value is the lower limit in Table 3 which is necessary to determine constants *C* and *m* to be used in **Eq. 2.47** for the evaluation of the average Nusselt number. Without the pre-established constants, $\overline{Nu}$ and consequently $\overline{h}$ cannot be evaluated. Hence, velocities lower than *3,0E-6 m/s* start to be critical for the determination of the characteristic time value for typical borehole diameters.

Franco Lý

Interpretation of Borehole Heat Exchangers Thermal Response Tests under groundwater influence: analysis of three case studies

3 Thermal Response Test analysis: Claviere case study

The first analyzed case study in this thesis is the Thermal Response Test of a pilot borehole heat exchanger located in Claviere, which raw data were managed and kindly supplied by PhD geothermal consultant Andrea Zille.

3.1 Geographical Background

The project site is located in Claviere district (TO) in Italy, in via Nazionale. This municipality is located about 94 kilometers west of Torino, in an area called Alta Val di Susa, on the border with France. Claviere has an elevation of *1760 m* above sea level and its residential area rises on the eastern edge of the wide plateau of Colle del Monginevro, along the country borderline. At north the locality is dominated by the massif of Chaberton (*3130 m*).
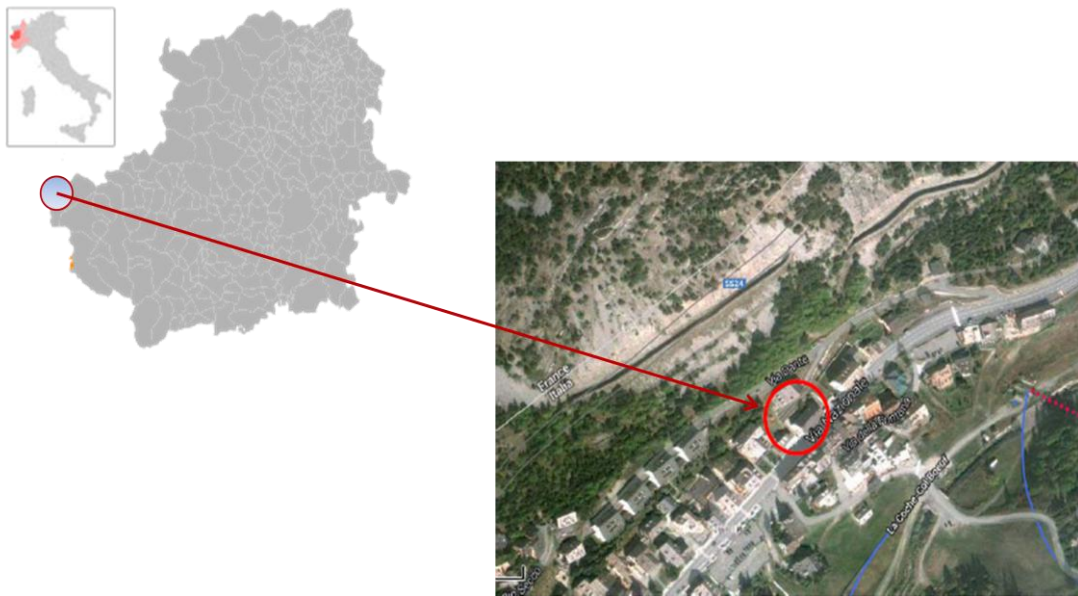
Figure 3-1 - Project site: geographical location.

Franco Lý

Interpretation of Borehole Heat Exchangers Thermal Response Tests
under groundwater influence: analysis of three case studies

3.2 Hydro-Geological Background

From a geological point of view, the area results to be very varied, as it is well underlined by the extract of the National Geological Map in Figure 3-2.
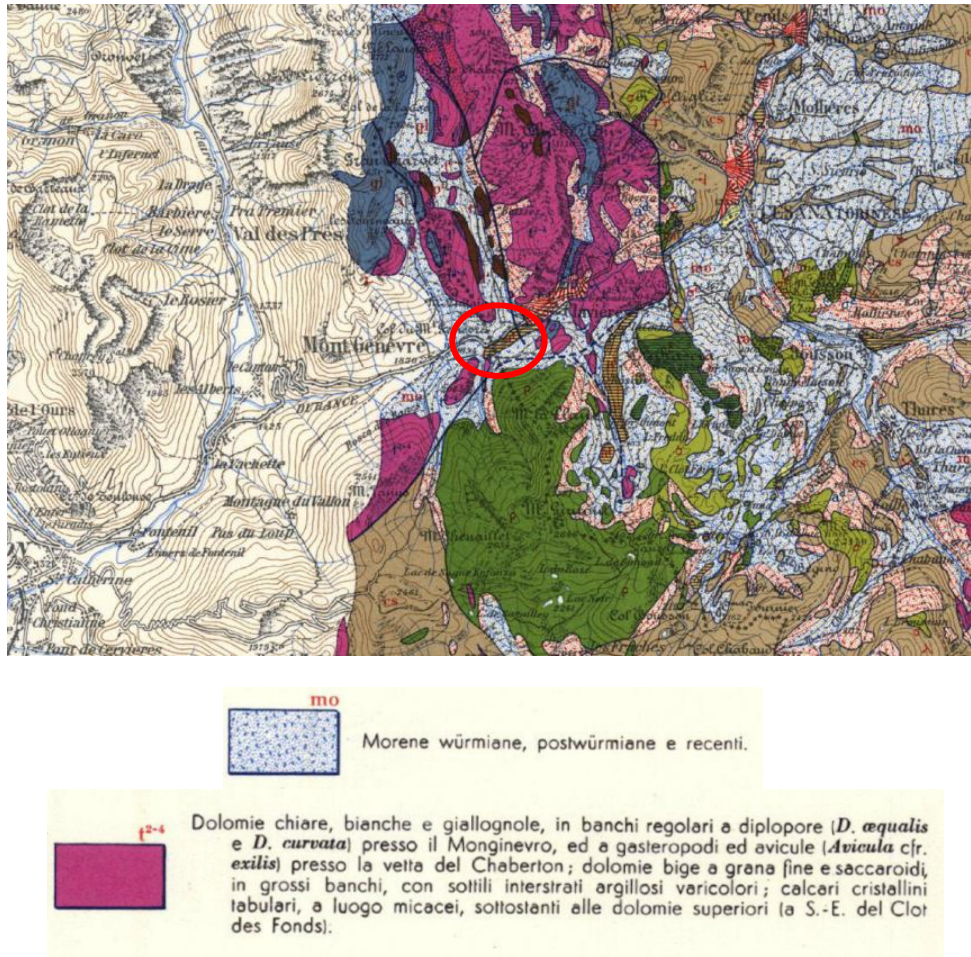
Figure 3-2 - Extract from the National Geological Map (Italy).

By means of situ drillings, it was mainly spotted the presence of pale white-yellow dolostones with fine granulometry and saccharoids present in large banks with shallow clayish interpositions, laying on a level of compact crystalline limestone located at the final 20 meters of the borehole which is *170m* deep. The presence of gypsum in the area has to be source of particular attention for the risk of swelling that this kind of geological material can originate when in contact with water. In addition, the perforations have identified three levels of aquifer, respectively at *2m*, *22m* and *150m* of depth from ground level. No precise permeability and aquifers direction data are available, but by means of the general surveys performed during the drilling operations, aquifer flow is deducible to be relevant.

Franco Lý

*Interpretation of Borehole Heat Exchangers Thermal Response Tests
under groundwater influence: analysis of three case studies*

3.3 Thermal Response Test

The initial purpose of the test is to estimate the mean subsurface thermal conductivity λ_{eff} and the thermal resistance R_b of the pilot borehole heat exchanger. This approach corresponds to the standard TRT analysis which has the limit to assume a pure conductive heat transport (Infinite Line Source solution) as described in section 2.5. However, for this dataset, another analysis is additionally carried out, based on Moving Line Source theory described in section 2.6. This latter technique permits to execute a parameter estimation involving both conduction and advection phenomena.

3.3.1 Test Equipment

The test is carried out in situ with mobile equipment *GEOgert 2.0*, ad hoc designed to try out geothermal heat exchange (pressure test, flow test, undisturbed ground temperature measurement and geothermal response test).

Figure 3-3 - *GEOgert 2.0*, module 1.

The equipment is constituted by two modules. The measurement module (Figure 3-3) includes:
- a hydraulic loop composed by a circulating pump and a series of regulating, interception and safety valves;
- a measurement system made up of two temperature probes *PT100* for the circulating fluid, a temperature probe for the external air, an electromagnetic flow-meter and a piezo-resistive pressure transducer;

Franco Lý

Interpretation of Borehole Heat Exchangers Thermal Response Tests
under groundwater influence: analysis of three case studies

– a system for data acquisition and data storage.

The second module is specific for the performance of the TRT and consists of :

– a hot water heater provided with three electric resistances (two of *3,5 kW* and one of *1 kW*);

– a hydraulic loop composed of a circulating pump, an expansion vessel and a series of safety valves.

In order to evaluate the thermal properties of the system, it is necessary that the fluid properties, the geometrical and thermal characteristics of the pipes, the stratigraphy of the ground as well as the undisturbed soil temperature are well-known.

Furthermore, it is necessary to wait until the injecting grout in the borehole reaches its maturity, minimizing the risk of having alterations in the TRT due to the development of the thermal energy. From a technical point of view, *GEOgert 2.0* mobile equipment is elaborated to perform TRTs based on principles scheme developed at Luleå University of Technology in Figure 3-4.
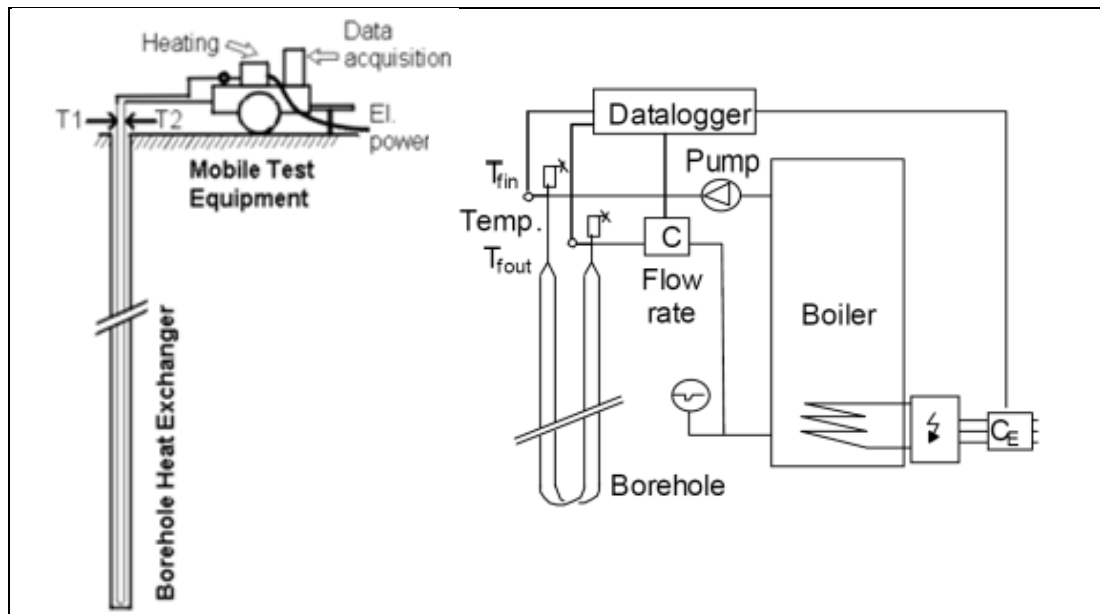
Figure 3-4 - **Mobile test equipment and scheme for the execution of a TRT.**

This system supplies a constant known thermal power generated by the electrical resistances to the flow rate; meanwhile it records inlet and outlet temperatures time series from the borehole heat exchanger. Differently from Figure 3-4, the mobile test equipment is provided with 3 resistances which allow to module the electrical power of the boiler, in order to best suit BHEs of different lengths.

Franco Lý

*Interpretation of Borehole Heat Exchangers Thermal Response Tests
under groundwater influence: analysis of three case studies*

In Table 5 the main characteristics of the equipment are summarized, while in the next Tables 6, 7 and 8 the main specification of the flow-meter, temperature probe and pressure transducer are reported.

Table 5 - Minimal datasheet of the equipment, GEOgert 2.0.

- vertical closed pipe loop type	single or double U, suitable to concentric type
- nominal diameters (external)	DN25, DN32, DN40 and DN50 mm
- material	HDPE PN16, HDPE PN10, HDPE-RC PN16
- pipe loop producer	indifferent
- borehole length	20 to 500 m (standard)
- max pressure for leakage test	16 bar
- max discharge for TRT	2300 l/h
- max electrical power TRT modulus	8 kW
- A/D converter	24 bit
- sampling frequency	2 seconds upwards
- thermal exchange measure precision	1-3% depending on BHEs configurations
- modules communication system	wireless
- electrical link : module 1	plug CEI 230 V 16A (industrial blue single phase)
- electrical link : module 2	plug CEI 400 V 16A (industrial red small 3P+N+E)

Table 6 - Electromagnetic flow-meter characteristics.

General description	Electromagnetic flow-meter
Environment temperature range	-40…+60°C
Storage temperature range	50…+70°C
Maximum operational pressure	16 bar
Maximum measurement error	±0,2% from measured value + 1mm/s

Table 7 - Temperature probe characteristics.

General description	High precision temperature probe
Sensor type	RTD PT100 cl. 1/3 DIN
Temperature range	- 55/+110°C
Lead time (agitated fluid)	≤ 10 sec.
Insulation resistance	≥ 20MΩ
Resolution	< 0,01 °C

Table 8 - Pressure transmitter characteristics.

Full scale value (FSV)	25 bar, relative
Over Pressure	90 bar, relative
Precision (%FSV)	≤0,25
Calibration	On limit point according to DIN 16086
Repeatability	≤ 0,15% FSV
Thermal drift	≤0,03% FSV/°C
Annual drift	≤ 0,2% FSV
Operating fluid temperature	25 …+85 °C
Environment temperature	25 …+85 °C
Storage temperature	25 …+85 °C
Lead time (10…90%)	< 3 ms

	Compensated temperature range	0…+80°C
	Measurement sensor	Piezo-resisitive
	Filling fluid	Silicone oil

3.3.2 Borehole Heat Exchanger Description

The test geothermal exchanger consists of a drilled borehole *170 m* deep with a diameter of *152 mm* filled with specific filling material for geothermal applications. It is made up of a double U-pipe with external pipe diameter of *40 mm* and internal of *32,6 mm*. The pipe material is high-density polyethylene (HDPE Pe100 RC PN20 De40).
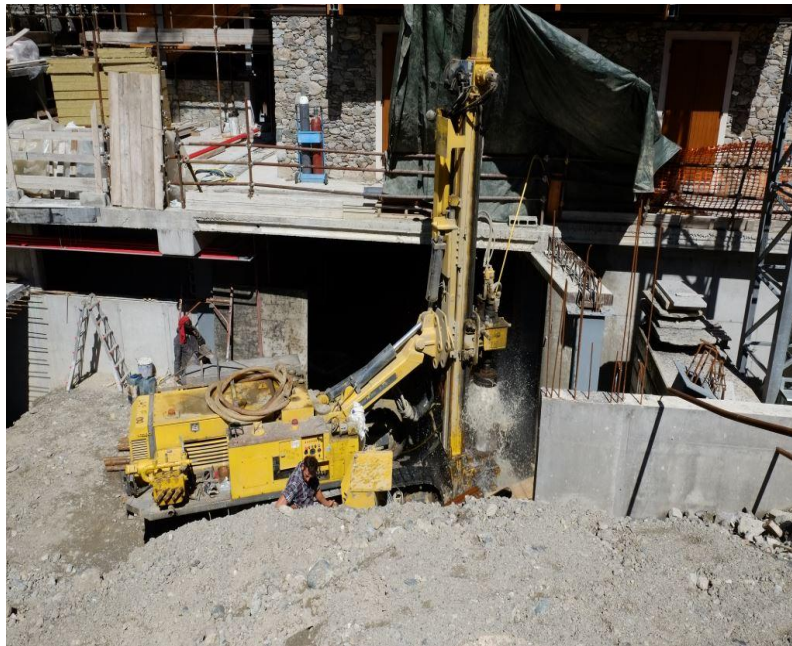
Figure 3-5 - Perforation of the pilot borehole heat exchanger.

The material adopted to seal the borehole is called Termoplast PLUS® which is a premixed specially designed for the filling of geothermal wells. According to the (VDI4640/part2), Termoplast PLUS® is a special blend of blast furnace cement binders, bentonite with high plastic value and selected sands that can guarantee the efficiency of the full GSHP system (Table 9). The grout thermal conductivity depends on the ratio powder/water as reported in Table 10. In Claviere case the expected grout conductivity is *2,0 W/(m·K)*.

Franco Lý

Interpretation of Borehole Heat Exchangers Thermal Response Tests under groundwater influence: analysis of three case studies

The grout hardening process started on *29/08/2014,* about two weeks before the Thermal Response Test in order to have a sufficient period for the mortar to reach its maturity, spreading the heat that the process has generated before starting the TRT.

Table 9 - Characteristics of the components for Termoplast Plus.

Binding component:	the exclusive cementitious binding components used allow for excellent workability in the first four hours, a high sulphate resistance (DIN 1164/ sec. 10) and finally a strong resistance to freezing without the use of additives, until -15 ° C (*VDI 4640*).
Bentonite:	the high performance bentonites specially selected for use in geothermal wells allow the achievement of the required performance with a limited quantity, still maintaining the necessary characteristics of swelling, as required by many of the requirements of local legislation in Germany.
Selected sands:	with high fineness (<0,25 mm) and high thermal conductivity allow a good fluidity during pumping operations of the cement mixture.

Table 10 - Example of mixture formulations.

A	Thermal Conductivity λ 2,3 W/m·K* Composition of mixture Soft water 780 l - Termoplast PLUS 875 Kg Ratio powder / water per m^3 1,1 Number of bags per m^3 of mud 35 ca Mixture that can be produced with a 25 kg bag 28-30 l
B	Thermal Conductivity λ 2,0 W/m·K* Composition of mixture Soft water 705 l - Termoplast PLUS 705 Kg Ratio powder / water per m^3 1,0 Number of bags per m^3 of mud 28 ca Mixture that can be produced with a 25 kg bag 34-36 l
C	Thermal Conductivity λ 1,6 W/m·K* Composition of mixture Soft water 720 l - Termoplast PLUS 585 Kg Ratio powder / water per m^3 0,8 Number of bags per m^3 of mud 23 ca Mixture that can be produced with a 25 kg bag 42-44 l

(*) determination method UNI EN 12664

3.3.3 Flow Test

The flow test is performed independently on the two vertical closed loops of the BHE. The measure of the pressure drop was repeated for three different flow rate values for loop 1 and four discharge values for loop 2. Based on the different point "discharge/pressure leakage", the characteristic curves of the two hydraulic loops have been respectively traced in Figure 3-6 and Figure 3-7.
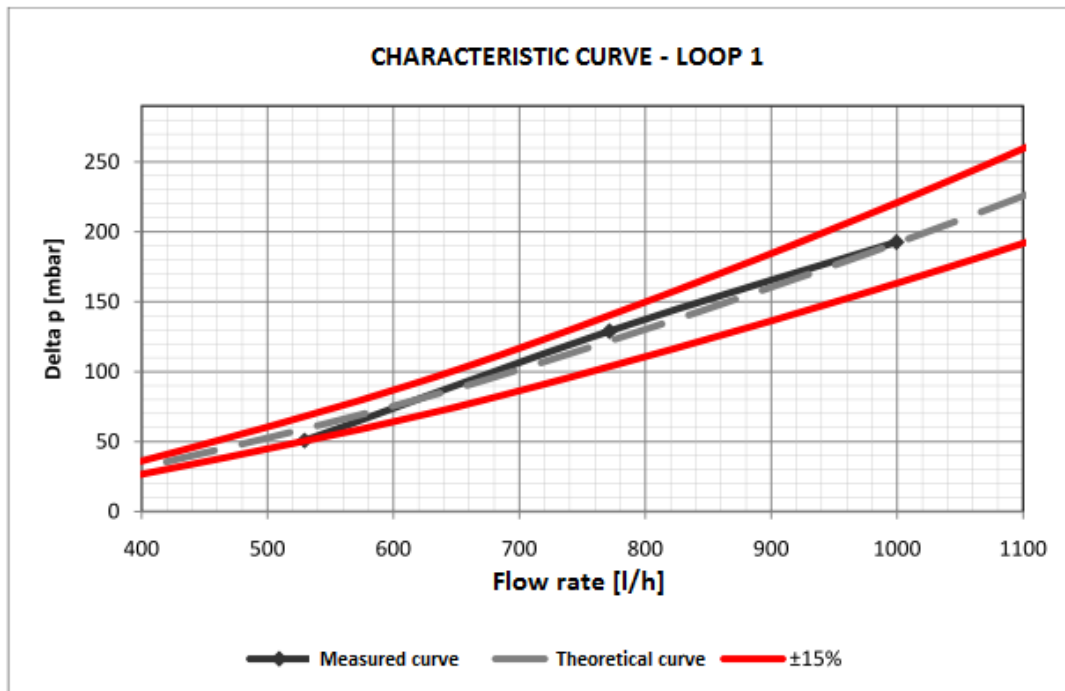
Figure 3-6 - Characteristic curve for loop 1

Concerning loop 1, the points corresponding to the measured couples of values lie inside the acceptance interval according to the Swiss legislation (SIA384/6, 2010) and are located very closely to the theoretical curve of a BHE having the same characteristics.

The same cannot be stated for loop 2, since all the measures exhibit a pressure drop slightly higher than acceptable values from the legislation. In any case the differences between measured value and theoretical value do not indicate a particularly critical situation of the BHE: it can be ruled out significant crushing or clogging and no doubts are concerned about the realization quality. The phenomenon is very likely to be connected to a soft out of round wear of the pipes due to the winding in reel. The difference of behavior between loop 1 and 2 does not involve any critical conditions suggesting a correction intervention.
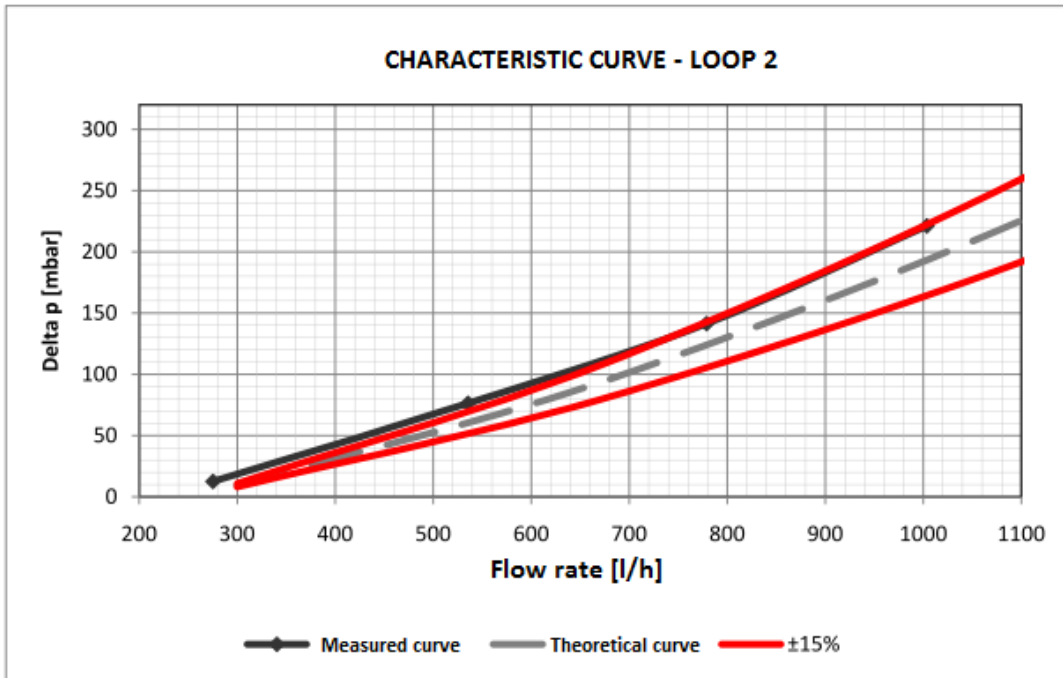
Figure 3-7 - Characteristic curve for loop 2

Franco Lý

*Interpretation of Borehole Heat Exchangers Thermal Response Tests
under groundwater influence: analysis of three case studies*

3.3.4 Test Operating Conditions

The thermal response test is carried out with constant thermal injection, starting at 11:30 on *15/09/2014* and lasting until *18/09/2014* for *62h 27min.*

The supplied power set on machinery is *7,5 kW* by means of the three electrical resistances. Its corresponding specific power, i.e. averaged along the length of the borehole, turns out to be *44,2 W/m*. Nevertheless, the effective electrical and thermal power result to be lower than this value due to mechanical and thermal dissipation that the heat carrier fluid, propylene glycol in this case, generates along its path within the closed pipe loops. This fluid consists in a transparent, slightly sweet and odorless liquid, miscible with water in any proportion. The raw formula of the propylene glycol is $C_3H_8O_2$, but since it is a chiral molecule, it can naturally exist in two different isotopes equally stable and represented in equal parts in industrial products (racemic mixture) (Delmastro, 2011). The molecular mass is equal to *76,09 g/mol* .

The flow rate is constantly measured by the electromagnetic flow-meter with a sampling time set to *1 min*, resulting to an average of *1542 l/h* with a standard deviation of *3,6 l/h* equal to *0,24%* . Referring to this value of flow rate, the relative time necessary to the liquid mass to complete a loop is computed as:

$$t_{loop} = \frac{2L}{(Q/\pi r_i^2)}$$

Eq. 3.1

where:

- *L* is the borehole heat exchanger length, *170 m*;

- *Q* is the fluid mass flow rate occurring in the vertical closed pipe loops [*m³/s*];

- *r_i* is the internal radius for a HDPE Pe100 RC PN20 De40 pipe [*m*] .

This approach does not consider a short extent of pipes external to the BHE connected to the mobile equipment (about *2 m*). However, compared to *170 m*, this segment does not significantly affects the estimation, that considers a perfect installation of the pipes underground without any damaging/drifts. The evaluated time for the fluid to fulfill a complete loop is about *663s*, i.e. *11 minutes*. This information will be useful to reduce the computational efforts for the following MLS analysis, since the sampling frequency can be inferior to this value in order to have a good description of mean fluid temperature according to (UNI11466, 2012). Then, guaranteeing an adequate precision, it can be chosen a higher sampling time than *1 minute* adopted by the data acquisition system, involving a significant improvement in diminishing the computational time for parameters estimation.

Franco Lý

Interpretation of Borehole Heat Exchangers Thermal Response Tests
under groundwater influence: analysis of three case studies

3.3.5   Undisturbed Ground Temperature

At first, a thermal log profile is performed by circulating water at known flow rate with a sampling time measurement at the outlet pipe of about *2 s*. Thus, for a certain time, the relative depth is calculated. The procedure is applied to both the loops of the BHE as shown in Figure 3-8, in order to investigate on temperature gradient along the vertical.
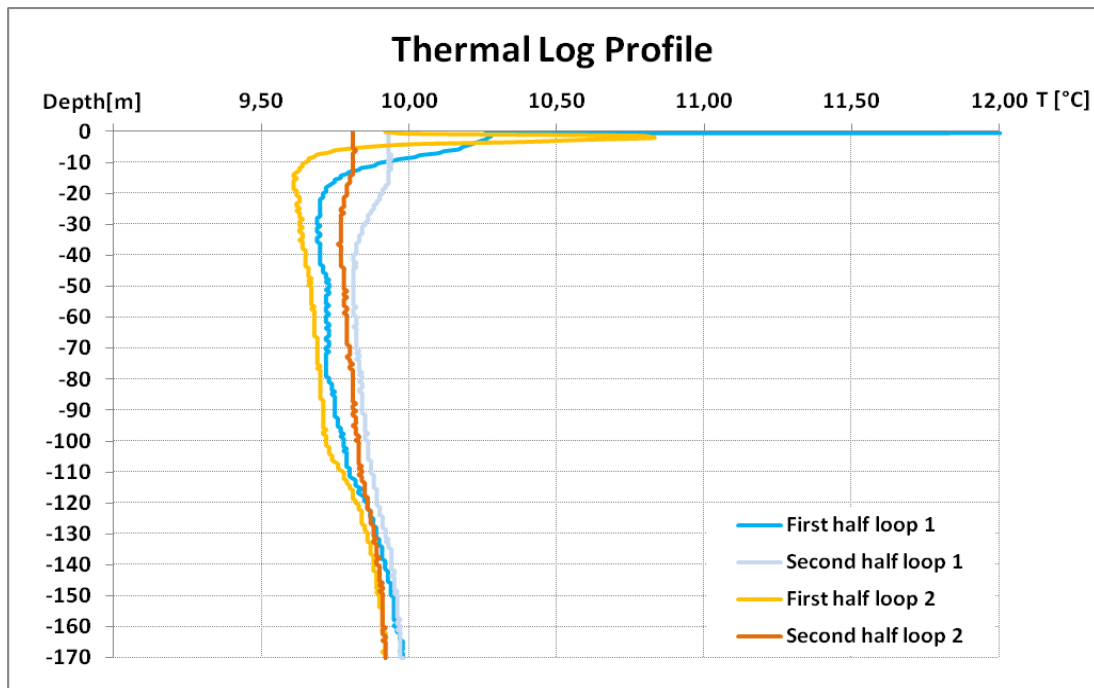
Figure 3-8 - Thermal log profile along the pilot borehole heat exchanger.

Then, the evaluation of the undisturbed ground temperature is carried out by circulating the heat carrier fluid inside the closed pipe loops without activating none of the three electrical resistances and illustrated in Figure 3-9.

The fluid can reach the thermal equilibrium with the surrounding environment and, thus about the same temperature of the ground. At this measurement, it is coupled the thermal log profile along the BHE and from their interpretations the undisturbed ground temperature value is estimated.

From the analysis of the results, it is considered *9,79 °C* to best represent the thermal level of the ground in undisturbed conditions T_0. This value has to be interpreted as the mean value averaged along the total drilled length and it will be assumed as undisturbed soil temperature for the following TRT analysis.
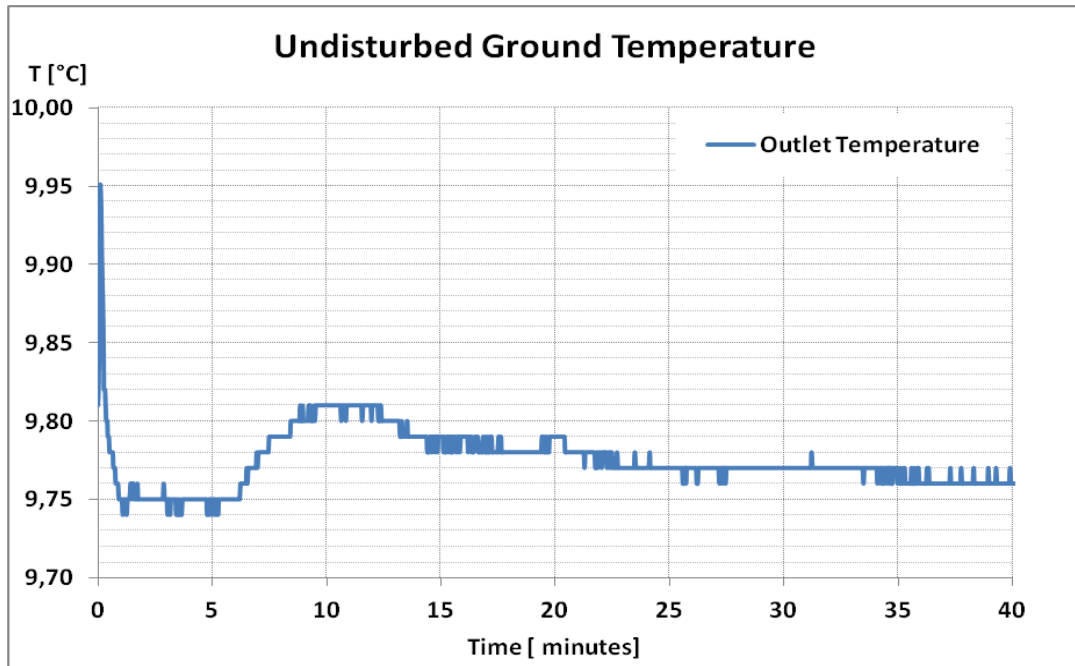
Figure 3-9 - Test to evaluate the undisturbed ground temperature.

3.3.6 Measurements

The first module of *GEOgert 2.0* mobile equipment is set to collect inlet and outlet fluid temperatures every minutes for the total duration of the TRT. In Figure 3-10 the plot of the measured inlet and outlet fluid temperature time series is reported.
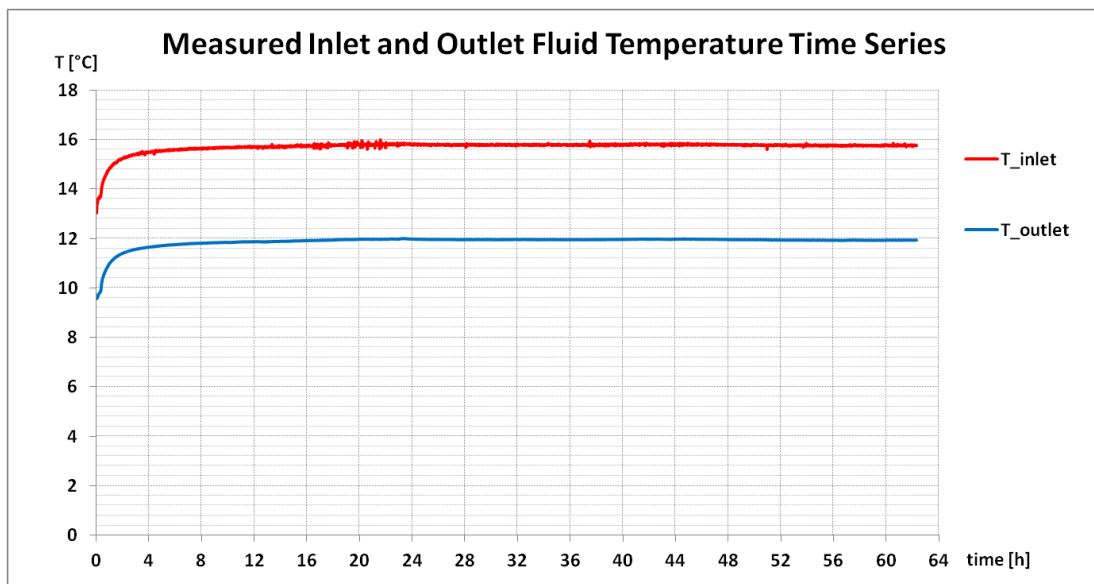
Figure 3-10 - Measured inlet and outlet fluid temperature time series.

The increasing trend of the two temperature time series is regular in the first part of the test. After about *20 hours* of test, the thermal steady state is reached; this behavior is characteristic for elevated heat dissipation system, which may be caused by convective movements due to groundwater flow.

The electromagnetic flow-meter has recorded the flow-rate in the vertical closed pipe loops, exhibiting a constant trend after an initial adjustment as shown in Figure 3-11. The mean volumetric flow rate results to be of *1542 l/h* with a standard deviation of *3,6 l/h* equal to *0,24%* of the mean value.
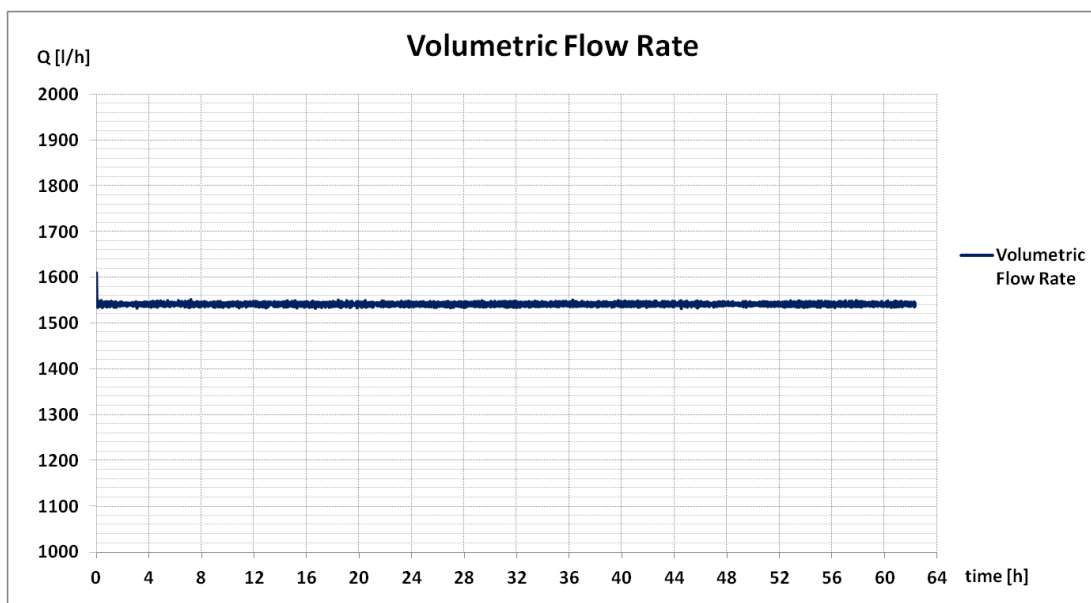
Figure 3-11 - Volumetric flow rate inside the vertical pipe loops.

The heat carrier fluid flow rate is sufficient to comply the recommendations given in (UNI11466, 2012), since it guarantees a temperature differences between inlet and outlet temperature comprised between *3K* and *7K* (in this case slightly lower than *4K*).

Concerning to the effective electrical (three phases) and thermal power, they are obtained at every minutes according to the following equations:

Effective electrical power $\qquad Q_{el} = \Sigma\ (V \cdot I \cdot cos\ \varphi)$ **Eq. 3.2**

where:

- *V* is the electrical potential measured for the three phases R, S and T every minute [*Volt*];

- *I* is the current intensity measured for the three phases R, S and T every minute [*Ampere*];

- *φ* is the offset angle measured for the three phases R, S and T every minute [°]

Effective thermal power $$Q_{th} = c_f \cdot Q \cdot \Delta T$$ **Eq. 3.3**

where:

- c_f is the fluid specific heat, for the propylene glycol *3930* [*kJ/(°C l)*];

- Q is the flow rate occurring in the vertical closed pipe loops [*l/min*];

- ΔT is the temperature difference between inlet and outlet pipes at every minute [*°C*]
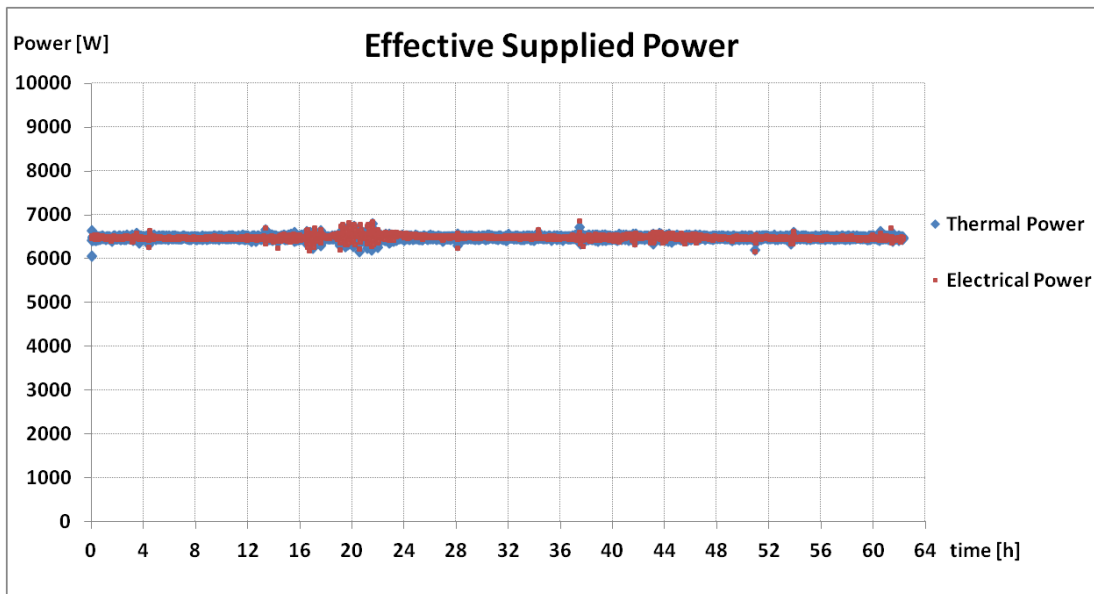
Figure 3-12 - Effective electrical and thermal power.

The effective mean thermal power averaged on the total duration results to be equal to *6478,8 W* with a standard deviation of *35,3 W* equal to *0,54%*; more precise than the effective electrical power with a mean of *6480,5 W* with a standard deviation of *43,5 W* equal to *0,67%*. According to (UNI11466, 2012) both standard deviations are lower than *±1,5%* of the mean value and thus both measurement are suitable for TRT analysis.

Considering the total length of the borehole, the resulting specific thermal and electrical power are calculated by means of the following equations:

Effective specific thermal power $$q_{th} = Q_{th}/L$$ **Eq. 3.4**

Effective specific electrical power $$q_{el} = Q_{el}/L$$ **Eq. 3.5**

From the calculations, they result to be respectively *38,11 W/m* and *38,15 W/m*.

3.4 TRT Analysis by means of Infinite Line Source Theory

In order to obtain the thermal properties of the system, the common approach adopted by geothermal designers to interpret TRT data is the Infinite Line Source model. As previously mentioned in section 2.5, this model assumes a pure conductive thermal exchange in the subsurface, considering negligible the convection contribute of the aquifers to the heat transport processes; in addition it does not account possible thermal exchange along the BHE vertical axis due to finite vertical dimension of the BHE.

First of all, to carry on a standard ILS approach, the mean fluid temperature time series is obtained from the arithmetic mean of two temperature time series.

$$T_{fm} = \frac{T_{in} - T_{out}}{2}$$

Eq. 3.6

It is compared with the inlet and outlet fluid temperature time series in Figure 3-13.
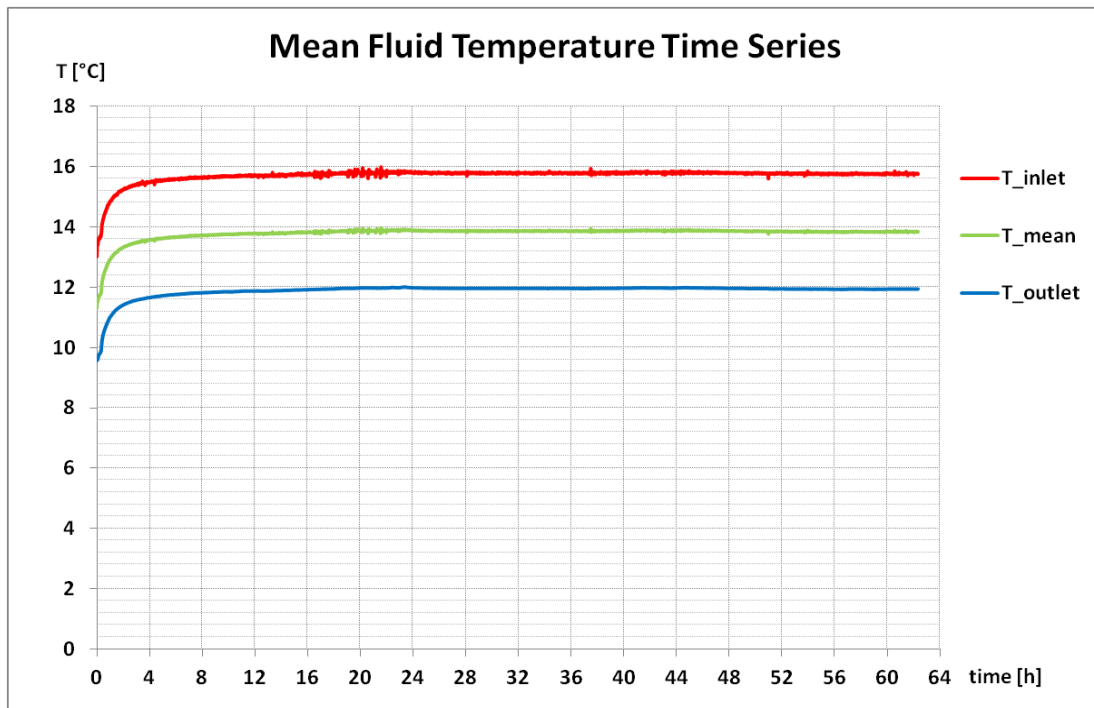
Figure 3-13 - Mean fluid temperature time series.

As previously presented in section 2.5, according to the LS approach, the heat carrier mean fluid temperature changes in time according to the following relation:

$$T_{fm} \approx \frac{q}{4\pi\lambda_{eff}} ln(t) + q\left[R_b + \frac{1}{4\pi\lambda_{eff}}\left(ln\left(\frac{4a}{r_{bw}^2}\right) - \gamma\right)\right] + T_0$$

Eq. 3.7

Franco Lý

*Interpretation of Borehole Heat Exchangers Thermal Response Tests
under groundwater influence: analysis of three case studies*

According to section 2.5 the criterion for the logarithmic approximation has to be fulfilled:

$$t \geq t_c \geq \frac{5r_{bw}^2}{a}$$

Eq. 3.8

A initial thermal diffusivity *a* is estimated to start the analysis; this is feasible since it consists in an iterative process, because the same *a* depends on the effective ground thermal conductivity λ_{eff} that has to be obtained by linear interpolation.

$$a = \frac{\lambda_{eff}}{C}$$

Eq. 3.9

where *C* is the volumetric thermal capacity deductible from geological maps and here estimated equal to *2,3 MJ/(m³·K)*. While for the thermal conductivity it is individuated a value equal to *2,7 W/(m·K)* corresponding to the mean value for dolostones according to (UNI11466, 2012). Thus, a value of thermal diffusivity *a* is derived of *1,17E-6 m²/s*.

Adopting this initial value for the diffusivity, the time criterion is fulfilled for times larger of *6,83 hours*. The first *7 hours* are disregarded to evaluate the thermal conductivity by linear interpolation of mean fluid temperature time series with x-axis the logarithm of time. Thus, t_{in} = *7 hours* is adopted as initial time for TRT interpretation by means of Line Source model.

3.4.1 Estimate of the Effective Ground Thermal Conductivity

Then, the thermal conductivity is indirectly estimated by the slope *A* of the interpolating straight line for the measurement in a plot where x-axis corresponds to the logarithm of time:

$$\lambda_{eff} = \frac{q}{4 \cdot \pi \cdot A}$$

Eq. 3.10

The conductivity estimation is carried on varying t_{end} from *30 hours* to *62 hours* i.e. the total duration of the test with *4 hours* step, the results are illustrated in Figure 3-15.
This method permits to understand the sensitivity of the thermal conductivity to the final time of the TRT, that is considering a time window which ends at a certain time before the real end of the test. An example of linear interpolation is illustrated for t_{end} = *62 hours* (complete test duration) in Figure 3-14.
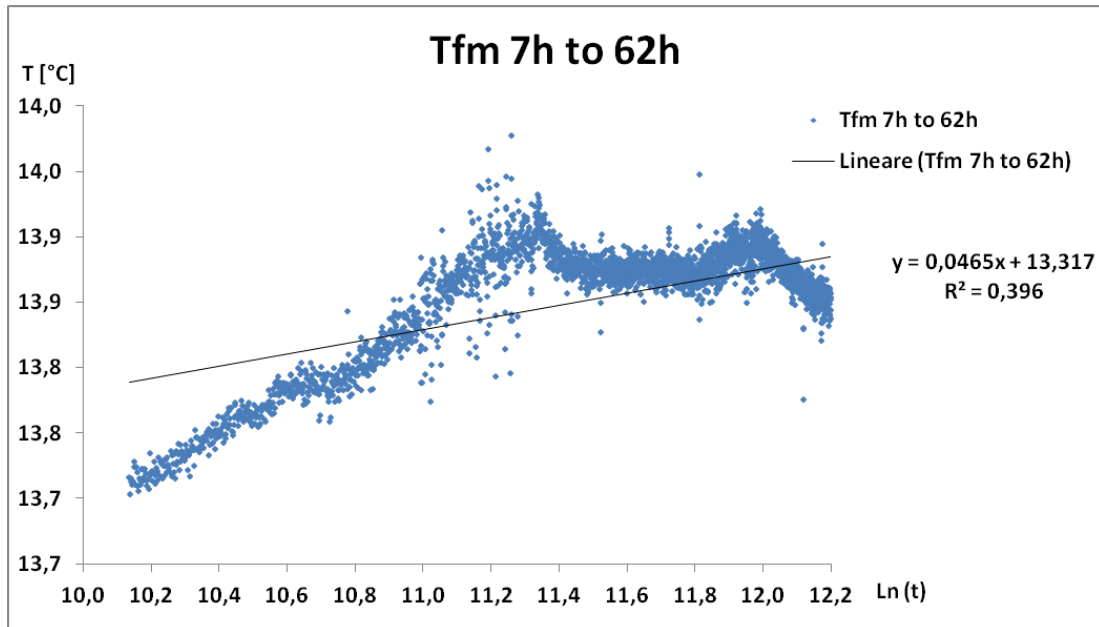
Figure 3-14 - Linear interpolation for data interval from 7h to 62h.

The theoretical model of test interpretation expects that temperature time series represented in a plot with *ln*(*t*) in the x-axis to be almost rectilinear. In this case, the trend does not match the time series. In addition, the drop of angular coefficient in time means that the reference model for this analysis, purely conductive, is not suitable.
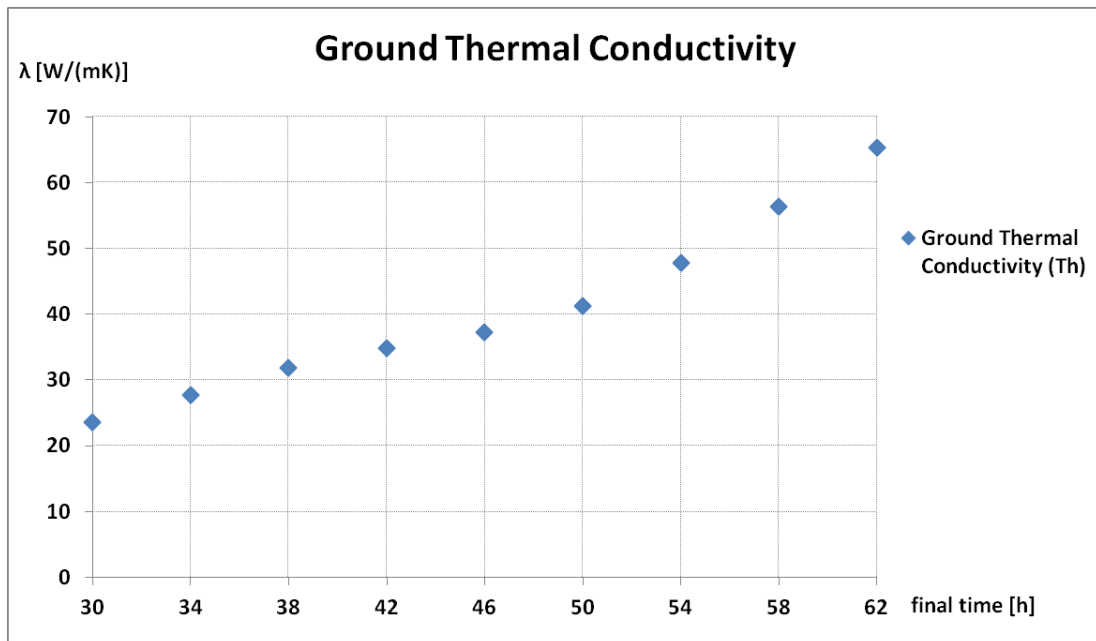
Figure 3-15 - Ground thermal conductivity trend for increasing t_{end}.

The estimation is performed just considering thermal specific power, since in relation to electrical specific power there are no significant differences, as deducted in section 3.3.6. The ground thermal conductivity λ_{eff} quickly increases for large t_{end} without any sign of a possible convergence to stable value as outlined in Figure 3-15. These characteristics may indicate the presence of an advection-dominated system as suggested by some authors e.g. (Witte H. , 2001). The conductivity values series estimated by ILS approach exhibits an increasing trend, not corresponding to a pure conductive heat exchange system. The values are in any way much larger than *2,7 W/(m·K)*, the mean expected value for the ground thermal conductivity in situ. Further considerations are discussed in section 3.4.3.

3.4.2   Estimate of the Borehole Thermal Resistance

The borehole thermal resistance is evaluated in a similar approach, increasing the final time t_{end} from *30 h* to *62 h* with a step *Δt* of *4h* and keeping fixed t_{in} = *7 hours*:

$$R_b = \frac{B - T_0}{q} - \frac{1}{4\pi\lambda_{eff}}\left[ln\left(\frac{4a}{r^2}\right) - \gamma\right]$$

Eq. 3.11

Figure 3-16 illustrates the borehole thermal resistance values for thermal specific power. The estimated values for large t_{end} approach to *0,106 m·K/W*. The plot shows a slight increase of the borehole resistance values. It is likely that a longer TRT would have supported a more precise parameter evaluation. Nonetheless, the results are satisfying and considered valid to describe R_b, differently from thermal conductivity values trend.
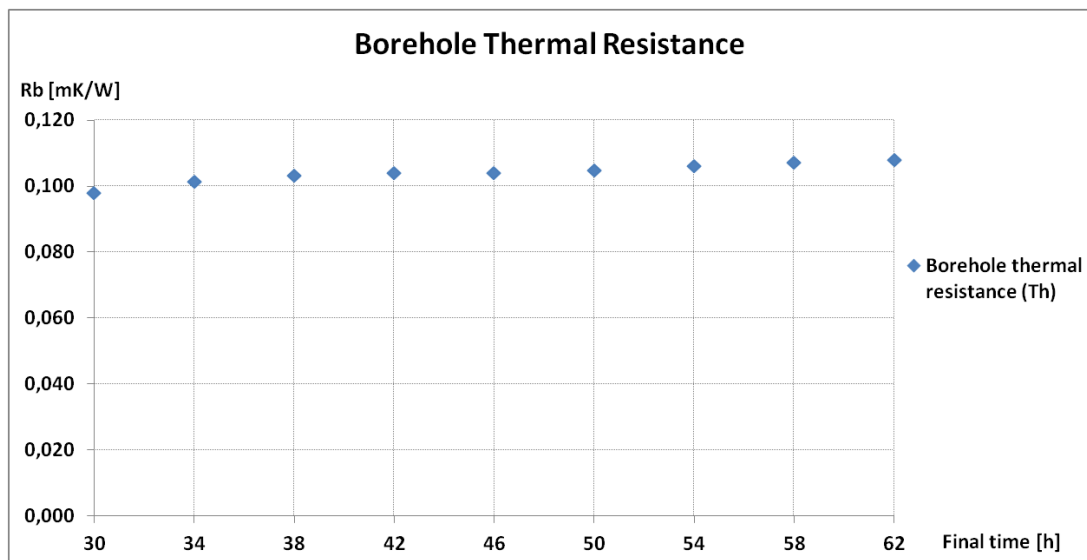
Figure 3-16 - Borehole thermal resistance values for increasing t_{end}.

Franco Lý

Interpretation of Borehole Heat Exchangers Thermal Response Tests
under groundwater influence: analysis of three case studies

3.4.3 Results Discussion

As a purely conductive transport model is assumed, (UNI11466, 2012) recommends that, if the T_{fm} trend, function of $ln(t)$ is not linear, then a significant thermal interaction with groundwater flow or external environmental disturbances can be present, as demonstrated by several studies (Witte H. a., 2006) and (Bandos, 2011) respectively. In these cases, ILS model cannot be applied. This non-linear behavior is evident in Figure 3-14, where the coefficient of determination R^2 returned a very low value, that is *0,396* indicating how data improperly fit the linear interpolation.

Assuming an appropriate insulation from external disturbances and considering this specific geological site, where three aquifer levels are identified, an important groundwater flow influence is very likely. In aquifers, advective heat transfer due to groundwater flow can be significant e.g. (Witte H. , 2001)**.** Accordingly the effective thermal conductivity obtained based on ILS solution is an apparent parameter, known to increase with Darcy velocity.

The influence of groundwater flow is examined by several theoretical studies. For instance, (Chiasson, 2000) numerically simulated TRTs to analyze the role of groundwater flow velocity and different evaluation periods with respect to the value of that λ_{eff} would be obtained by the Line Source approach. They demonstrated that the resulting thermal conductivity value is an effective one that does not represent the thermal conductivity of the subsurface. (Signorelli, 2007) comprehensively analyzed those effects and confirmed the findings of (Witte H. , 2001) that λ_{eff} increase continuously with evaluation time.

Therefore, the effective ground thermal conductivity values trend for increasing evaluation time in Figure 3-15, coupled with a short time to achieve the thermal steady state in Figure 3-10 suggests a remarkable groundwater flow influence as confirmed by Witte's studies. While the borehole thermal resistance value can be feasibly in agreement with the borehole typology of double U-pipe. Nevertheless, it is comprehensible that the result of the LS analysis cannot be used for representing the correct estimation of ground thermal conductivity and besides, it cannot manage to describe the groundwater flow characteristics that strongly affect this advection-dominated system.

3.5 Coupled Conductive - Advective Analysis by means of Moving Line Source Theory

The results obtained from the standard TRT interpretation suggest a strong ground water flow influence, which cannot be accounted for the standard method of analysis. Therefore, the MLS theory of section 2.6 is applied to the experimental data in order to determine adequate parameters for the simultaneous heat transport by advection and conduction.

As previously commented in section 2.6.1, the script in MATLAB used for a 3 parameters estimation, neglects the effect of thermal longitudinal and transversal dispersivity. This approximation is necessary in order to simplify the complex governing equations and reduce the computational efforts of the runs.

3.5.1 MLS Analysis Settings

The script is ad hoc implemented to embed specific geological site features and borehole geometrical characteristics in order to reproduce conductive and advective heat exchange processes (appendix 7.1). In particular, mean subsurface density, undisturbed ground temperature and borehole radius of the tested BHE are essential information to represent the physical model.

The script is run in order to estimate 3 parameters, minimizing the *RMSE* between measured and simulated temperature time series:

- Ground thermal conductivity λ [$W/(m \cdot K)$]
- Darcy velocity v [m/s]
- Borehole thermal resistance R_b [$m \cdot K/W$]

To appropriately understand the influence of initial parameters, it is proposed to originate a 120 combinations matrix, thus constituted by 120 sets of the three parameters. This systematic scheme of initial parameters is defined based on considerations hereafter explained and will be used for further parameters estimation for this specific case study.

About ground thermal conductivity, the few available geological information suggests to use a wide range of possible values shown in Table 11.

Table 11 - Ground thermal conductivity initial values used for MLS solution fit.

Ground Thermal Conductivity [$W/(m \cdot K)$]	1,5	2,0	2,5	3,0	3,5	4,0

Concerning Darcy velocity, expecting elevated hydraulic heads in this specific site and considering the geological subsurface, relatively high velocity are considered, however accounting for a large possible interval as reported in Table 12.

Table 12 - Darcy velocity initial values used for MLS solution fit.

Aquifer Darcy Velocity [m/s]	1,0E-3	1,0E-4	1,0E-5	1,0E-6	1,0E-7
Aquifer Darcy Velocity [m/day]	86,4	8,64	0,864	0,0864	0,00864

The same values are shown both in *m/s* and *m/day*, since they are both commonly used.

Regarding borehole thermal resistance, a range of values commonly recurrent for the double U-pipe configuration is suggested (Table 13), with a specific advice for the superior limit of the interval:

Table 13 - Borehole thermal resistance initial values used for MLS solution fit.

Borehole Thermal Resistance [m·K/W]	0,06	0,08	0,10	0,11*

*The superior limit for R_b can be obtained once the steady-state temperature is observed graphically.

It can be noticed in Figure 3-13, that after about *20 hours* the temperature values reach a steady condition, which persists until the end of the TRT. Hence, a steady state temperature can be simply evaluated as illustrated in Figure 3-17 where mean fluid temperature time series is reported after *36 hours* until the end of the thermal response test. This practical consideration is very helpful to constrain the range of the parameter initial value.

The steady state temperature $T_s = T_{fm}$ ($t = \infty$) is about *13,95°C*; since reasonably T_{fm} ($t = 0$) is inferior to T_{fm} ($t = \infty$) for TRT in heat injection condition, then it is possible to deduct the superior limit $R_{b,max}$ as shown in the following equations:

$$T_{fm} \, (t = 0) \leq T_{fm} \, (t \to \infty)$$

$$T_0 + q \cdot R_b \leq T_{fm} \, (t \to \infty) = T_s = 13,95°C$$

$$R_b \leq R_{b,max} = \frac{T_s - T_0}{q} = \frac{13,95°C - 9,79°C}{38,11 \, W/m} = 0,109 \, m \cdot K/W$$

Hence, a superior limit of R_b equal to *0,11 m·K/W* is estimated.
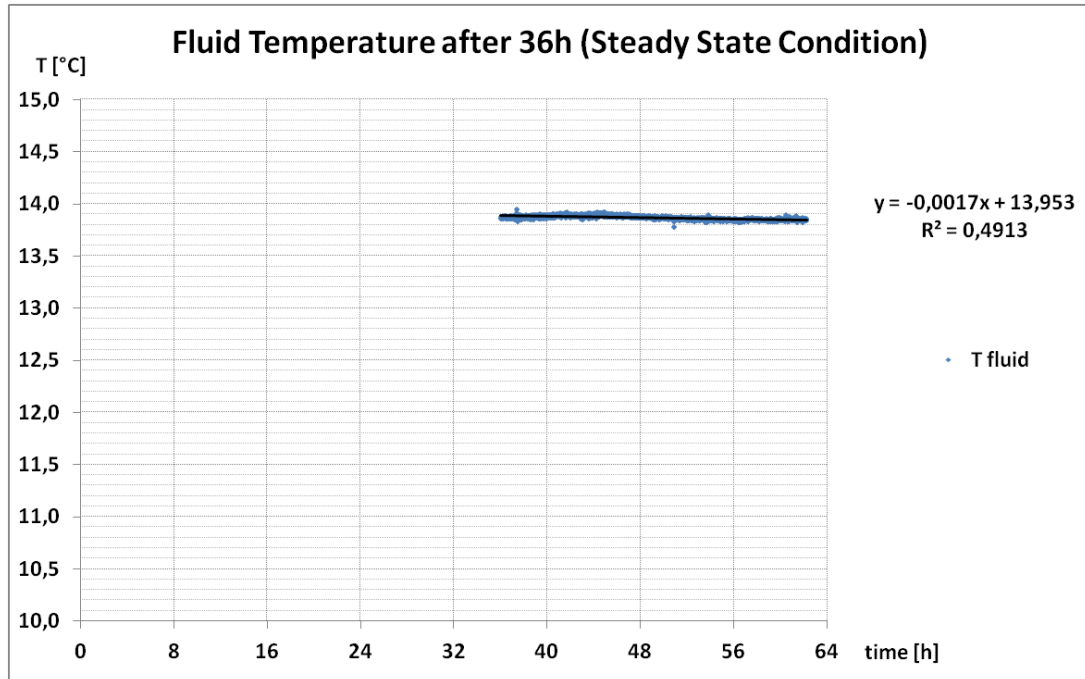
Figure 3-17 - Mean fluid temperature time series after 36 hours.

Additional issues are considered before running the fits in order to estimate the parameters. One of these is the numerical step for the integral function in **Eq. 2.23**, after some systematic attempts, the maximum step attainable with no script run interruption is *1E-4*. Using this value for performing fits, it returns same results that using *1E-3* would provide, but with remarkable superior evaluation time. A numerical step of *1E-3* is so kept constant for all the fits.

Furthermore, since the loop circulation time is equal to *11 minutes* as calculated by **Eq. 3.1**, the (UNI11466, 2012) recommends sampling time lower than the loop circulation time. Then, it is adopted a sampling time of *3 minutes* equivalent to about a fourth of the loop circulation time (*11 minutes*). This is very compliant in reducing the dataset, diminishing of two thirds the amount of data used to run the minimization process by MATLAB.

Franco Lý

Interpretation of Borehole Heat Exchangers Thermal Response Tests
under groundwater influence: analysis of three case studies

3.5.2 Time Criterion for Initial Data Significativity

Assuming a parallel approach to Infinite Line Source model for TRT interpretation, a time criterion for data significativity is proposed as described in section 2.6.2. Briefly, the characteristics time is defined as 4-5 times the thermal time constant. This constant depends on flow geometries, fluid characteristics and convection coefficient. The mean surface convection coefficient $\bar{h}$ is calculated by inverting the empirical correlation formula due to Hilpert (**Eq. 2.47**) in conditions of forced convection for external flow, specifically a cylinder in cross flow and valid for $Pr \geq 0,7$. It consists in simplified method assuming lumped thermal capacitance and an overall convection coefficient.

According to borehole and injection material characteristics, and fluid properties at undisturbed ground temperatures (Incropera, 2011), the surface average convection coefficient can be obtained in an iterative procedure, since a initial Darcy velocity has to be provided in order to determine Reynolds number (**Eq. 2.48**). This procedure is similar to the time criterion adopted when the logarithmic approximation is accounted in the ILS approach, but providing an initial value of effective thermal conductivity to calculate the thermal diffusivity used in the time criterion.

For a initial $v = 1E\text{-}5\ m/s$ and $T_0 = 9,79°C$ the following parameters are evaluated:

$$Re_L = \frac{\rho \cdot v \cdot L}{\mu} = \frac{1000 \cdot 10^{-5} \cdot 0,152}{1,31 \cdot 10^{-3}} = 1,16$$

$$Pr = \frac{\nu}{a} = 9,53$$

$$\overline{Nu} = C\ Re_L^m\ Pr^{1/3} = 0,989 \cdot 1,16^{0,33} \cdot 9,53^{1/3} = 2,20$$

$$\bar{h} = \frac{\overline{Nu} \cdot \lambda}{L} = \frac{2,20 \cdot 0,586}{0,152} = 8,50\ ^W/_{m^2 K}$$

Recalling **Eq. 2.41**, the thermal time constant is interpreted as:

$$\tau_t = \frac{\rho_g \cdot r_b \cdot c_g}{h \cdot 2} = 0,8\ h$$

And the characteristic time t_c (**Eq. 2.42**) is determined as:

$$t_c = (4 \div 5)\ \tau_t = 3,2 \div 4,0\ h$$

The criterion is subsequently validated by an initial time sensitivity analysis for Claviere site.

Franco Lý

*Interpretation of Borehole Heat Exchangers Thermal Response Tests
under groundwater influence: analysis of three case studies*

3.5.3 Final Time Sensitivity Analysis

Prior to apply the time criterion to the fits, a round of fits are carried out with an initial time t_{in} = 0 h and a final time t_{end} = 60 h in order to have a first insight of the solutions.

It will be showed how plots comparing MLS temperature time series and experimental data exhibit a systematic error in initial data fitting. This is caused by MLS model itself, that already at early times, accounts for a specific power injection at the beginning of the test. As a result, the thermal inertia of the borehole in the initial times is neglected. In order to reduce this systematic problem, an initial time sensitivity analysis will be performed in section 3.5.4.

The sets of parameters obtained by the estimation procedure are characterized by a *RMSE*, calculated by means of **Eq. 2.35**. The first run of the script generates multiple solutions described in Table 14. For each solution, the correspondent frequency and *RMSE* are also indicated.

The solutions obtained by the 120 fits with the above imposed conditions are 51 sets of three parameters with *RMSE* ranging from *0,108°C* to *0,192°C*. The most recurrent solution covers the *46,67%* of the fits. Besides, another solution interests the 8,33% of the fits while there are 45 solutions that result singularly from the fits.

Table 14 - Solutions from MLS analysis with t_{in} = 0 h and t_{end} = 60 h

Solution	Fitted Parameter Values			f [%]	RMSE [°C]
	λ [W/mK]	v [m/s]	Rb [mK/W]		
1	0,05	2,2E-04	0,087	46,67%	0,108
2	6,01	5,7E-05	0,099	8,33%	0,141
3	0,06	2,5E-04	0,089	2,50%	0,111
4	0,05	2,1E-04	0,087	1,67%	0,108
5	0,05	2,4E-04	0,089	1,67%	0,109
6	0,06	2,8E-04	0,091	1,67%	0,119
7	0,34	6,8E-10	0,105	0,83%	0,186
8	0,34	1,3E-09	0,105	0,83%	0,186
9	0,34	1,3E-07	0,105	0,83%	0,186
10	1,68	6,2E-05	0,099	0,83%	0,134
11	18,79	-6,4E-07	0,098	0,83%	0,141
12	18,79	1,5E-08	0,098	0,83%	0,141
13	2,83	6,1E-05	0,099	0,83%	0,135
14	18,79	-1,6E-07	0,098	0,83%	0,141
15	2,89	6,1E-05	0,099	0,83%	0,135

Franco Lý

Interpretation of Borehole Heat Exchangers Thermal Response Tests
under groundwater influence: analysis of three case studies

16	0,05	-2,0E-04	0,086	0,83%	0,109
17	18,79	-6,8E-08	0,098	0,83%	0,141
18	3,72	6,1E-05	0,099	0,83%	0,135
19	0,06	-2,0E-04	0,088	0,83%	0,108
20	1,41	-6,3E-05	0,099	0,83%	0,134
21	0,45	3,9E-10	0,104	0,83%	0,192
22	0,45	1,7E-07	0,104	0,83%	0,192
23	0,45	1,7E-08	0,104	0,83%	0,192
24	2,60	-6,0E-05	0,099	0,83%	0,142
25	16,56	-3,0E-07	0,098	0,83%	0,145
26	2,27	6,1E-05	0,099	0,83%	0,142
27	16,56	-4,2E-07	0,098	0,83%	0,145
28	18,79	3,2E-07	0,098	0,83%	0,141
29	2,58	-6,1E-05	0,099	0,83%	0,134
30	0,34	-1,1E-09	0,105	0,83%	0,186
31	0,34	1,7E-07	0,105	0,83%	0,186
32	2,97	-6,1E-05	0,099	0,83%	0,135
33	18,79	-6,8E-07	0,098	0,83%	0,141
34	0,11	-1,6E-04	0,092	0,83%	0,112
35	4,10	-6,0E-05	0,099	0,83%	0,135
36	18,79	-6,6E-08	0,098	0,83%	0,141
37	18,79	-4,1E-08	0,098	0,83%	0,141
38	3,47	6,1E-05	0,099	0,83%	0,135
39	18,79	-1,3E-07	0,098	0,83%	0,141
40	1,76	6,2E-05	0,099	0,83%	0,134
41	0,34	4,4E-11	0,105	0,83%	0,186
42	0,34	1,1E-07	0,105	0,83%	0,186
43	4,76	6,0E-05	0,099	0,83%	0,135
44	0,20	-1,2E-04	0,094	0,83%	0,117
45	0,06	2,7E-04	0,091	0,83%	0,116
46	18,79	-1,0E-06	0,098	0,83%	0,141
47	0,12	-1,7E-04	0,092	0,83%	0,112
48	0,17	7,4E-04	0,100	0,83%	0,175
49	0,07	-1,8E-04	0,089	0,83%	0,109
50	18,79	-2,1E-07	0,098	0,83%	0,141
51	18,79	-2,2E-07	0,098	0,83%	0,141

In order to have a general overview of the estimation results, a summary plot from all the fits is given for each fitted parameter.
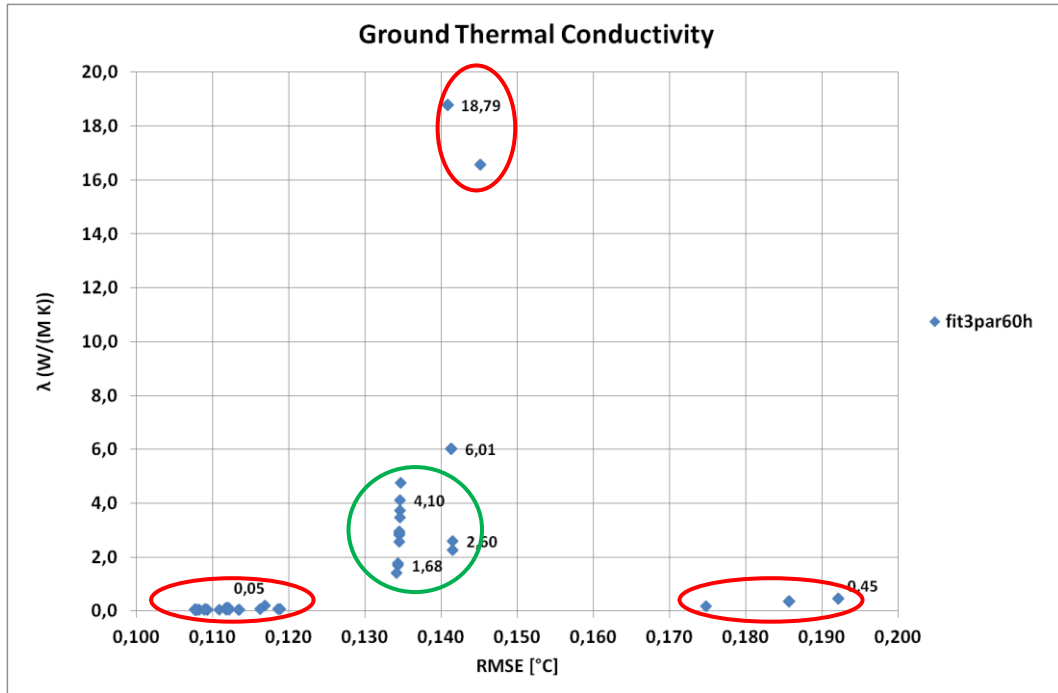
Figure 3-18 - Summary plot of fitted ground thermal conductivity values for t_{in} = 0 h and t_{end} = 60 h.

Figure 3-19 - Summary plot of fitted Darcy velocity values for t_{in} = 0 h and t_{end} = 60 h.

Relative to thermal conductivity summary plot in Figure 3-18, four different groups of values can be individuated. Lower *RMSE* values from *0,107°C* to *0,120°C* correspond to unfeasible conductivity values which are too low to realistically describe the ground thermal properties, as well as for a second group of *RMSE* values larger than *0,170°C*. Another group is also not reasonable, since values of λ superior to *4-5 W/(m·K)* are not plausible and very rare in nature. These groups of values are enclosed by red circles. A last group (enclosed by a green circle) presents physically acceptable values of λ from *1,5 W/(m·K)* to *4,5 W/(m·K)* around RMSE values of *0,135°C*.

Regarding Darcy velocity summary plot in Figure 3-19, only absolute values are reported in order to be represented in a logarithmic scale. Negative values can be ordinarily obtained by MLS solution since in theory advection is free to be orientated in both horizontal directions. In the plots, negative values are converted to positive to be depicted altogether with the positive values. The corresponding values of this parameter for the group of lower *RMSE* exhibit extremely high values. While for the group of acceptable thermal conductivities previously identified around *RMSE* values of *0,135°C* correspond a Darcy velocity absolute values of about *5,7E-5 m/s* (enclosed by a green circle). Other values of Darcy velocity are low to affirm that a groundwater flow is recognizable, these are however referred to unfeasible thermal ground conductivity and/or larger *RMSE* values.

Figure 3-20 - Summary plot of fitted borehole thermal resistance values for t_{in} = *0 h* and t_{end} = 6*0 h*.

Franco Lý

Interpretation of Borehole Heat Exchangers Thermal Response Tests
under groundwater influence: analysis of three case studies

Concerning the borehole thermal resistance summary plot in Figure 3-20, three evident groups can be identified. The lower *RMSE* values correspond to R_b values around *0,09 m·K/W*; while for the group of acceptable thermal conductivities around *RMSE* values of *0,135°C* correspond R_b slightly lower than *0,10 m·K/W* (enclosed by a green circle). Additionally the group with higher *RMSE* matches R_b values a bit larger than *0,10 m·K/W*.

To sum up, the fitting procedure results in many solutions corresponding to the three parameters ranging in wide intervals, except for the borehole thermal resistance. Additional considerations on physical meaning of some values and solutions *RMSE* comparison along relative plots can help to discriminate some solutions in favor to others. Critical comments will be provided after carrying out the initial time sensitivity analysis and the results discussion is presented in section 3.5.6.

A series of fits are carried on to perform a final time sensitivity analysis, since the achievement of steady state condition is observed for early time period in Figure 3-13. This analysis has the purpose to understand if in cases like this or with similar heat transfer conditions, where the mean fluid temperature time series reaches steady values after few hours (about 20 hours) it can possibly be recommended to reduce the duration of TRT.

Two indices are introduced in order to describe the solutions obtained by MLS fits:

- $RMSE_{average}$
- $RMSE_{best\_fit}$

$RMSE_{average}$ is the mean of the *RMSEs* obtained by the fits performed starting from the scheme of 120 combinations of initial parameters described in section 3.5.1.

$$RMSE_{average} = \sum_{i=1}^{n} \frac{RMSE}{n} \qquad \textbf{Eq. 3.12}$$

where *n* corresponds to *120* in this case study, that is the number of the fits performed for a single run of the script in appendix 7.1.

$RMSE_{best\_fit}$ is relative to the solution with physically acceptable values of each parameter, lowest *RMSE* value and also a good matching plot between MLS temperature time series and experimental data. Parameter values which does not have physical meaning are disregarded, in Figure 3-18 they are enclosed by a red circle. Thus, comparing the results, not only the *RMSE* has to be used to distinguish a good solution from another, but it is also necessary to check that the fit is able to catch the fundamental behavior of the measured trend.

The parameters estimations by MLS MATLAB script are performed using as initial parameters the systematic scheme already described of 120 combinations for 5 times, increasing the final time t_{end} from *36 hours* to *60 hours* with a step *Δt = 6 hours*.

Table 15 - Final time values used for the sensitivity analysis.

Final time t_{end} [hours]	36	42	48	54	60

Even if it requires longer computational times, an increase of the final time strongly influences the fitted parameters and the relative *RMSE*. In fact, passing from *36 hours* to *60 hours* the $RMSE_{average}$ passes from *0,165°C* to *0,125°C* as shown in Figure 3-21. This observation suggests to use a final time of *60 hours* as the most suitable time for parameters estimation.
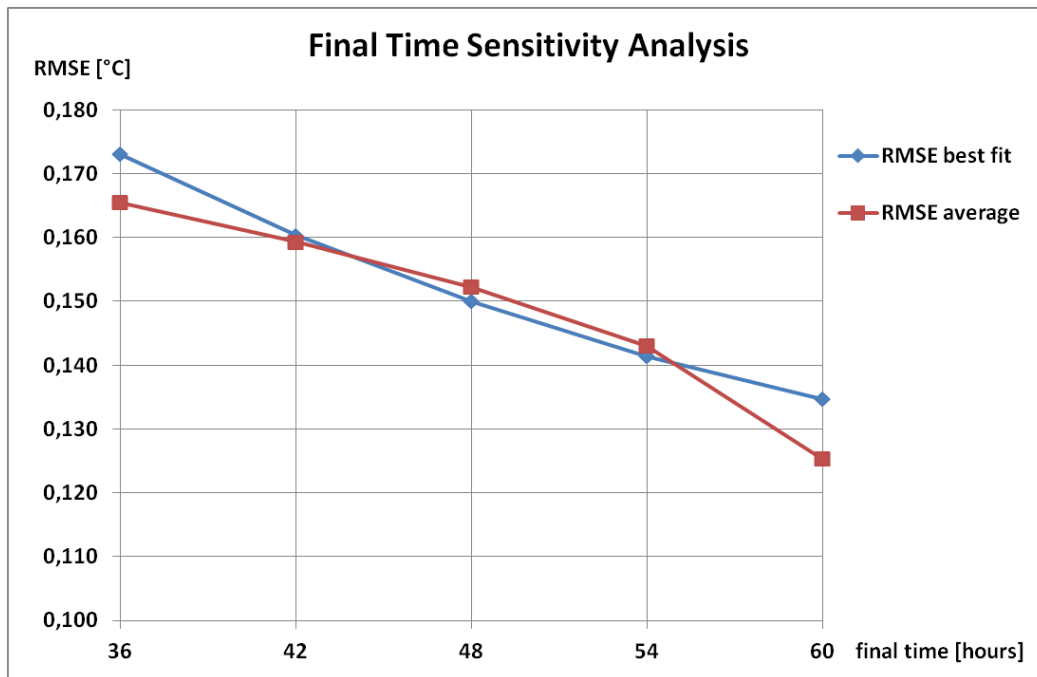
Figure 3-21 - RMSE trend for increasing final time t_{end}.

For instance, some resulting plots of the Moving Line Source model fits are illustrated in the following figures corresponding to the three most frequent solutions of Table 14.

Solution 1 and solution 3 generate temperature time series which are not representative of the experimental data. Solution 2 exhibits a good matching plot; however all the solutions present the initial systematic error in initial data fitting as previously mentioned. None of these recurrent solutions has physically acceptable values of ground thermal conductivity.
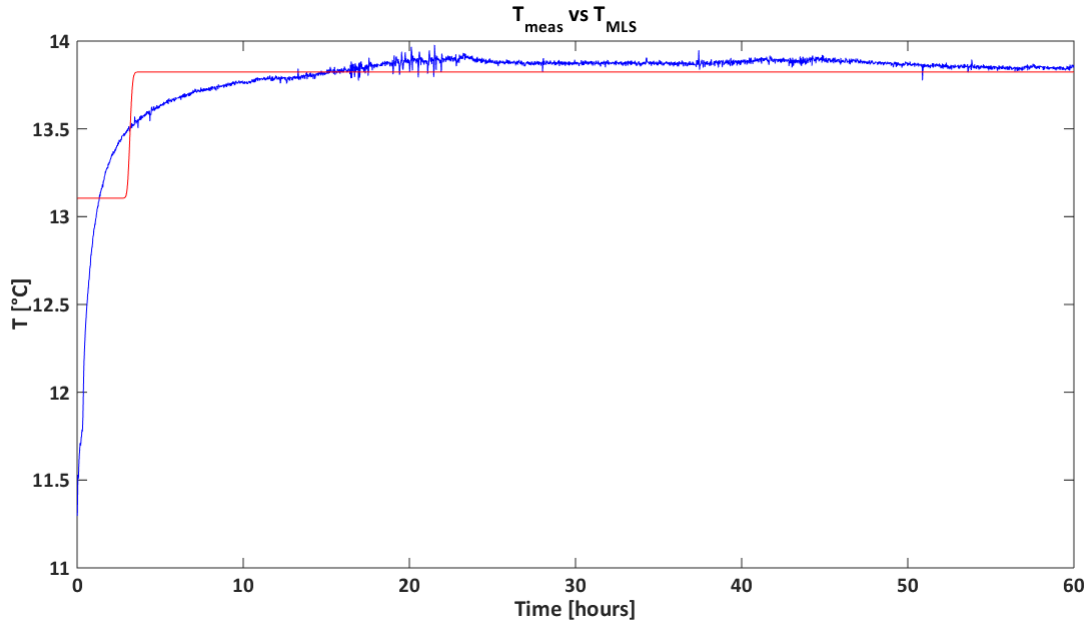
Figure 3-22 - Plot of measured data (blue line) vs. MLS temperature time series (red line) for t_{in} = 0 h and t_{end} = 60 h, solution 1 of Table 14.
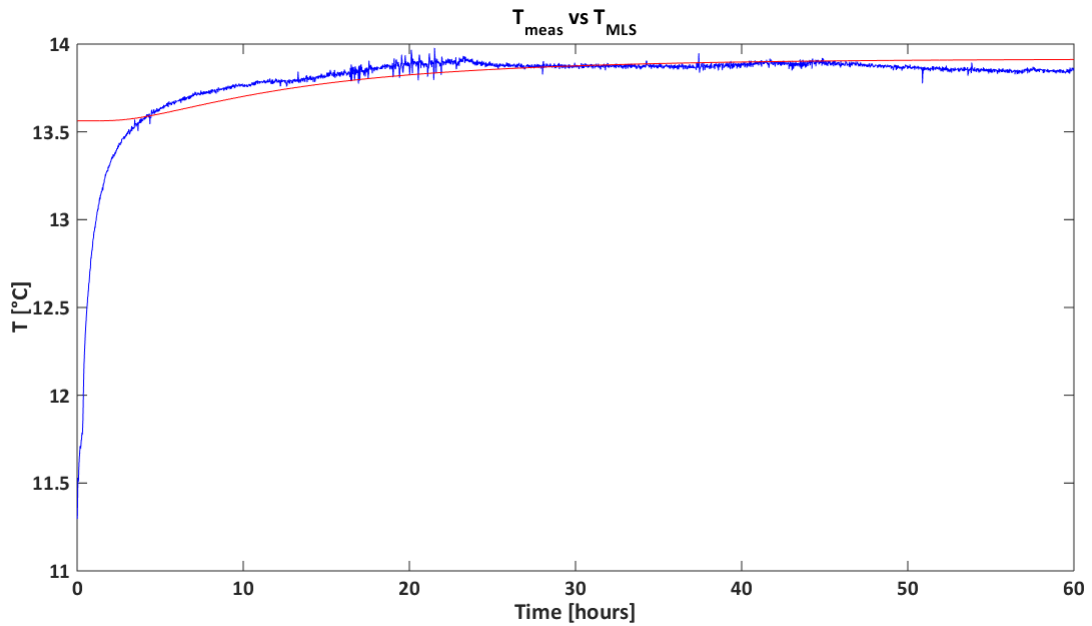
Figure 3-23 - Plot of measured data (blue line) vs. MLS temperature time series (red line) for t_{in} = 0 h and t_{end} = 60 h, solution 2 of Table 14.
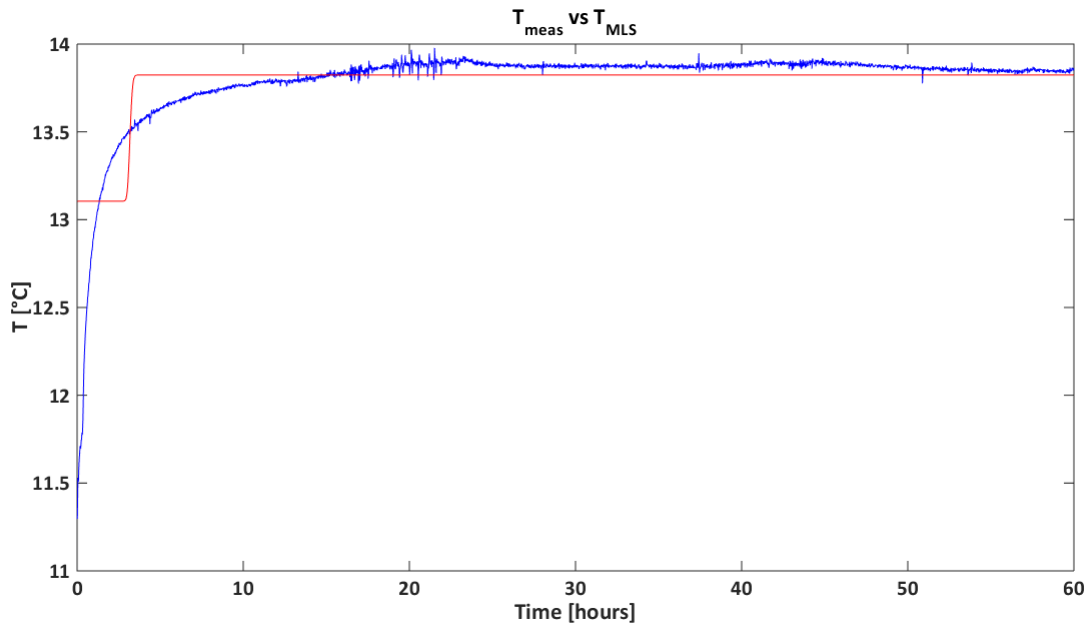
Figure 3-24 - Plot of measured data (blue line) vs. MLS temperature time series (red line) for t_{in} = 0 h and t_{end} = 60 h, solution 3 of Table 14.

Consequently, in order to extensively investigate MLS approach and also solve this systematic issue, an initial time sensitivity analysis is performed, providing large improvement in *RMSE* results from the fits when data related to initial times are disregarded.

3.5.4   Initial Time Sensitivity Analysis

After the results obtained by the final time sensitivity analysis, which are complex to be interpreted due to the amount of different solutions. Another series of fits are carried on with the aim of understanding initial time influence to MLS model fit and to validate the time criterion for data significativity proposed in section 2.6.2.

Time criterion for Claviere case study returns a characteristics time of *4 hours* (section 3.5.2), thus a round of fits are carried out with an initial time t_{in} = *4 h* and a final time t_{end} = *60 h*, in order to have an overview of the solutions before to go ahead with the initial time sensitivity analysis.

The sets of parameters obtained by the estimation procedure are characterized by a *RMSE*, calculated by means of **Eq. 2.35**. This run of the script generates multiple solutions described in Table 16.

Franco Lý

Interpretation of Borehole Heat Exchangers Thermal Response Tests under groundwater influence: analysis of three case studies

The solutions obtained by the 120 fits with the above imposed conditions are 44 sets of three parameters with *RMSE* ranging from *0,019°C* to *0,062°C*. The two most recurrent solutions cover the *64,17%* of the fits (77 solutions on 120 fits), which actually coincide if the absolute value of Darcy velocity is considered. Along the results, solution 3 is present twice, while there are 41 solutions that result singularly from the fits.

Table 16 - Solutions from MLS analysis with t_{in} = 4 h and t_{end} = 60 h.

Solution	Fitted Parameter Values			f [%]	RMSE [°C]
	λ [W/mK]	v [m/s]	Rb [mK/W]		
1	2,77	7,6E-05	0,100	36,67%	0,019
2	2,77	-7,6E-05	0,100	27,50%	0,019
3	0,21	1,1E-06	0,106	1,67%	0,062
4	0,22	5,3E-09	0,106	0,83%	0,062
5	1,06	5,3E-04	0,104	0,83%	0,062
6	0,22	1,1E-07	0,106	0,83%	0,062
7	1,40	5,3E-04	0,104	0,83%	0,062
8	1,75	5,3E-04	0,104	0,83%	0,062
9	39,63	1,1E-07	0,102	0,83%	0,040
10	2,09	5,3E-04	0,105	0,83%	0,062
11	2,44	5,2E-04	0,105	0,83%	0,062
12	39,63	-1,3E-08	0,102	0,83%	0,040
13	2,78	5,2E-04	0,105	0,83%	0,062
14	39,63	3,3E-07	0,102	0,83%	0,040
15	1,33	8,0E-04	0,105	0,83%	0,062
16	0,22	8,9E-08	0,106	0,83%	0,062
17	1,77	8,0E-04	0,105	0,83%	0,062
18	2,21	8,0E-04	0,105	0,83%	0,062
19	2,66	8,0E-04	0,105	0,83%	0,062
20	39,63	5,0E-07	0,102	0,83%	0,040
21	3,10	8,0E-04	0,105	0,83%	0,062
22	3,54	8,0E-04	0,105	0,83%	0,062
23	1,48	1,0E-03	0,105	0,83%	0,062
24	0,22	3,1E-09	0,106	0,83%	0,062
25	0,22	1,7E-07	0,106	0,83%	0,062
26	1,98	1,0E-03	0,105	0,83%	0,062
27	39,63	-9,5E-07	0,102	0,83%	0,040
28	2,46	1,0E-03	0,105	0,83%	0,062
29	2,94	9,9E-04	0,105	0,83%	0,062
30	3,41	9,9E-04	0,105	0,83%	0,062

31	39,63	-1,7E-07	0,102	0,83%	0,040
32	3,90	9,9E-04	0,105	0,83%	0,062
33	1,58	1,0E-03	0,105	0,83%	0,062
34	0,22	7,6E-08	0,106	0,83%	0,062
35	0,22	7,6E-09	0,106	0,83%	0,062
36	2,12	1,0E-03	0,105	0,83%	0,062
37	39,62	-2,0E-06	0,102	0,83%	0,040
38	2,64	1,0E-03	0,105	0,83%	0,062
39	3,17	1,0E-03	0,105	0,83%	0,062
40	39,63	-6,2E-07	0,102	0,83%	0,040
41	3,70	1,0E-03	0,105	0,83%	0,062
42	39,63	-8,3E-07	0,102	0,83%	0,040
43	4,23	1,0E-03	0,105	0,83%	0,062
44	39,63	-7,4E-07	0,102	0,83%	0,040

To have a general overview of the parameters estimation results, a summary plot from all the fits for an initial time t_{in} = *4 hours* and a final time t_{end} = *60 h* is given for each fitting parameter (ground thermal conductivity, Darcy velocity and borehole thermal resistance).
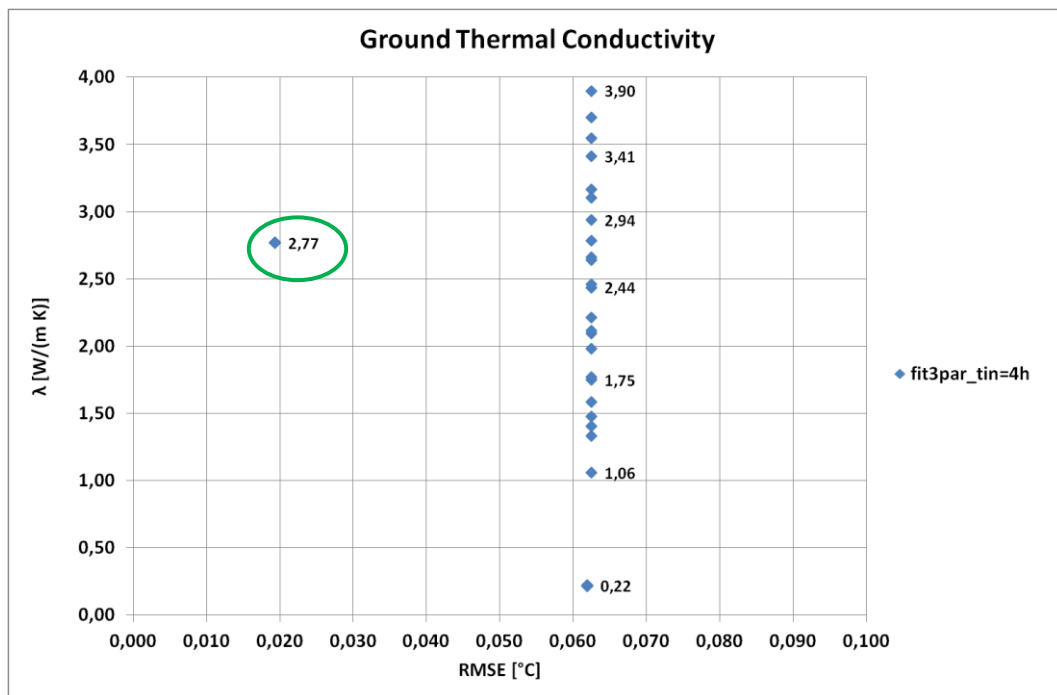
Figure 3-25 - Summary plot of fitted ground thermal conductivity values for t_{in} = 4 h and t_{end} = 60 h.

Relative to the ground thermal conductivity summary plot in Figure 3-25, the lowest *RMSE* value of *0,019°C* corresponds to a ground thermal conductivity of *2,77 W/(m·K)* of solutions

Franco Lý

Interpretation of Borehole Heat Exchangers Thermal Response Tests
under groundwater influence: analysis of three case studies

1 and 2 of Table 16 (in total 77 solutions on 120 fits). Parameter values larger than *4,0 W/(m·K)* are filtered out, since it would have scaled out the plot, but such high value of conductivity is not considered physically possible for this case (as previously mentioned values of *λ* superior to *4-5 W/(m·K)* are very rare in nature).

The group of *RMSE* around *0,062°C* which also involves several different solutions (*29* on *120* fits) comprehends a large interval of conductivity values, from a very low values group lower than *0,30 W/(m·K)* to values larger than *3,50 W/(m·K)*. Even if some *λ* values of this interval could be accepted, however, they respectively correspond to *RMSE* values more than two times the best fit *RMSE*.
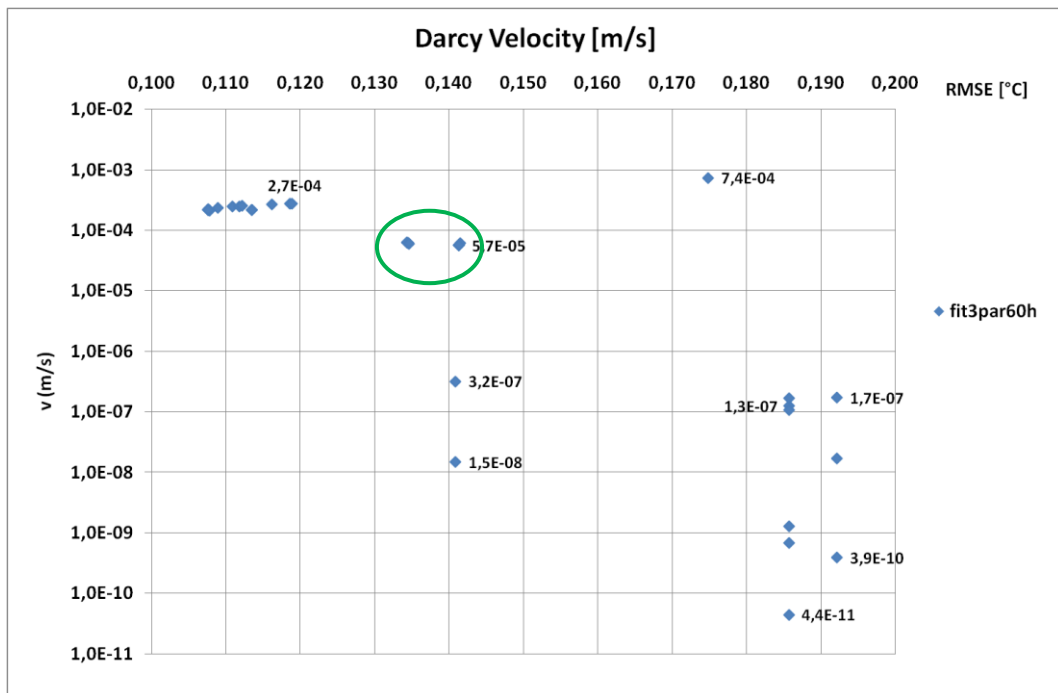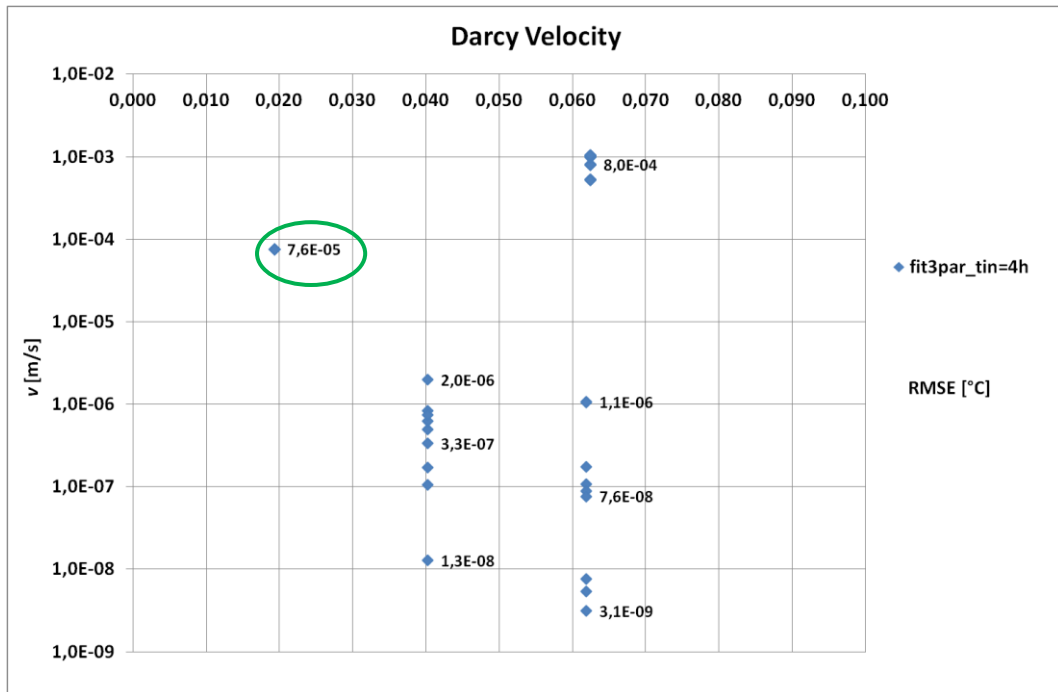

Figure 3-26 - Summary plot of fitted Darcy velocity values for t_{in} = 4 h and t_{end} = 60 h.

Regarding Darcy velocity summary plot in Figure 3-26, only absolute values are reported in order to represent the parameter on a logarithmic scale. In the plot the negative values are converted to positive to be plotted altogether with the already estimated positive values. The corresponding value of Darcy velocity for the lowest group of *RMSE* is *7,6E-5 m/s* in absolute value.

Other values of Darcy velocity are between *2,0E-6 m/s 1,3E-8 m/s* for *RMSE* around *0,040°C*. While for *RMSE* around *0,062°C* Darcy velocity values are about *1,0E-3 m/s* or inferior to *1,0E-6 m/s.* However, these solutions respectively correspond to *RMSE* values more than two times the $RMSE_{best\_fit}$.
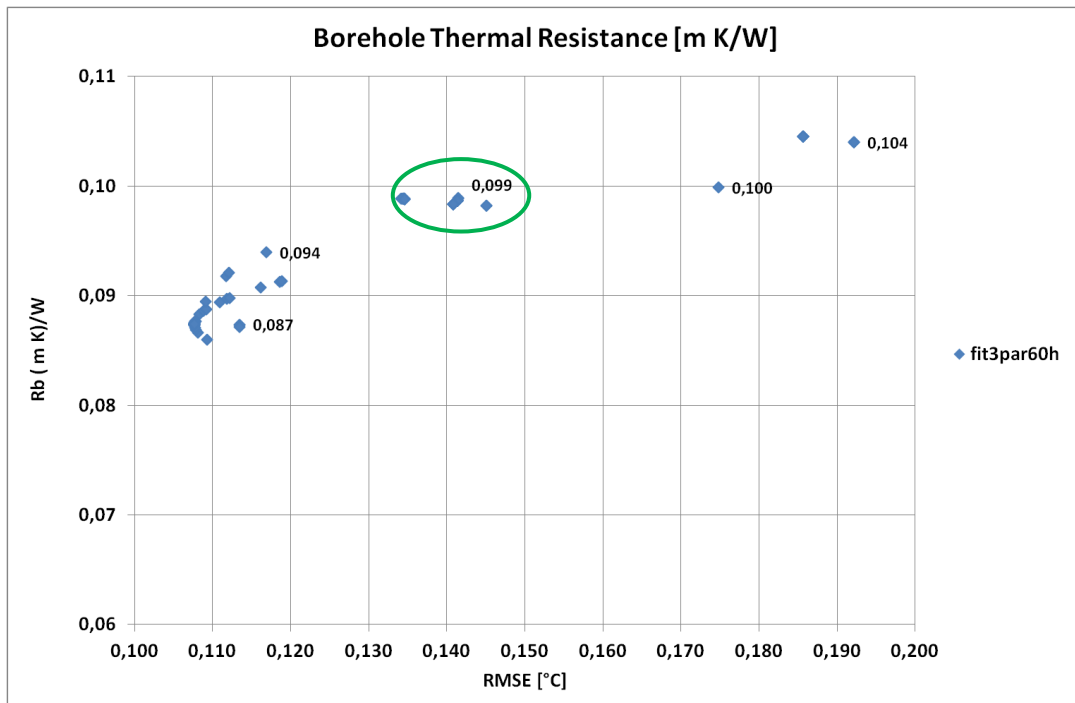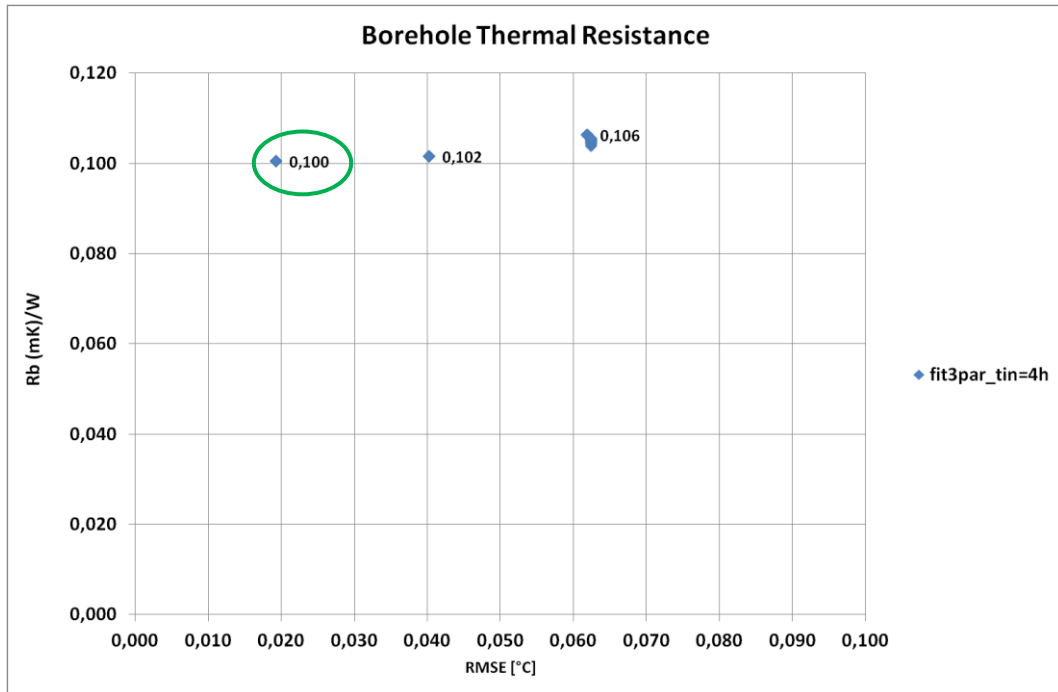
Figure 3-27 - Summary plot of fitted borehole thermal resistance values for t_{in} = 4 h and t_{end} = 60 h.

Concerning the borehole thermal resistance summary plot in Figure 3-27, three evident groups can be identified. The lowest *RMSE* value corresponds to a R_b value of *0,100 m·K/W*; while *RMSE* values around *0,040°C* correspond to a R_b value *0,102 m·K/W*. *RMSE* of *0,062°C* denotes a larger interval of parameter values between *0,104 m·K/W* and *0,106 m·K/W*.

Similarly to the previous analysis, the parameters estimation by MLS script is performed using as initial parameters the systematic scheme already described of 120 combinations for 6 times, disregarding initial data according to Table 17. The final time t_{end} = *60 h* is kept constant for all the fits as suggested by the final time sensitivity analysis.

Table 17 - Initial time values used for the sensitivity analysis.

Initial time t_{in}	18 min	2 hours	3 hours	4 hours	5 hours	6 hours

The time value of *18 minutes* is not randomly chosen, but is the value around which the mean temperature time series seems graphically to be affected by the heat injection and so start to increase with a different slope as depicted in Figure 3-28. Considering that the time required by the fluid to flow along the U-pipe is estimated in 11 minutes (section 3.3.4), the time interval of *18 minutes* roughly means twice the necessary time. This was the result of a

first attempt to understand how to disregard initial data. then, the time criterion for data significativity will be considered as an reliable procedure for the MLS approach.
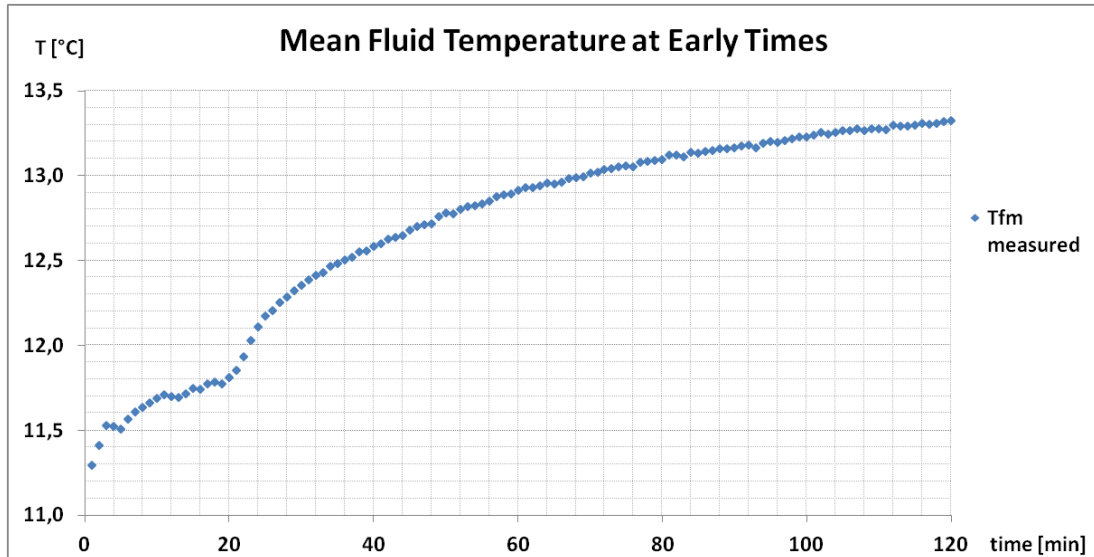
Figure 3-28 - Mean fluid temperature at early times.

A great improvement of both $RMSE_{average}$ and $RMSE_{best\_fit}$ by increasing the initial time t_{in} can be noticed in Figure 3-29. In both cases, the diminishment in percentage is around *60-70%* from disregarding first *18 minutes* to *2 hours*. It can be reasonably stated that *RMSE* values after disregarding two hours converge to stable values for increasing initial times, as a smooth trend of *RMSE* values can be observed approaching to an initial time t_{in} = *6 hours*.
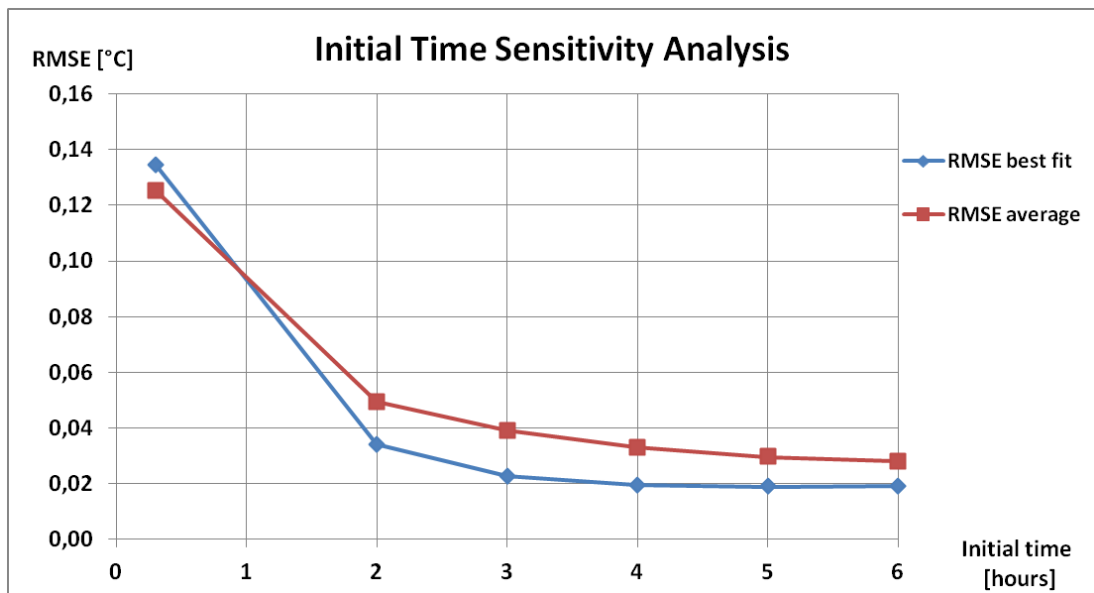
Figure 3-29 - RMSE trend for increasing initial time.

For instance, some resulting plots of the Moving Line Source model fits are illustrated in the following figures corresponding to the three most frequent solutions of Table 16. MLS temperature time series obtained with solution 3 does not follow experimental data trend.
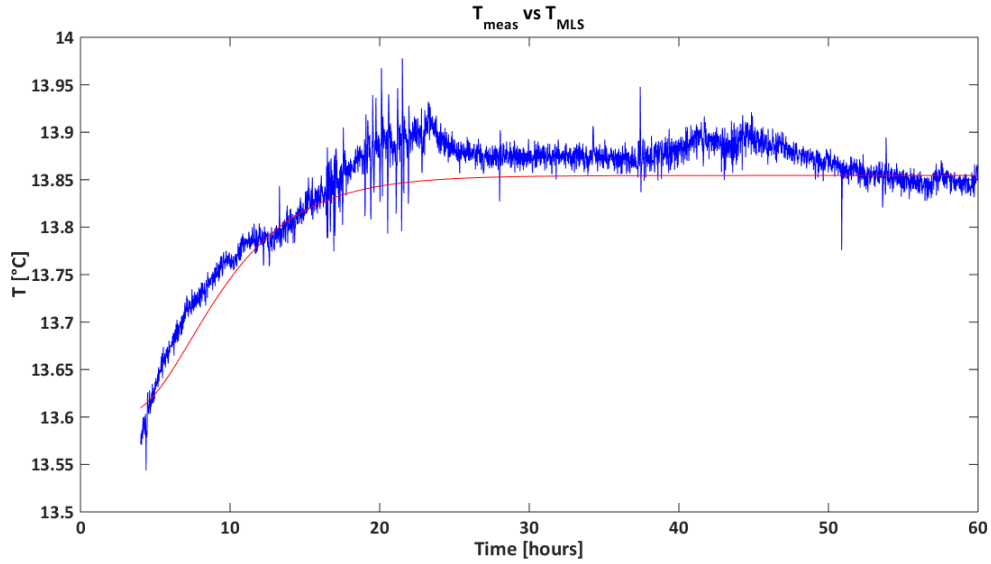
Figure 3-30 - Plot of measured data (blue line) vs. MLS temperature time series (red line) for t_{in} = 0 h and t_{end} = 60 h, solution 1 and 2 of Table 14.
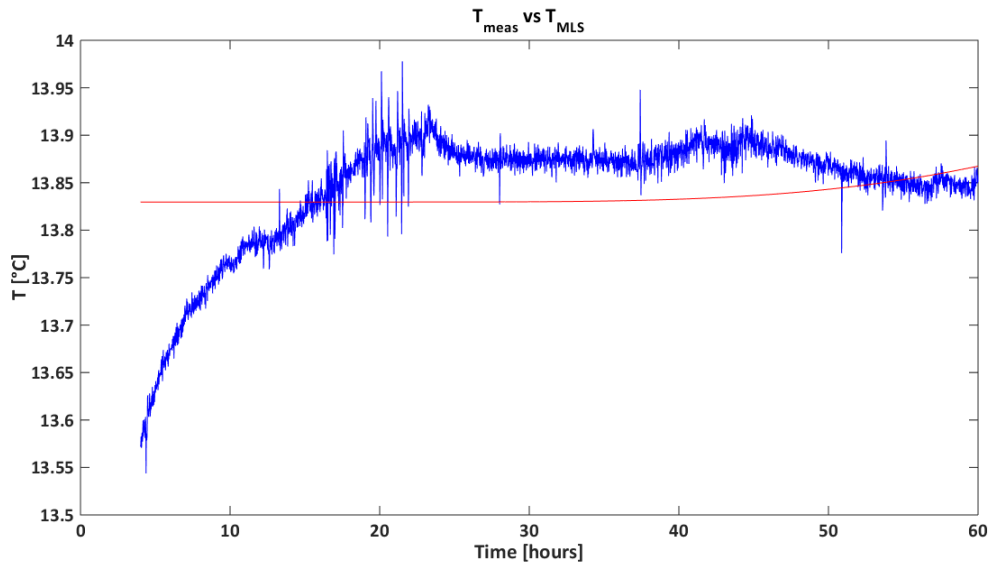
Figure 3-31 - Plot of measured data (blue line) vs. MLS temperature time series (red line) for t_{in} = 0 h and t_{end} = 60 h, solution 3 of Table 14.

Solution 1 and solution 2 generate the same MLS temperature time series which seems to represent very well the experimental data as reported in Figure 3-30. Other solutions presents higher *RMSE* values, solution 9 (*RMSE = 0,040°C*) and solution 11 (*RMSE = 0,062°C*) are presented in the following figure exhibiting in both the cases a clear mismatching trend.
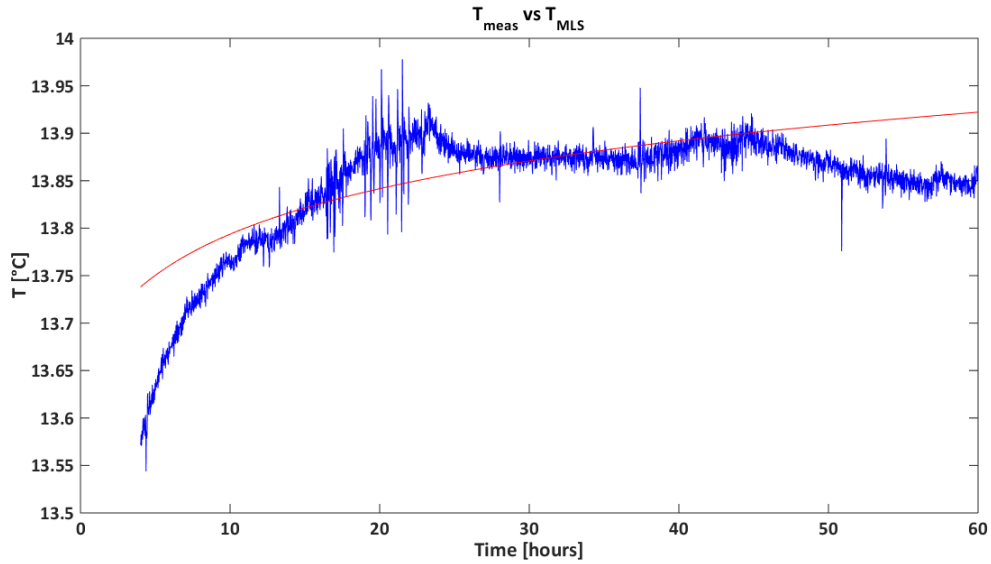
Figure 3-32 - Plot of measured data (blue line) vs. MLS temperature time series (red line) for t_{in} = 0 h and t_{end} = 60 h, solution 9 of Table 14.
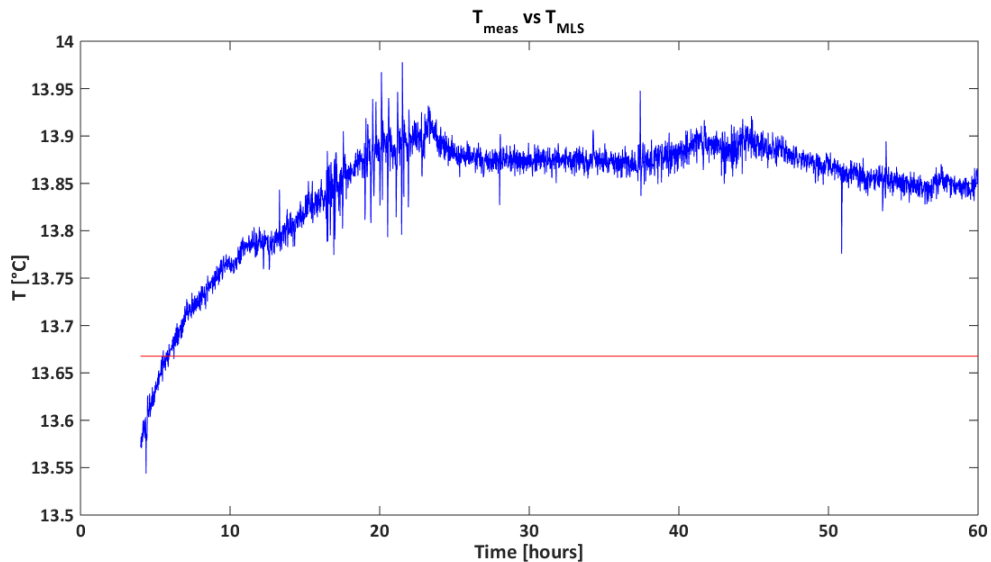
Figure 3-33 - Plot of measured data (blue line) vs. MLS temperature time series (red line) for t_{in} = 0 h and t_{end} = 60 h, solution 11 of Table 14.

Franco Lý

Interpretation of Borehole Heat Exchangers Thermal Response Tests under groundwater influence: analysis of three case studies

With the lowest RMSE of *0,019°C*, solution 1 and 2 return satisfying matching plot between measured and MLS temperature time series, with ground thermal conductivity value of *2,77 W/(m·K)* close to the mean expected value for the site (*2,7 W/(m·K)*), same groundwater flow absolute value of *7,6E-05 m/s* and borehole thermal resistance value equal to *0,100 m·K/W*. They are the most recurrent solutions with very good matching plot to experimental data and lowest *RMSE* among all the fits. All the estimated parameters can be reasonably acceptable and they are in agreement with the expectations considering specific site hydrogeological characteristics. Therefore, this set of parameters is considered the *best fit solution*.

Concerning the other solutions, the plots indicate the minimization procedure has identified local minima, since the MLS temperature time series is not able to reproduce the fundamental behavior of measured data.

For example, solution 9 does not generate a temperature series that well fit graphically as shown Figure 3-32, above all because it does not seem to reach a steady state condition for large times. It also corresponds to extremely large values of thermal conductivity that cannot in any way be descriptive of the site subsurface. MLS temperatures time series from solution 11 results in a straight line trend, that is located well under the experimental data as reported in Figure 3-33.

The *best fit solution* trends are represented in Figure 3-34 and in Figure 3-35 for each parameter increasing the initial time and keeping constant the final time t_{end} = *60 h.* Each parameter exhibits a converging behavior approaching from an initial time of *2 hours* to *6 hours*, especially Darcy velocity and borehole thermal resistance. While, the thermal conductivity seems to be slower to reach a stable value. The *RMSE* trend improves significantly after an initial time of *2 hours* reaching a good stability after *4 hours*.
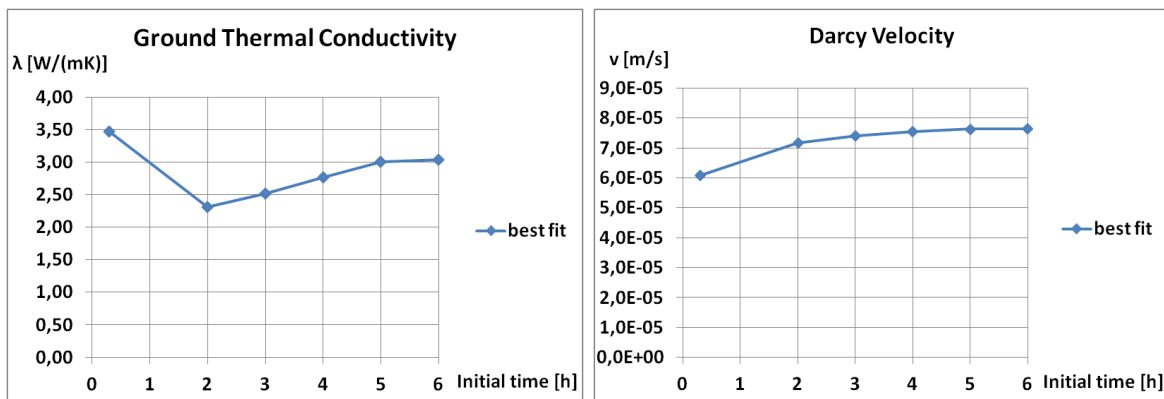
Figure 3-34 - Thermal conductivity and Darcy velocity trends for increasing initial time and fixed final time.
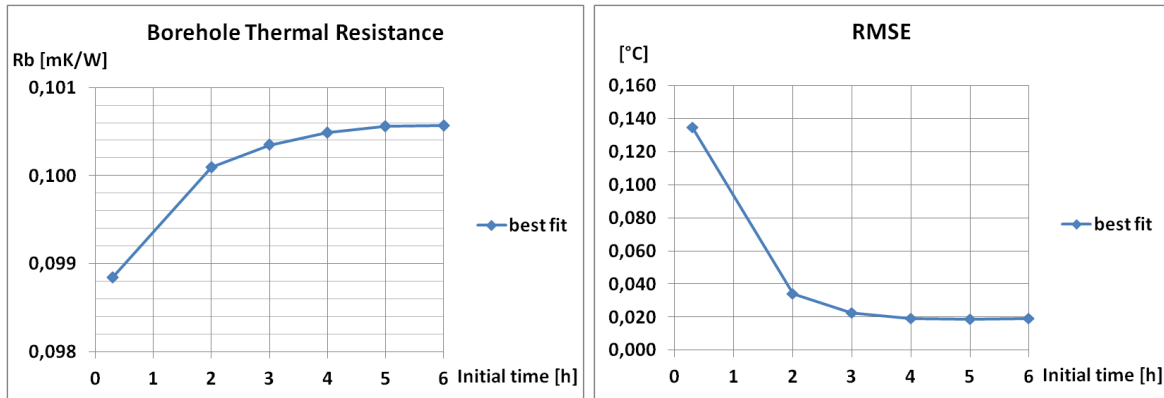
Figure 3-35 - Borehole thermal resistance and *RMSE*_{best_fit} trends for increasing initial time and fixed final time.

The MLS *best fit solution* involves a Darcy velocity *v* of *7,6E-5 m/s*, then the re-calculated characteristic time is obtained following the previously applied procedure:

$$Re_L = \frac{\rho \cdot v \cdot L}{\mu} = \frac{1000 \cdot 7,6 \cdot 10^{-5} \cdot 0,152}{1,31 \cdot 10^{-3}} = 8,84$$

$$Pr = \frac{\nu}{a} = 9,53$$

$$\overline{Nu} = C\ Re_L^m\ Pr^{1/3} = 0,911 \cdot 8,84^{0,385} \cdot 9,53^{1/3} = 4,47$$

$$\bar{h} = \frac{\overline{Nu} \cdot \lambda}{L} = \frac{4,47 \cdot 0,586}{0,152} = 17,23\ W/_{m^2K}$$

The thermal time constant is now updated:

$$\tau_t = \frac{\rho_g \cdot r_b \cdot c_g}{h \cdot 2} = 0,4\ h$$

And the characteristic time t_c becomes:

$$t_c = (4 \div 5)\ \tau_t = 1,6 \div 2,0\ h$$

The initial time sensitivity analysis has confirmed that after disregarding *2 hours*, as the characteristic time obtained by the time criterion for data significativity using a "best fit solution" Darcy velocity *v* of *7,6E-05 m/s*, the fits starting from systematic scheme of initial parameters yield a large amount of valid fitted parameters results with optimal *RMSE* and a good convergence of parameters values. All the 3 estimated parameters exhibit a satisfying trend, able to reach a stable value after having disregarded *4-5 hours* of data measurement as demonstrated in Figure 3-34 and Figure 3-35.

Franco Lý

*Interpretation of Borehole Heat Exchangers Thermal Response Tests
under groundwater influence: analysis of three case studies*

3.5.5 Two-Parameters Fit for Analysis Check

A further check analysis is carried out to verify the goodness of the 3 parameters estimation fit. The borehole thermal resistance is kept fixed as the best fit result from initial time sensitivity analysis for initial time of *4 hours,* being equal to *0,100 m·K/W.*

Therefore, a 2 parameters estimation approach is performed to evaluate ground thermal conductivity and Darcy velocity. The script is a simplified version of the original one able to minimize the RMSE between measured and simulated data acting only on 2 parameters instead of 3.

The possible combinations keeping fixed the borehole thermal resistance are 30 initial parameters vectors, shown in Table 18 with the relative solutions from the fit procedure. The results confirm the expectations, returning identical values yielded with the 3 parameters approach without constraining borehole thermal resistance parameter.

It can be observed that for low values of initial conductivities the fits individuate local minima more often than for larger initial conductivities. The lowest RMSE of *0,019°C* considered as the best fit (*16* cases out of *30*), corresponds to a ground thermal conductivity of *2,78 W/(m·K)* and a Darcy velocity of *7,6E-05 m/s.*

Other results fall back into much larger RMSE with not feasible thermal conductivity values (too low, from *0,18* to *0,58 W/(m·K)*) and Darcy velocity extremely large or very proximal to null groundwater flow.

Table 18 - Two parameters estimation results for an initial time of 4h with fixed borehole thermal resistance.

Initial parameters values			Fitted parameters values		
set	*λ [W/mK]*	*v [m/s]*	*λ [W/mK]*	*v [m/s]*	*RMSE [°C]*
1	1,50	1E-03	0,27	1,2E-03	0,1113
2	1,50	1E-04	**2,78**	**7,6E-05**	**0,0193**
3	1,50	1E-05	0,58	4,0E-09	0,1667
4	1,50	1E-06	0,58	-7,7E-10	0,1667
5	1,50	1E-07	0,58	1,1E-07	0,1667
6	2,00	1E-03	0,58	-1,6E-09	0,1667
7	2,00	1E-04	**2,78**	**7,6E-05**	**0,0193**
8	2,00	1E-05	0,58	5,3E-12	0,1667
9	2,00	1E-06	0,58	-2,5E-09	0,1667
10	2,00	1E-07	0,58	-1,6E-09	0,1667
11	2,50	1E-03	0,18	6,3E-04	0,0624
12	2,50	1E-04	**2,78**	**7,6E-05**	**0,0193**
13	2,50	1E-05	**2,78**	**7,6E-05**	**0,0193**
14	2,50	1E-06	0,58	-4,4E-10	0,1667
15	2,50	1E-07	0,58	-1,5E-09	0,1667

16	3,00	1E-03		0,18	6,3E-04	0,0624
17	3,00	1E-04		**2,78**	**7,6E-05**	**0,0193**
18	3,00	1E-05		**2,78**	**7,6E-05**	**0,0193**
19	3,00	1E-06		**2,78**	**7,6E-05**	**0,0193**
20	3,00	1E-07		**2,78**	**7,6E-05**	**0,0193**
21	3,50	1E-03		0,17	6,7E-04	0,0624
22	3,50	1E-04	➡	**2,78**	**7,6E-05**	**0,0193**
23	3,50	1E-05		**2,78**	**7,6E-05**	**0,0193**
24	3,50	1E-06		**2,78**	**7,6E-05**	**0,0193**
25	3,50	1E-07		**2,78**	**7,6E-05**	**0,0193**
26	4,00	1E-03		0,16	7,0E-04	0,0624
27	4,00	1E-04		**2,78**	**7,6E-05**	**0,0193**
28	4,00	1E-05		**2,78**	**7,6E-05**	**0,0193**
29	4,00	1E-06		**2,78**	**7,6E-05**	**0,0193**
30	4,00	1E-07		**2,78**	**7,6E-05**	**0,0193**

3.5.6 Results Discussion

Both in case of 3 and 2 parameters estimation procedure, multiple solutions result from fits comprehending absolute and local minima. This is due to fminsearch algorithm that finds minimum of unconstrained multivariable function using derivative-free method (Lagarias, 1998). More in general, the inverse problem under examination can result in multiple solutions, as also reported by (Wagner V. a., 2013).

Therefore, the fitted parameters can depend on the initial parameters values. In order to comprehensively account for this issue, a systematic scheme of initial parameters was generated involving until 120 different combinations of:

- Ground thermal conductivity λ [$W/(m \cdot K)$]
- Darcy velocity v [m/s]
- Borehole thermal resistance R_b [$m \cdot K/W$]

This approach was able to guarantee an adequate range of possible solutions including the absolute minimum, since the initial parameters choice fell back into feasible values interval for all three parameters. This issue has been validated by the results from initial time sensitivity analysis. Therefore, the choice of initial parameters interval has to be careful and led by physical considerations and geological site-specific characteristics.

At the same time, it is important to choose a variation step quite close within each parameter interval, but not such to increase exaggeratedly the number of combinations.

However, the variation step can be later improved after a first round of fits, if not sufficiently reliable results are obtained.

Generally, the main indicator which can point out a good fit is the *RMSE* (standard deviation of the differences between simulated and observed temperature values); however, it has been proved the necessity to couple it with a graphical check of the fit that has to catch the fundamental behavior of the measured trend. Thus, among all the results, if the *RMSE* is good but the plot presents a mismatching trend, then obviously the fitted parameters have to be ignored and disregarded.

Along the report from both sensitivity analysis, it is demonstrated how some results have no physical meaning and thus can be discriminated and filtered out. In particular, for the evaluation time sensitivity analysis a significant group of thermal conductivity values stands lower than *0,40 W/(m·K)*. Even if some of these belong to the lowest group of *RMSE*, such low thermal conductivity values can only represent dry sand, dry gravel or peat whose conformations are not characteristic of the specific geological site.

In addition, thermal conductivity values larger than *4-5 W/(m·K)* cannot be commonly found in nature and hence disregarded. Consequently, once these conductivity values and the relative Darcy velocity and borehole resistance values are removed from interest, only acceptable fitted parameters are left to be considered.

Even also for the initial time sensitivity analysis, the same logical procedure of filtering is followed yielding optimal results. For initial times of *4-5-6 hours* the analysis has given back for about *65%* (77, 79 and 78 on 120 total combinations) of the total cases with the same estimate of λ, v and R_b for the lowest RMSE value coupled with good matching plot.

Therefore, the application of the MLS approach for data interpretation of the TRT in Claviere case study results in the following best estimate of the thermo-physical parameters of the ground and of the BHE:

- λ = 2,77 W/(m·K)
- v = 7,6E-5 m/s
- R_b = 0,100 m·K/W

This result involves a correct initial parameters interval and variation step choice for each parameter such to foster the recurrent localization of the absolute minimum even starting from different initial sets of parameters.

Time criterion for data significativity (namely for disregarding initial data) returns a characteristics time of *2 hours* for Darcy velocity of *7,6E-05 m/s*, which is consistent with

Franco Lý

Interpretation of Borehole Heat Exchangers Thermal Response Tests
under groundwater influence: analysis of three case studies

the initial time analysis sensitivity findings. Then, it is considered reliable, at least for this case study. Nevertheless, it has to be underlined that it holds two important assumptions. The first is the lumped thermal capacitance of the borehole and the second is that convection coefficient is an overall average one. Further analysis are necessary to assess if these assumptions are acceptable to determine a valid characteristics time, in addition to its validity range.

To sum up, it can be assessed that results from sensitivity analysis are optimal if the total duration of the test is accounted and initial times longer than *2 hours* are considered. In fact, the ground thermal conductivity and Darcy velocity turn to be coherent with the hydro-geological characteristics of the site previously estimated by geological maps and observations from in-situ drillings; similarly the borehole thermal resistance is consistent with the borehole geometry and filling material adopted for tested BHE. Results of MLS approach are fully compared with LS ones in section 3.6.1.

According to (Wagner V. a., 2013), who analyzed the suitability of Moving Line Source equation for determination of the Darcy velocity, possible errors fitting TRT data can be caused from violating the homogeneous medium assumption. Indeed, a BHE is made up of different materials with specific property values. The R_b should not be influenced by groundwater flow in the BHE-surrounding porous medium and its value may be determined separately (Wagner V. a., 2013). He compared the known values of *v* specified in a FEFLOW model with the effective Darcy velocity evaluated by MLS using numerically generated TRT temperature time series (influenced by different Darcy velocities). It is resulted that true value of Darcy velocity, *v*, was underestimated, and the calculated conformance ratio even decreases non-linearly for higher groundwater velocities (Figure 3-36).
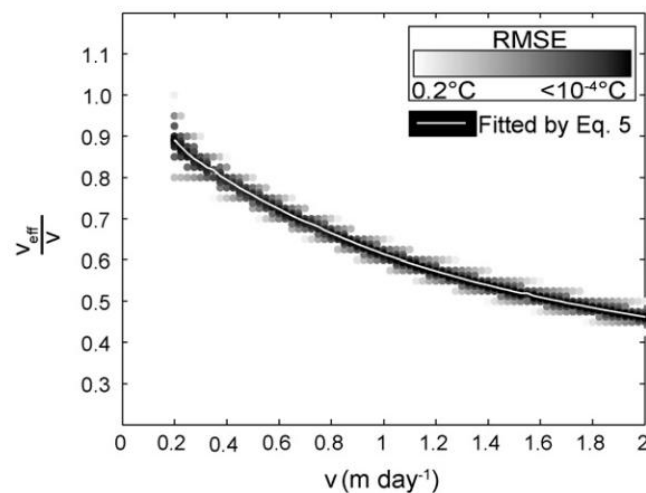
Figure 3-36 - Result of the evaluation of numerically generated TRT temperature time series (influenced by different Darcy velocities) based on the MLS equation. Max tolerance of fitting error is set to a RMSE of 0,2°C.

This discrepancy between input and best-fitted Darcy velocity is mainly caused by the difference between the hydraulic conductivities of the grouting material and the aquifer, in which it is many order of magnitude higher than that of the grout. Thus, the Darcy velocity is noticeably reduced in the vicinity of the source, which also explains why the best fitted Darcy velocities are increasingly underestimated for increasing input *v* (Wagner V. a., 2013).

Hence, he suggested a parametric approach for practical applications in order to correct this systematic error. A correction term *C* is introduced to balance the difference between v_{eff} and *v:*

$$v = \frac{v_{eff}}{C}$$

Eq. 3.13

A defined field of application of *C* for a thermal conductivity range of the porous medium from *1,2* to *5,2* W/(m·K) and a Darcy velocity *v* interval from *0,01* to *3,5 m/day.* The ratio v_{eff}/*v* is calculated for three different R_b values and four different extraction/injection rates, exhibiting no significant variations. Thus, only averages v_{eff}/*v* are quantified in Figure 3-37.

In our study case, differently from (Wagner V. a., 2013) MLS solution is performed on experimental TRT temperature time series, in addition, R_b is an unknown parameter and not pre-determined separately. However, trying to comply with his estimation procedure, a correction factor for the Darcy velocity has been evaluated.

By the initial time sensitivity analysis, the solution disregarding the first 4 hours of dataset has yielded a Darcy velocity value v_{eff} of *6,6 m/day* (i.e. *7,6E-5 m/s*), considered as the *best fit solution*. But, this value does not lie inside the range of Darcy velocity values investigated by (Wagner V. a., 2013), involving the necessity to survey larger values interval for the determination of the correction factor *C*.
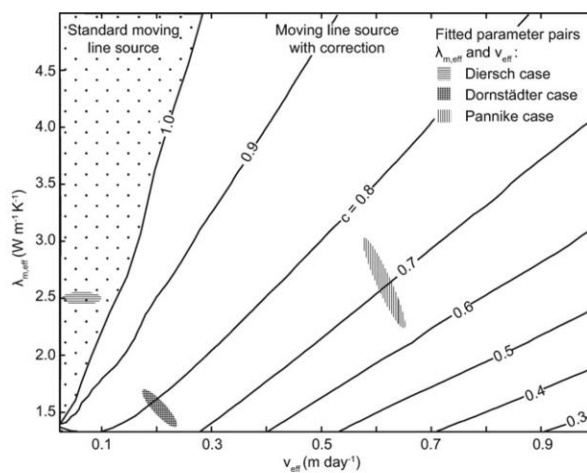
Figure 3-37 - Relation between the resulting parameters of the TRT evaluation based on MLS equation and the determined correction term *C*. For the white parameter range a correction of v_{eff} is based on Eq. 3.13.

Franco Lý

Interpretation of Borehole Heat Exchangers Thermal Response Tests under groundwater influence: analysis of three case studies

3.6 Infinite Line Source vs. Moving Line Source Approach for Claviere TRT

3.6.1 Results Comparison

By means of the MLS model an alternative method, with respect to the standard LS, to interpret TRT dataset was applied, in order to also account for advection heat exchange. Actually the Claviere TRT analysis has indicated the presence of an important groundwater flow such that the purely conductive Line Source model cannot afford to return an adequate ground thermal conductivity. A comparison between the two applied method results is then presented in Table 19.

Table 19 - Comparison between Infinite Line Source vs. Moving Line Source results.

TRT analysis / estimated parameter	ILS results	MLS *best fit solution*
Ground Thermal Conductivity [$W/(m·K)$]	Not eligible, increasing values with increasing evaluation time.	*2,77*
Borehole Thermal Resistance [$m·K/W$]	*0,106*	*0,100*
Aquifer Darcy Velocity [m/s]	Cannot be estimated by this approach.	*7,6E-05*

Ground thermal conductivity mean value is expected from geological maps evaluation to be *2,7 W/(m·K)* which is very close to the value estimated by MLS solution.

Regarding borehole thermal resistance, both ILS and MLS solutions return a reasonable value, that can be characteristic of borehole heat exchanger. Indeed borehole thermal resistance value with BHE backfilling mixture formulation B (Termoplast thermal conductivity of *2,0 W/(m·K)*) is expected to be comprised between a range of *0,070 ÷0,120 m·K/W* (Delmastro, 2011)*.

Franco Lý

*Interpretation of Borehole Heat Exchangers Thermal Response Tests
under groundwater influence: analysis of three case studies*

Table 20 - Thermal conductivity and borehole resistances values range for common filling materials, valid for both single and double-U pipe configuration (Delmastro, 2011).

Material filling type	Thermal conductivity (W/m·K)	Borehole Resistance (m·K/W)
Thermally enhanced	2,0	0,07÷0,12
Thermally enhanced	1,6	0,12÷0,16
Concrete and bentonite	0,6÷1,2	0,16÷0,20
Saturated sand	2,0÷2,5	0,04÷0,10
Dry sand	0,3÷0,6	0,20÷0,30

Aquifer Darcy velocity value is expected to be elevated because of the geological characteristics of the site, by the way, there are no comparison terms for the result since no hydraulic tests are carried out in situ. These tests would be a good practice to validate the groundwater flow values obtained by MLS method.

Comparing the two approaches used to analyze this case study, it can be stated that both analytical solutions are very effective in describing the borehole thermal resistance, while the thermal ground conductivity cannot be properly evaluated by ILS model and only MLS gives back a valid estimate according to geological preliminary assessment. Eventually, a estimated Darcy velocity is obtained by Moving Line Source model, which can support the evaluation of the hydraulic properties of the present aquifers. However, multiple solutions to the inverse problem are generally found by applying the MLS model, requiring a careful analysis based on physical consideration and solutions *RMSE* comparison to discriminate among them.

Franco Lý

Interpretation of Borehole Heat Exchangers Thermal Response Tests
under groundwater influence: analysis of three case studies

4 Thermal Response Test analysis: Trento case study

The second analyzed case study in this work is the Thermal Response Test of a pilot borehole heat exchanger located in Trento, which raw data were managed and kindly furnished by PhD geothermal consultant Andrea Zille.

4.1 Geographical Background

A geothermal survey is carried out at "Archivio Regione Trentino Alto Adige" site located in San Lazzaro, Gardolo in the municipality of Trento (TN) at the border with the district of Lavis. Placed close to a hill in West direction in respect of the same, the site is characterized by a declined ground level in South/South-West direction (Figure 4-1). The geothermal field is located on a ground level at an average elevation of about *225 m* above sea level. The area is actually occupied by building site and prefabricated frame (appendix 7.2).

Figure 4-1 - Project site : geographical location.

The test is performed with the aim to provide information about the geological background and determine the thermo-physical characteristics of the specific site in order to support the design of a new low-temperature geothermal plant with vertical BHEs.

Franco Lý

Interpretation of Borehole Heat Exchangers Thermal Response Tests
under groundwater influence: analysis of three case studies

4.2 Hydro-Geological Background

The studied area belongs to the proximal sector of the geo-morphological domain of Avisio stream alluvial conoid, recognizable in the fan-shape morphology with the extremity centered near Lavis residential area, gradually declined towards Adige river (Figure 4-2). The conoid structure has developed for debris accretion carried by Avisio stream at the outlet in the valley floor over alluvial deposits of Adige river (of glacial origins, rehashed in fluvial environment). Concerning the superior solid transport capacity of Avisio stream, the granulometry of the conoid is on average much substantial (frequent porphyritic findings) than alluvial deposits of Adige river (oozy sandy gravels/ oozy sands).

Figure 4-2 - Regional geological frame of the surveyed area, San Lazzaro (Trento).

A static water table is identified at a depth of *30÷32 m* and aquifer recharge is linked to the water from Avisio Stream along with water infiltration from surface rainfalls in the area. A deeper aquifer is localized after *100 m* in the calcareous bedrock.

Franco Lý

*Interpretation of Borehole Heat Exchangers Thermal Response Tests
under groundwater influence: analysis of three case studies*

4.2.1   Ground Stratigraphy and Thermo-Physical Characterization

The details of the stratigraphy are measured in situ, considering the resistance to drilling progress and the cores extracted in surface. On the basis of the surveyed stratigraphy during perforations phases, the subsurface can be divided into five significant geological layers. From the estimated stratigraphy, obtained in order to assess a preliminary characterization of potential heat exchange, it is possible to estimate the thermo-physical properties of the crossed layers adopting reference values from (UNI11466, 2012) for thermal conductivity (Table 21) and volumetric heat capacity (Table 23) and from (VDI4640/part2) specific heat coefficient (Table 22) and thermal diffusivity (Table 24). Considering the whole depth, weighted averages over the layer thicknesses are subsequently estimated as follows:

- the weighted average ground thermal conductivity turns out to be *2,23 W/(m·K),* while minimum and maximum values are *1,87* and *2,59 W/(m·K)* respectively*;*

- the weighted average specific heat is *911 J/(kg·K)*;

- the mean volumetric thermal capacity is *2,09 MJ/(m³K),* while, minimum and maximum values are *1,92* and *2,27 MJ/(m³K)* respectively;

- the weighted average thermal diffusivity is *0,081m²/day*

Table 21 - Subsurface column stratigraphy with associated thermal conductivity (UNI11466, 2012).

Layer depth range [m]	Layer description	Thermal conductivity [W/(m·K)]		
		Min	Max	Mean
0,0 - 2,0	Backfill of pebbly ground (dry gravel)	0,3	0,6	0,45
2,0 - 31,5	Porphyritic findings and dry gravel	1,3	1,8	1,55
31,5 -60,5	Porphyritic findings and saturated gravel	1,8	2,4	2,1
60,5 - 71,5	Sand and silt with saturated gravel	1,8	2,4	2,1
71,5 - 115	Calcareous bedrock	2,4	3,4	2,9

Table 22 - Subsurface column stratigraphy with associated specific heat (VDI4640/part2).

Layer depth range [m]	Layer description	Specific Heat [J/(kg·K)]
0,0 - 2,0	Backfill of pebbly ground (dry gravel)	800
2,0 - 31,5	Porphyritic findings and dry gravel	840
31,5 -60,5	Porphyritic findings and saturated gravel	960
60,5 - 71,5	Sand and silt with saturated gravel	960
71,5 - 115	Calcareous bedrock	920

Table 23 - Subsurface column stratigraphy with associated volumetric thermal capacity (UNI11466, 2012).

Layer depth range [m]	Layer description	Volumetric thermal capacity [MJ/(m³·K)]		
		Min	Max	Mean
0,0 - 2,0	Backfill of pebbly ground (dry gravel)	1,3	1,6	1,5
2,0 - 31,5	Porphyritic findings and dry gravel	1,3	1,6	1,5
31,5 -60,5	Porphyritic findings and saturated gravel	2,2	2,6	2,4
60,5 - 71,5	Sand and silt with saturated gravel	2,2	2,8	2,5
71,5 - 115	Calcareous bedrock	2,1	2,4	2,3

Franco Lý

Interpretation of Borehole Heat Exchangers Thermal Response Tests under groundwater influence: analysis of three case studies

Table 24 - Subsurface column stratigraphy with associated thermal diffusivity (VDI4640/part2).

Layer depth range [m]	Layer description	Thermal diffusivity [m^2/day]
0,0 - 2,0	Backfill of pebbly ground (dry gravel)	0,045
2,0 - 31,5	Porphyritic findings and dry gravel	0,056
31,5 -60,5	Porphyritic findings and saturated gravel	0,078
60,5 - 71,5	Sand and silt with saturated gravel	0,078
71,5 - 115	Calcareous bedrock	0,103

4.3 Thermal Response Test

The purpose of the test is to estimate the effective subsurface thermal conductivity λ_{eff} and to evaluate the thermal resistance R_b of the pilot borehole heat exchanger. As a general approach in this thesis, at first, a standard TRT interpretation is performed according to the ILS method. Secondly, an additional analysis by MLS approach is carried out and the results are compared with the standard approach.

4.3.1 Test Equipment

The test is carried out in situ with mobile equipment *GEOgert 2.0*, ad hoc designed to try out geothermal heat exchange. It comprises two modules, previously described in detail in section 3.3.1 as the equipment used for Claviere site is the same. However, the scheme concerning the mobile equipment *GEOgert 2.0* is reported in Figure 4-3. The measurement instruments are of the same kind used for Claviere TRT. Technical details of the instruments are provide in section 3.3.1.
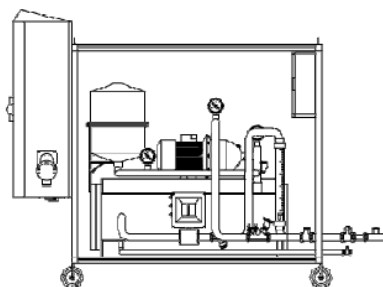
Figure 4-3 - Scheme of principle *GEOgert 2.0* mobile equipment

Franco Lý

Interpretation of Borehole Heat Exchangers Thermal Response Tests
under groundwater influence: analysis of three case studies

4.3.2 Borehole Heat Exchanger Description

The geothermal exchanger consists of a drilled borehole *115 m* deep with a diameter of *127 mm* filled with specific filling material for geothermal applications. It is made up of 2 vertical closed pipe loops with external pipe diameter of *32 mm* and internal of *26 mm*. The pipe material is high-density polyethylene, in particular HDPE Pe100 PN16 De32.

The perforation is carried out on *15/07/2013* until *17/07/2013* by GeoB S.r.l., it is performed by rotary-percussive technique with compressed air circulation and a *4''* hammer at borehole bottom equipped with borer "Odex" by means of tracked probe Atlas Copco Mustang A66 with single rotary head.

Well casings has taken place until *75 m* from ground level. Then, the work continued with only the batch of beams since the ground is constituted by calcareous bedrock, thus without risk of rockslide of the borehole walls.

The filling material adopted to fill the borehole is named Termoplast Plus. According to the(VDI4640/part2), Termoplast PLUS ® is a special blend of blast furnace cement binders, bentonite high value plastic and selected sands that can guarantee the efficiency of the full GSHP system.

Characteristics of the components for Termoplast Plus have been already illustrated in Table 9, while examples of mixture formulations are described in Table 10.

The grout hardening process started on *17/07/2013* in order to have a sufficient period (usually at least a week) for the mortar to reach its maturity, spreading the heat that the process has generated before starting the TRT.

4.3.3 Flow Test

Since the Thermal Response Test has interested a double U pipe loops, it is necessary to proceed in advance to the hydraulic connection by two delivery pipes and two runback.

Linked the pipes, the next procedure is to fill the loops. To facilitate the expulsion of air, the pipes section between borehole and machinery is declined with the highest point towards the equipment. The flow test is executed with site-water and the set pressure in the machinery is larger than *1 bar*. Once the circuit is in pressure, it is verified no presence of fluid leakage at hydraulic connections. The flow reaches the steady condition of *1234 l/h* before carrying on the Thermal Response Test.

Figure 4-4 - Connection of the two delivery pipes and two runback, GEOgert 2.0.

4.3.4 Test Operating Conditions

The response test is carried on with constant thermal injection, starting on *26/07/2013* at 11:00 and lasting until *29/07/2013* at 12:00 for *73h 00min.* However, since an unexpected blackout occurred, the effective total duration is actually equal to *58h 28min*.

The supplied nominal power set on machinery is *7,0 kW* by means of the three electrical resistances. Its corresponding specific power, i.e. averaged along the length of the borehole turns out to be *60,9 W/m*. Notwithstanding, the effective electrical and thermal power values result to be slightly inferior to this value due to mechanical and thermal dissipations that the heat carrier fluid, propylene glycol in this case, generates along its path within the closed pipe loops.

The flow rate is constantly measured by the electromagnetic flow-meter with a sampling frequency of *1 minute*, resulting to an average of *1234 l/h* with a standard deviation of *3,0 l/h* equal to *0,23%* of the mean value. Referring to this value of flow rate, the time necessary to the fluid mass to complete a loop is computed as:

$$t_{loop} = \frac{2L + L_e}{(Q/\pi r_i^2)}$$
Eq. 4.1

where:

- *L* is the borehole heat exchanger length, *115 m*;

- L_e is the total pipe length external to the borehole connected to mobile equipment, *6 m*;

- *Q* is the flow rate occurring in the vertical closed pipe loops [m^3/s];

- r_i is the internal radius for a standard HDPE Pe 100 PN16 De32 pipe [*m*].

This approach does consider the extent of pipes external to the borehole connected to the mobile equipment. The estimated time to the fluid to fulfill a complete loop is about 3*66 seconds*, i.e. about *6 minutes*. This information is useful to reduce the computational efforts for the following MLS analysis, since the sampling time has to be lower than this value (*6 minutes*) in order to have a good description of mean fluid temperature according (UNI11466, 2012). Therefore, guaranteeing an adequate precision, it can be chosen a higher sampling time than *1 minute* adopted by the data acquisition system, involving a significant improvement in diminishing the computational times for parameters estimation.

4.3.5 Undisturbed Ground Temperature

At first, a thermal log is performed with a sampling frequency of about *1 m* both for the inlet pipe (delivery) and outlet pipe (runback), for the two loops of the borehole heat exchanger in order to investigate on temperature trend at increasing depth from ground level (Figure 4-5).
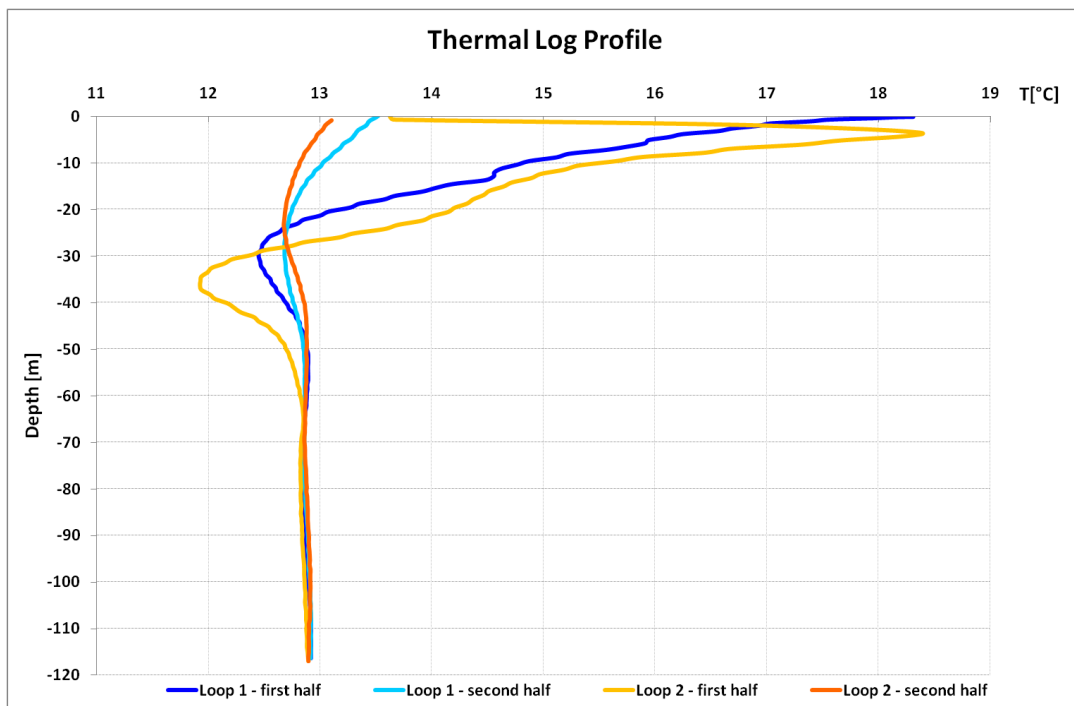
Figure 4-5 - Thermal log profile.

From the analysis of the thermal log profile, it is evident :

- the remarkable influence of the first aquifer between *30-35 m*, underlined by a negative temperature variation;
- the absence of evidences that proves the influence of temperature geothermal gradient due to the remarkable influence of groundwater flow.

The measure of the undisturbed ground temperature T_0 is carried out by circulating a fluid inside the closed pipe loops without activating none of the three electrical resistances, while data-logger is still recording. The total duration of the test is of *19,2 minutes* with a sampling time of *2 seconds*. Therefore, the fluid can reach the thermal equilibrium with the surrounding environment and, thus about the same temperature of the ground. In steady condition, the mean temperature is fixed at *13,13°C*. The thermal equilibrium is illustrated in Figure 4-6.
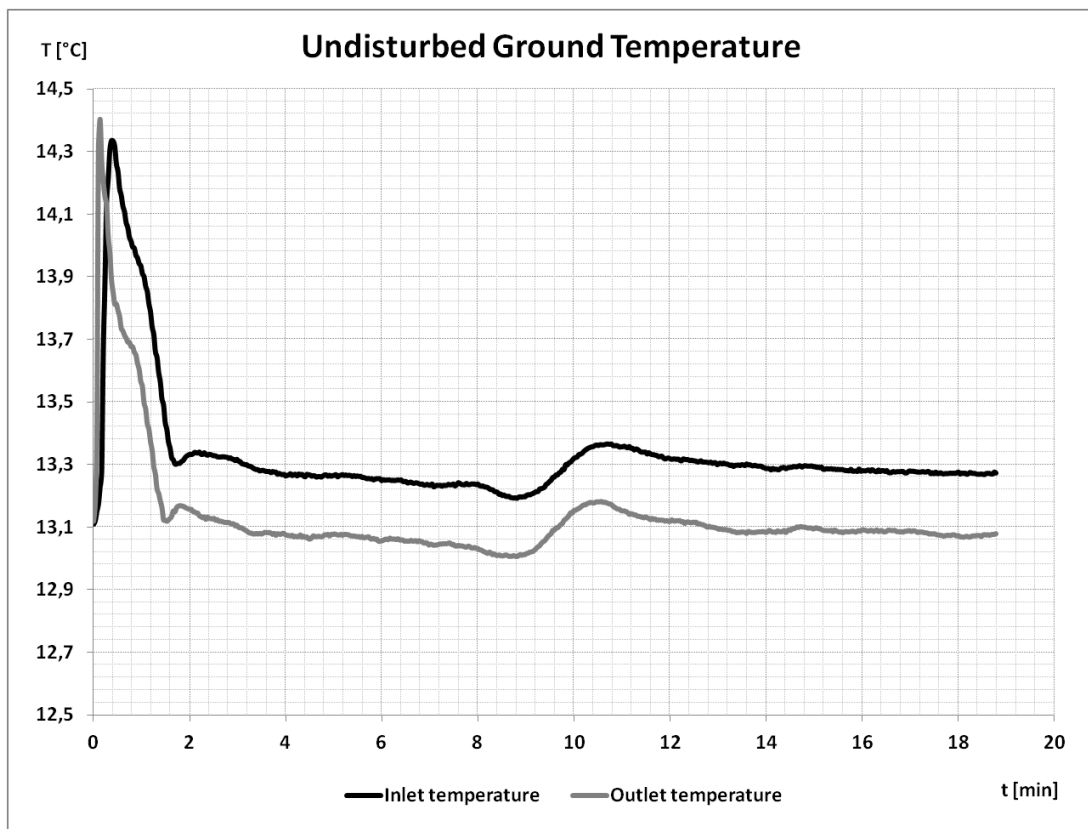
Figure 4-6 - Thermal equilibrium to evaluate undisturbed ground temperature.

4.3.6 Measurements

The first module of *GEOgert 2.0* mobile equipment is set to collect inlet and outlet fluid temperature every minutes for the total duration of the Thermal Response Test. As mentioned in section 4.3.4 the total duration is not *73 hours* as planned, but less, equal to *58 hours 28 minutes*, since an unexpected blackout occurred. However, the measurements are considered long enough in order to avoid repeating the TRT according to international recommendations, which suggests test duration longer than *50 hours*.

It is reported in Figure 4-7 the plot of the measured inlet and outlet fluid temperature time series.
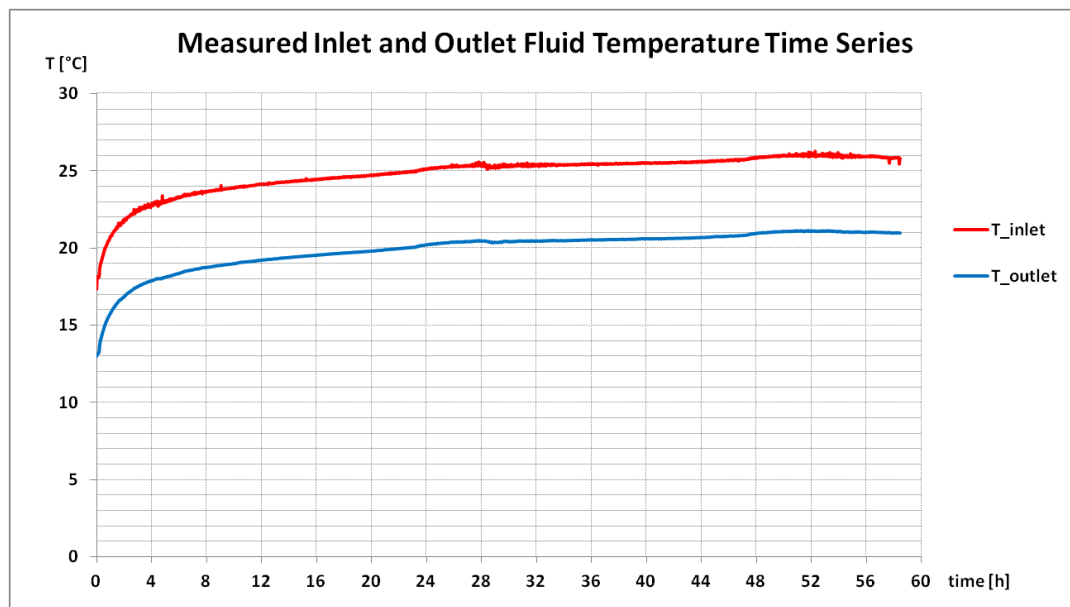
Figure 4-7 - Measured inlet and outlet fluid temperature time series.

The increasing logarithmic trend of the two temperature time series is regular along the test with just some scattering around *28 hours* and *52 hours*.

The electromagnetic flow-meter has recorded the flow-rate in the vertical closed pipe loops, exhibiting a constant trend in time after an initial stabilization, as reported in the Figure 4-8. The mean volumetric flow rate results to be of *1234 l/h* with a standard deviation of *3,0 l/h* equal to *0,23%* of the mean value.
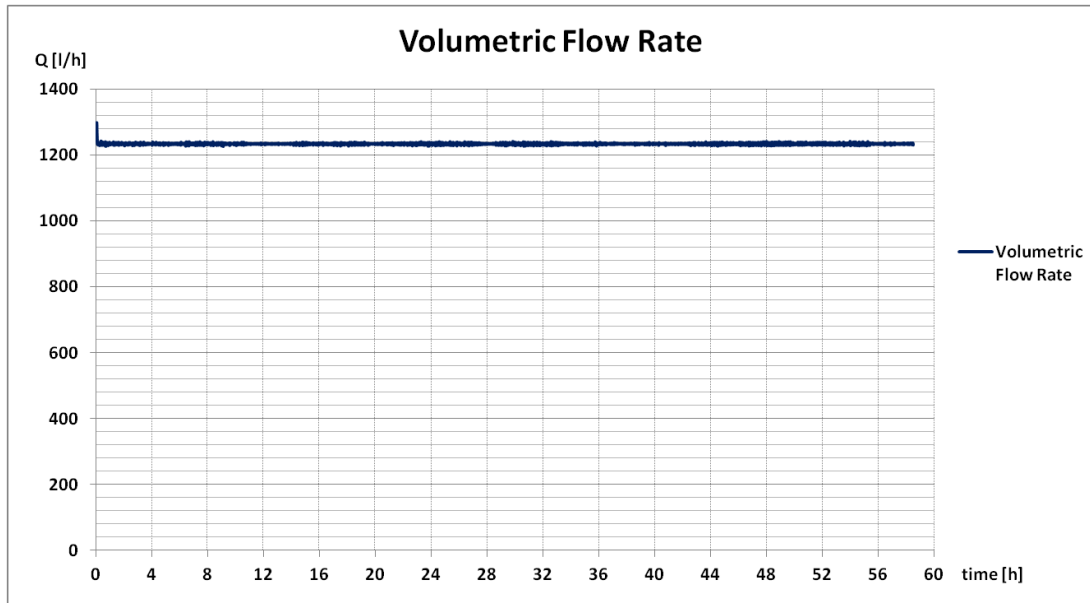
Figure 4-8 - Volumetric Flow Rate inside the vertical pipe loops.

The heat carrier fluid flow rate is sufficient to comply the recommendations given in (UNI11466, 2012), since it guarantees a temperature differences between inlet and outlet temperature comprised between *3K* and *7K* (in this case about *4,8K*).

Concerning to the effective electrical (three phases) and thermal power, they are obtained at every minutes according to the following equations :

Effective electrical power $\qquad Q_{el} = \Sigma \ (V \cdot I \cdot cos \ \varphi)$ **Eq. 4.2**

where:

- *V* is the electrical potential measured for the three phases R, S and T every minute [*Volt*];

- *I* is the current intensity measured for the three phases R, S and T every minute [*Ampere*];

- *φ* is the offset angle measured for the three phases R, S and T every minute [°]

Effective thermal power $\qquad Q_{th} = c_f \cdot Q \cdot \varDelta T$ **Eq. 4.3**

where:

- c_f is the fluid specific heat, for the propylene glycol *3930* [*kJ/(°C l)*];

- *Q* is the flow rate occurring in the vertical closed pipe loops [*l/min*];

- *ΔT* is the temperature difference between inlet and outlet pipes at every minute [*°C*]
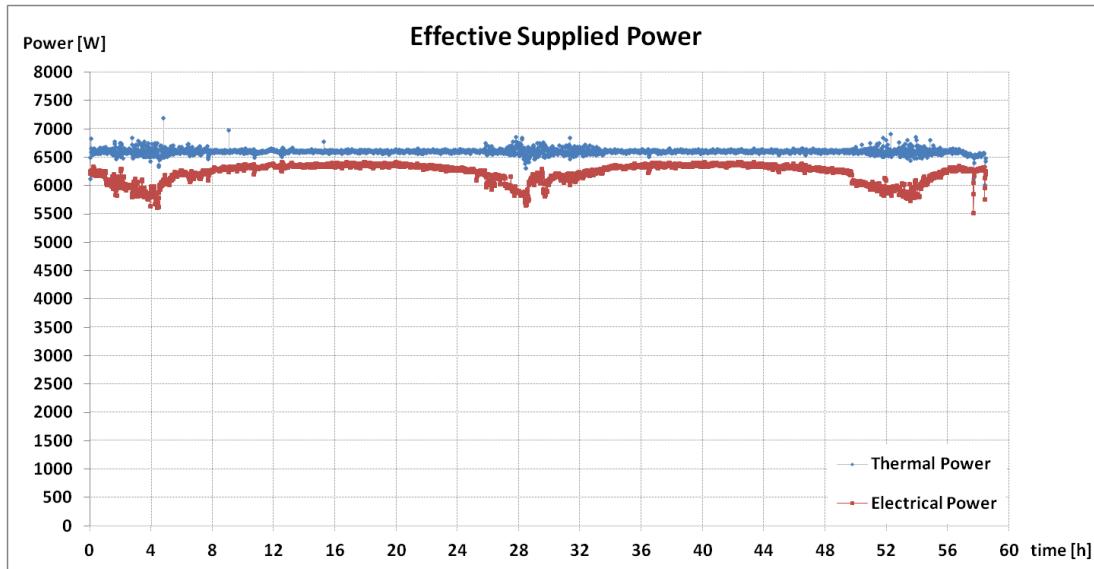
Figure 4-9 - Effective electrical and thermal power.

The effective mean thermal power averaged on the total duration results to be equal to *6598,6 W* with a standard deviation of *47,7 W* equal to *0,72%*. This value is more precise than the effective electrical power, which has a mean of *6228,6 W* with a standard deviation of *158,6 W* equivalent to *2,55%*. The difference of *5,61%* between mean power values is evident in Figure 4-9, where the electrical power trend exhibits leaks of supply in three time intervals. The blackout event can be also noticed at the end of test. However, both thermal and electrical power values will be used for standard TRT analysis by Infinite Line Source theory. According to (UNI11466, 2012) both standard deviations have to be lower than ±*1,5%* of the mean value. In this case only the thermal power complies this recommendation, while the electrical power standard deviation exceeds the limit of *1,5%*. Thus, it is clear that thermal power trend is more reliable than electrical power one.

Considering the total length of the borehole, the resulting specific thermal and electrical power are calculated by means of the following equations:

Effective specific thermal power $q_{th} = Q_{th}/L$ **Eq. 4.4**

Effective specific electrical power $q_{el} = Q_{el}/L$ **Eq. 4.5**

From the calculations, they result to be respectively *57,40 W/m* and *54,40 W/m,* where the effective specific thermal power is considered to be more reliable.

4.4 TRT Analysis by means of Infinite Line Source Theory

The first analysis to evaluate the TRT is based on ILS theory. This approach approximates the BHE as an infinite line source in a homogeneous, isotropic and infinite medium, which injects or extract a constant amount of energy by conductive heat transport only (Wagner V. a., 2013).

First of all, to conduct a line source analysis, the mean fluid temperature time series is obtained from the instantaneous arithmetic mean of two temperature time series.

$$T_{fm} = \frac{T_{in} - T_{out}}{2}$$ **Eq. 4.6**

It is compared with inlet and outlet fluid temperature time series as showed in Figure 4-10.
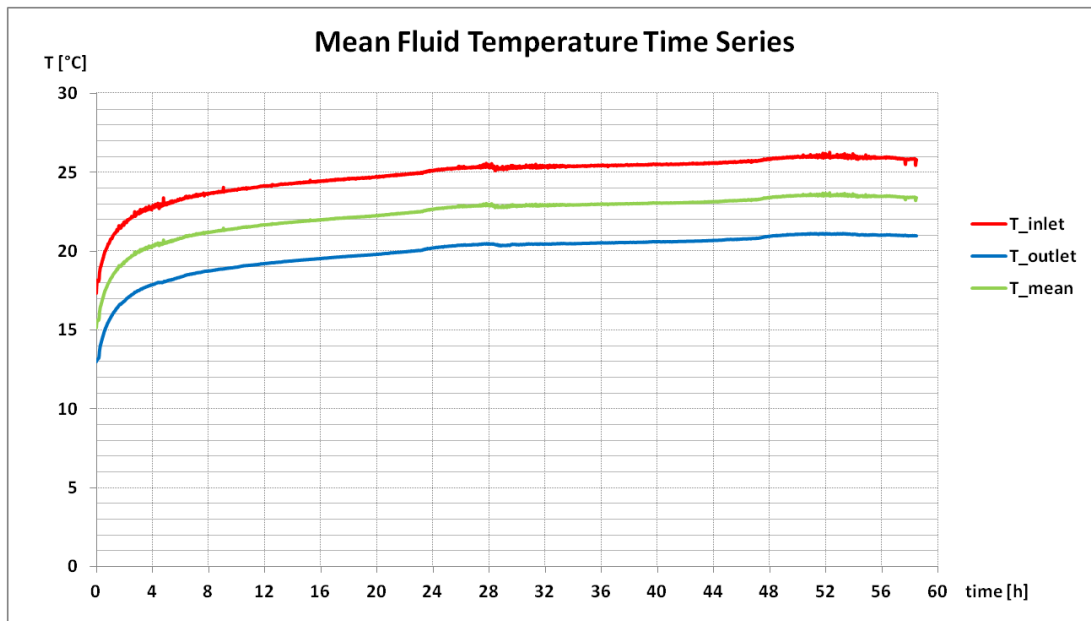
Figure 4-10 - Mean fluid temperature time series.

As previously presented in section 2.5, according to the LS approach, the heat carrier mean fluid temperature change in time according to the following relation:

$$T_{fm} \approx \frac{q}{4\pi\lambda_{eff}} ln(t) + q\left[R_b + \frac{1}{4\pi\lambda_{eff}}\left(ln\left(\frac{4a}{r_{bw}^2}\right) - \gamma\right)\right] + T_0$$ **Eq. 4.7**

Franco Lý

Interpretation of Borehole Heat Exchangers Thermal Response Tests
under groundwater influence: analysis of three case studies

According to section 2.5 the criterion for the logarithmic approximation has to be fulfilled:

$$t \geq t_c \geq \frac{5r_{bw}^2}{a}$$

Eq. 4.8

As a first guess, previously estimated values (see section 4.2.1) for thermal capacity and thermal conductivity are used, namely *C = 2,27 MJ/(m³·K)* and *λ = 2,23 W/(m·K)*. Thus, a value of thermal diffusivity *a* is derived equal to *9,8E-7 m²/s*.

Adopting this value, the time criterion is fulfilled for times larger than *5,69 hours*. Thus, t_{in} = *6 hours* is adopted as initial time for TRT interpretation by means of Infinite Line Source model.

4.4.1 Estimate of the Effective Ground Thermal Conductivity

Therefore, the thermal conductivity is indirectly estimated by the slope *A* of the interpolating straight line for the measurement in a plot where x-axis corresponds to the logarithm of time:

$$\lambda_{eff} = \frac{q}{4 \cdot \pi \cdot A}$$

Eq. 4.9

The conductivity estimation is carried on varying t_{end} from *30 hours* to *58 hours* i.e. the total duration of the test before the blackout with a *4 hours* step. This method permits to understand the sensitivity of the thermal conductivity to the evaluation time of the TRT. An example of linear interpolation is illustrated for *t $_{end}$ = 58 hours* in Figure 4-12.

The theoretical model of test interpretation expects that temperature time series represented in a plot with *ln(t)* in the x-axis to be almost rectilinear. In this specific case, the trend does match the fluid mean temperature time series, even if some evident irregularities around *28* and *52 hours* are however present in Figure 4-12. This scattered measurement that does not follow the linear trend may be caused by external disturbance due to daily temperature fluctuations along with not adequately insulated pipe at the head of the double U-pipe.

From Figure 4-11 the small temperature oscillations may be correlated to external noise influence due to warm air temperature and solar radiation in the hottest hours of the day. In addition, the influence is underlined by the fact that the TRT is run exactly in the middle of July, a very warm month that emphasize daily temperature fluctuations.
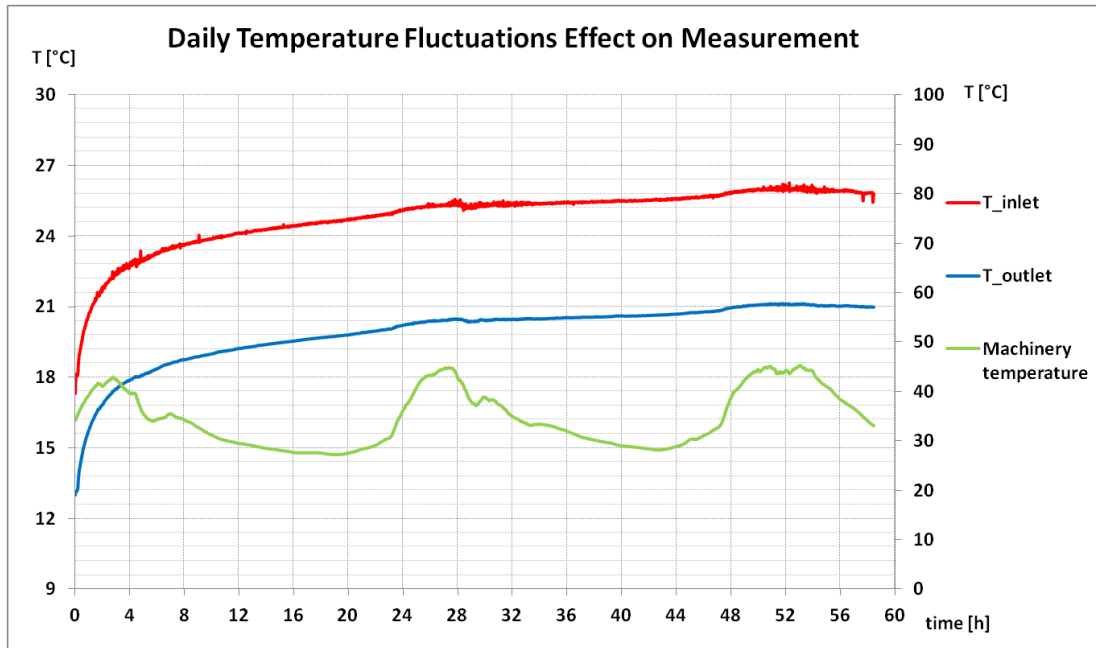
Figure 4-11 - Correlation between external influence and measured temperature time series

From the linear interpolation in Figure 4-12, in the semi-log plot, the coefficient of determination R^2 returned a value of *0,9835* proximal to the unity, indicating an elevated level of correspondence between measured values and estimated values by trend.
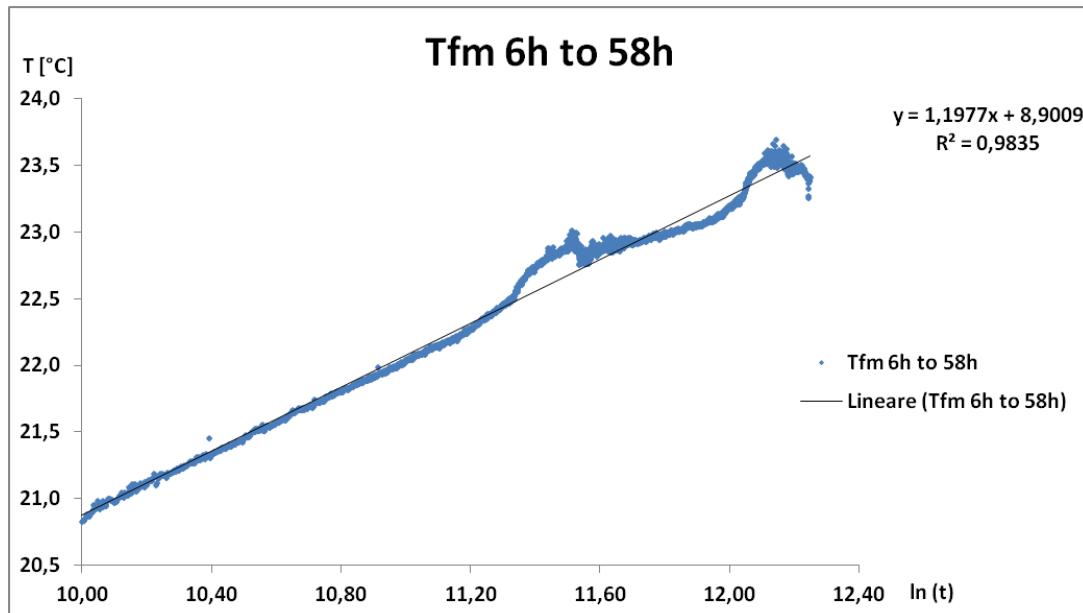
Figure 4-12 - Linear interpolation for data interval from 6h to 58h

Franco Lý

Interpretation of Borehole Heat Exchangers Thermal Response Tests
under groundwater influence: analysis of three case studies

The ground thermal conductivity estimation is performed considering both thermal and electrical specific power. Their trends Figure 4-13 shows an initial increase of conductivity values until a stabilization for larger t_{end}, although ground thermal conductivity values obtained from electrical specific power are always slightly lower due to the fact that recorded electrical power is resulted to be inferior to calculated thermal power.

Observing the plot in Figure 4-13, however, the estimated conductivity values are always located well above the expected conductivity of the specific subsurface column estimated by literature values. This high values may be explained by the influence of an important groundwater presence which enhances the effective ground thermal conductivity. This aspect will be further analyzed in section 4.4.3.

The conductivity values trend estimated by Infinite Line Source approach seems to indicate light oscillations at increasing t_{end}, even if for late evaluation time they seem to converge.

Therefore, considered these light variations, it is preferred to choose the arithmetic mean of the last 4 estimated values for both ground thermal conductivity series (thermal and electrical), resulting respectively *3,81 W/(m·K)* and *3,62 W/(m·K)*. As a consequence, these values differs each other of *5,02%*. In case of longer duration of the test (as it was planned of *73 hours*), it would have been an assist to understand if the values were converging to a stable value. A margin of uncertainty is present, but it cannot be solved by this analysis.
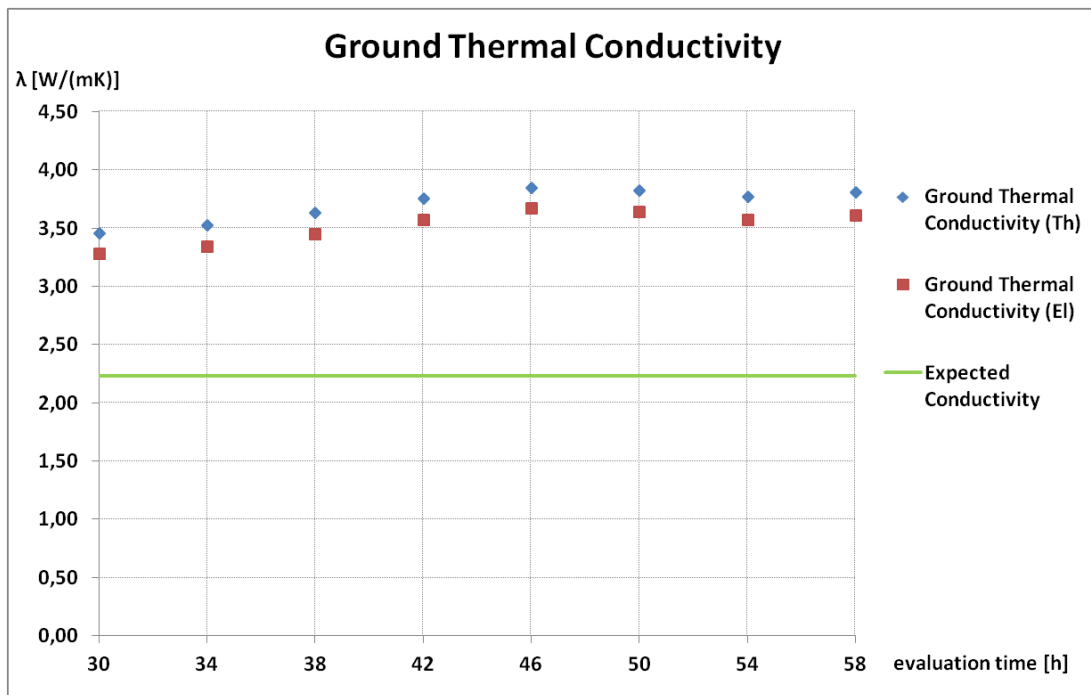
Figure 4-13 - Ground thermal conductivity trend for increasing evaluation time.

4.4.2 Estimate of the Borehole Thermal Resistance

According to ILS theory, the borehole thermal resistance is thus evaluated in a similar approach, i.e. increasing the evaluation time from *30 hours* to *58 hours* with a time step *Δt* of *4 hours*.

$$R_b = \frac{B - T_0}{q} - \frac{1}{4\pi\lambda_{eff}}\left[ln\left(\frac{4a}{r^2}\right) - \gamma\right]$$ **Eq. 4.10**

The plot in Figure 4-14 depicts the borehole thermal resistance values for both thermal and electrical specific power. The estimated values for larger evaluation times approach to *0,074 m·K/W* and *0,078 m·K/W* respectively. The trend exhibits light oscillations of the borehole thermal resistance series for electrical and thermal cases. In this case, it is very likely that a longer TRT would have supported a more precise evaluation of the parameter. Nevertheless, the results are quite satisfying and are considered valid to describe borehole thermal resistance, like for thermal conductivity values trend.
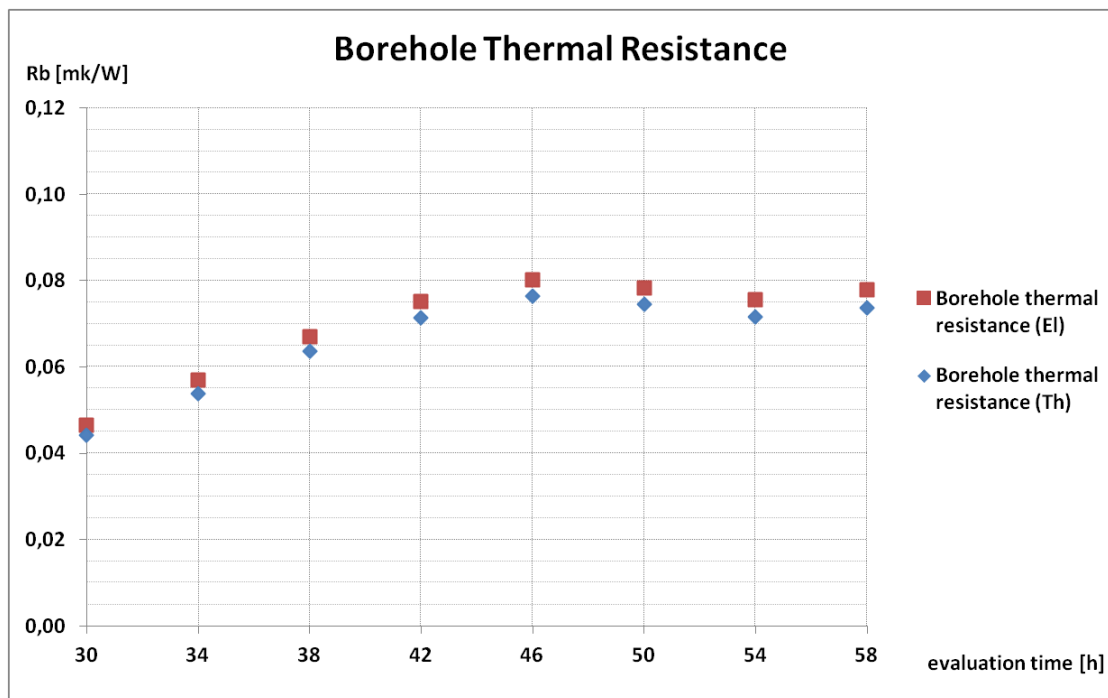
Figure 4-14 - Borehole thermal resistance values for increasing evaluation time.

Franco Lý

Interpretation of Borehole Heat Exchangers Thermal Response Tests under groundwater influence: analysis of three case studies

4.4.3   Results Discussion

In general, the Infinite Line Source approach for TRT interpretation of Trento case study has yielded satisfying results, even if the total duration of the tested data was limited to about *58 hours 28 minutes*, due to an unexpected blackout. The difference in effective specific supplied power, between thermal and electrical mean power of *5,61%*, has originated a *5,02%* difference between estimated effective thermal ground conductivity and a *5,01%* difference between estimated borehole thermal resistance.

However, if (UNI11466, 2012) recommendations were fulfilled, effective electrical power would have been disregarded, since standard deviation has to be inferior to *±1,5%* of the mean value. In fact, the electrical power standard deviation exceeds the limit of *1,5%*, entailing the effective thermal power values as the reliable constant power to be considered for ground conductivity and borehole thermal resistance.

ILS model adequately fits data measurement, in fact the linear interpolation in the semi-log plot gives back a coefficient of determination R^2 of *0,9835* proximal to the unity guaranteeing the goodness of the following calculations to estimate thermal properties within this method.

Estimated ground thermal conductivity values for increasing evaluation time have demonstrated to be sufficiently stable for large times approaching to *3,84 W/(m·K)* in case of thermal power values; however, as previously mentioned the duration of the test was meant to be *73 hours* and not *58 hours*. This additional hours would have helped to be more confident with the results from the effective ground thermal conductivity estimation.

Furthermore, the evaluated λ_{eff} turns out to be larger than expected mean value estimated by literature table by about *70%* (expected ground thermal conductivity estimated by stratigraphy analysis equal to *2,23 W/m·K*). This remarkable increase may be explained by the significant influence of groundwater flows in the aquifers localized at *30÷32 m* and at *100 m* below ground level, which enhances heat exchange phenomena.

Relatively to the borehole thermal resistance, the estimated values for larger evaluation times approach to *0,073 m·K/W* using the thermal power measurements. This value is quite reliable and predictable considering the borehole geometry, the filling material conductivity and the fact that is a double U-pipe loop.

In fact borehole thermal resistance value with a mixture formulation B (estimated Termoplast thermal conductivity of *2,0 W/m·K*) is expected to be comprised between a range of *0,070 ÷0,120 m·K/W* as reported in Table 20.

Franco Lý

Interpretation of Borehole Heat Exchangers Thermal Response Tests
under groundwater influence: analysis of three case studies

4.5 Coupled Conductive - Advective Analysis by means of Moving Line Source Theory

The results obtained from Trento TRT interpretation by Infinite Line Source approach proved to be not entirely satisfying, since ground thermal conductivity appears to be overestimated with respect to literature. Moreover observations from thermal log profile and the presence of groundwater suggests an additional analysis to verify the validity of the TRT interpretation and to evaluate groundwater flow velocity.

As previously commented in section 2.6.1, the MLS script in MATLAB used for a 3 parameters estimation, neglects the effect of thermal longitudinal and transversal dispersivity according to (Wagner V. a., 2013).

4.5.1 MLS Analysis Settings

The script is updated to embed specific geological site features and borehole characteristics for Trento TRT and the script is run in order to estimate λ, v and R_b.

To appropriately comprehend the influence of initial parameters, it is proposed to originate a 100 combinations matrix, thus constituted by 100 line vectors of the three parameters. This systematic scheme of initial parameters is defined based on considerations hereafter explained and will be used for further parameters estimation for this specific case.

About ground thermal conductivity, the available geological information indicates to use a wide a range of possible values (Table 25).

Table 25 - Ground thermal conductivity initial values used for MLS solution fit.

Ground Thermal Conductivity [$W/(m \cdot K)$]	1,5	2,0	2,5	3,0	3,5

Concerning Darcy velocity, identified an important groundwater presence in this specific site and considered the geological subsurface characteristic, relatively significant velocity are considered, however accounting for a large possible interval as shown in Table 26.

Table 26 - Darcy velocity initial values used for MLS solution fit.

Aquifer Darcy Velocity [m/s]	1,0E-4	1,0E-5	1,0E-6	1,0E-7	1,0E-8

Aquifer Darcy Velocity [m/day]	8,64	0,864	0,0864	0,00864	0,000864

The same values are shown both in *m/s* and *m/day*, since they are both commonly used.

Regarding borehole thermal resistance, a range of values commonly recurrent for the double U pipe loop scheme are suggested in Table 27.

Table 27 - Borehole thermal resistance initial values used for MLS solution fit.

Borehole Thermal Resistance [m·K/W]	0,06	0,09	0,12	0,15

A numerical step of *1E-3* is so kept constant for all the fits according to the consideration discussed in section 3.5.1.

Furthermore, since the loop circulation time is equal to *6 minutes* as previously calculated, (UNI11466, 2012) suggests sample time lower than the loop circulation time. Then, it is adopted a sampling time of *2 minutes* equivalent to about a third of the loop circulation time (*6 minutes*). This is very compliant in reducing the dataset, diminishing the computational efforts to run the minimization process by MATLAB.

4.5.2   Time Criterion for Initial Data Significativity

Assuming a parallel approach to ILS model for TRT interpretation, a time criterion for data significativity is proposed in section 2.6.2. A first guess Darcy velocity is required, such to roughly estimate the time that is necessary for the borehole volume to almost reach steady state.

Hence, taking into consideration the hydrogeological characteristics of the site a initial Darcy velocity *v* of *5E-6 m/s* is supposed. For an undisturbed ground temperature T_0 = *13,13°C* the following parameters are evaluated:

$$Re_L = \frac{\rho \cdot v \cdot L}{\mu} = \frac{1000 \cdot 5 \cdot 10^{-6} \cdot 0,127}{1,23 \cdot 10^{-3}} = 0,52$$

$$Pr = \frac{v}{a} = 8,81$$

$$\overline{Nu} = C \, Re_L^m \, Pr^{1/3} = 0,989 \cdot 0,52^{0,33} \cdot 8,81^{1/3} = 1,64$$

Franco Lý

Interpretation of Borehole Heat Exchangers Thermal Response Tests under groundwater influence: analysis of three case studies

$$\overline{h} = \frac{\overline{Nu} \cdot \lambda}{L} = \frac{1,64 \cdot 0,586}{0,127} = 7,59 \, W/_{m^2 K}$$

Recalling the thermal time constant (**Eq. 2.41**) interpreted as:

$$\tau_t = \frac{\rho_g \cdot r_b \cdot c_g}{h \cdot 2} = 0,76 \, h$$

And the characteristic time t_c (**Eq. 2.42**) is defined as:

$$t_c = (4 \div 5) \, \tau_t = 3,0 \div 3,8 \, h$$

4.5.3 Initial Time Sensitivity Analysis

Time criterion returns about an approximate characteristics time of *4 hours*, which will be considered as one of the initial time values of the sensitivity analysis (Table 29).

A round of fits is carried out with an initial time t_{in} = *10 h* and a final time t_{end} = *58h 28min* in order to have an outline of the solutions.

The sets of parameters obtained by the estimation procedure are characterized by a *RMSE*, calculated by means of **Eq. 2.35**. The script generates MLS solutions described in Table 28.

The results obtained by the 100 fits with the above imposed conditions are 48 sets of three parameters with *RMSE* ranging from *0,131°C* to *0,145°C*. Negative values of *v* are converted to positive for further analysis. The most recurrent solution cover the *45,0%* of the fits (45 solutions on 100 fits). 54 solutions result to have same λ and R_b, but different *v* values.

Table 28 - Solutions from MLS analysis with t_{in} = *10 h* and t_{end} = *58 h 28 min*.

Solution	Fitted Parameter Values			f [%]	RMSE [°C]
	λ [W/mK]	v [m/s]	Rb [mK/W]		
1	0,60	2,1E-05	0,152	45,00%	0,131
2	2,18	1,1E-07	0,149	3,00%	0,145
3	2,18	1,1E-08	0,149	3,00%	0,145
4	2,18	2,5E-08	0,149	2,00%	0,145
5	2,18	8,5E-07	0,149	2,00%	0,145
6	2,18	8,6E-08	0,149	2,00%	0,145
7	2,18	8,6E-09	0,149	2,00%	0,145
8	2,18	2,5E-09	0,149	1,00%	0,145
9	2,18	2,5E-10	0,149	1,00%	0,145

10	2,14	1,6E-06	0,150	1,00%	0,145
11	2,18	5,0E-07	0,149	1,00%	0,145
12	2,18	5,0E-08	0,149	1,00%	0,145
13	2,18	5,0E-09	0,149	1,00%	0,145
14	2,18	2,0E-09	0,149	1,00%	0,145
15	2,18	2,0E-10	0,149	1,00%	0,145
16	2,18	2,0E-11	0,149	1,00%	0,145
17	2,18	2,3E-07	0,149	1,00%	0,145
18	2,18	2,3E-08	0,149	1,00%	0,145
19	2,18	2,3E-09	0,149	1,00%	0,145
20	2,18	2,5E-07	0,149	1,00%	0,145
21	2,18	2,4E-09	0,149	1,00%	0,145
22	2,18	9,1E-08	0,149	1,00%	0,145
23	2,18	8,9E-09	0,149	1,00%	0,145
24	2,18	8,9E-10	0,149	1,00%	0,145
25	2,18	7,5E-07	0,149	1,00%	0,145
26	2,18	7,5E-08	0,149	1,00%	0,145
27	2,18	7,5E-09	0,149	1,00%	0,145
28	2,18	4,0E-07	0,149	1,00%	0,145
29	2,18	4,0E-08	0,149	1,00%	0,145
30	2,18	4,0E-09	0,149	1,00%	0,145
31	2,18	8,5E-08	0,149	1,00%	0,145
32	2,18	8,5E-09	0,149	1,00%	0,145
33	2,18	7,0E-07	0,149	1,00%	0,145
34	2,18	7,0E-08	0,149	1,00%	0,145
35	2,18	7,0E-09	0,149	1,00%	0,145
36	2,18	6,6E-07	0,149	1,00%	0,145
37	2,18	6,6E-08	0,149	1,00%	0,145
38	2,18	6,6E-09	0,149	1,00%	0,145
39	2,18	8,9E-07	0,149	1,00%	0,145
40	2,18	8,0E-08	0,149	1,00%	0,145
41	2,18	8,0E-09	0,149	1,00%	0,145
42	2,18	1,1E-06	0,150	1,00%	0,145
43	2,18	9,4E-08	0,149	1,00%	0,145
44	2,18	9,4E-09	0,149	1,00%	0,145
45	2,18	1,0E-07	0,149	1,00%	0,145
46	2,18	1,0E-08	0,149	1,00%	0,145
47	2,18	1,2E-07	0,149	1,00%	0,145
48	2,18	1,2E-08	0,149	1,00%	0,145

To have a general overview of the parameters estimation results, a summary plot from all the fits for an initial time t_{in} = *10 hours* and t_{end} equal to the total duration of the test is given for each fitting parameter (λ, R_b and v).
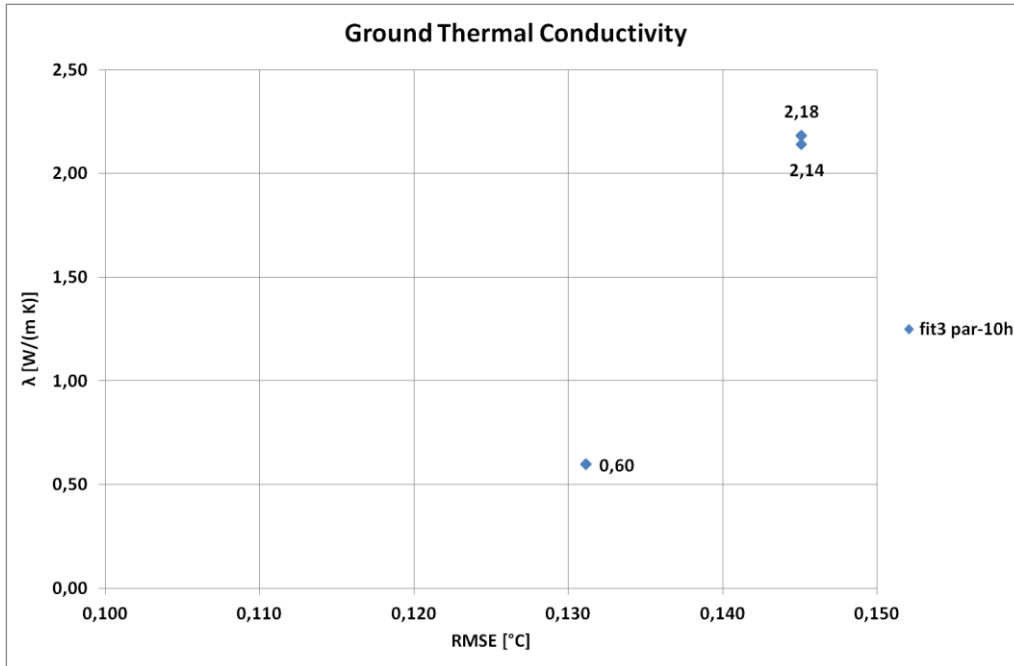
Figure 4-15 - Summary plot of fitted ground thermal conductivity values for t_{in} = 10 h and t_{end} = 58 h 28 min.
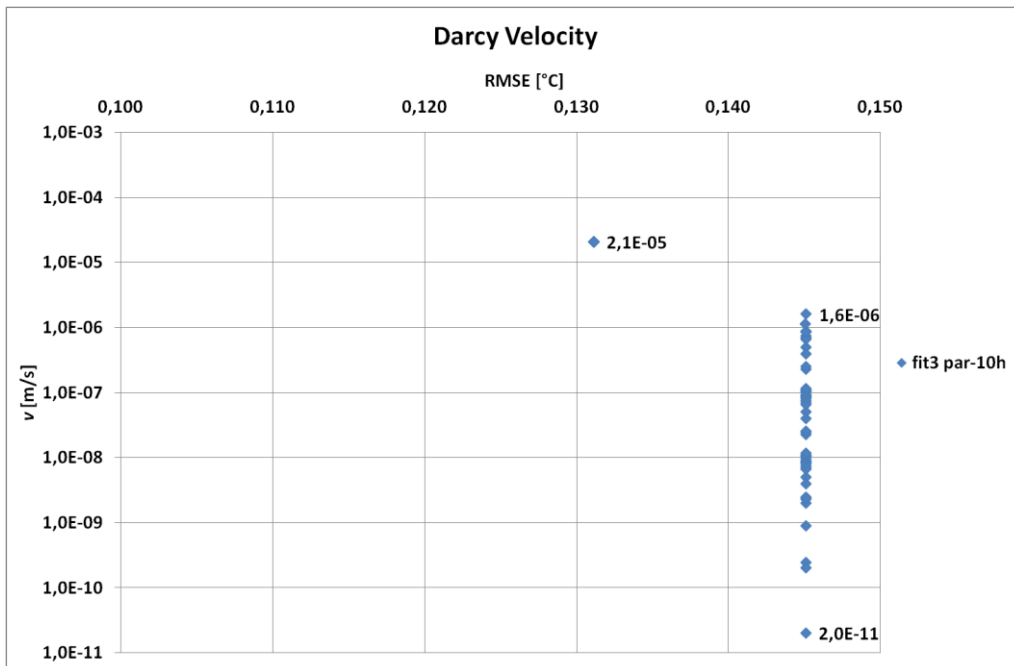
Figure 4-16 - Summary plot of fitted Darcy velocity absolute values for t_{in} = 10 h and t_{end} = 58 h 28 min.

Franco Lý

Interpretation of Borehole Heat Exchangers Thermal Response Tests under groundwater influence: analysis of three case studies

Relative to fitted ground thermal conductivity summary plot in Figure 4-15, the lowest *RMSE* value of *0,131°C* corresponds to a very low ground thermal conductivity of *0,60 W/m·K* (*45* solutions on *100*). The remaining solutions with *RMSE* around *0,145°C* refer to a more realistic thermal conductivity of *2,18 W/m·K* except for a single value of *2,14 W/m·K* (solution 10). It has to be remarked that they correspond to *RMSE* values which are only slightly larger than the best fit *RMSE*.

Regarding fitted Darcy velocity summary plot in Figure 4-16, the corresponding value of this parameter for the lowest values of *RMSE* is *2,1E-5 m/s* in absolute value. All the other values of Darcy velocity are relative to a slightly higher *RMSE* of *0,145°C*, which range on a very large interval from *2,0E-11 m/s* to *1,6E-6 m/s*. However, these values are all coupled with the same ground thermal conductivity of *2,18 W/m·K* and resulting in the same MLS temperature time series. Further considerations will be given in next section 4.5.4 and 4.6.
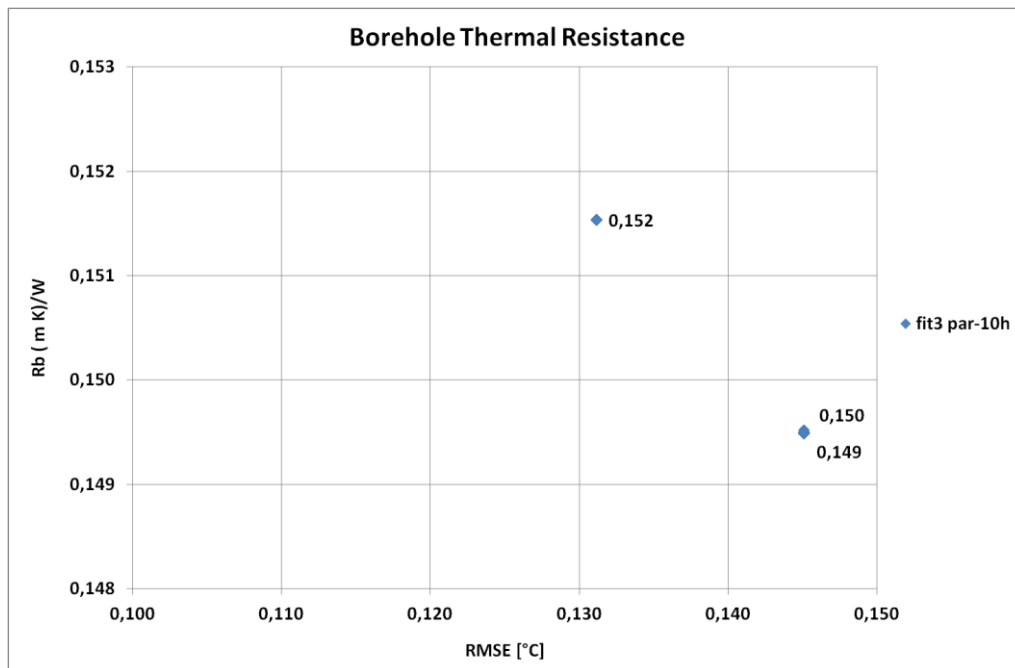
Figure 4-17 - Summary plot of fitted borehole thermal resistance values for *t_{in} = 10 h* and *t_{end} = 58 h 28 min*.

Concerning the fitted borehole thermal resistance summary plot in Figure 4-17, three different values can be identified. The lowest *RMSE* value correspond to R_b values slightly lower than *0,152 m·K/W*; while for *RMSE* values around *0,145°C* corresponds R_b = *0,149 m·K/W*. Solution 10 presents a R_b = *0,150 m·K/W*.

Franco Lý

*Interpretation of Borehole Heat Exchangers Thermal Response Tests
under groundwater influence: analysis of three case studies*

Differently from the previous case study, the final time sensitivity analysis is not performed since no steady state conditions are reached in the fluid profile temperature profile. Nevertheless, a series of fits are carried out with the aim of understanding initial time influence to Moving Line Source solution and trying to validate the time criterion for data significativity previously established in section 2.6.2.

The parameters estimation by MLS script is performed using as initial parameters the systematic scheme already described of 100 combinations (section 4.5.1) for 6 times, disregarding initial data according to Table 29. The considered evaluation time is the total duration of the test kept constant for all the fits equal to *58 hours 28 minutes*.

<div align="center">**Table 29 - Initial time values used for the sensitivity analysis.**</div>

Initial time	12 min	2 hours	4 hours	6 hours	8 hours	10 hours

The time value of *12 minutes* is the value around which the mean temperature time series seems graphically to be affected by the heat injection and so start to increase (Figure 4-18). This was the result of a first attempt to understand how to disregard initial data.
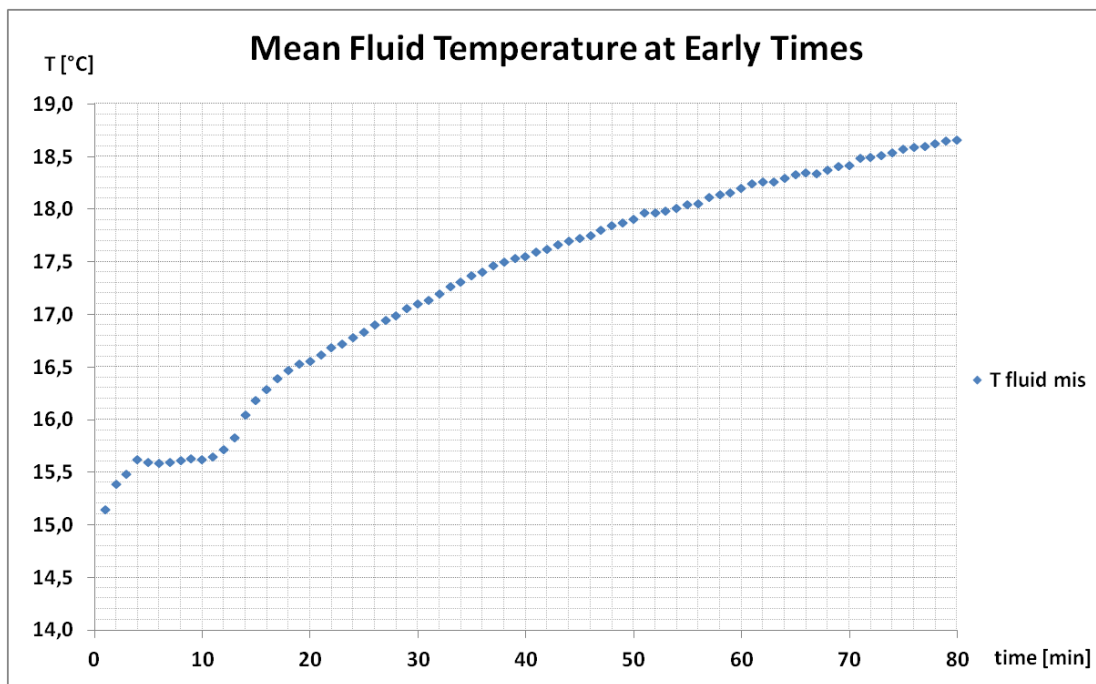
<div align="center">**Figure 4-18 - Mean fluid temperature at early times.**</div>

Franco Lý

Interpretation of Borehole Heat Exchangers Thermal Response Tests under groundwater influence: analysis of three case studies

A great improvement of $RMSE_{average}$ by increasing the initial time t_{in} can be noticed in Figure 4-19. The diminishment of $RMSE$ is already about *41%* from disregarding first *12 minutes* to *2 hours*. It can be reasonably stated that $RMSE$s of the solutions, after disregarding two hours converge to stable values for increasing initial times, as a smooth trend of $RMSE$ values can be observed approaching to an initial time t_{in} = *10 hours*.
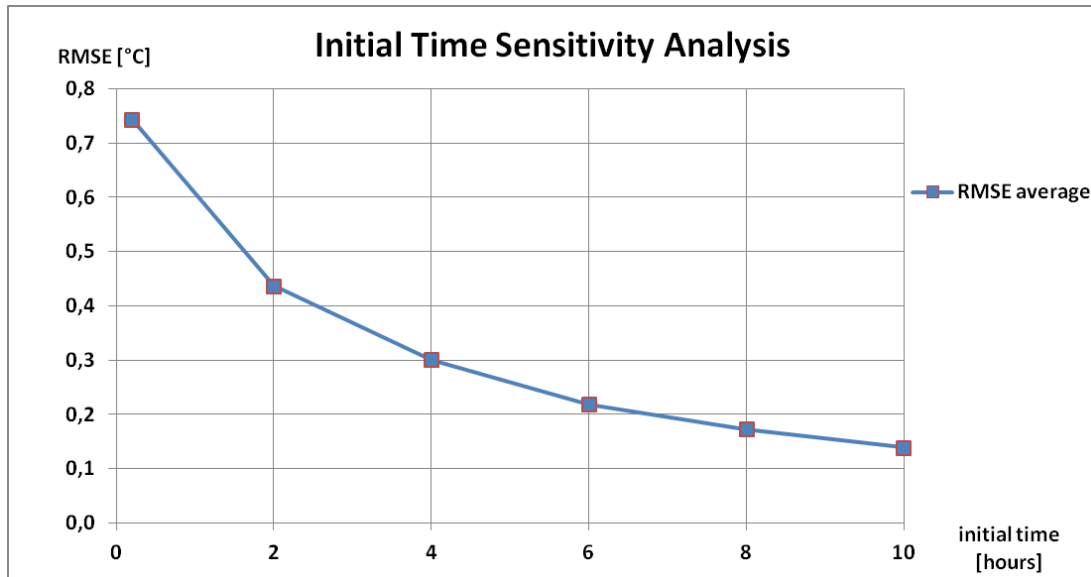
Figure 4-19 - $RMSE_{average}$ trend for increasing initial time.

Then, the initial time sensitivity analysis allows to individuate t_{in} = *10 h* as the initial time value to be considered for its low $RMSE_{average}$. Therefore, some examples of resulting plots of the Moving Line Source model fits are illustrated for an initial time t_{in} = *10 h*.

As reported in Table 28, solution 1 covers the *45%* of the fits, for a final time t_{end} = *58h 28min*. With the exception of solution 10, the other solutions consist in the *54%* of the total fits. They are characterized by the same λ, R_b and $RMSE$ values, but fitted Darcy velocity values range in a wide interval from *2,0E-11 m/s* to *1,1E-6 m/s*.

Aside from solution 10, which is illustrated in Figure 4-20, there are two main solutions that cover the *99%* of the results:

— solution **1** [*λ = 0,60 W/(m·K); v = 2,1E-5 m/s; R_b = 0,152 m·K/W*];

— solution **a** [*λ = 2,18 W/(m·K); v = 2,0E-11 ÷ 1,1E-6 m/s; R_b = 0,152 m·K/W*]

Solution **1** is illustrated in Figure 4-21, while solution **a** is depicted in Figure 4-22.
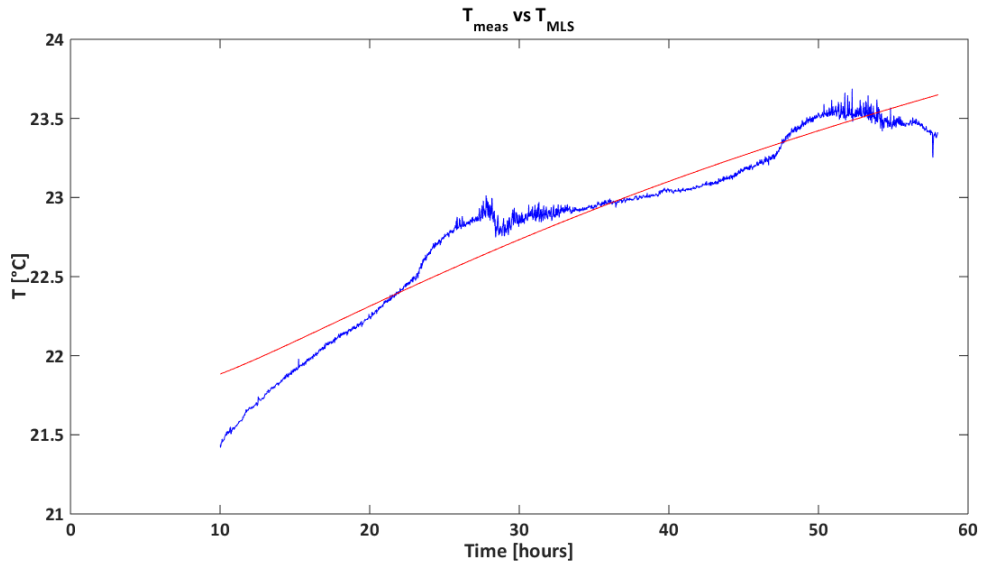
Figure 4-20 - Plot of measured data (blue line) vs. MLS temperature time series (red line) for t_{in} = 10 h and t_{end} = 58 h 28 min, solution 10 of Table 28.
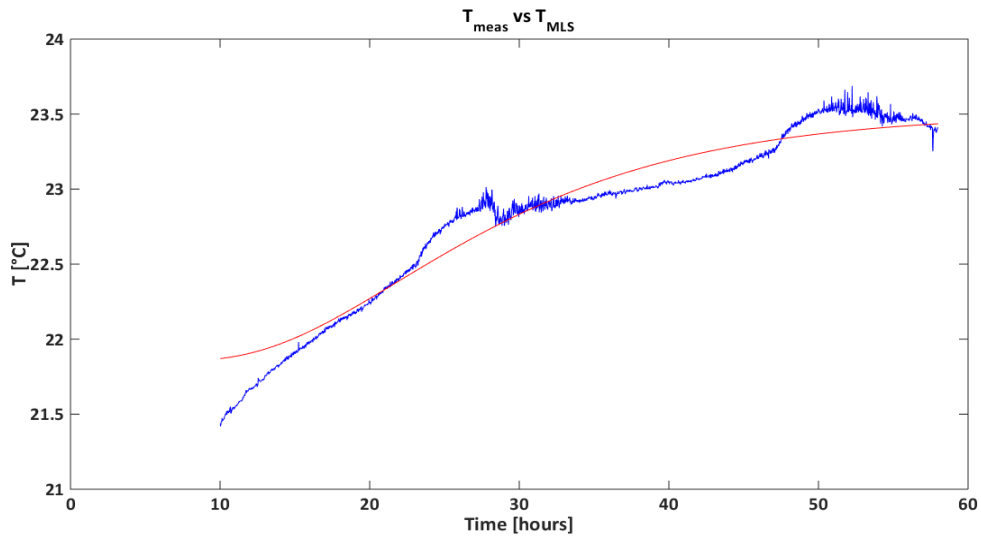
Figure 4-21 - Plot of measured data (blue line) vs. MLS temperature time series (red line) for t_{in} = 10 h and t_{end} = 58 h 28 min, solution 1 [λ = 0,60 W/(m·K); v = 2,1E-5 m/s; R_b = 0,152 m·K/W].

With the lowest *RMSE* equal to *0,131*, solution **1** returns satisfying matching plot (Figure 4-21) between measured and simulated temperature time series, but with thermal conductivity value not close to the mean expected value for the geological site of *2,23 W/(m·K)*, a significant groundwater flow absolute value of *2,1E-5 m/s* and borehole thermal resistance value equal to *0,152 m·K/W*.
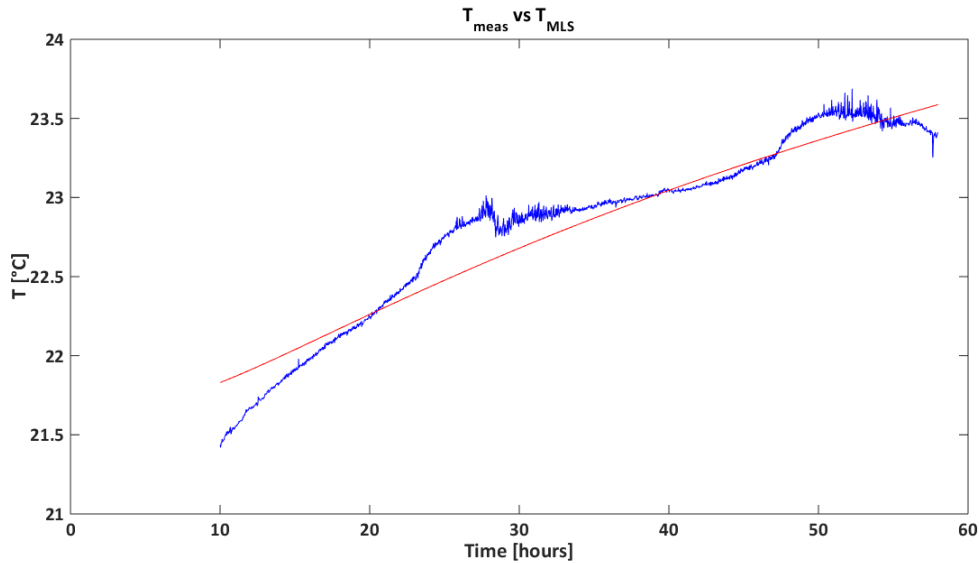
Figure 4-22 - Plot of measured data (blue line) vs. MLS temperature time series (red line) for t_{in} = *10 h* and t_{end} = *58 h 28 min*, solution a [$λ$ = *2,18 W/(m·K)*; v = *2,0E-11 ÷ 1,1E-6 m/s*; R_b = *0,152 m·K/W*].

Solutions 10 and **a**, which relative plots are in Figure 4-20 and Figure 4-22 return higher values of *RMSE* than solution **1**. They denote a thermal conductivity very close to the mean expected value for the geological site, similar borehole thermal resistance to solution **1**, but relative low values for Darcy velocity, not in agreement with the expectations considering the hydro-geological context.

MLS solution **1** determined a Darcy velocity *v* of *2,1E-5 m/s*, which can be reasonably representative of the groundwater flow. Then, the time criterion for data significativity is updated with this estimated value. The resulting characteristic time is obtained following the previously applied procedure:

$$Re_L = \frac{\rho \cdot v \cdot L}{\mu} = \frac{1000 \cdot 2,1 \cdot 10^{-5} \cdot 0,127}{1,23 \cdot 10^{-3}} = 2,18$$

$$Pr = \frac{v}{a} = 8,81$$

$$\overline{Nu} = C\ Re_L^m\ Pr^{1/3} = 0,989 \cdot 2,18^{0,33} \cdot 8,81^{1/3} = 2,64$$

$$\bar{h} = \frac{\overline{Nu} \cdot \lambda}{L} = \frac{2,64 \cdot 0,586}{0,127} = 12,18\ ^W/_{m^2K}$$

Recalling the thermal time constant interpreted as:

Franco Lý

*Interpretation of Borehole Heat Exchangers Thermal Response Tests
under groundwater influence: analysis of three case studies*

$$\tau_t = \frac{\rho_g \cdot r_b \cdot c_g}{h \cdot 2} = 0,47 \; h$$

And the characteristic time t_c is defined as:

$$t_c = (4 \div 5) \; \tau_t = 1,9 \div 2,4 \; h$$

This characteristic time value according to Figure 4-19 corresponds to a very good $RMSE_{average}$ improvement, however more elevated initial times are necessary in order to make $RMSE$ values more stable.

Darcy velocity values from solutions **a** or 10 cannot be taken into consideration, since velocities lower than *3,0E-6 m/s* are critical for the determination of the characteristic time value for typical borehole diameter of *127 mm* as previously described in section 2.6.2.

4.5.4 Results Discussion

By means of a 3 parameters estimation procedure, multiple solutions result from initial time sensitivity analysis comprehending different minima, as it happened in the first case study analyzed in chapter 3, namely Claviere case study.

As already cited, the script fits generated MLS temperature time series to experimental data, minimizing *RMSE* starting from a large combinations of initial parameters. This approach aims to guarantee an adequate range of possible solutions including the absolute minimum, if the initial parameters choice falls back into feasible values interval for all three parameters. In this case study, it was not possible to validate the results from initial time sensitivity analysis. Perhaps, it could have been important to choose a variation step closer than the actual within each parameter interval, but we are rather confident with the adopted variation step to generate enough dense initial values (*Δλ = 0,5 W/(m·K)*, *Δv = 10^1 m/s* and *ΔR$_b$ 0,03 m·K/W*; sets of initial parameter in section 4.5.1).

Throughout the report from initial time sensitivity analysis, it is explained how some results have no physical meaning and thus should be discriminated and not considered.

Solution **1** resulted in a thermal conductivity value *λ* equal to *0,60 W/(m·K)*. Even if this estimated value corresponds to the lowest *RMSE*, such low thermal conductivity value can only represent soil conformations that are not characteristic of the specific geological site. Consequently, this *λ* value, its relative *v* and *R$_b$* values of the same set of fitted parameters should be not considered as possible correct solution (solution **1**). The issue is that this set of fitted parameters is responsible for generating the best matching plot between MLS

Franco Lý

Interpretation of Borehole Heat Exchangers Thermal Response Tests
under groundwater influence: analysis of three case studies

temperature time series and experimental data for this specific case study as outlined in Figure 4-21.

Then, the interpretation of the MLS solutions results to be inconsistent and not trivial: not feasible fitted parameters generate best matching plot with also the lowest *RMSE* value. The coupled value of Darcy velocity is *2,1E-05 m/s* indicating a rather relevant groundwater flow and it would be reasonably in agreement with the hydro-geological conditions, although actually no precise information on hydraulic properties are available. Thus, further hydraulic tests are recommended for this specific site in order to have a term of comparison.

Solutions 10 and **a** return higher values of *RMSE*. They denote a thermal conductivity very close to the mean expected value for the geological site, but relative low values for Darcy velocity, not in agreement with the expectations considering the hydro-geological context. Besides, the MLS curve follows the measured data trend for most of the dataset but, in the last part the two series seem to detach one to each other, with the MLS curve mainly going upward as outlined in Figure 4-20 and Figure 4-22. Then, the fit is not able to catch the fundamental behavior of the measured trend.

The borehole thermal resistance values obtained from all the fits are consistent between them, ranging from *0,147* to *0,153 m·K/W*. It results to be the most constrained parameter after having carried out the initial time sensitivity analysis. However, the values seem a bit larger than the expectations, especially taking into account the filling material and the double U-pipe configuration (Table 20).

Time criterion for data significativity returns a characteristics time of *2,4 hours* relatively for a Darcy velocity of *2,1E-05 m/s*, which is in agreement with the initial time analysis sensitivity findings. Indeed removing about the first two hours, the largest decrease rate in $RMSE_{average}$ is achieved. In disregarding more hours the *RMSE* does not have the same improvement rate, in fact from Figure 4-19 it can be noticed a smooth trend of *RMSE* values approaching to an initial time of *10 hours*.

To sum up, the sets of parameters (the solutions) attained by MLS script are multiple, confirming the findings of (Wagner V. a., 2013), that TRT evaluation based on **Eq. 2.23**. and its simplified form **Eq. 2.34** is an ill-posed problem, where solutions to the inverse problem are non-unique. Only performing hydraulic tests like a pumping test more detailed information can be compared to MLS solutions to verify the goodness of the parameter estimation procedure.

Franco Lý

*Interpretation of Borehole Heat Exchangers Thermal Response Tests
under groundwater influence: analysis of three case studies*

4.6 Infinite Line Source vs. Moving Line Source Approach for Trento TRT

4.6.1 Results Comparison

By means of the MLS model an alternative method to interpret TRT dataset is applied able to account also for advection heat exchange. Unlike the Claviere case study, the standard TRT interpretation is possible in Trento case. However, the presence of an important groundwater flow is inferred from the resulting ground thermal conductivity, which is enhanced by 70% with respect to literature tables.

Performing an initial time sensitivity analysis using MLS approach, two sets of estimated parameters are obtained comprising the *99%* of the results, namely solutions **1** and solution **a**. They are compared with the solution attained by ILS model in Table 30.

Differently from Claviere case study, the interpretation of the TRT by MLS approach is not straightforward, on the contrary it turned out to be complex. Solution **1** exhibits the best matching plot and plausible Darcy velocity, but very low thermal conductivity. Solution **a**, corresponding to slightly larger *RMSE* than solution **1**, returns a ground thermal conductivity in agreement with literature table, but low Darcy velocity values ranging in a very broad range. In addition, the MLS temperature time series of solution **a** does not seem to catch the fundamental behavior of the measured trend.

Table 30 - Comparison between Infinite Line Source vs. Moving Line Source results.

TRT analysis / estimated parameter	ILS solution	MLS solution 1	MLS solution a
Ground Thermal Conductivity [$W/(m \cdot K)$]	*3,84*	*0,60*	*2,18*
Borehole Thermal Resistance [$m \cdot K/W$]	*0,074*	*0,152*	*0,149*
Aquifer Darcy Velocity [m/s]	Cannot be estimated by this approach.	*2,1E-5*	*2,0E-11 ÷ 1,1E-6*

Franco Lý

Interpretation of Borehole Heat Exchangers Thermal Response Tests
under groundwater influence: analysis of three case studies

MLS solution **a** gives back a very good ground thermal conductivity close to the literature based estimation of *2,23 W/(m·K)*. Unfortunately multiple Darcy velocities are coupled with this ground thermal conductivity, ranging in a very wide interval as described in Table 30. This behavior is rather unusual, since the relative plots of MLS temperature time series are the same: it seems that if Darcy velocity is any in that range, it does not affect the thermal exchange between the source and the surrounding environment, yielding the same mean fluid temperature variation.

The set of parameters of solution **1** obtained by the RMSE minimization algorithm occurs 45 times on 100. It generates the best matching plot in Figure 4-21. The problem in accepting this set of parameters is mainly about the ground thermal conductivity as previously underlined. However, Darcy velocity may actually be representative of the advective conditions present in the site.

If we had considered Darcy velocity from solution **1** in order to deduce Wagner's correction factor, we would have obtained a value *v = 1,8 m/day*, which coupled with a thermal conductivity of *0,60 W/(m·K)* is not represented in Figure 3-37. In this case the correction factor cannot be determined.

On the other hand, If we had considered Darcy velocity values from solution **a**, we would have obtained values lower than *v = 0,1 m/day* which coupled with a thermal conductivity of *2,18 W/(m·K)* do not require a correction factor according to (Wagner V. a., 2013).

Concerning estimated borehole thermal resistance, MLS approach returns larger values with respect to ILS. Indeed both solutions **a** and **1** are roughly the double of the value obtained by the standard TRT interpretation, corresponding to an important difference. It seems that ILS approach, not considering the advective processes, leads not only to an overestimation of the ground thermal conductivity λ_{eff}, but also an underestimation of the borehole thermal resistance R_b. This consideration is actually in agreement with the necessity of ILS approach to take into account a more effective heat exchange than the only pure conductive one, in presence of a significant groundwater flow.

Franco Lý

Interpretation of Borehole Heat Exchangers Thermal Response Tests under groundwater influence: analysis of three case studies

5 Thermal Response Test analysis: Lodi case study

The third analyzed case study in this work is the Thermal Response Test of a pilot borehole heat exchanger in Lodi, which raw data were provided by my academic supervisor Adriana Angelotti.

5.1 Introduction

The site is located in Pianura Padana, in the municipality of Lodi, within the Experimental Zoo-technical Centre, used by the researchers of the Faculty of Veterinary Medicine of the Università Statale of Milan as a center where to carry out food and veterinary experimentations. The pilot borehole heat exchanger (named BHE4) is part of a low-temperature geothermal plant installed for monitoring purpose (EcoZoo Project). The geothermal field is located at an average elevation of about *76 m* above sea level.

<p align="center">**Figure 5-1 - Project site: geographical location.**</p>

In Figure 5-2 it can be appreciated a detailed technical map that depicts the location of the boreholes and piezometers in the site. The environment that needs to be heated/cooled by the geothermal system is the piglets room highlighted in color rose in the figure, placed inside a warehouse (green in the figure).

Franco Lý

*Interpretation of Borehole Heat Exchangers Thermal Response Tests
under groundwater influence: analysis of three case studies*

Figure 5-2 - Technical map of the site, with boreholes and piezometers location.

Differently from the two previous case studies analyzed in this thesis, a hydrogeological investigation of the subsoil was performed in this case. Actually, the Zoo-technical Centre was interested by pumping tests in order to estimate hydraulic conductivity of the ground (piezometers pz1 and pz2). A pumping test consists in decreasing the piezometric level by means of a hydraulic pump and monitoring the phase of resurgence after having switched off the pump. The results of the tests were previously calibrated by a numerical model of transport by a *trial & error* approach (Marocchi, 2015).

Additionally, a numerical model of heat transport in the aquifers was implemented (Marocchi, 2015) to calibrate the hydro-geological parameters of the site, but setting the thermo-physical properties (thermal conductivity and heat capacity) from a literature review. If in this thesis a correct interpretation of an in situ TRT is carried out, the obtained thermal parameters can largely improve the calibration performed in the previous work.

5.2 Hydro-Geological Background

From a geological point of view, the area results to be rather uniform, as it is well underlined by the extract of the National Geological Map (Figure 5-3).

The borehole heat exchanger is situated in the shallowest hydro-stratigraphic group of the Pianura Padana area called *Aquifer Group A* which has developed in Pleistocene period. By means of in situ drillings, it was detected the presence of a thin layer of clayish silt at around *30 m* of depth, dividing the ground column in two aquifers, a free aquifer starting from about *5,4 m* of depth and a confined aquifer under the layer of silt.

The depth achieved by the perforation of the boreholes is approximately *60 m*, and samples of the overall ground column were extracted in borehole BHE1 (close to borehole BHE4, where the TRT is performed, see Figure 5-2) to identify the subsurface stratigraphy in a detailed way (section 5.2.1).

The shallow aquifer comprises about *24 m* of ground characterized by silt with fine grained sand. The deep aquifer in turn is mostly constituted of coarse-medium grained sand with gravel and has a thickness of about *30 m.*
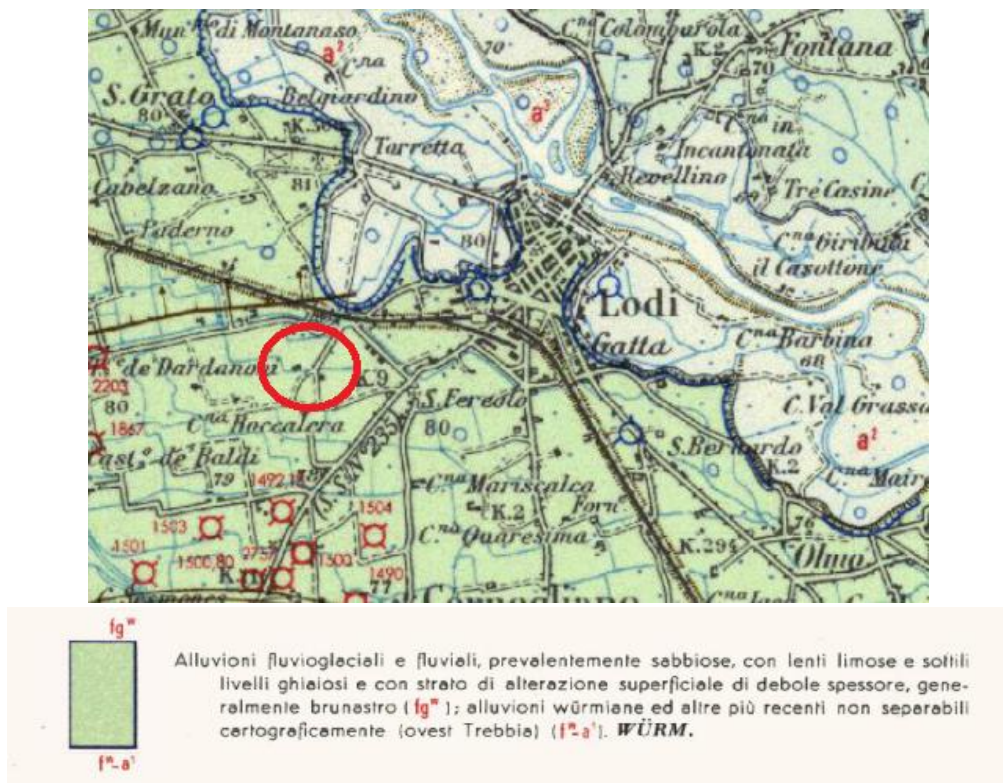
Figure 5-3 - Extract from the National Geological Map (Italy).

Franco Lý

Interpretation of Borehole Heat Exchangers Thermal Response Tests under groundwater influence: analysis of three case studies

5.2.1 Ground Stratigraphy and Thermo-Physical Characterization

From the extracted stratigraphy (appendix 7.5), in order to obtain a preliminary characterization of potential heat exchange, it is possible to estimate the thermo-physical properties of the crossed layers adopting reference values from (UNI11466, 2012) for thermal conductivity (Table 31) and volumetric heat capacity (Table 32).

Considering the whole depth, weighted averages over the layer thicknesses are subsequently estimated as follows:

− the weighted average ground thermal conductivity turns out to be *2,33 W/(m·K),* while minimum and maximum values are *1,79* and *2,86 W/(m·K)* respectively*;*

− the mean volumetric thermal capacity is *2,41 MJ/(m³K),* while, minimum and maximum values are *2,11* and *2,71 MJ/(m³K)* respectively.

Table 31 - Subsurface column stratigraphy with associated thermal conductivity (UNI11466, 2012).

Layer depth range [m]	*Layer description*	*Thermal conductivity [W/(m·K)]*		
		Min	*Max*	*Mean*
0 - 1,0	Gravel with pieces of lay-brick and sand	0,4	0,9	0,65
1,0 - 2,3	Yellowish sandy loam	0,4	1,0	0,7
2,3 - 3,3	Yellowish slimy sand	0,4	0,9	0,65
3,3 - 4,4	Compact yellow-grey loam	0,4	1,0	0,7
4,4 - 6,6	Slimy fine sand	2,0	3,0	2,5
6,6 - 9,4	Grey sandy loam	1,1	3,1	2,1
9,4 - 12,7	Fine-medium grained sand	2,0	3,0	2,5
12,7 - 13,5	Dark grey loam	1,1	3,1	2,1
13,5 - 18,0	Slimy fine-medium grained sand	2,0	3,0	2,5
18,0 - 29,4	Coarse grained sand	2,0	3,0	2,5
29,4 - 30,5	Light slimy fine grained sand	2,0	3,0	2,5
30,5 - 33,0	Compact plastic dark grey clayey loam	1,1	3,1	2,1
33,0 - 38,0	Coarse grained sand with gravel	2,0	3,0	2,5

38,0 - 42,0	Sand and gravel	2,0	3,0	2,5
42,0 - 44,0	Medium grained sand	2,0	3,0	2,5
44,0 - 45,5	Coarse grained sand	2,0	3,0	2,5
45,5 - 60,0	Medium grained sand	2,0	3,0	2,5

Table 32 - Subsurface column stratigraphy with associated volumetric thermal capacity (UNI11466, 2012).

Layer depth range [m]	Layer description	Volumetric thermal capacity [$MJ/(m^3 K)$]		
		Min	Max	Mean
0 - 1,0	Gravel with pieces of lay-brick and sand	1,3	1,6	1,5
1,0 - 2,3	Yellowish sandy loam	1,5	1,6	1,6
2,3 - 3,3	Yellowish slimy sand	1,3	1,6	1,5
3,3 - 4,4	Compact yellow-grey loam	1,5	1,6	1,6
4,4 - 6,6	Slimy fine sand	2,0	2,8	2,4
6,6 - 9,4	Grey sandy loam	2,0	2,8	2,4
9,4 - 12,7	Fine-medium grained sand	2,2	2,8	2,5
12,7 - 13,5	Dark grey loam	2,0	2,8	2,4
13,5 - 18,0	Slimy fine-medium grained sand	2,2	2,8	2,5
18,0 - 29,4	Coarse grained sand	2,2	2,8	2,5
29,4 - 30,5	Light slimy fine grained sand	2,2	2,8	2,5
30,5 - 33,0	Compact plastic dark grey clayey loam	2,0	2,8	2,4
33,0 - 38,0	Coarse grained sand with gravel	2,2	2,8	2,5
38,0 - 42,0	Sand and gravel	2,2	2,8	2,5
42,0 - 44,0	Medium grained sand	2,2	2,8	2,5
44,0 - 45,5	Coarse grained sand	2,2	2,8	2,5
45,5 - 60,0	Medium grained sand	2,2	2,8	2,5

Franco Lý

Interpretation of Borehole Heat Exchangers Thermal Response Tests
under groundwater influence: analysis of three case studies

5.3 Thermal Response Test

The purpose of the test is to estimate the effective subsurface thermal conductivity λ_{eff} and the thermal resistance R_b of the pilot BHE. According to the general approach of this thesis, a standard TRT interpretation is initially performed by Infinite Line Source approach. Then, elevated scattering of power values suggests to adopt an extended version of ILS model, accounting for variable heat injection rates (VHI-ILS). Eventually, an additional analysis by MLS model is carried out to account for convective phenomena.

5.3.1 Test Equipment

The test is carried out in situ with a mobile equipment constructed by an Italian company (VECOS SRL), with a similar machinery to the equipment called *TED*, elaborated to perform TRT based on principles scheme developed at Luleå University of Technology. It is ad hoc designed to try out geothermal heat exchange (pressure test, flow test, undisturbed ground temperature measurement and geothermal response test).

Figure 5-4 - Vecos TRT mobile unit.

The equipment is constituted by:

− a measurement system made up of two temperature probes *PT100* for the circulating fluid, a temperature probe for the external air, a temperature probe for the internal air in the machinery, an electromagnetic flow-meter and a piezo-resistive pressure transducer;
− a system for data acquisition and data storage;
− a hot water heater provided with electric resistances to module the power
− a hydraulic loop composed of a circulating pump, an expansion vessel and a series of safety valves.

Main characteristics of the mobile test equipment VECOS TED are provided in Table 33.

<div align="center">Table 33 - Minimal datasheet of the equipment, VECOS TED.</div>

- vertical closed pipe loop type	single or double U, suitable to concentric type
- nominal diameters (external)	DN25, DN32, DN40 and DN50 mm
- material	HDPE PN16, HDPE PN10, HDPE-RC PN16
- pipe loop producer	indifferent
- borehole length	20 to 500 m (standard)
- max pressure for leakage test	16 bar
- max discharge for TRT	4-6 m^3/h
- max electrical power TRT modulus	10-12 kW
- A/D converter	24 bit
- sampling frequency	1 seconds upwards
- thermal exchange measure precision	1-3% depending on BHEs configurations

The measurement instruments are of the same kind used for Claviere site. Technical details of the instruments are provided in section 3.3.1.

Franco Lý

Interpretation of Borehole Heat Exchangers Thermal Response Tests
under groundwater influence: analysis of three case studies

5.3.2 Borehole Heat Exchanger Description

The geothermal exchanger consists of a drilled borehole *60 m* deep with a diameter of *127 mm* filled with specific filling material based on cement and bentonites for geothermal applications. It is made up of a single U-pipe with external pipe diameter of *40 mm* and internal of 3*2,6 mm*. The pipe material is the typically adopted high-density polyethylene (HDPE Pe100 PN16 De40).

5.3.3 Test Operating Conditions

The response test is carried on with constant thermal injection on BHE4, starting on *07/01/2014* at 11.55 and lasting until *09/01/2014* at 12.35 for a total duration of *72h 40min.*

The supplied power set on the machinery is *4 kW* by means of the electrical resistances. Its corresponding specific power, i.e. the supplied power averaged along the length of the borehole turns out to be *66,7 W/m*. The flow rate is constantly measured by the electromagnetic flow-meter with a sampling frequency of *1 minute*, resulting to an average of *1773 l/h* with a standard deviation of *19,5 l/h* equal to *1,10%* . Referring to this value of flow rate, the time necessary to the liquid mass to complete a loop is computed as:

$$t_{loop} = \frac{2L + L_e}{(Q/\pi r_i^2)}$$
Eq. 5.1

where:

- *L* is the borehole heat exchanger length, *60 m*;

- *L_e* is the total pipe length external to the borehole connected to mobile equipment, *6 m*;

- *Q* is the flow rate occurring in the vertical closed pipe loops [*m^3/s*];

- *r_i* is the internal radius for a standard HDPE Pe 100 PN16 De40 pipe [*m*].

This approach does consider the short extent of pipes external to the borehole connected to the mobile equipment. The estimated time to the fluid to fulfill a complete loop is about *214 seconds*, i.e. *3 minutes 34 seconds*. This information could be useful to reduce the computational efforts for the following MLS analysis, since the sampling frequency can be lower than this value in order to have a good description of mean fluid temperature (UNI11466, 2012). However, a sampling time of *1 minute* adopted by the data acquisition system will be kept for further analysis.

Franco Lý

Interpretation of Borehole Heat Exchangers Thermal Response Tests under groundwater influence: analysis of three case studies

5.3.4 Undisturbed Ground Temperature

The measure of the undisturbed ground temperature T_0 is carried out by circulating the fluid inside the closed pipe loops in BHE4 without activating electrical resistances, while data-logger is recording. The total duration of the test is of *60 minutes* with an irregular sampling time. Therefore, the fluid can reach the thermal equilibrium with the surrounding environment and, thus about the same temperature of the ground. In steady condition, the mean temperature reaches *17,4°C*. The thermal equilibrium is illustrated in Figure 5-5 .
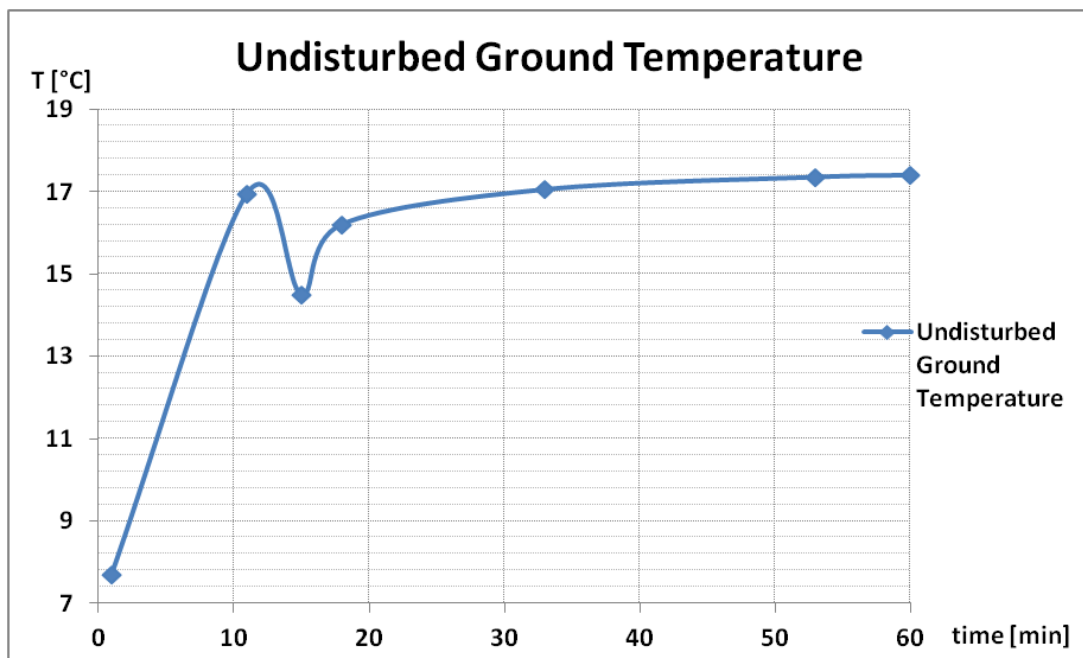
Figure 5-5 - Thermal equilibrium to evaluate undisturbed ground temperature.

There are some doubts about the procedure to assess T_0 because guidelines from (ASHRAE, 2007) recommends short circulation period from *10* to *20 minutes*. This because heat produced by mechanical work of the pump can be transferred to the water in the pipes and thus introduces a bias in the measured temperature (Gehlin S. E., 2003). Additionally, it is commonly proposed to perform short interval fluid temperature logging to have an estimation close to the undisturbed ground temperature, e.g. in (UNI11466, 2012) and (Gehlin S. E., 2003) a sampling time of *10 seconds* is recommended. Moreover the resulting temperature T_0 = *17,4°C* appears overestimated with respect to expectations based on the experience on the geographical area.

Therefore, while the TRT was started in BHE4, a thermal log profile in the nearby piezometer pz1 was performed by means of a phreatimeter with a sampling frequency of ca. *5 m*. Additionally for the same purpose a PT100 sensor is lowered four times at different

Franco Lý

*Interpretation of Borehole Heat Exchangers Thermal Response Tests
under groundwater influence: analysis of three case studies*

depths. Measured values obtained by both the devices are illustrated in Figure 5-6. An average temperature equal to 15,9°C and 15,1°C is obtained with the phreatimeter and with the PT100 sensor respectively. Such temperature levels are in agreement with expectations for the site. However the question arises on the motivations why the measurements in BHE4 based on fluid flow results in about 2°C higher temperature. The possibility that a temperature anomaly is present nearby BHE4 is considered. Therefore the considered value of T_0 for further analysis is set to *17,4°C*.
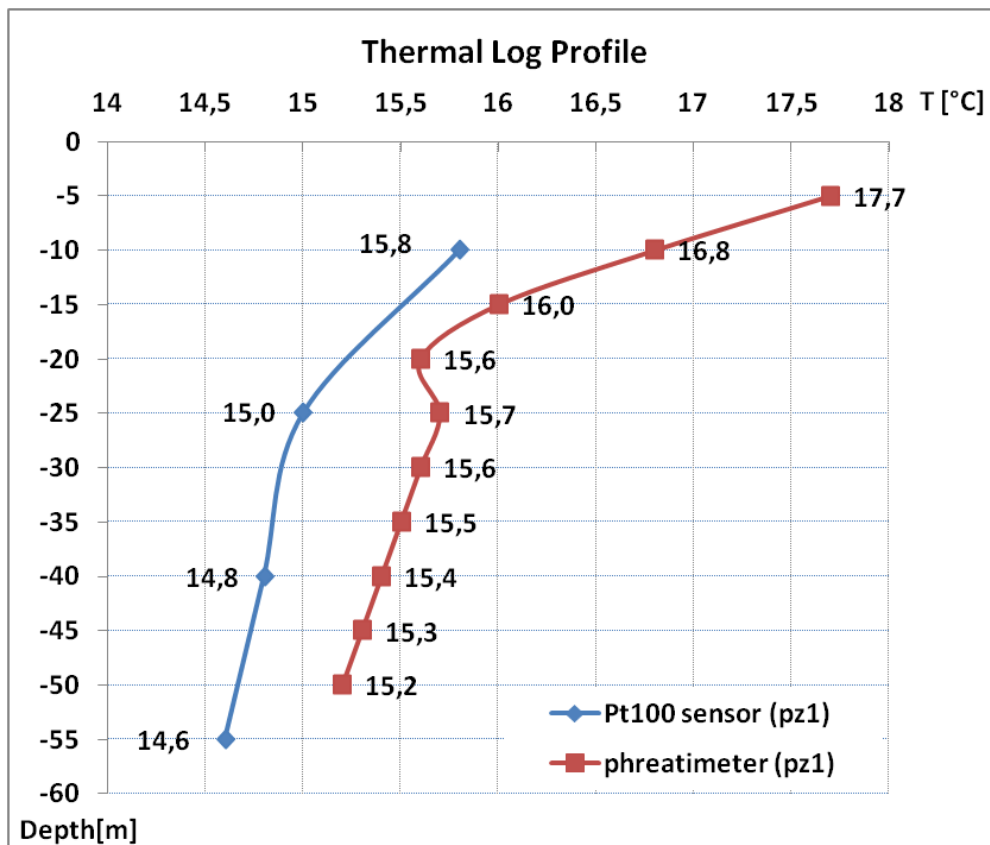
Figure 5-6 - Thermal log profile in piezometer pz1 by phreatimeter and Pt100 sensor.

5.3.5 Measurements

The mobile equipment is set to collect inlet and outlet fluid temperature every minutes for the total duration of the Thermal Response Test. The plot of the measured inlet and outlet fluid temperature time series is reported Figure 5-7.

Franco Lý

*Interpretation of Borehole Heat Exchangers Thermal Response Tests
under groundwater influence: analysis of three case studies*
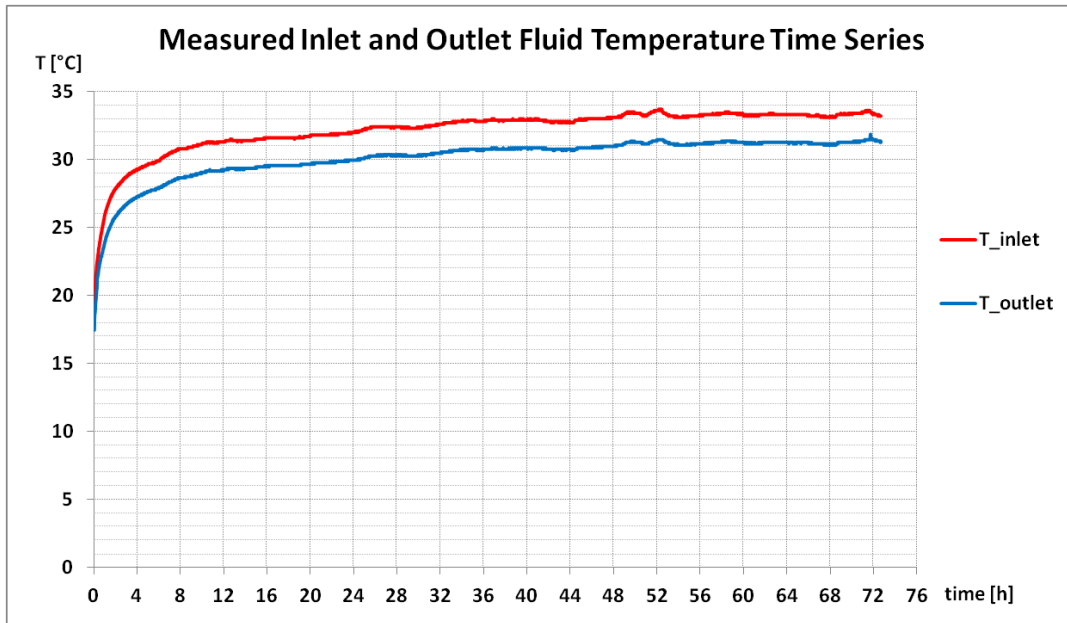
Figure 5-7 - Measured inlet and outlet fluid temperature time series.

The increasing logarithmic trend of the two temperature time series is regular along the test with just some scattering around *48-52 hours*.

The electromagnetic flow-meter has recorded the flow-rate in the vertical closed pipe loops, exhibiting a constant trend in time after an initial stabilization. The volumetric flow rate results to be of *1773 l/h* with a standard deviation of *19,6 l/h* (*1,10*% of the mean).
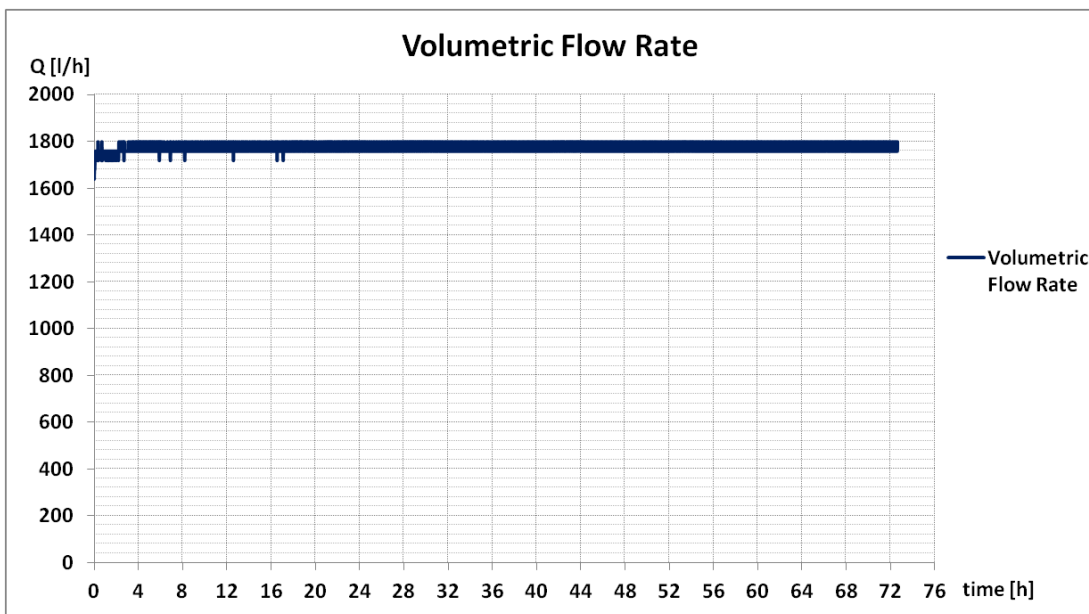
Figure 5-8 - Volumetric Flow Rate inside the vertical closed pipe loop.

It has to be noticed that the heat carrier fluid flow rate does not comply the recommendations given in (UNI11466, 2012), since it cannot guarantees a temperature differences between inlet and outlet temperature comprised between *3K* and *7K* (in this case about *2,1K*).

Concerning the effective electrical (three phases) and thermal power, they are obtained at every minutes according to the following equations :

Effective electrical power $\qquad Q_{el} = \Sigma \, (V \cdot I \cdot cos \, \varphi)$ **Eq. 5.2**

where:

- *V* is the electrical potential measured for the three phases R, S and T every minute [*Volt*];

- *I* is the current intensity measured for the three phases R, S and T every minute [*Ampere*];

- *φ* is the offset angle measured for the three phases R, S and T every minute [°]

Effective thermal power $\qquad Q_{th} = c_f \cdot Q \cdot \Delta T$ **Eq. 5.3**

where:

- c_f is the fluid specific heat, for the water *4186* [*kJ/(°C l)*];

- *Q* is the flow rate occurring in the vertical closed pipe loops [*l/min*];

- *ΔT* is the temperature difference between inlet and outlet pipes at every minute [*°C*]
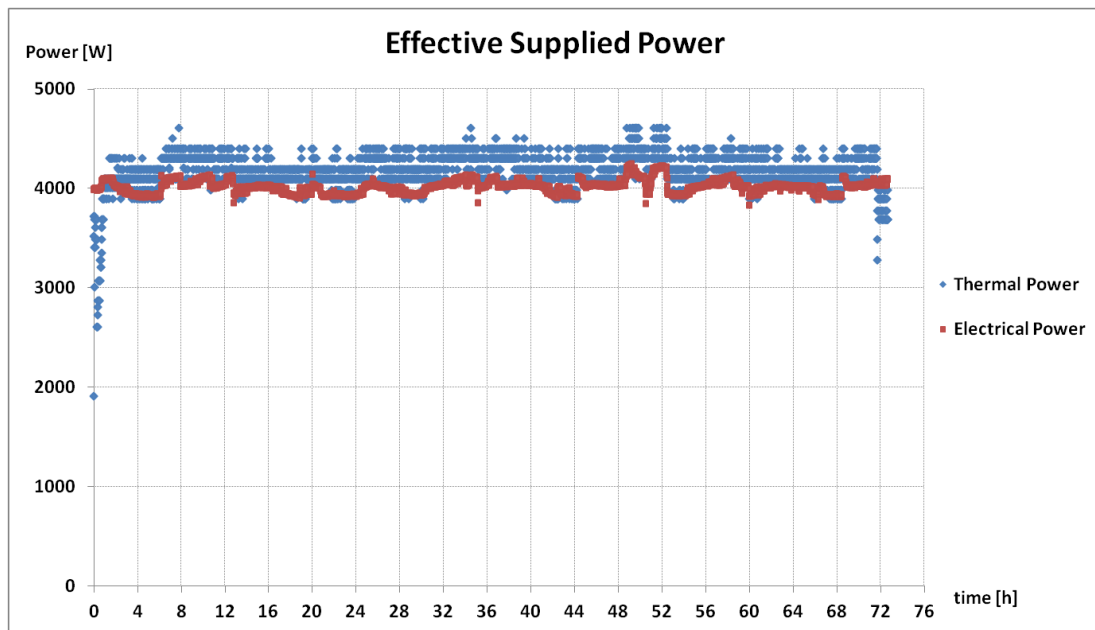
Figure 5-9 - **Effective electrical and thermal power.**

The effective mean thermal power averaged on the total duration results to be equal to *4172,2 W* with a standard deviation of *172,2 W* equal to *4,13%*. It is less accurate than the effective electrical power characterized by a mean value of *4013,2 W* and a standard deviation of *64,3 W* equivalent to *1,60%*. The difference of *3,81%* between mean power values is evident in Figure 5-9, where the electrical power trend exhibits more stability and remains always below the thermal power trend. In fact the wide-range scattering of thermal power corresponds to considerable standard deviation.

According to (UNI11466, 2012) both standard deviations have to be lower than *±1.5%* of the mean value. In this case, only the electrical power results to almost comply this recommendation, while the thermal power standard deviation exceeds of almost three times the limit of *1.5%*. Thus, it is clear that electrical power trend is more reliable than thermal power one. However, both thermal and electrical power values will be used for standard TRT analysis by Infinite Line Source theory.

Considering the total length of the borehole, the resulting specific thermal and electrical power per unit length are calculated resulting in *69,81 W/m* and *66,86 W/m* respectively.

5.3.6 Injection Power Check

Since in this case the thermal power standard deviation is significant, the influence of the heat exchange between the connecting pipes and the outside environment is checked by calculating the overall linear thermal resistance of such pipes (UNI11466, 2012), according to:

$$R_c = \frac{1}{2\pi}\left(\frac{1}{\lambda_1}ln\left(\frac{r_2}{r_1}\right) + \frac{1}{\lambda_e}\left(\frac{r_3}{r_2}\right)\right)$$

Eq. 5.4

where:
- λ_1 is the pipe thermal conductivity equal to *0,4 W/(m·K)*;
- λ_2 is the insulating layer thermal conductivity equal to *0,035 W/(m·K)*;
- r_1 is the pipe internal radius equal to *16,3 mm*;
- r_2 is the pipe external radius equal to *20 mm*;
- r_3 is the overall radius (pipe external radius + insulating layer thickness) equal to *35 mm.*

The overall linear thermal resistance R_c results to be 2,63 *m·K/W.*

Franco Lý

*Interpretation of Borehole Heat Exchangers Thermal Response Tests
under groundwater influence: analysis of three case studies*

In conditions of thermal difference equal to (T_{fm} - T_e) *°C*, where T_e is the external air temperature [*°C*] and T_{fm} is the mean fluid temperature [*°C*], the overall thermal power burnt off by the pipes (of length L_{TOT}) is equal to:

$$\dot{Q} = (T_{fm} - T_e) \cdot \frac{L_{TOT}}{R_c}$$

Eq. 5.5

And it has to be inferior to *1,5%* of the supplied power.

The external insulating layer has to be always shielded by solar radiation by means of opportune protection. In this specific TRT, since the thermal power values result to be very scattered this control is convenient to test if there is any possible correlation.
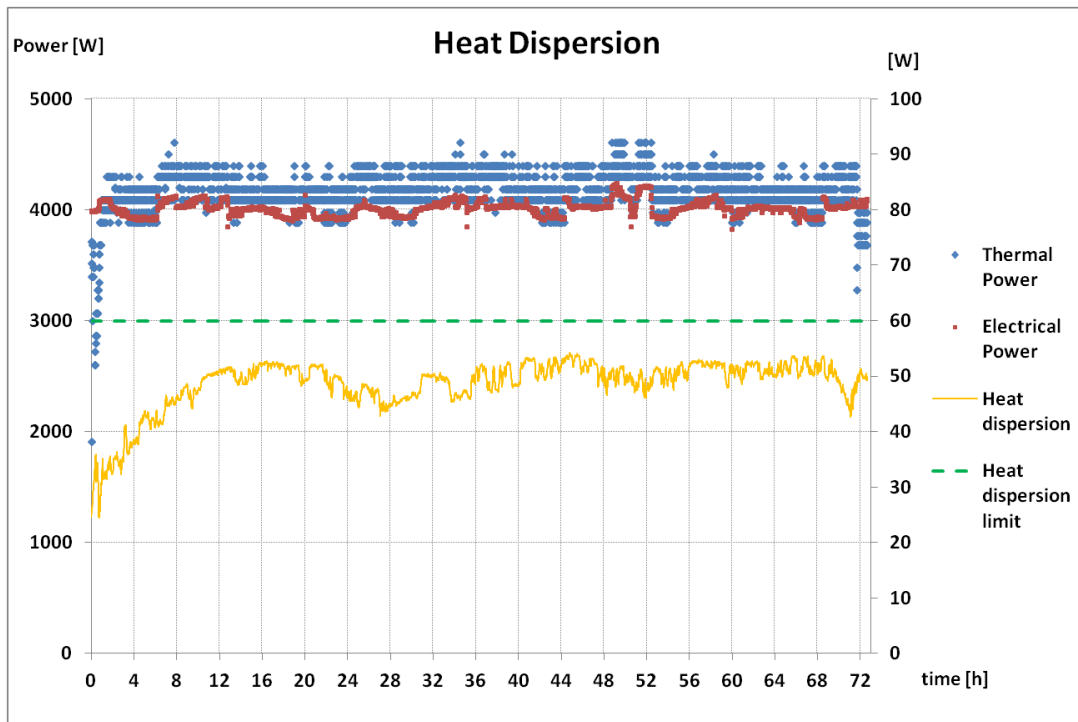
Figure 5-10 - Heat dispersion vs. effective supplied power

The limit imposed according to (UNI11466, 2012) recommendation, in this case equal to about *60 W* as shown in Figure 5-10 (considering electrical mean power value) is never exceeded by heat dispersion time series Therefore, the heat dispersion cannot be considered a relevant issue.

Franco Lý

*Interpretation of Borehole Heat Exchangers Thermal Response Tests
under groundwater influence: analysis of three case studies*

5.4 TRT Analysis by means of Infinite Line Source Theory

First of all, to carry on a line source analysis, the mean fluid temperature time series is obtained from the instantaneous arithmetic mean of two temperature time series.

$$T_{fm} = \frac{T_{in} - T_{out}}{2}$$ **Eq. 5.6**

In Figure 5-11 it is compared with inlet and outlet fluid temperature time series.
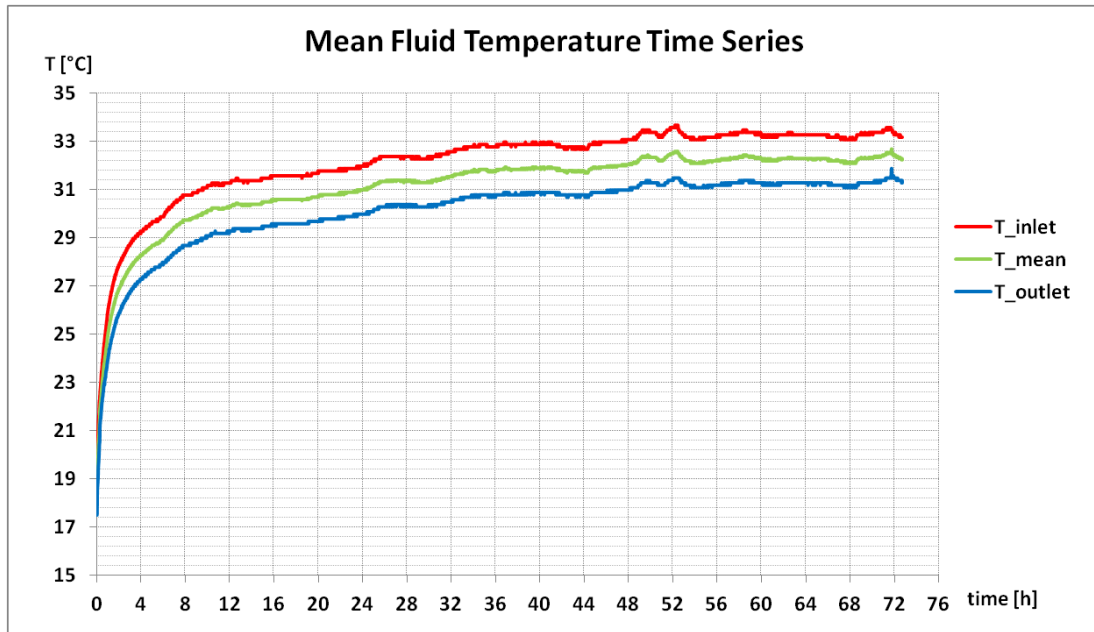
Figure 5-11 - Mean fluid temperature time series.

As previously presented in section 2.5, according to the LS approach, the heat carrier mean fluid temperature change in time according to the following relation:

$$T_{fm} \approx \frac{q}{4\pi\lambda_{eff}} ln(t) + q\left[R_b + \frac{1}{4\pi\lambda_{eff}}\left(ln\left(\frac{4a}{r_{bw}^2}\right) - \gamma\right)\right] + T_0$$ **Eq. 5.7**

According to section 2.5 the criterion for the logarithmic approximation has to be fulfilled:

$$t \geq t_c \geq \frac{5r_{bw}^2}{a}$$ **Eq. 5.8**

As a first guess previously estimated values (see section 5.2.1) for thermal capacity and thermal conductivity are used, namely *C = 2,41 MJ/(m³·K)* and *λ = 2,33 W/(m·K)*. Thus, a value of thermal diffusivity *a* is derived equal to *9,6E-7 m²/s*.

Franco Lý

*Interpretation of Borehole Heat Exchangers Thermal Response Tests
under groundwater influence: analysis of three case studies*

Adopting this value, the time criterion is fulfilled for times larger than *5,81 hours*. Thus, t_{in} = *6 hours* is adopted as initial time for TRT interpretation by means of ILS model.

5.4.1 Estimate of the Effective Ground Thermal Conductivity

Hence, the ground thermal conductivity is indirectly estimated by the slope *A* of the interpolating straight line for the measurement in a plot where x-axis corresponds to the logarithm of time:

$$\lambda_{eff} = \frac{q}{4 \cdot \pi \cdot A}$$

Eq. 5.9

The estimation is carried on varying t_{end} from *32 hours* to *72 hours* i.e. the total duration of the test is increased with a *4 hours* step. This method permits to understand the sensitivity of the thermal conductivity to the evaluation time of the TRT. An example of linear interpolation is illustrated for *t_{end} = 72 hours* in Figure 5-13. The theoretical model of test interpretation expects that temperature time series represented in a plot with *ln(t)* in the x-axis to be almost rectilinear. In this specific case, the trend does match in the fluid mean temperature time series, even if some irregularities are remarkable in Figure 5-13. The small temperature oscillations may be correlated to external noise influence due to solar radiation during the day as it can be inferred from Figure 5-12.
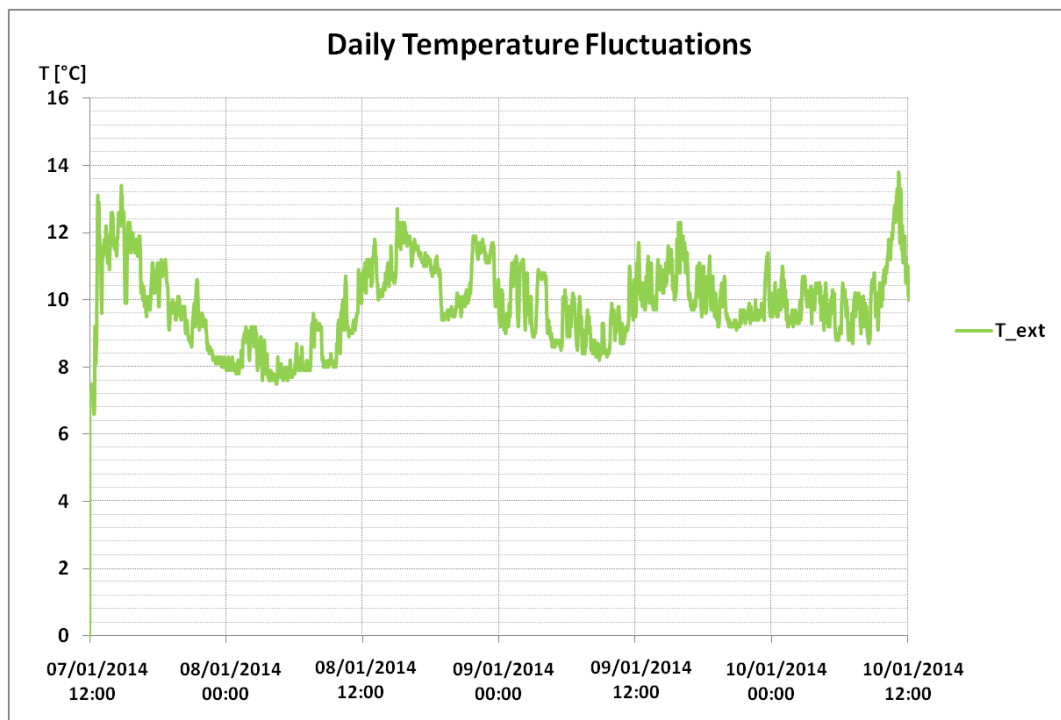
Figure 5-12 - Daily temperature fluctuations.

Franco Lý

Interpretation of Borehole Heat Exchangers Thermal Response Tests
under groundwater influence: analysis of three case studies
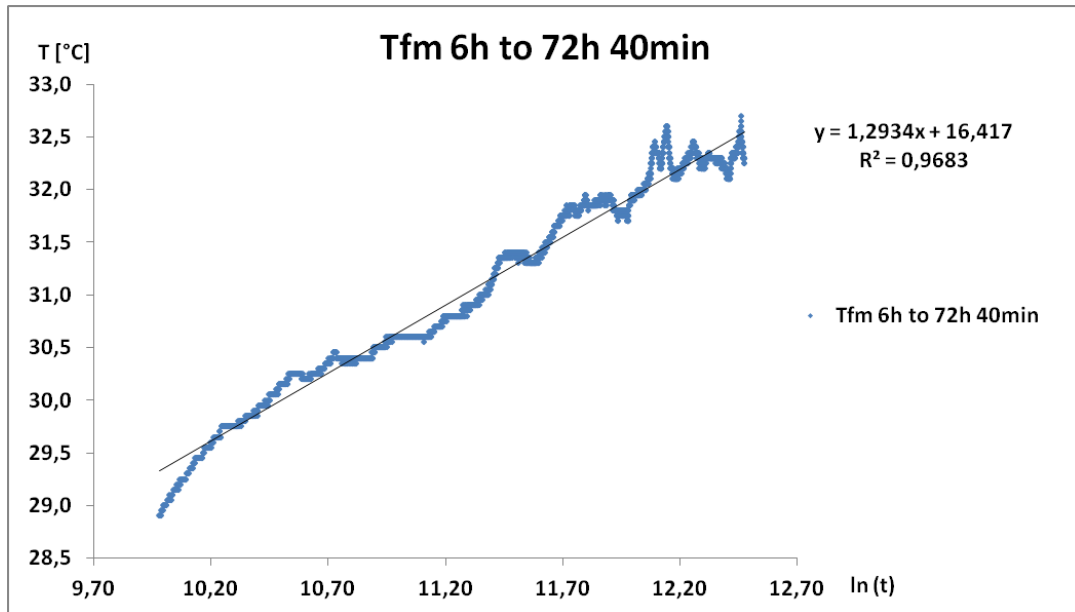
Figure 5-13 - Linear interpolation for data interval from *10 hours* to *72 hours*.

From the linear interpolation in Figure 5-13, in the semi-log plot, the coefficient of determination R^2 returned a value of 0,9683 proximal to the unity, indicating an elevated level of correspondence between measured values and estimated values by trend.
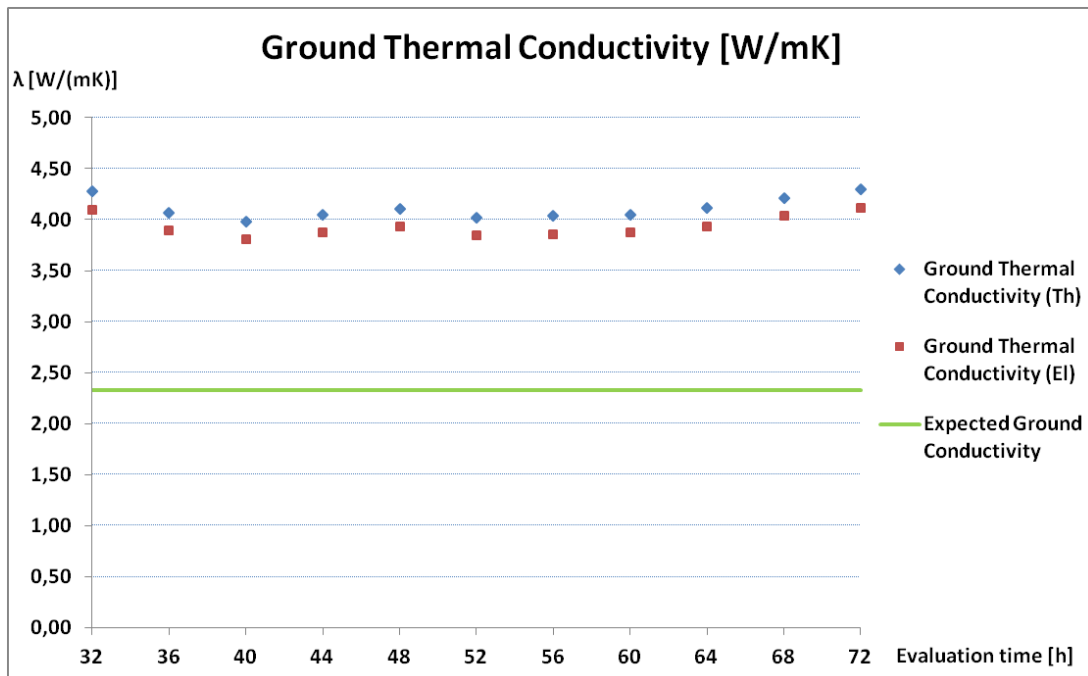
Figure 5-14 - Ground thermal conductivity trend for increasing evaluation time.

Franco Lý

Interpretation of Borehole Heat Exchangers Thermal Response Tests under groundwater influence: analysis of three case studies

The ground thermal conductivity estimation is performed considering both thermal and electrical specific power. Their trends (Figure 5-14) show an initial fluctuations and then a slight increase for larger t_{end}. In cases like this, it would be opportune to perform longer TRT to verify if the trend is going to converge to a stable value or not. If the estimated conductivity does not converge, a significant groundwater flow is present, as verified by (Witte H. , 2001). Ground thermal conductivity values obtained from electrical specific power are always slightly lower since recorded electrical power resulted to be inferior to calculated thermal power.

Observing the plot, however, the estimated conductivity values are always located well above the expected conductivity of the specific subsurface column estimated by literature values, namely 2,33 $W/(m \cdot K)$ with a maximum value equal to 2,86 $W/(m \cdot K)$. This high values may be explained by the influence of an important groundwater flow, which increases the effective ground thermal conductivity. The ground thermal conductivity series, both thermal and electrical ones, approach respectively *4,12* and *3,94 W/(m·K)*. Thus, these values differs each other of *4,35%*; further considerations will be provided in section 5.4.4.

5.4.2   Estimate of the Borehole Thermal Resistance

The borehole thermal resistance is thus evaluated in a similar approach, i.e. by increasing the evaluation time from *32 hours* to *72 hours* with a time step *Δt* of *4 hours*.

$$R_b = \frac{B - T_0}{q} - \frac{1}{4\pi\lambda_{eff}}\left[ln\left(\frac{4a}{r^2}\right) - \gamma\right] \qquad \textbf{Eq. 5.10}$$
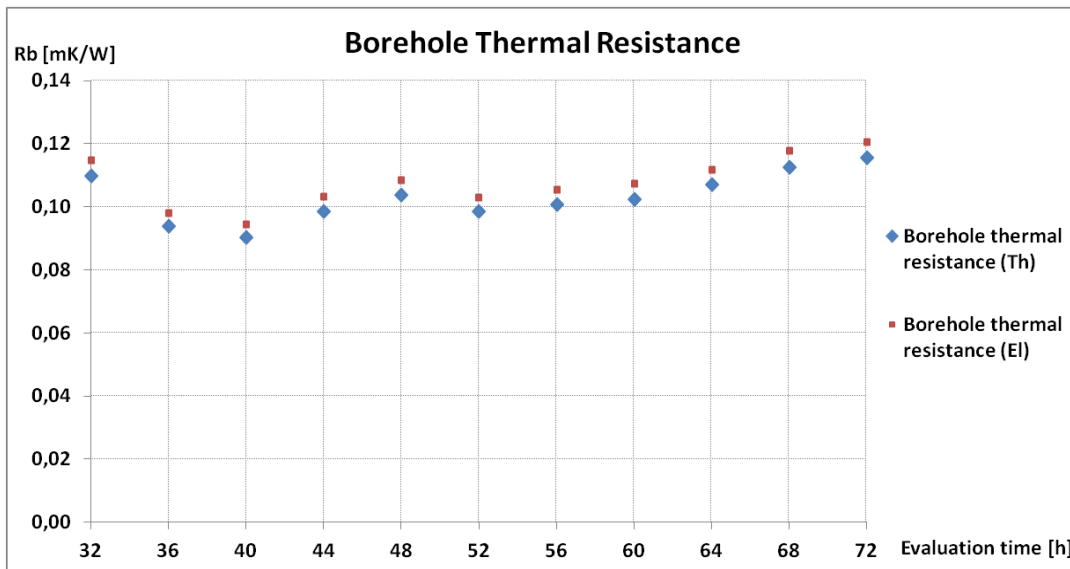
Figure 5-15 - Borehole thermal resistance values for increasing evaluation time.

The plot in Figure 5-15 illustrates the borehole thermal resistance values for both thermal and electrical specific power. The R_b values show an increasing trend for large t_{end}. The estimated values for t_{end} = *72 hours* approach to *0,115* and *0,121 m·K/W* respectively, which are low values for single U-pipes according to Table 20.

In this TRT, it is likely that a longer evaluation time would have supported a more precise evaluation of the parameter. Nevertheless, the results are considered valid to describe R_b.

5.4.3 Borehole Thermal Resistance Sensitivity to Undisturbed Ground Temperature

It is commonly known that the estimate of borehole thermal resistance R_b is strongly affected by T_0. For this specific TRT, the adopted T_0 is *17,4°C* as previously mentioned. However, the thermal log profile executed in the geothermal field, precisely in pz1, has surveyed lower temperature values of the ground in respect to the determined T_0 in BHE4 as discussed in section 5.3.4. Due to this high level of uncertainty on the correct value of parameter to be applied, a sensitivity analysis of R_b is carried out accounting for varying T_0 from *15,0°C* to *17,4°C* with a temperature interval ΔT_0 = *0,2°C.* The analysis accounts only for lower values of T_0 since a overestimation is more likely according to (Gehlin S. E., 2003).
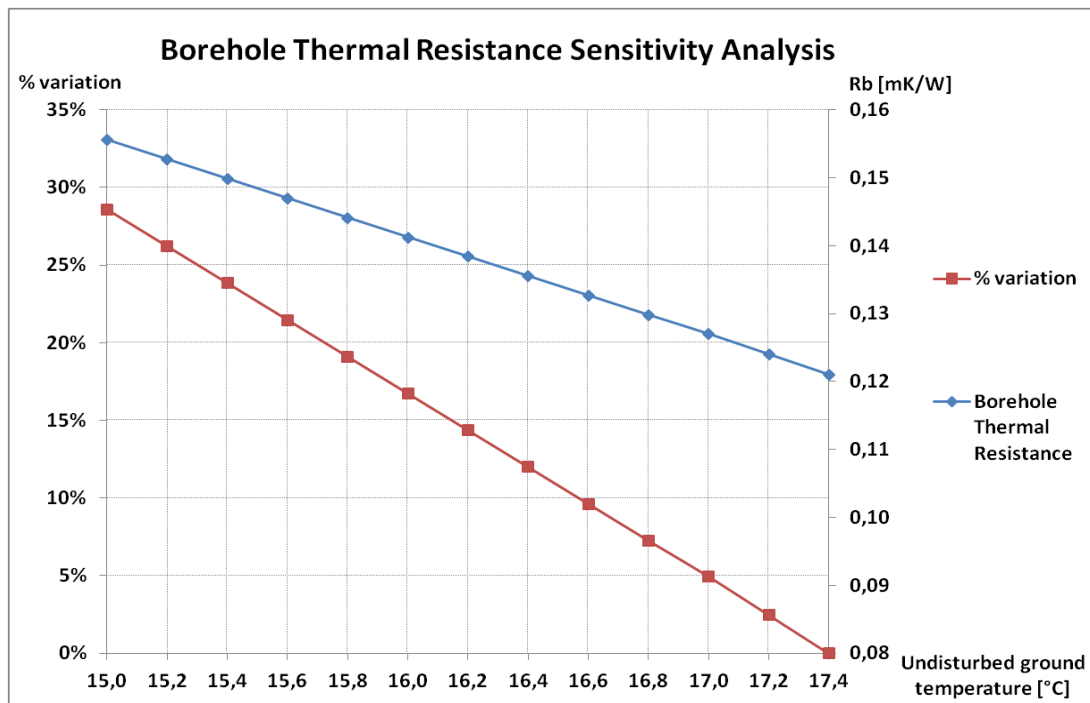
Figure 5-16 - Borehole thermal resistance sensitivity analysis to undisturbed ground temperature.

Franco Lý

Interpretation of Borehole Heat Exchangers Thermal Response Tests under groundwater influence: analysis of three case studies

In Figure 5-16 it can be noticed that with decreasing undisturbed ground temperature, the borehole thermal resistance tends to increase linearly up to *28,6%* with respect to the R_b value for T_0 of *17,4°C*, approaching a value of *0,156 m·K/W.* Therefore, if the undisturbed ground temperature is overestimated, a lower borehole thermal resistance is consequently determined. Then, an overestimation of the heat exchange with the surrounding is performed leading to an under-sizing of the BHEs length.

5.4.4 Results Discussion

In general, the ILS approach for TRT interpretation has yielded almost satisfying results, although mainly thermal conductivity extracted appears to be high. It has to be remarked that two main conditions in test itself are not respected according to (UNI11466, 2012):

- the total duration of the test respects minimum recommendation of *72 hours,* but temperature difference between inlet and outlet pipe is lower than the inferior limit of 3°C;
- effective electrical and thermal power standard deviation are larger than *±1,5%* of the mean value.

The difference in effective specific supplied power, between thermal and electrical mean power of *3,81%*, has originated a *4,35%* difference between estimated effective thermal ground conductivity and a *4,41%* difference between estimated borehole thermal resistance.

If (UNI11466, 2012) recommendations had to be fulfilled, both effective electrical and thermal power would be disregarded. In fact, the thermal power standard deviation is of *4,1%,* while electrical power standard deviation is of *1,6%,* indicating the effective electrical power values as the most reliable "constant" power to be considered for ground conductivity and borehole thermal resistance. In order to take into account a variable heat injection rate a specific interpretation model will be applied in the next section 5.5.

The pilot BHE length in this case study is of *60 m*, a short extent if typical geothermal applications are considered. Indeed, if an ILS analysis is adopted, a limit of exactly *60 m* is mentioned in (UNI11466, 2012), where for shorter length the heat exchange along the vertical axis is not negligible anymore and numerical modeling is usually preferred in order to estimate thermo-physical properties of the ground. A further development of this study could take into account adopting a Moving Finite Line Source approach (Molina-Giraldo N. a., 2011) in this case.

Franco Lý

Interpretation of Borehole Heat Exchangers Thermal Response Tests under groundwater influence: analysis of three case studies

Infinite Line Source model turns out to be adequate in fitting Lodi TRT data, in fact the linear interpolation in the semi-log plot gives back a coefficient of determination R^2 of *0,9683* proximal to the unity guaranteeing the goodness of the following estimation in the method: ground thermal conductivity and borehole thermal resistance.

Estimated ground thermal conductivity values for increasing evaluation time have demonstrated to be slightly increasing for large times, averaging to a mean of the last four values of *3,94 W/(m·K)* in case of electrical power values; however, the duration of the test was of about *73 hours,* usually considered sufficient; indeed no longer tests are common practice among geothermal energy experts. Nevertheless few additional hours would have helped to be more confident with the results from effective ground thermal conductivity estimation.

Compared to expected value, the evaluated λ_{eff} turns out to be larger than expected mean value estimated by literature value tables of about *70%*, a noteworthy increase that may be explained by the significant influence of two aquifers present in situ.

Relatively to the borehole thermal resistance, the estimated values for larger evaluation times approach to *0,121 m·K/W* considering the electrical power measurements and an undisturbed ground temperature of *17,4°C*. This value is not completely reliable considering that the adopted procedure to evaluate T_0 does not comply recommendations from (ASHRAE, 2007) and (UNI11466, 2012), and also it is not in agreement with Gehlin's instruction (Gehlin S. E., 2003). By means of a borehole thermal resistance sensitivity analysis, it is proved that an overestimation of T_0 will lead to compute a reduced borehole thermal resistance value.

5.5 Infinite Line Source Solution with Variable Heat Injection

The standard interpretation of TRT has demonstrated a high level of scattering for both thermal and electrical power, without fulfilling standard deviation recommendation of (UNI11466, 2012). An extended version of the Infinite Line Source solution (with Variable Heat Injection or VHI) using the superposition principle is then applied to comprehensively account for variable heat injections. The analytical solution is described in **Eq. 2.21** in section 2.5.2 and implemented in MATLAB.

The expression is recalled:

$$T_{fm}(t) = q(t)R_b + \sum_{i=1}^{n}(q_i - q_{i-1})\frac{ln\left(\frac{4a(t - t_{i-1})}{r_{bw}^2}\right) - \gamma}{4\pi\lambda_{eff}} + T_0 \qquad \textbf{Eq. 5.11}$$

Franco Lý

Interpretation of Borehole Heat Exchangers Thermal Response Tests under groundwater influence: analysis of three case studies

Hence, it is necessary to generate a step function for the supplied power (Figure 5-9), dividing the time series in intervals where heat injection rate can be assumed reasonably constant. The procedure should improve the representation of the supplied power, decreasing the overall standard deviation. A step function is proposed in Table 34 and plotted in Figure 5-17.

Table 34 - Proposed thermal power step values for VHI-ILS solution.

interval dt [min]	mean [W]	std dev [W]	std dev [%]
0-50	3301	357	10,8%
50-450	4118	125	3,0%
450-800	4246	105	2,5%
800-1500	4128	92	2,2%
1500-1600	4270	97	2,3%
1600-1900	4181	109	2,6%
1900-2300	4270	108	2,5%
2300-2700	4155	121	2,9%
2700-2800	4254	110	2,6%
2800-2900	4203	108	2,6%
2900-3150	4341	139	3,2%
3150-4300	4170	113	2,7%
4300-4360	3793	135	3,6%
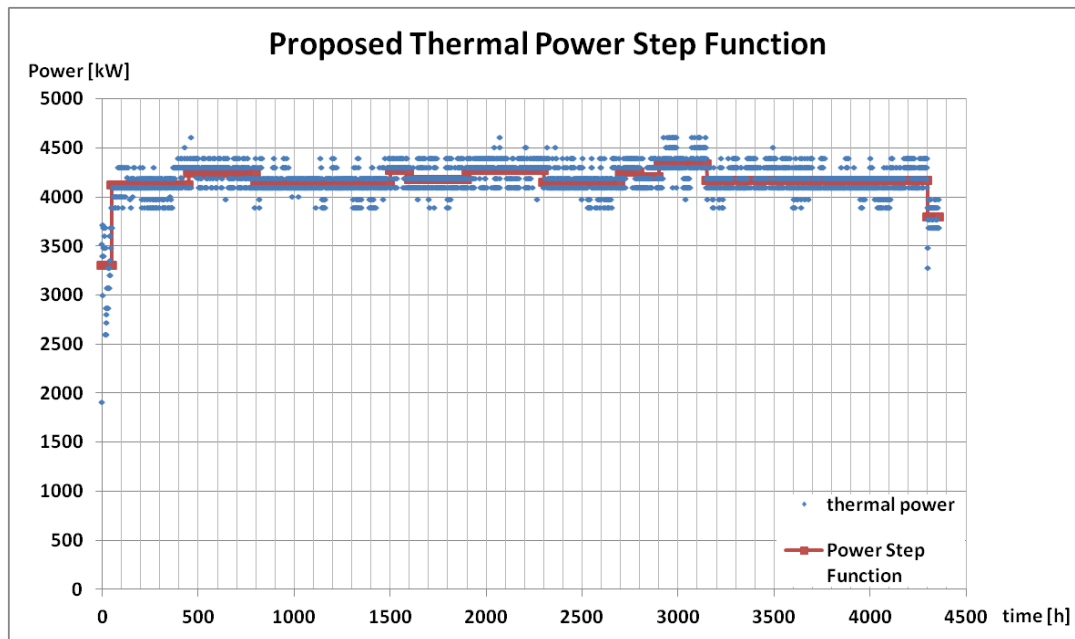
Figure 5-17 - Proposed thermal power step function for ILS solution with variable heat injection.

Franco Lý

*Interpretation of Borehole Heat Exchangers Thermal Response Tests
under groundwater influence: analysis of three case studies*

From Table 34, it can be observed that from a standard deviation of 4,1% considering all the dataset, a general standard deviation inferior to 3% is achieved for most of the chosen intervals (10 on 13), if the first and the last interval are disregarded. These two intervals are the most scattered, since for early time large variations occur and in the last period a large decrease is verified. In Figure 5-17 the step function tries to reproduce the experimental thermal power trend.

5.5.1   VHI - ILS Analysis Settings

A script in MATLAB is implemented in order to reproduce conductive heat exchange process with variable heat injection rates (appendix 7.4). Volumetric thermal capacity, thermal diffusivity, undisturbed ground temperature and borehole radius of the pilot BHE are necessary parameter of the model. The recorded TRT data are fitted by a two-variable parameter estimation technique, minimizing the *RMSE* between measured and generated temperature time series by varying a pair of initial parameters constituted by:

- Ground thermal conductivity λ [$W/(m \cdot K)$]
- Borehole thermal resistance R_b [$m \cdot K/W$]

To appropriately comprehend the influence of initial parameters, it is proposed to originate a 18 combinations set, thus constituted by 18 pairs of the two parameters. This scheme of initial parameters is defined based on considerations hereafter explained and will be used for the initial time sensitivity analysis for this specific case.

About ground thermal conductivity, the available geological information indicate to use a wide a range of possible values with a superior limit of *3,0 W/(m·K)*. The corresponding values are shown in Table 35.

Table 35 - Ground thermal conductivity initial values used for VHI-ILS solution fit.

Ground Thermal Conductivity [$W/(m \cdot K)$]	0,5	1,0	1,5	2,0	2,5	3,0

Regarding borehole thermal resistance, a range of values recurrent for a filling material based on cement and bentonites and single U-pipe configuration are considered (Table 36).

Table 36 - Borehole thermal resistance initial values used for VHI-ILS solution fit.

Borehole Thermal Resistance [$m \cdot K/W$]	0,10	0,15	0,20

Franco Lý

*Interpretation of Borehole Heat Exchangers Thermal Response Tests
under groundwater influence: analysis of three case studies*

The step specific power function (q_i) is obtained from step function of the supplied thermal power dividing it in each interval by the BHE length of *60 m*. The calculated values are used as input in **Eq. 5.11** as well the step specific power variation (q_i - q_{i-1}) to generate the mean heat carrier fluid by means of VHI-ILS solution. In Figure 5-18 the step specific power variation series is depicted, that is the series of the single specific power input, positive or negative that superimposes to the previous one at the beginning of each interval, with q_0 = *0* and t_0 = *0* assumed as initial conditions of the Thermal Response Test.
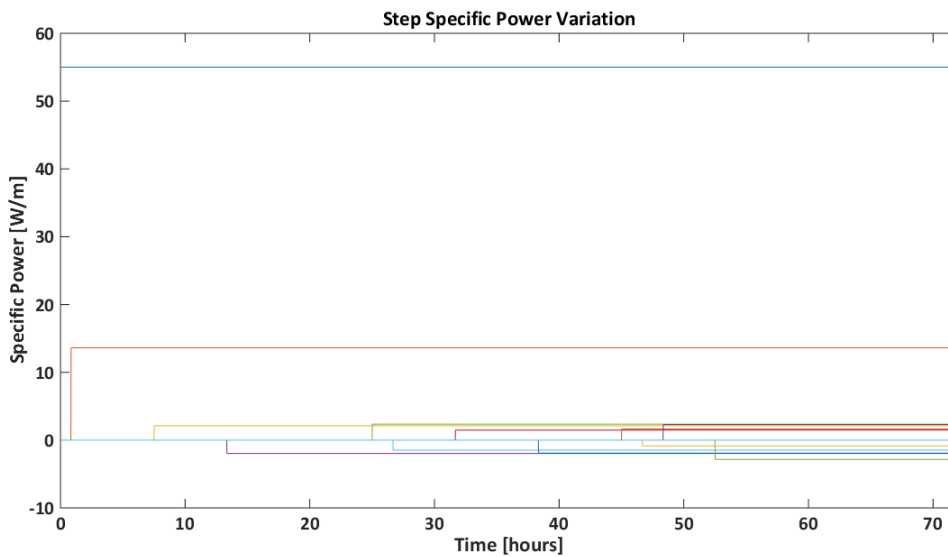
Figure 5-18 - Step specific power variation series as input for ILS solution with variable heat injection.

The choice of a different power step function implies a different specific power step variation, which can be more or less precise based on the number of intervals earlier defined. This procedure is not pre-determined but can be arranged in order to locally reduce the standard deviations, such they are lower than an established value in each interval. In this study, only the step power function provided in Table 34 is evaluated in order to estimate ground thermal conductivity and borehole thermal resistance.

5.5.2   Initial Time Sensitivity Analysis

A series of fits are performed with the aim of understanding initial time influence to Infinite Line Source model with variable heat injection rates and to confirm ILS time criterion for data significativity of *5,81 hours* (**Eq. 5.8**) previously determined.

A round of fits is carried out with an initial time t_{in} = *6 h* and a final time t_{end} = *72h 40min* in order to have an outline of the solutions. The sets of parameters obtained by the

Franco Lý

Interpretation of Borehole Heat Exchangers Thermal Response Tests
under groundwater influence: analysis of three case studies

estimation procedure are characterized by a *RMSE*, calculated in an analogous way to **Eq. 2.35**. The script generates VHI-ILS solutions described in Table 37. The results obtained by the 18 fits lead to a unique solution:

− λ = *2,88 W/(m·K)*
− R_b = *0,203 m·K/W*

Table 37 - Solution from VHI-ILS analysis with t_{in} = 6 h and t_{end} = 72h 40min.

Initial Parameter Values		Fitted Parameter Values		RMSE [°C]
λ [W/mK]	Rb [mK/W]	λ [W/mK]	Rb [mK/W]	
0,50	0,100	2,88	0,203	0,760
1,00	0,100	2,88	0,203	0,760
1,50	0,100	2,88	0,203	0,760
2,00	0,100	2,88	0,203	0,760
2,50	0,100	2,88	0,203	0,760
3,00	0,100	2,88	0,203	0,760
0,50	0,150	2,88	0,203	0,760
1,00	0,150	2,88	0,203	0,760
1,50	0,150	2,88	0,203	0,760
2,00	0,150	2,88	0,203	0,760
2,50	0,150	2,88	0,203	0,760
3,00	0,150	2,88	0,203	0,760
0,50	0,200	2,88	0,203	0,760
1,00	0,200	2,88	0,203	0,760
1,50	0,200	2,88	0,203	0,760
2,00	0,200	2,88	0,203	0,760
2,50	0,200	2,88	0,203	0,760
3,00	0,200	2,88	0,203	0,760

The parameters estimation by VHI-ILS script is then performed using as initial parameters the systematic scheme already described of 18 pairs of λ and R_b for 6 times and by varying t_{in}, according to Table 38. The considered evaluation time t_{end} is the total duration of the test and kept constant for all the fits equal *72 hours*.

Table 38 - Initial time values used for the sensitivity analysis.

Initial time	0 hours	2 hours	4 hours	6 hours	8 hours	10 hours

Franco Lý

*Interpretation of Borehole Heat Exchangers Thermal Response Tests
under groundwater influence: analysis of three case studies*

By increasing t_{in} an improvement of the fit quality can be noticed (Figure 5-19). The diminishment of *RMSE* is about *22%* from disregarding first *0 hours* to *6 hours* and improves by an other *24%* passing from disregarding *6 hours* to *8 hours* (Table 39 shows obtained *RMSE* values).
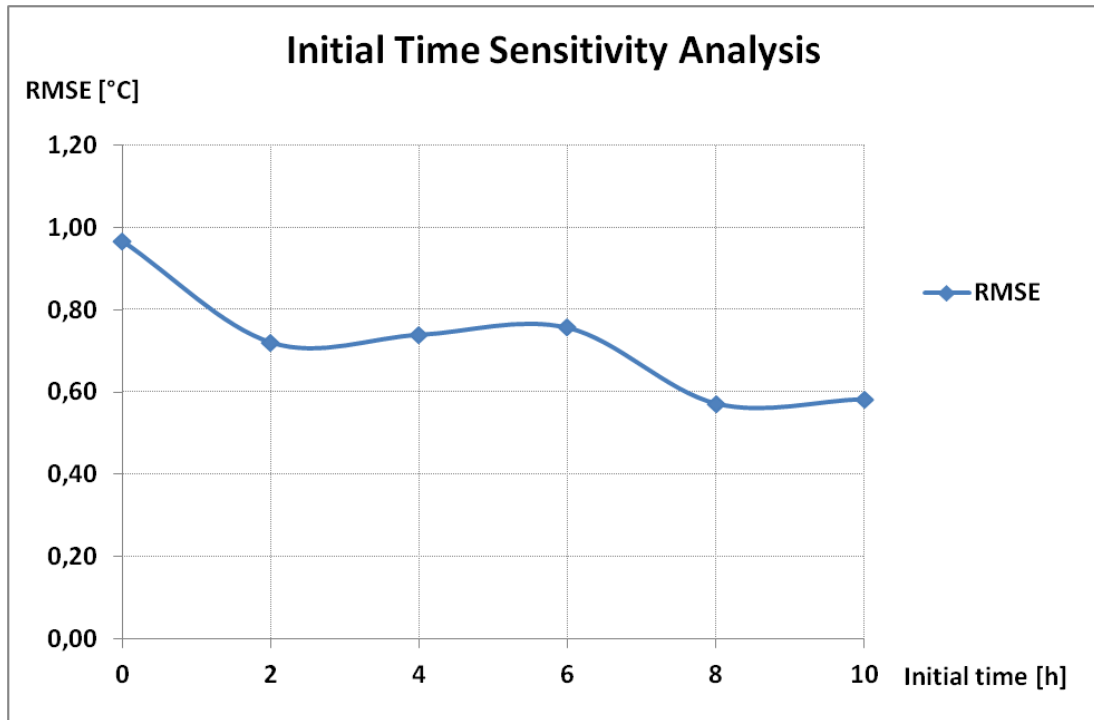
Figure 5-19 - RMSE trend for increasing initial time.

The initial time sensitivity analysis returns unique pairs of parameters (solutions) for each initial time reported in Table 39. The ground thermal conductivity seems to stabilize after disregarding *6 hours*, approaching to a value of about *2,69 W/m·K* for an initial time of *10 hours* (Figure 5-20). While borehole thermal resistance values are rather steady, slightly superior to *0,200 m·K/W* as illustrated in Figure 5-21.

Table 39 - Estimated pairs of parameters by VHI-ILS solution for increasing initial time.

Initial time [h]	λ [W/mK]	R_b [mK/W]	RMSE [°C]
0	2,17	0,200	0,97
2	3,03	0,203	0,72
4	3,00	0,203	0,74
6	2,88	0,203	0,76
8	2,75	0,206	0,57
10	2,69	0,206	0,58
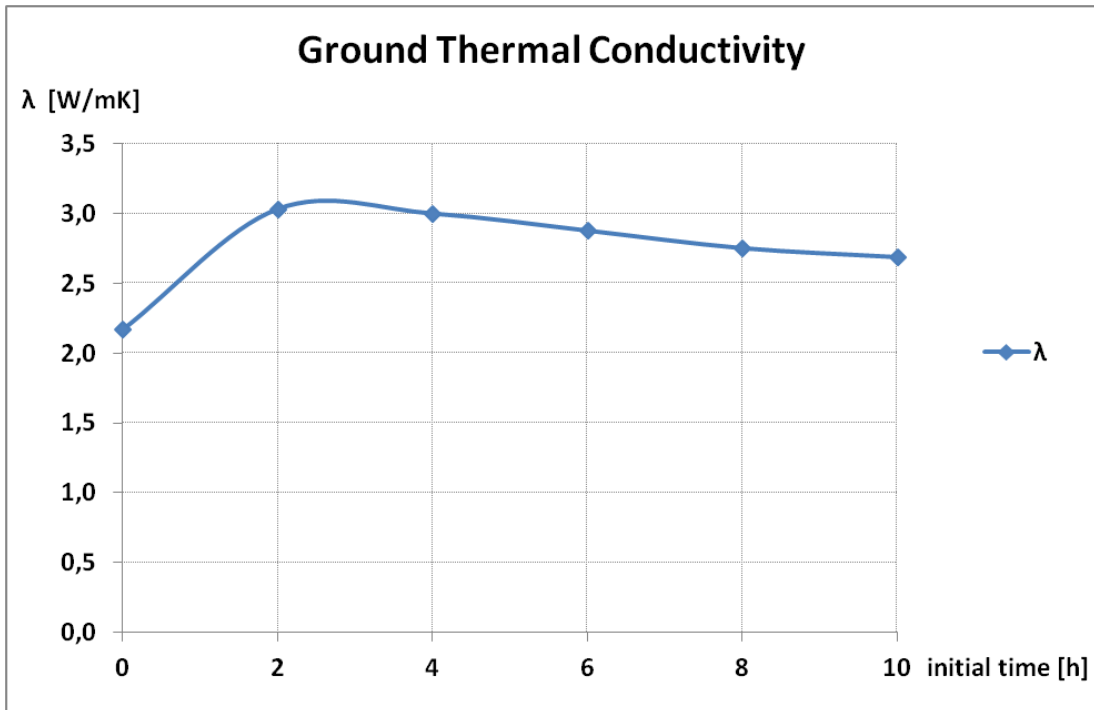
Figure 5-20 - Estimated ground thermal conductivity values for increasing initial time by VHI-ILS solution.
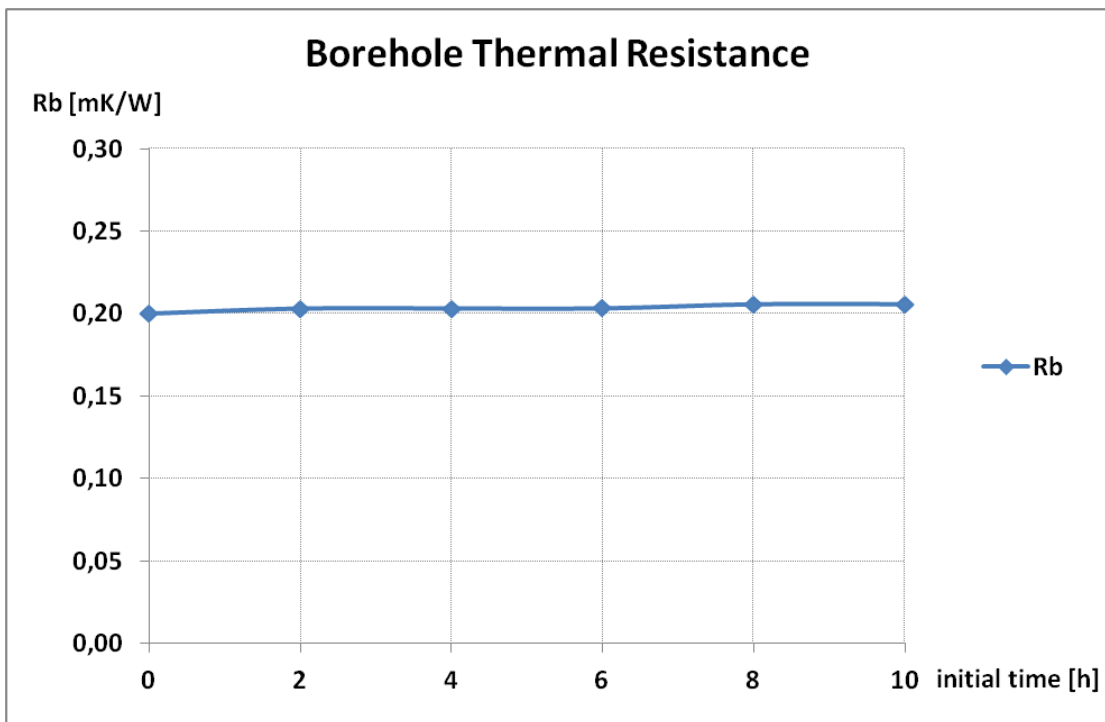
Figure 5-21 - Estimated borehole thermal resistance values for increasing initial time by VHI-ILS solution.

The obtained temperature time series by ILS solution with variable heat injection rates disregarding first *10 hours* of the dataset is depicted in Figure 5-22. Similar plots are obtained for different tested initial time and thus they are not reported.
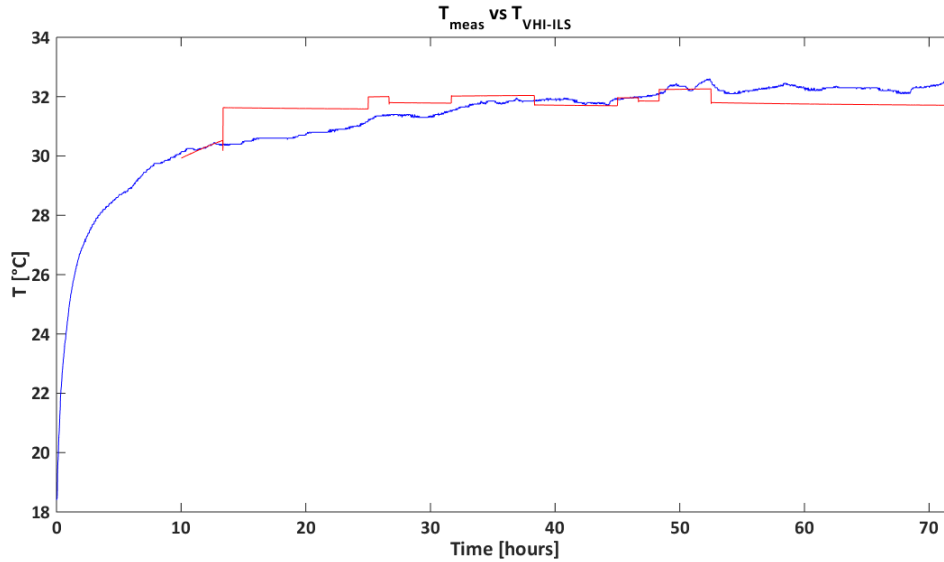
Figure 5-22 - Experimental data (blue line) vs. simulated temperature time series by VHI-ILS solution (red line) for an initial time t_{in} = 10 h.

5.5.3 Results Discussion

By means of a two-variables parameter estimation procedure according to the inverse modeling of **Eq. 5.11**, which is the logarithmic approximation of VHI-ILS equation, unique solutions result from fitting generated temperature time series to experimental data starting from different pairs of initial parameters.

The scheme of initial parameters involves until 18 different combinations of λ and R_b. The results seems to indicate the independence of the solution with respect to the initial parameters values.

The procedure is validated by the results from initial time sensitivity analysis, which has proved to originate consistent values of λ and R_b with decreasing *RMSE* values for larger initial time (tested until *10 hours*). However, the choice of initial parameters interval is constrained and led by physical consideration and geological site-specific characteristics.

Franco Lý

Interpretation of Borehole Heat Exchangers Thermal Response Tests under groundwater influence: analysis of three case studies

Concerning ground thermal conductivity, the estimated values are comprised between *2,17* and *3,03 W/m·K* as illustrated in Figure 5-20. In particular after an initial increase for an initial time of 2 hours the conductivity values seems to slowly decrease approaching to a stable value of about *2,69 W/m·K* for an initial time of *10 hours*.

Regarding borehole thermal resistance, the estimated values are certainly more stable than thermal conductivity, standing around *0,200 m·K/W* as shown in Figure 5-21.

Time criterion for data significativity returns a characteristics time of *5,81 hours* for a thermal diffusivity *a* of *9,6E-7 m^2/s* (**Eq. 5.8**), which has proved to be coherent with the initial time analysis sensitivity findings.

To sum up, it can be assessed that results from initial time sensitivity analysis are reliable if the total duration of the test is accounted and initial time longer than *6 hours* are considered. In fact, the ground thermal conductivity turns to be coherent with the geological characteristics of the site previously evaluated by geological maps and observations from in-situ drillings; while the borehole thermal resistance values seems to be slightly overestimated with respect to the borehole geometry and filling material adopted for tested BHE.

In section 5.7, VHI-ILS solution is compared with the conventional TRT analysis results with constant heat injection and with MLS solution results.

5.6 Coupled Conductive - Advective Analysis by means of Moving Line Source Theory

The results obtained from Lodi TRT interpretation by Infinite Line Source approach has proved to be not completely satisfying, since ground thermal conductivity appears to be overestimated with respect to literature. Moreover, the presence of two aquifers suggests an additional analysis to verify the validity of the TRT interpretation and to evaluate groundwater flow velocity.

As previously commented in section 2.6.1, the MLS script in MATLAB used for a 3 parameters estimation, neglects the effect of thermal longitudinal and transversal dispersivity according to (Wagner V. a., 2013).

5.6.1   MLS Analysis Settings

The script is updated to embed specific geological site features and borehole characteristics for Lodi TRT and the script is run in order to estimate λ, v and R_b.

To appropriately comprehend the influence of initial parameters, it is proposed to originate a 80 combinations matrix, thus constituted by 80 line vectors of the three parameters. This systematic scheme of initial parameters is defined based on considerations hereafter explained and will be used for further parameters estimation for this specific case.

About ground thermal conductivity, the available geological information indicate to use a wide a range of possible values with a superior limit of *3,0 W/(m·K)* (see Table 40).

<div align="center">Table 40 - Ground thermal conductivity initial values used for MLS solution fit.</div>

Ground Thermal Conductivity [W/(m·K)]	1,5	2,0	2,5	3,0

Concerning Darcy velocity, identified an groundwater presence in this specific site and considered the geological subsurface characteristic, relatively important velocity are considered, however accounting for a large interval as shown in Table 41.

<div align="center">Table 41 - Darcy velocity initial values used for MLS solution fit.</div>

Aquifer Darcy Velocity [m/s]	1,0E-4	1,0E-5	1,0E-6	1,0E-7	1,0E-8
Aquifer Darcy Velocity [m/day]	8,64	0,864	0,0864	0,00864	0,000864

Regarding borehole thermal resistance, a range of values commonly recurrent for the single U-pipe configuration are suggested:

<div align="center">Table 42 - Borehole thermal resistance initial values used for MLS solution fit.</div>

Borehole Thermal Resistance [m·K/W]	0,09	0,12	0,15	0,18

A numerical step of *1E-3* is kept constant for all the fits according to the consideration discussed in section 3.5.1.

Franco Lý

Interpretation of Borehole Heat Exchangers Thermal Response Tests under groundwater influence: analysis of three case studies

5.6.2 Time Criterion for Initial Data Significativity

Assuming a parallel approach to ILS model for TRT interpretation, a time criterion for data significativity is established in section 2.6.2. A first guess Darcy velocity is required, such to roughly estimate the time that is necessary for the borehole volume to almost reach steady state.

Hence, taking into consideration the hydrogeological characteristics of the site a initial Darcy velocity *v* of *5E-6 m/s* is supposed. For an undisturbed ground temperature T_0 = *17,4°C* the following parameters are evaluated:

$$Re_L = \frac{\rho \cdot v \cdot L}{\mu} = \frac{1000 \cdot 5 \cdot 10^{-6} \cdot 0,127}{1,08 \cdot 10^{-3}} = 0,59$$

$$Pr = \frac{v}{a} = 7,56$$

$$\overline{Nu} = C \, Re_L^m \, Pr^{1/3} = 0,989 \cdot 0,59^{0,33} \cdot 7,56^{1/3} = 1,63$$

$$\bar{h} = \frac{\overline{Nu} \cdot \lambda}{L} = \frac{1,63 \cdot 0,586}{0,127} = 7,52 \, W/_{m^2 K}$$

Recalling the thermal time constant (**Eq. 2.41**) interpreted as:

$$\tau_t = \frac{\rho_g \cdot r_b \cdot c_g}{h \cdot 2} = 0,76 \, h$$

And the characteristic time t_c (**Eq. 2.42**) is defined as:

$$t_c = (4 \div 5) \, \tau_t = 3,0 \div 3,8 \, h$$

5.6.3 Initial Time Sensitivity Analysis

Time criterion returns about a characteristics time of *4 hours*, which will be considered as one of initial time values of the sensitivity analysis as reported in Table 44. A round of fits is carried out with an initial time t_{in} = *10 h* and a final time t_{end} = *72h 40min* in order to have an outline of the solutions. The sets of parameters obtained by the estimation procedure are characterized by a *RMSE*, calculated by means of **Eq. 2.35**. The script generates MLS solutions described in Table 43.

The results obtained by the 80 fits with the above imposed conditions are 33 solutions (sets of three parameters) with *RMSE* ranging from *0,113°C* to *0,182°C*. Negative values of *v* are

Franco Lý

*Interpretation of Borehole Heat Exchangers Thermal Response Tests
under groundwater influence: analysis of three case studies*

converted to positive for the most recurrent solution which covers the *57,5%* of the fits (46 solutions on 80 fits). 34 solutions result to have same *λ* and R_b, but different *v* values.

Table 43 - Solutions from MLS analysis with t_{in} = 10 h and t_{end} = 72 h 40 min.

Solution	Fitted Parameter Values			f [%]	RMSE [°C]
	λ [W/mK]	v [m/s]	Rb [mK/W]		
1	0,53	2,1E-05	0,186	57,50%	0,113
2	2,84	4,8E-08	0,184	2,50%	0,182
3	2,84	4,8E-09	0,184	2,50%	0,182
4	2,84	2,8E-08	0,184	1,25%	0,182
5	2,84	2,8E-09	0,184	1,25%	0,182
6	2,84	4,2E-08	0,184	1,25%	0,182
7	2,84	4,2E-09	0,184	1,25%	0,182
8	2,84	1,7E-07	0,184	1,25%	0,182
9	2,84	1,7E-08	0,184	1,25%	0,182
10	2,84	1,1E-07	0,184	1,25%	0,182
11	2,84	1,1E-08	0,184	1,25%	0,182
12	2,84	7,6E-07	0,184	1,25%	0,182
13	2,84	7,4E-08	0,184	1,25%	0,182
14	2,84	7,4E-09	0,184	1,25%	0,182
15	2,84	7,6E-08	0,184	1,25%	0,182
16	2,84	7,6E-09	0,184	1,25%	0,182
17	2,84	7,0E-08	0,184	1,25%	0,182
18	2,84	7,0E-09	0,184	1,25%	0,182
19	2,84	-3,3E-08	0,184	1,25%	0,182
20	2,84	-3,3E-09	0,184	1,25%	0,182
21	2,84	3,1E-07	0,184	1,25%	0,182
22	2,84	3,0E-08	0,184	1,25%	0,182
23	2,84	3,0E-09	0,184	1,25%	0,182
24	2,84	1,2E-07	0,184	1,25%	0,182
25	2,84	1,2E-08	0,184	1,25%	0,182
26	2,84	8,8E-08	0,184	1,25%	0,182
27	2,84	8,8E-09	0,184	1,25%	0,182
28	2,84	6,9E-08	0,184	1,25%	0,182
29	2,84	6,9E-09	0,184	1,25%	0,182
30	2,84	9,4E-08	0,184	1,25%	0,182
31	2,84	9,3E-09	0,184	1,25%	0,182
32	2,84	1,0E-07	0,184	1,25%	0,182
33	2,84	1,0E-08	0,184	1,25%	0,182

Franco Lý

Interpretation of Borehole Heat Exchangers Thermal Response Tests
under groundwater influence: analysis of three case studies

To have a general overview of the parameters estimation results, a summary plot from all the fits for an initial time t_{in} = *10 hours* and t_{end} equal to the total duration of the test is given for each fitting parameter (λ, R_b and v).
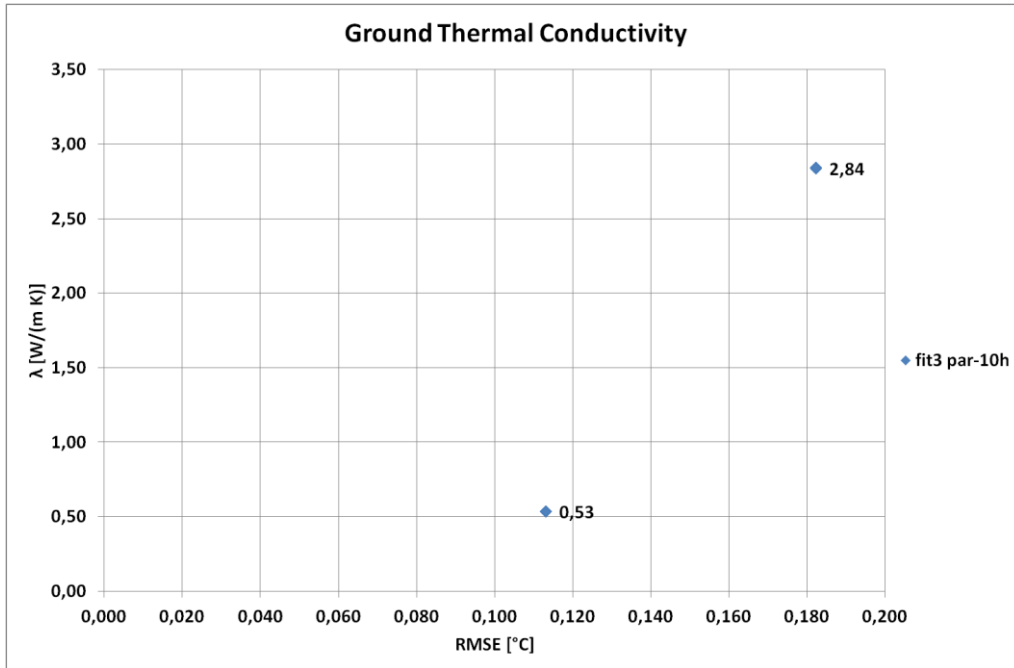
Figure 5-23 - Summary plot of fitted ground thermal conductivity values for initial time t_{in} = 10 h.
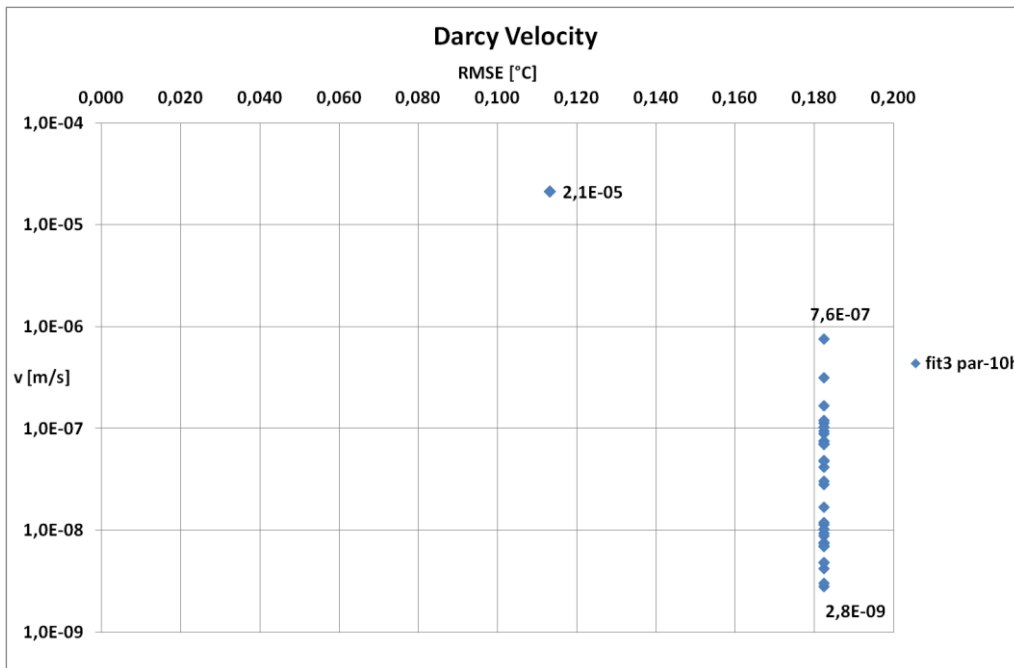
Figure 5-24 - Summary plot of fitted Darcy velocity absolute values for initial time t_{in} = 10 h.

Franco Lý

Interpretation of Borehole Heat Exchangers Thermal Response Tests
under groundwater influence: analysis of three case studies

Relative to thermal conductivity summary plot in Figure 5-23, the lowest *RMSE* value of *0,113°C* corresponds to a ground thermal conductivity of *0,53 W/(m·K)* (solution 1 of Table 43). The remaining solutions with *RMSE* around *0,182°C* refer to the same thermal conductivity of *2,84 W/(m·K)* (solutions 2 ÷ 33 of Table 43).

Regarding Darcy velocity summary plot in Figure 5-24, the corresponding value of this parameter for the lowest values of *RMSE* is *2,1E-5 m/s* in absolute value (solution 1).

All the other values of Darcy velocity are relative to a higher *RMSE* equal to *0,182°C*, which range on a large interval, specifically from *2,8E-9 m/s* to *7,6E-7 m/s*. These low values are all coupled with the same ground thermal conductivity of *2,84 W/(m·K)*. Further considerations are provided in sections 5.6.4 and 5.7.
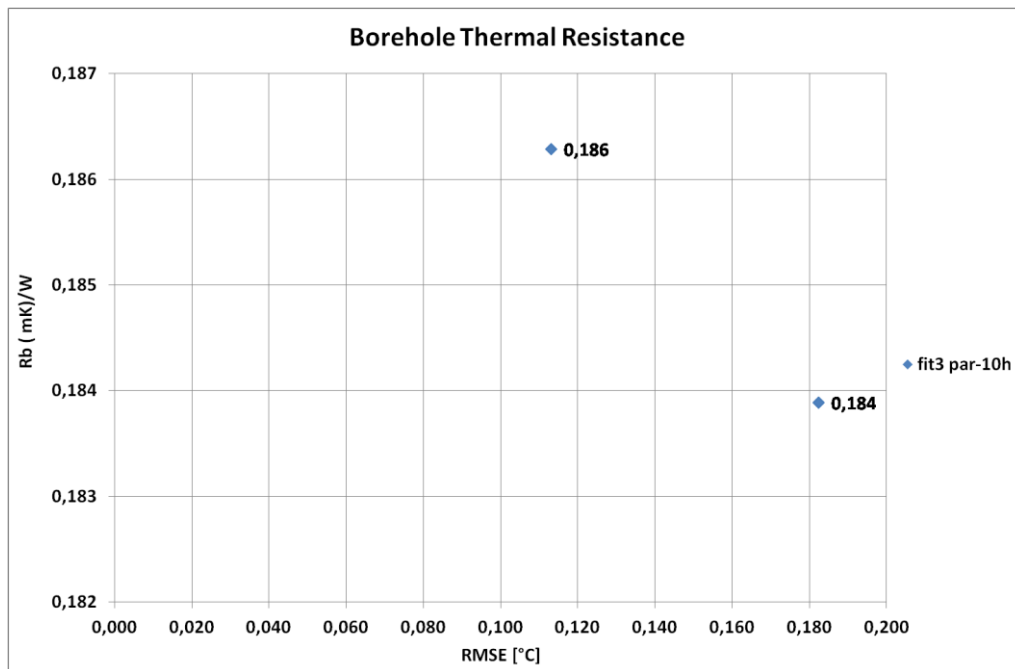
Figure 5-25 - Summary plot of fitted borehole thermal resistance values for initial time t_{in} = 10 h.

Concerning the borehole thermal resistance summary plot in Figure 5-25, two very similar values can be identified. The lowest *RMSE* value correspond to a R_b value slightly lower than *0,186 m·K/W*; while for *RMSE* values around *0,182°C* it corresponds *0,184 m·K/W*. The two values have a not significant difference of only *1,3%* between each other.

Franco Lý

Interpretation of Borehole Heat Exchangers Thermal Response Tests under groundwater influence: analysis of three case studies

Similarly to the Trento case study, the final time sensitivity analysis is not performed since no steady state condition is reached in the fluid profile temperature profile. Nonetheless, a series of fits are carried out with the aim of understanding initial time influence to Moving Line Source model fit and trying to validate the time criterion for data significativity previously established in section 2.6.2.

The parameters estimation by Moving Line Source script is performed using as initial parameters the systematic scheme already described of 80 combinations (section 5.6.1) for 6 times, disregarding initial data according to Table 44. The considered evaluation time is the total duration of the test kept constant for all the fits equal to *72 hours 40 minutes*.

Table 44 - Initial time values used for the sensitivity analysis.

Initial time	8 min	2 hours	4 hours	6 hours	8 hours	10 hours

The time value of about *8 minutes* is the value around which the mean temperature time series seems graphically to be affected by the heat injection and so start to rise (Figure 5-26). This was the result of a first attempt to understand how to disregard initial data.
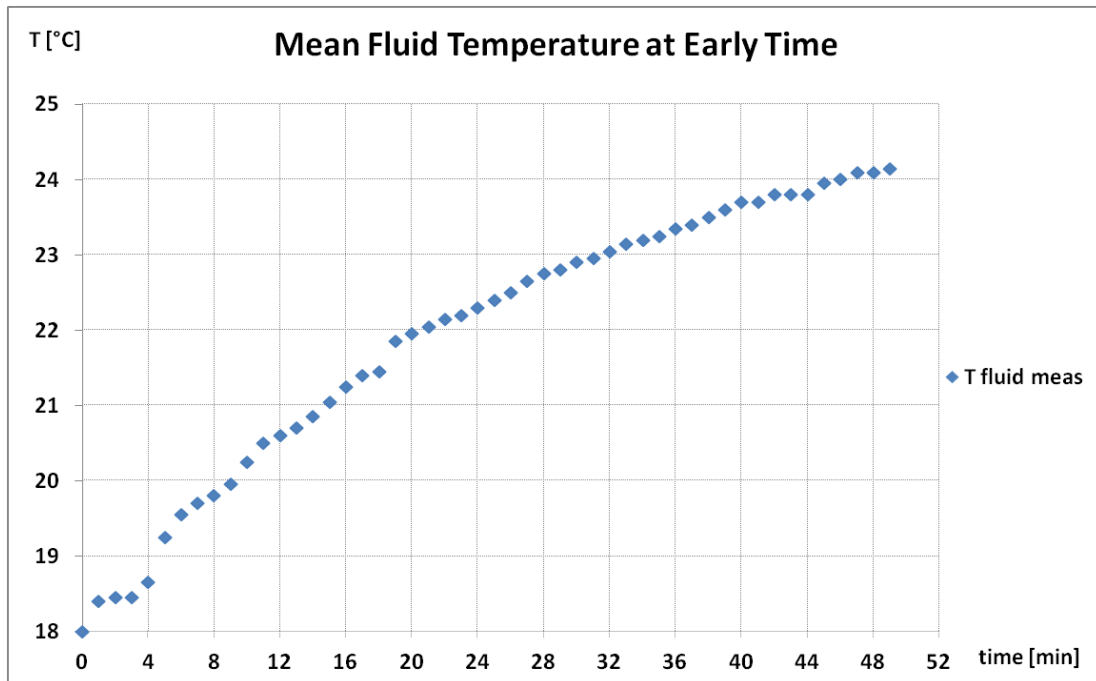
Figure 5-26 - Mean fluid temperature at early times.

A great improvement of $RMSE_{average}$ by increasing the initial time t_{in} can be noticed in Figure 5-27. The diminishment of $RMSE$ is already about *49%* when passing from disregarding first *8 minutes* to *2 hours*. It can be coherently stated that $RMSE$ values after disregarding *2 hours* converge to stable values for increasing initial times, as a smooth trend of $RMSE$ values can be detected approaching to an initial time t_{in} = *10 hours*.
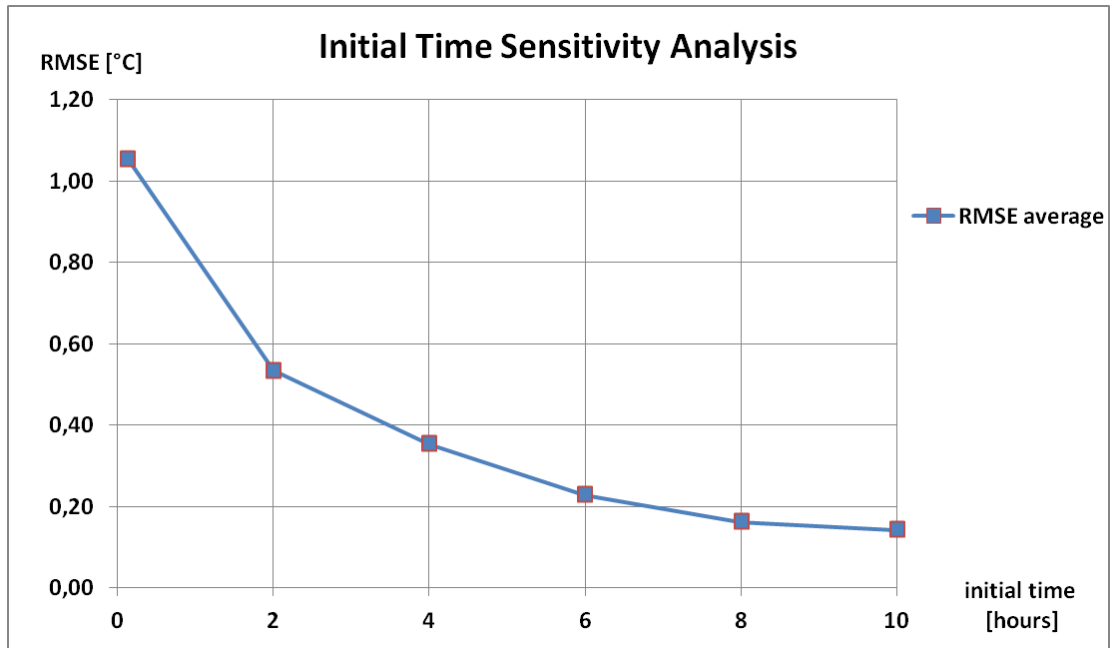
Figure 5-27 - RMSE trend for increasing initial time.

Then, the initial time sensitivity analysis allows to individuate t_{in} = *10 h* as the initial time value to be considered for its corresponding stable and low $RMSE_{average}$. Therefore, some examples of resulting plots of the Moving Line Source model fits are illustrated for an initial time t_{in} = *10 h*.

There are two main solutions that cover the totality of the results:

− solution **1** [*λ = 0,53 W/(m·K); v = 2,1E-5 m/s; R_b = 0,186 m·K/W*];

− solution **a** [*λ = 2,84 W/(m·K); v = 2,8E-9 ÷ 7,6E-7 m/s; R_b = 0,184 m·K/W*]

Solution **1** is shown in Figure 5-28, while solution **a** in Figure 5-29.

Franco Lý

*Interpretation of Borehole Heat Exchangers Thermal Response Tests
under groundwater influence: analysis of three case studies*
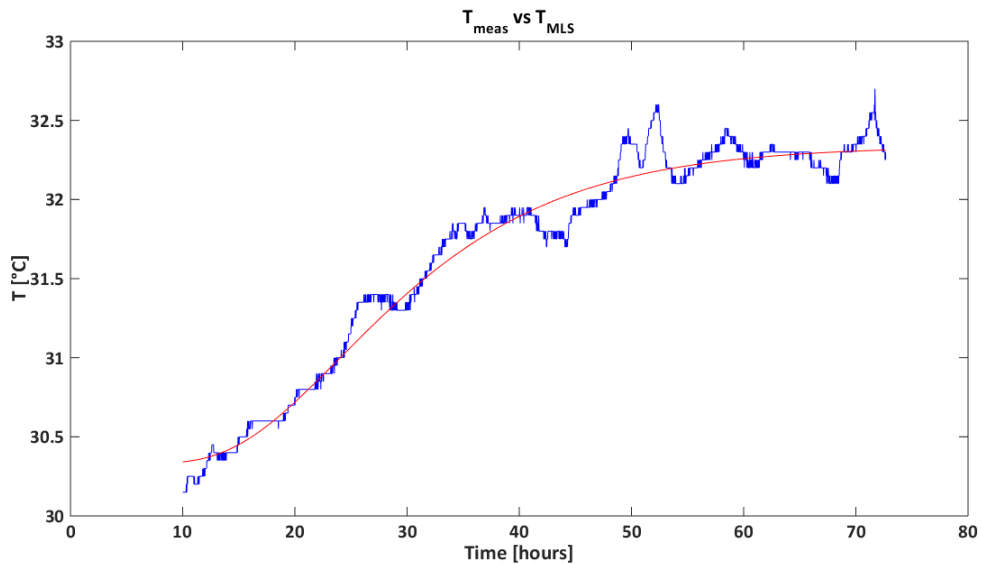
Figure 5-28 - Plot of measured data (blue line) vs. MLS temperature time series (red line) for t_{in} = 10 h and t_{end} = 72 h 40 min, solution 1 [λ = 0,53 W/(m·K); v = 2,1E-5 m/s; R_b = 0,186 m·K/W].

With the lowest *RMSE* equal to *0,113°C*, solution **1** returns satisfying matching plot (Figure 5-28) between measured and simulated temperature time series, but with thermal conductivity value not close to the mean expected value for the geological site equal to *2,33 W/(m·K)*, a significant groundwater flow in absolute value of *2,1E-5 m/s* and a feasible borehole thermal resistance value equal to *0,186 m·K/W*.
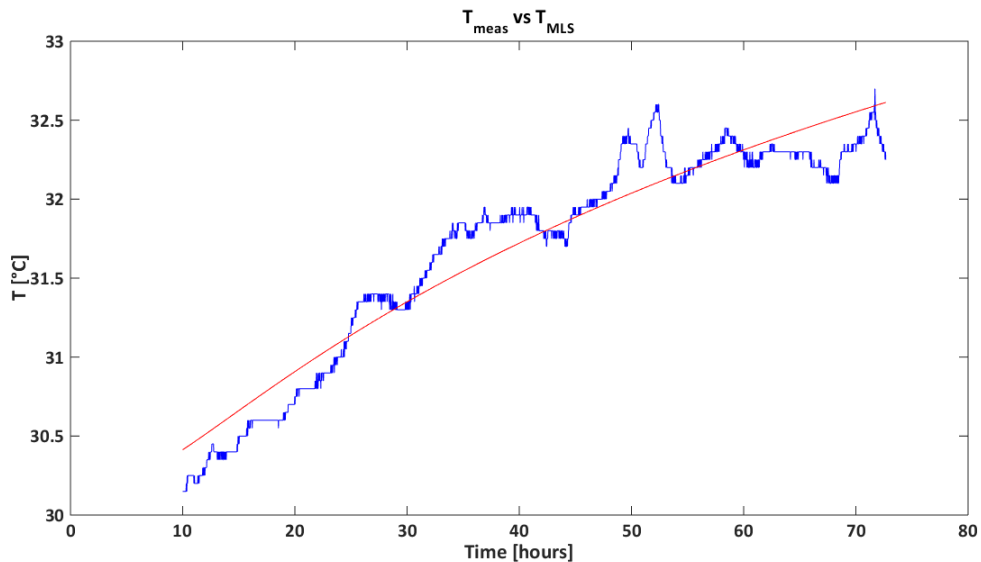
Figure 5-29 - Plot of measured data (blue line) vs. MLS temperature time series (red line) for t_{in} = 10 h and t_{end} = 72 h 40 min, solution a [λ = 2,84 W/(m·K); v = 2,8E-9 ÷ 7,6E-7 m/s; R_b = 0,184 m·K/W].

Franco Lý

Interpretation of Borehole Heat Exchangers Thermal Response Tests
under groundwater influence: analysis of three case studies

Solution **a**, which relative plot is in Figure 5-29 returns higher values of *RMSE* equal to *0,182°C*. They denote a thermal conductivity of *2,84 W/(m·K)* close to the mean expected value for the geological site, borehole thermal resistance equal to *0,184 m·K/W* similar to solution **1**, but low values for Darcy velocity, not in agreement with the expectations considering the hydro-geological context.

MLS solution **1** determined a Darcy velocity *v* of *2,1E-5 m/s*, which could be reasonably representative of the groundwater flow. Then, the time criterion for data significativity is updated with this estimated value. The resulting characteristic time is obtained following the previously applied procedure:

$$Re_L = \frac{\rho \cdot v \cdot L}{\mu} = \frac{1000 \cdot 2,1 \cdot 10^{-5} \cdot 0,127}{1,08 \cdot 10^{-3}} = 2,47$$

$$Pr = \frac{v}{a} = 7,56$$

$$\overline{Nu} = C\ Re_L^m\ Pr^{1/3} = 0,989 \cdot 2,47^{0,33} \cdot 7,56^{1/3} = 2,62$$

$$\bar{h} = \frac{\overline{Nu} \cdot \lambda}{L} = \frac{2,62 \cdot 0,586}{0,127} = 12,07\ {W}/{m^2 K}$$

Recalling the thermal time constant interpreted as:

$$\tau_t = \frac{\rho_g \cdot r_b \cdot c_g}{h \cdot 2} = 0,47\ h$$

And the characteristic time t_c is defined as:

$$t_c = (4 \div 5)\ \tau_t = 1,9 \div 2,4\ h$$

This characteristic time value according to Figure 5-27 corresponds to a very good *RMSE_{average}* improvement, however larger initial times are necessary in order to make *RMSE* values more stable.

Darcy velocity values from solution **a** cannot be taken into consideration, since velocities lower than *3,0E-6 m/s* are critical for the determination of the characteristic time value for typical borehole diameter of *127 mm* as previously described in section 2.6.2.

5.6.4 Results Discussion

By means of a 3 variable parameters estimation procedure, multiple solutions result from initial time sensitivity analysis comprehending different minima, as it happened in the other two case studies analyzed in chapter 3 and 4.

As already cited, the script fits MLS temperature time series to experimental data, minimizing *RMSE* starting from a large combinations of initial parameters. This approach aims to guarantee an adequate range of possible results including the absolute minimum, if the initial parameters choice falls back into feasible values interval for all three parameters. As for Trento case study, it was not possible to validate the results from initial time sensitivity analysis. Maybe, it could have been important to choose a variation step closer than the actual within each parameter interval, but we are rather confident with the adopted variation step to generate enough dense initial values ($\Delta\lambda$ = *0,5 W/(m·K)*, Δv = *10^1 m/s* and ΔR_b *0,03 m·K/W*; sets of initial parameter in section 4.5.1).

Throughout the report from initial time sensitivity analysis, it is explained how some results have no physical meaning and thus should be discriminated and not considered.

Solution **1** resulted in a thermal conductivity value λ equal to *0,53 W/(m·K)*. Even if this estimated value corresponds to the lowest *RMSE*, such low thermal conductivity value can only represent soil conformations that are not characteristic of the specific geological site. Consequently, this λ value, its relative *v* and R_b values of the same set of fitted parameters should be not considered as possible correct solution (solution **1**). The issue is that this set of fitted parameters is responsible for generating the best matching plot between MLS temperature time series and experimental data for this specific case study as outlined in Figure 5-28.

Then, the interpretation of the MLS solutions results to be inconsistent and not trivial: not feasible fitted parameters generate best matching plot with also the lowest *RMSE* value. The coupled value of Darcy velocity is *2,1E-05 m/s* indicating a rather relevant groundwater flow and it would be in agreement with the result of ILS approach. However, no precise information on hydraulic properties are available.

Solution **a** returns higher values of *RMSE*. It denotes a thermal conductivity close to the mean expected value for the geological site, but low values for Darcy velocity, not in agreement with the expectations considering the hydro-geological context.

Pumping tests in situ have determined an overall hydraulic conductivity of *3,35E-4 m/s* accounting both shallow and deep aquifers. An hydraulic gradient of *0,4%* for the shallow aquifer is identified and also assumed for the confined aquifer because of the lack of wells

Franco Lý

Interpretation of Borehole Heat Exchangers Thermal Response Tests
under groundwater influence: analysis of three case studies

deeper than *30 m* in a radius of *1 Km* from the site (Marocchi, 2015). After a first calibration of the heat transfer model with only one stress period, the confined aquifer hydraulic gradient was reduced to *0,25%* leading to great benefits to the goodness of the model. The Darcy velocity can be roughly averaged over the aquifers thicknesses resulting *1,06E-6 m/s.* Both MLS solutions **1** and **a** do not comprises this value. Further considerations are provided in section 5.9.

Finally, the MLS curve follows the measured data trend for most of the dataset but, in the last part the two series seem to detach one to each other, with the MLS curve mainly going upward as outlined in Figure 5-29.

The borehole thermal resistance values obtained from all the fits are consistent, ranging in small interval, from *0,184* to *0,186 m·K/W*. R_b turns to be the more constrained parameter after having carried out the initial time sensitivity analysis. The values confirm the expectations, especially considering the filling material i.e. cement and bentonites and the single U-pipe configuration (Table 20).

Time criterion for data significativity returns a characteristics time of *2,4 hours* relatively for a Darcy velocity of *2,1E-05 m/s*, which is in agreement with the initial time analysis sensitivity findings. Indeed removing about the first *2 hours*, the largest decrease rate in $RMSE_{average}$ is achieved. In disregarding more hours the *RMSE* does not have the same improvement rate, in fact from Figure 5-27 it can be noticed a smooth trend of *RMSE* values approaching to an initial time of *10 hours*.

To sum up, the sets of parameters attained by MLS script are multiple, confirming the findings of (Wagner V. a., 2013), that TRT evaluation based on **Eq. 2.23**. and its simplified form **Eq. 2.34** is an ill-posed problem, where solutions to the inverse problem are non-unique. The obtained MLS results for Lodi case study are similar to Trento case study, where two main solutions are obtained, resulting difficult the choice of the best fit solution. This because in both case studies a solution (solution **1**) is characterized by the lowest *RMSE* presenting reasonable Darcy velocity, but very low ground thermal conductivity altogether with a good matching plot of temperature time series. While a second group of solutions (solution **a**) is distinguished by the same thermal conductivity in agreement with literature table, similar borehole thermal resistance to solution **1**, but low Darcy velocity values although important aquifers are identified in the subsurface. Thus, choosing the correct parameters to describe thermal properties of the subsurface and the boreholes is not simple in these two case studies. Only performing hydraulic tests or by means of numerical modeling, more detailed information can be compared to MLS solutions to verify the goodness of the parameter estimation procedure. A comparison of MLS solutions with numerical modeling results in MODFLOW is provided in section 5.9.

Franco Lý

*Interpretation of Borehole Heat Exchangers Thermal Response Tests
under groundwater influence: analysis of three case studies*

5.7 Infinite Line Source vs. Moving Line Source Approach for Lodi TRT

5.7.1 Results Comparison

For this TRT case study, three different analytical solutions were applied to determine subsurface and borehole thermal properties. At first, the TRT interpretation was carried out with the standard ILS approach, leading to two main final considerations: elevated power values oscillation and ground thermal conductivity overestimation. Consequently, variable heat injection rates and advection heat exchange were taken into account by means of more complex analytical solutions and compared to the conventional ILS solution.

In fact, a high level of scattering for both thermal and electrical power time series, without fulfilling standard deviation recommendation of (UNI11466, 2012) was detected as outlined in Figure 5-9. Therefore, an extended version of the ILS solution using the superposition principle is then applied to comprehensively account for variable heat injections rates. The analysis managed to improve the ground thermal conductivity estimation, but it overestimated the borehole thermal resistance if compared to conventional ILS results. However, the solution has a high level of dependence on the proposed step power function, for which only one attempt was tested in this work (see Table 34). With further refinement of the proposed input heat injection function to the analytical solution, it is very likely that a better parameter estimation can be achieved.

Besides, by means of the MLS model an alternative method to interpret TRT dataset is applied able to account also for advection heat exchange. As just mentioned, the standard TRT interpretation has indicated the presence of an important groundwater flow such that the purely conductive ILS model returned a *70%* enhanced ground thermal conductivity than the estimated from literature tables. Performing an initial time sensitivity analysis using MLS script, two sets of estimated parameters are obtained comprising the totality of the results: solutions **1** and **a** described in section 5.6.3. Differently from Claviere case study, the interpretation of the TRT was not straightforward, it turned out to be complex. The two sets of parameter values are compared with the solution attained by ILS model and its extended version able to account variable heat injection rates (VHI-ILS).

To recall the preliminary assessment, the mean expected ground thermal conductivity that was estimated by literature tables from the extracted stratigraphy is *2,33 W/(m·K)*. While the borehole thermal resistance should be comprised between *0,16 ÷ 0,20 m·K/W* (Delmastro, 2011) considering the filling material i.e. concrete and bentonite and the single U-pipe configuration (Table 20).

Franco Lý

Interpretation of Borehole Heat Exchangers Thermal Response Tests
under groundwater influence: analysis of three case studies

Table 45 - Comparison among ILS, VHI-ILS and MLS results.

TRT analysis / estimated parameter	ILS	VHI-ILS	MLS (solution **1**)	MLS (solution **a**)
Ground Thermal Conductivity [$W/(m·K)$]	*3,84*	*2,69*	*0,53*	*2,84*
Borehole Thermal Resistance [$m·K/W$]	*0,121*	*0,206*	*0,186*	*0,184*
Aquifer Darcy Velocity [m/s]	Cannot be estimated by this approach.	Cannot be estimated by this approach.	*2,1E-5*	*2,8E-9 ÷ 7,6E-7*

The set of parameters of solution **1** obtained by the MLS solution is univocal considering the absolute value of Darcy velocity (*57,5%* of the fits) and it generates the best matching plot as described in Figure 5-28.

The sets of parameters of solution **a** obtained by the MLS solution are multiple considering that ground thermal conductivity and borehole thermal resistance always correspond to the same values respectively, but the Darcy velocity (*42,5%* of the fits) ranges in interval of values, though they generate the same plot as described in Figure 5-29.

Concerning ground thermal conductivity, the VHI-ILS (*RMSE = 0,76°C*) and MLS solution **a** (*RMSE = 0,18°C*) provide close estimates to the expected value of *2,33 W/($m·K$)* remaining under max values of *2,86 W/($m·K$)* from Table 31. While standard ILS model gives an overestimation of the parameter since it consists in an effective ground thermal conductivity, which is known to increase with Darcy velocity. MLS solution **1** is not able to estimate an acceptable value of thermal conductivity which is too low in respect to the real geological conditions (*RMSE = 0,113°C*). It is likely that the Darcy velocity parameter is so prevalent in this case, that it dominates the influence of the ground thermal conductivity in the solution, identifying a local minimum (for more details see sections 2.6 and 2.6.1.)

About borehole thermal resistance, VHI-ILS and MLS solutions (**a** and **1**) give back similar results, respectively *0,206 m·K/W*, *0,184 m·K/W* and *0,186 m·K/W*, which are in agreement to the filling material characteristics of the borehole. However, MLS solutions are characterized by lower *RMSEs, 0,182°C* and *0,113°C,* respectively for solutions **a** and **1**.

Franco Lý

Interpretation of Borehole Heat Exchangers Thermal Response Tests under groundwater influence: analysis of three case studies

Thus, MLS solutions are believed to be more reliable. The standard ILS approach provides an underestimation of the parameter with respect to expected value and it can be risky for a correct sizing of the geothermal BHEs field.

The absolute value of Darcy velocity is *2,1E-05 m/s* obtained by MLS solution **1** indicates a rather relevant groundwater flow. The value seems a bit overestimated respect to a preliminary assessment accomplished by pumping tests.

While, for MLS solution **a**, multiple Darcy velocities are coupled with the same ground thermal conductivity and borehole thermal resistance values, ranging in a broad interval as described in Table 45. This behavior is rather unusual, since the relative plot of MLS temperature time series is the same, independently to the Darcy velocity values if it is any in that range (Figure 5-29). It seems to do not affect the thermal exchange between the source and the surrounding environment, yielding the same mean fluid temperature variation.

Summarizing the comparison of ILS solutions with MLS solutions suggests these remarks:

- the MLS solution **a** determines the more reliable ground thermal conductivity value;

- the MLS and VHI-ILS solutions provides the more appropriate borehole thermal resistance values, although MLS solutions have lower *RMSEs* than VHI-ILS one;

- the MLS solution **1** manages to determine a feasible Darcy velocity value representing the overall groundwater flow of the vertical ground column.

The choice of the best analytical solution is not trivial in this case. Basically considering the three different approaches, it seems that MLS solution **1** gives the best results but, the problem in accepting this set of parameters is mainly due to the ground thermal conductivity as previously underlined. However, only this model is able to account advective heat exchange determining a Darcy velocity value which could actually be representative of the hydro-geological conditions present in the site.

In order to better study the effect of Darcy velocity on MLS solutions, a sensitivity analysis to Darcy velocity values with constant ground thermal conductivity and borehole thermal resistance values is finally carried out and shown in next section 5.8.1. It is found (Figure 5-30) that Darcy velocity values inferior to *1,0E-6 m/s* do not significantly modify MLS temperature time series, while the thermal properties are kept fixed at $\lambda = 3,0 \ W/m \cdot K$ and $R_b = 0,184 \ m \cdot K/W$.

Franco Lý

Interpretation of Borehole Heat Exchangers Thermal Response Tests under groundwater influence: analysis of three case studies

If we had considered Darcy velocity from solution **1** in order to deduce Wagner's correction factor, we would have obtained a value *v = 1,8 m/day*, which coupled with a thermal conductivity of *0,53 W/(m·K)* is not represented in Figure 3-37. In this case the correction factor cannot be calculated.

On the other hand, If we had considered Darcy velocity values from solution **a**, we would have obtained values lower than *v = 0,1 m/day*, which coupled with a thermal conductivity of *2,84W/(m·K)* do not require a correction factor according to (Wagner V. a., 2013).

Concerning estimated borehole thermal resistance, MLS approach returns larger values with respect to ILS. Indeed both MLS solutions **a** and **1** are larger than the value obtained by the standard TRT interpretation. It seems that ILS approach, not considering the advective processes, leads not only to an overestimation of the ground thermal conductivity λ_{eff}, but also to an underestimation of the borehole thermal resistance R_b. This consideration is in agreement with the necessity of ILS approach to take into account a more effective heat exchange than the only pure conductive one, in presence of a significant groundwater flow.

5.8 Parametric Study on MLS

5.8.1 Sensitivity Analysis to Darcy Velocity

The plot in Figure 5-30 shows the influence of Darcy velocity value on the MLS solution for Lodi case study. Darker blue curve are referred to more elevated groundwater flow velocity values which are responsible for lowering the curve at larger time. Indeed, advective processes can enhance heat exchange between the borehole and the surrounding environment, diminishing the mean heat carrier fluid temperature inside the pipes and leading the temperature to a more steady temperature.
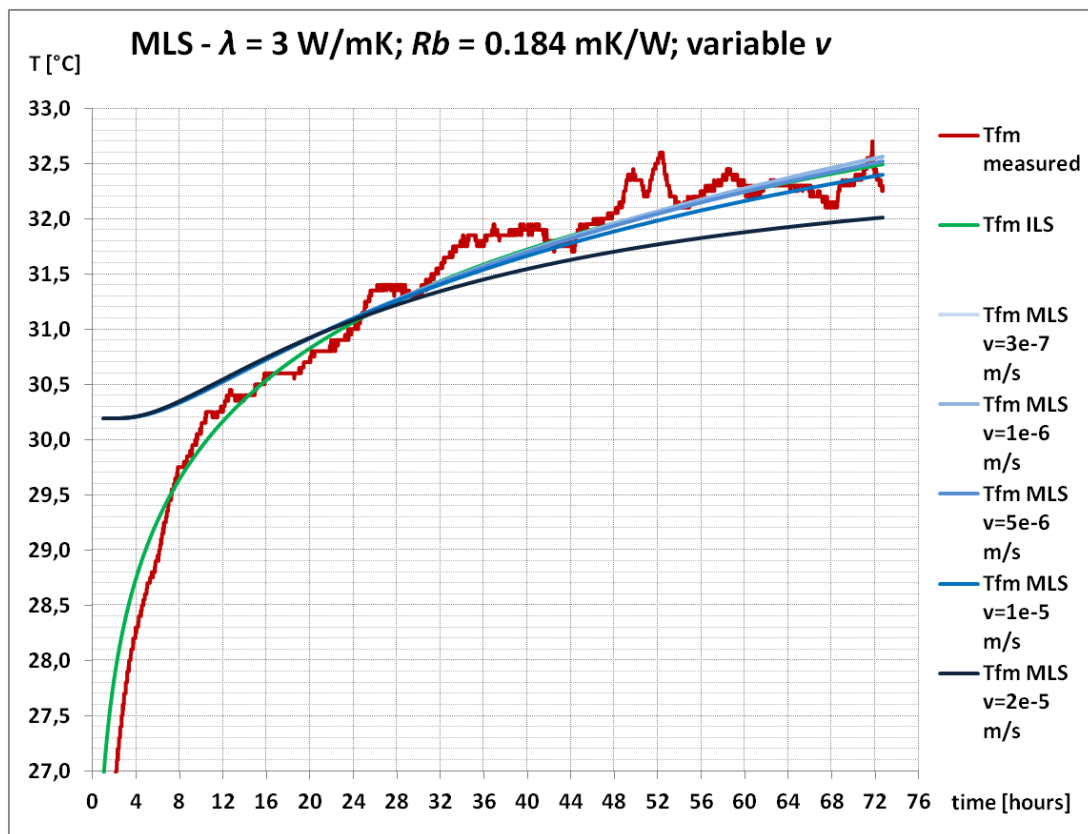
Figure 5-30 - Sensitivity analysis to Darcy Velocity on MLS solution.

From Figure 5-30 it can be noticed that for initial times the ILS solution manages to represent the experimental data, while MLS solution starts from higher temperature values which do not concur with measurement. This different behavior is due to the intrinsic dissimilarity of the two analytical solutions and it can be only solved by means of a time criterion able to disregard the correct amount of initial data for both approaches.

Franco Lý

*Interpretation of Borehole Heat Exchangers Thermal Response Tests
under groundwater influence: analysis of three case studies*

5.8.2   Sensitivity Analysis to Ground Thermal Conductivity

The plot in Figure 5-31 shows the influence of ground thermal conductivity value on the MLS solution for Lodi case study. Darker grey curve are referred to more elevated ground thermal conductivity values which are responsible for generating a point of inflection. The curves for $\lambda > 1,5$ *W/m·K* change from being convex to concave.

Indeed larger thermal conductivity values involve superior heat exchange between the borehole and the surrounding environment, diminishing the mean heat carrier fluid temperature increment in time avoiding thermal buildup in the site.

Similar plots are obtained varying λ exactly in the same way, keeping fixed R_b and adopting Darcy velocity values in a range between *3E-7 m/s* and *1E-5 m/s*. Larger values of *v* has showed to assist the attainment of inflection point, while lower values slow down this behavior.
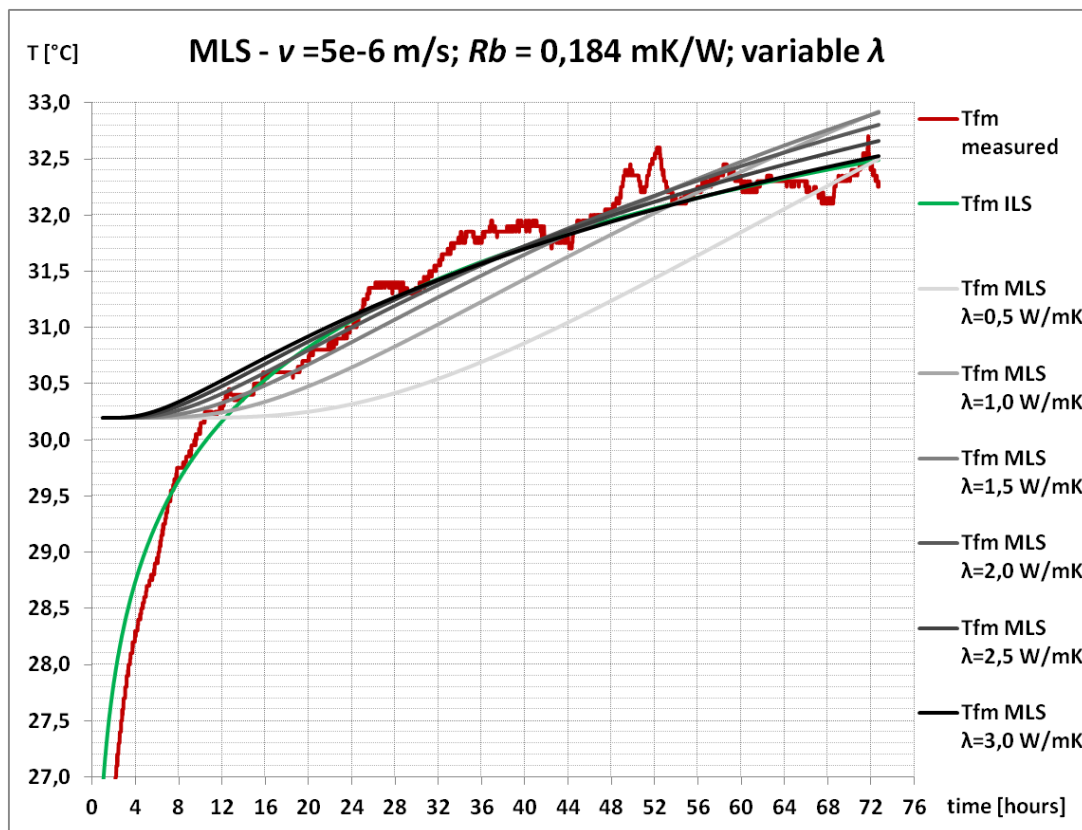
Figure 5-31 - Sensitivity analysis to ground thermal conductivity on MLS solution.

Franco Lý

Interpretation of Borehole Heat Exchangers Thermal Response Tests under groundwater influence: analysis of three case studies

5.8.3   Sensitivity Analysis to Borehole Thermal Resistance

The plot in Figure 5-32 shows the influence of ground thermal conductivity value on the MLS solution for Lodi case study. Darker brown curve are referred to more elevated borehole thermal resistance values which are responsible for determining higher thermal trend maintaining the same curve shape.

This is reasonable since this parameter directly affect mean fluid temperature estimation by means of **Eq. 2.34**, which shows the dependence to the product between specific power and borehole thermal resistance itself.

Similar plots are obtained varying λ exactly in the same way keeping fixed v and adopting ground thermal conductivity values in a range between *0,5 W/m·K* and *3,5 W/m·K*. This analysis has demonstrated that R_b does not influence MLS curve shape but only the thermal level.
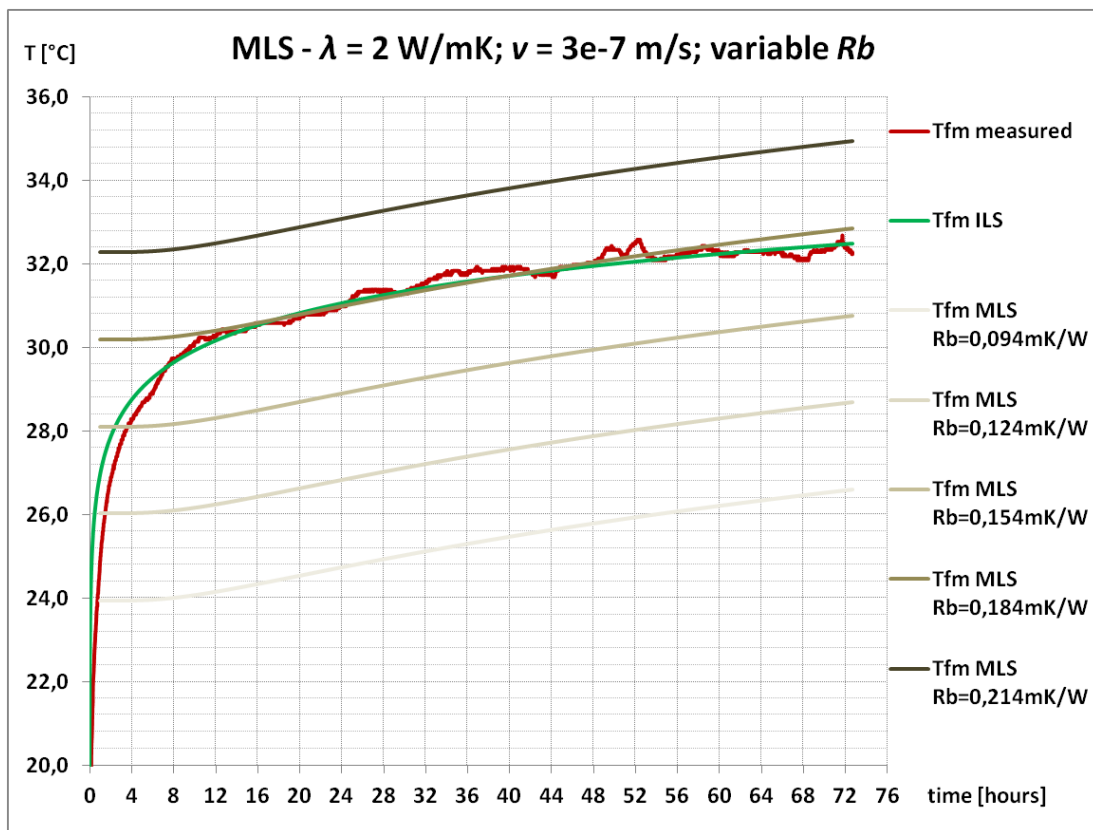
Figure 5-32 - Sensitivity analysis to borehole thermal resistance on MLS solution.

Franco Lý

*Interpretation of Borehole Heat Exchangers Thermal Response Tests
under groundwater influence: analysis of three case studies*

5.9 Comparison with Numerical Modeling in MODFLOW

In this section most important results from different simulations performed by a heat transport model of the aquifers involving Lodi pilot geothermal plant are pointed out and compared with results of TRT analysis in Lodi. Based on the numerical model of a single BHE, created by (Antelmi, 2010), and implemented by means of MODFLOW coupled with MT3DMS, *Marocchi* adjusted it to the specific case of Lodi and calibrated it using experimental data of a representative period of winter operation of the geothermal system (Marocchi, 2015). Later, *Antelmi* further adapted *Marocchi*'s model imposing the boundary conditions relative to the performed TRT before the startup of the geothermal system.

MODFLOW is a three-dimensional (3D) finite-difference groundwater model. It has a modular structure that allows it to be easily modified to adapt the code to a specific situation. It can simulate steady or transient flow in an irregularly shaped flow system where layers reproducing the aquifer can be confined, unconfined, or a combination of confined and unconfined. Different inlet flow, such as flow from wells, areal recharge, evapo-transpiration, flow to drains, and flow through river beds, can also be simulated. Hydraulic conductivities or transmissivities for any layer may differ spatially and be anisotropic and the storage coefficient may be heterogeneous (Harbaugh A. W., 2005). In hydrogeology MODFLOW/MT3DMS are generally used to model solute transport in porous media, but in this case the single particle of heat is considered as a pollutant. Consequently, MODFLOW/MT3DMS is also suitable to simulate the heat transport in the aquifers in analogous way as confirmed by (Hecht-Méndez, 2010).

As just mentioned, the heat transport model was calibrated with *18 days* operation measurement in winter 2015 by means of a *trial & error* approach for the estimation of the hydrogeological parameters (Marocchi, 2015). The thermal properties were initially deducted from literature tables. The geothermal system is made of five BHEs, but only the thermal perturbation of the *BHE1* was considered. Initial and boundary flow conditions were referred to ground water levels at the beginning of the plant operation (appendix 7.6), while initial temperatures were measured by four PT100 sensors at different depths. An hydraulic gradient of *0,4%* concerning the shallow aquifer was individuated and also assumed for the confined aquifer because of the lack of wells deeper than *30 m* in a radius of *1 Km* from the case study. The conceptual model helped to generate a mesh able to effectively represent the geometry of the vertical BHE and the characteristics of each layer. The vertical discretization of the domain was created according to the vertical heterogeneity (shown through a specific geognostic survey) and different hydraulic conductivity zones. In addition, heat carrier fluid properties and HDPE pipe characteristics were also necessary for the model and they were inferred from a literature research.

Franco Lý

*Interpretation of Borehole Heat Exchangers Thermal Response Tests
under groundwater influence: analysis of three case studies*

The inlet pipe temperature of the BHE is an input data depending on the operation of the geothermal plant. It consists in a boundary condition that can be temporally discretized resulting in an equivalent number of stress periods. Outlet pipe temperature depends on the heat exchange between the BHE and aquifer: it is an output of the model to be consequently compared with real data measurements.

Model calibration was performed for *1* or *18* stress periods cases, with better results in the latter case both at short and long times. After the first calibration of hydrogeological and thermal parameters in the heat transport model with only one stress period, the confined aquifer hydraulic gradient was reduced to *0,25%* leading to great benefits to the model. Moreover, the sensitivity analysis of the parameters has proved that the model results are more affected by hydrogeological parameters than the thermophysical ones (Marocchi, 2015).

Following the TRT analysis by means of MLS solution of this master thesis, *Antelmi* has updated the model to effectively reproduce the thermal perturbation generated by same Lodi TRT case. Result-oriented simulations were carried out by varying hydraulic conductivity, ground thermal conductivity and undisturbed ground temperature. MLS solutions allowed to preliminarily understand the direction to follow with MODFLOW simulations, defining the range of groundwater flow velocity values to be investigated.

A numerical model like the one implemented by *Antelmi* can account for non-homogeneous initial temperature distribution, specific thermal and hydraulic layer characteristics and above all it consider the three dimensionality of the heat exchange in the medium, especially the vertical axial heat exchange usually neglected in analytical solution.

In particular, concerning Lodi TRT, there was the issue regarding the uncertainty in the temperature surrounding the BHE: indeed the undisturbed ground temperature estimated at the beginning of the test resulted much higher if compared to the thermal log values in proximity of other wells. A thermal disturbance has probably occurred around *BHE4* due to tests carried out by the designated engineer, before the actual TRT beginning. Therefore, a higher temperature distribution of *17,4°C* as initial conditions was set around the BHE for a little rectangular area, while in the remaining part of the grid, four vertical thermal zones were left as previously set. The main simulation results are reported in Figure 5-33.
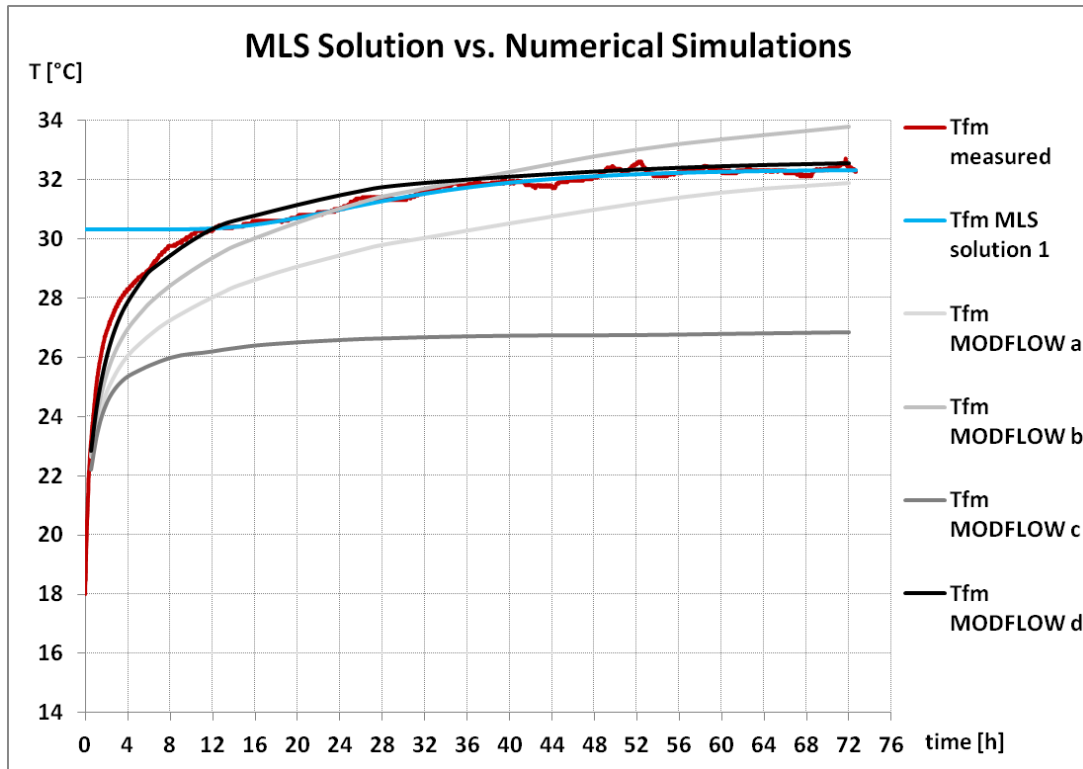
Figure 5-33 - Comparison between results of 4 numerical simulations in MODFLOW and MLS solution 1.

The ground thermal conductivity and Darcy velocity values concerning the illustrated simulations are described in Table 46. They refer to weighted average values among different layers.

Table 46 - Thermal and hydraulic properties set for the different simulations in MODFLOW. Tfm MLS set of parameters corresponds to MLS solution 1 of Table 45.

Simulation	λ [W/mK]	v [m/s]	R_b [mK/W]	notes
Tfm MLS solution **1**	0,53	2,10E-05	0,186	disregarding first 10 hours of dataset
Tfm MODFLOW a	2,66	2,20E-07	/	38 stress periods, mean Q_{th} = 4170 W
Tfm MODFLOW b	2,15	2,20E-07	/	38 stress periods, mean Q_{th} = 4170 W
Tfm MODFLOW c	2,66	5,50E-06	/	38 stress periods, mean Q_{th} = 4170 W
Tfm MODFLOW d	1,81	2,60E-06	/	38 stress periods, mean Q_{th} = 4170 W

Franco Lý

*Interpretation of Borehole Heat Exchangers Thermal Response Tests
under groundwater influence: analysis of three case studies*

From Figure 5-33, it can be observed how *Tfm MODFLOW d* well reproduces experimental data, with a very good correspondence both at short and large times. Besides, *Tfm MLS* solution **1** provides also a good matching plot, but with an initial systematic mismatch where the thermal inertia of the transient period is neglected.

Tfm MODFLOW a and Tfm MODFLOW b are not able to catch the trend of the mean fluid temperature time series, while *Tfm MODFLOW c* with a significant groundwater flow velocity leads to a quick achievement of thermal steady state, not consistent with the TRT dataset.

Comparing the results, it is evident the importance to have a detailed description of the borehole characteristics and properties, which is not possible in the analytical solution tested in this master thesis. The possibility to set a non-uniform initial temperature distribution in the grid played an important role in order to determine the thermal and hydraulic properties. Hence, without common shortcomings of an analytical solution, the heat exchange processes can be adequately performed by means of a numerical model.

However, the purposes of the researcher in testing a numerical model are substantially different from the reasons that stimulated this master thesis. The idea, that a analytical tool to effectively interpret TRT under groundwater influence is necessary, still remains.

Franco Lý

*Interpretation of Borehole Heat Exchangers Thermal Response Tests
under groundwater influence: analysis of three case studies*

Franco Lý

Interpretation of Borehole Heat Exchangers Thermal Response Tests under groundwater influence: analysis of three case studies

6 Conclusions

The conclusions of this study are here presented. The purpose of this chapter is to summarize the achieved results and introduces the possible future studies, which could be carried out on this topic, then described in section 6.1 .

The objective of this master thesis was to investigate experimental analytical approaches to interpret ground-water influenced thermal response tests of vertical borehole heat exchangers, in order to obtain the necessary thermo-physical parameters to properly design low-temperature geothermal systems.

Standard TRT interpretation by means of ILS model presumes a homogeneous subsurface, no axial heat transport, uniform initial temperature and it approximates the BHE shape as an infinite line. Constant heat injection/extraction is also an important requisite for the reliability of the test. However, the most important assumption is that only conductive heat transport is considered.

Therefore, to overcome some of these significant assumptions, in addition to the ILS analysis advised by (UNI11466, 2012), two alternative analytical solutions are taken into account and both implemented in MATLAB.

At first, an extended version of the ILS solution using the superposition principle is described to comprehensively account variable heat injections and then applied for Lodi case study, which has pointed out high levels of thermal power fluctuation.

Secondly, another equation is evaluated, which provides parameters more suitable for a detailed simulation of conductive and advective heat transport in the subsurface. This extended version of the ILS model, named Moving Line Source model, can account for the significant influence of groundwater flow and it is here tested for all the three case studies.

In the development of this master thesis the procedure of TRTs analysis is consistent. The interpretation starts with ILS approach, then from the evaluation of the results further analysis are carried out by means of MLS solution, while VHI-ILS solution is performed only for Lodi case study for the reason previously cited.

The results from ILS analysis of the three case studies have proved the overestimation of the effective ground thermal conductivity λ_{eff}, which is known to increase in presence of a significant groundwater flow. In particular for Claviere case study λ_{eff} value for increasing evaluation time has underlined an increasing trend without the attainment of a stable value. The convergence of this estimated parameter is also uncertain for Trento and Lodi

Franco Lý

Interpretation of Borehole Heat Exchangers Thermal Response Tests
under groundwater influence: analysis of three case studies

case studies, for which a more long-lasting test would have supported a better evaluation. Basically, it was observed remarkable enhanced thermal conductivity estimated by ordinary TRT interpretation, mainly caused by the advective phenomena.

Wagner et al. propose the adoption of the MLS theory to interpret TRT data in the presence of groundwater flow (Wagner V. a., 2013), but they do not provide any time criterion to disregard data related to initial times. In this thesis, a method is proposed in order to identify a characteristic time t_c necessary to determine the minimum time for data validity for TRTs analysis by means of MLS approach.

Then, according to MLS theory, a script was implemented in order to estimate Darcy velocity along with ground thermal conductivity and borehole thermal resistance. The initial time sensitivity analysis demonstrated to be a very effective tool for Claviere dataset in evaluating adequate parameters, on the other hand obtained multiple solutions for Lodi and Trento case studies were hardly analyzed and discriminated. The established time criterion turned out to be effective and coherent with the obtained results, demonstrating great improvements in *RMSE*, if data related to initial times are disregarded according to the criterion.

The large set of initial parameters combinations used in the fit procedure generated multiple solutions comprising absolute and local minima, which were assessed and discriminated according to *RMSE*, to physical considerations and to the capability of the fit to catch the fundamental behavior of the measured trend. The procedure led to optimal results for Claviere case study but it has turned to be complicated both for Lodi and Trento TRTs. In each of these case studies, two main solutions were obtained, of which the evaluation cannot be performed unless further tests are performed and results compared to validate MLS analysis. For instance, a preliminary hydro-geological assessment of the site can be very helpful in assist a groundwater influenced TRT interpretation by MLS theory such as a pumping test, although the experience in Lodi demonstrates that care should be taken in the presence of many aquifers.

On the basis of the work here presented, the following recommendations are provided:

- MLS approach can be a valid alternative for TRT interpretation if the ground thermal conductivity value cannot be estimated by standard ILS approach;

- if the presence of aquifers is detected, longer TRT should be performed in order to evaluate the convergence of effective ground thermal conductivity by means of a step by step interpretation.

Franco Lý

Interpretation of Borehole Heat Exchangers Thermal Response Tests
under groundwater influence: analysis of three case studies

6.1 Future Developments

Concerning MLS approach for the interpretation of TRT under groundwater influence, it would be interesting to study a larger set of TRT data relative to different hydrogeological conditions to better understand the capability of the analytical model to represent experimental data.

Moreover, along MLS script implementation process, some simplifications of the model were accepted in order to facilitate the parameter estimation procedure. For this reason, a script able to account for longitudinal and transversal dispersivity would be a great improvement of the analytical model, although adding further parameters into the estimation technique can enhance the ill-posed problem and increase the computational efforts to achieve a solution from the fit.

Remaining in the modeling field, a sensitivity study of the solutions to the integration step of MLS equation could be carried out. The results could help to optimize computational times in executing the multiple fits. It would be also interesting to perform two variable parameters estimation (i.e. ground thermal conductivity λ and Darcy velocity v) keeping fixed the borehole thermal resistance, which can be calculated by means of expressions implemented in specific software as DST, EED and GLHEPRO 4.0. Additionally, larger sets of initial parameters combinations should be considered in next TRTs analysis with the purpose to study the strength of the solutions obtained by MLS approach and in order to investigate further the problem of the influence of initial data on fit results.

In Lodi case study, the depth reached by the pilot borehole is *60 m*, a short length with respect to BHEs generally used in low-temperature geothermal applications, for which the heat exchange along the vertical axis should not be considered negligible. In this case, an improved interpretation could be performed by a Moving Finite Line Source model (Molina-Giraldo N. a., 2011), that takes into consideration both groundwater flow and axial effects.

If TRTs of BHEs located in different hydrogeological contexts will be analyzed, estimated Darcy velocity value by MLS approach could be likely found in the range evaluated by (Wagner V. a., 2013). Then, the suitability of the correction factor *C* can be assessed for experimental data and not numerically generated time series, if the results are compared with hydraulic test findings.

Eventually, the datasets obtained by in situ tests, like the three analyzed case studies, did not help to clarify the applicability study of MLS approach on TRTs. Therefore, datasets collected by laboratory experiments under controlled conditions could be used for a better understanding of the analytical solution.

Franco Lý

Interpretation of Borehole Heat Exchangers Thermal Response Tests
under groundwater influence: analysis of three case studies

Franco Lý

*Interpretation of Borehole Heat Exchangers Thermal Response Tests
under groundwater influence: analysis of three case studies*

7 Appendices and Attachments

7.1 MLS script (Claviere TRT)

- *main* used to perform multiple fits

```matlab
% Load observed temperature time series
load -ascii DatiClaviere60h.txt

t_in = 240; % initial time [minutes] (multiple of 3 to avoid float)
[min,n] = size(DatiClaviere60h);

% Sampling time every 3 minutes
m = (min - t_in)/3;
tau = zeros(1,m);
Tfm_mis = zeros(1,m);

% Create vector of time [minutes]
for i=1:(m)
    tau(1,i)= DatiClaviere60h(i*3+t_in,1);
end

% Create vector of measured temperature [°C]
for i=1:m
    Tfm_mis(1,i)= DatiClaviere60h(i*3+t_in,2);
end

% Setting of the initial sets of three parameters
% [Conductivity - Darcy Velocity - Borehole Resistance]
par_in = [1.5 , 1E-3, 0.06
           …  , …   , …
           4   , 1E-7, 0.06] ;

[w,b] = size(par_in);
result = zeros(w,b+1);
RMSE = zeros(w,1);

for e = 1 : w
        par = [par_in(e,1), par_in(e,2), par_in(e,3)];
        [par,RMSE] = fminsearch('Tfm_MLS_fit3',par,[],tau,Tfm_mis);

        result(e,1) = par(1,1);
        result(e,2) = par(1,2);
        result(e,3) = par(1,3);
        result(e,4) = RMSE;
end
```

– 'Tfm_MLS_fit3' MLS function

```
function [RMSE,Tfm_MLS] = Tfm_MLS_fit3(par,tau,Tfm_mis)
% par = [lambda_0, v_0, R_bh_0];
% lambda_0 = initial ground thermal conductivity [W/m.K]
% v = Darcy velocity [m/s]
% tau = times vector [s]
% Tfm_mis = measured mean heat carrier fluid temperature series [°C]

rho_s = 2650;    % solid matrix density [kg/mc]
c_s = 847;       % solid matrix specific heat  [J/kg.K]
eps = 0.035;     % total porosity [/]
T_0 = 9.79;      % undisturbed ground temperature [°C]
rho_w = 1000;    % water density [kg/mc]
c_w = 4186;      % water specific heat [J/kg.K]

% volumetric thermal capacity [J/mc.K]
C_0 = rho_s*c_s*(1-eps)+rho_w*c_w*eps;

q = 38.11;       % specific thermal power [W/m]
r_bh = 0.076;    % BHE radius [m]

dteta = 45*pi/180; % polar angle step [rad]
teta = (dteta:dteta:2*pi); % polar angles
est = (rho_w*c_w*par(2))^2*tau/(4*C_0*par(1)); % integration end

u=zeros(numel(tau),10^3);
f=zeros(numel(tau),10^3,numel(teta));
T=zeros(numel(tau),numel(teta));

for i=1:numel(tau)
    u(i,:)= ( est(i)*1E-3:est(i)*1E-3:est(i) )';
end

for j=1:numel(teta)
    f(:,:,j)=1./u.*exp(-u-
(r_bh)^2/par(1)*(rho_w*c_w*par(2))^2./(16*par(1)*u));
    % integral function calculated in 8 nodes
    for i=1:numel(tau)
    T(i,j) = T_0 +
q/(4*pi*par(1))*exp(rho_w*c_w*par(2)*r_bh*cos(teta(j))/(2*par(1)))*t
rapz(u(i,:),f(i,:,j),2);
    % borehole wall temperature at each node time series
    end
end
% representative borehole wall temperature
T_bw = mean(T');
% MLS mean fluid temperature time series
Tfm_MLS = q*par(3) + T_bw;
% RMSE [°C]
RMSE=(sum((Tfm_MLS-Tfm_mis).^2)/length(tau))^0.5;
```

Franco Lý

Interpretation of Borehole Heat Exchangers Thermal Response Tests
under groundwater influence: analysis of three case studies

7.2 Geothermal BHEs Field (Trento Case Study)

7.3 Functional Scheme of the Space Heating/Cooling System with Geothermal Heat Pump
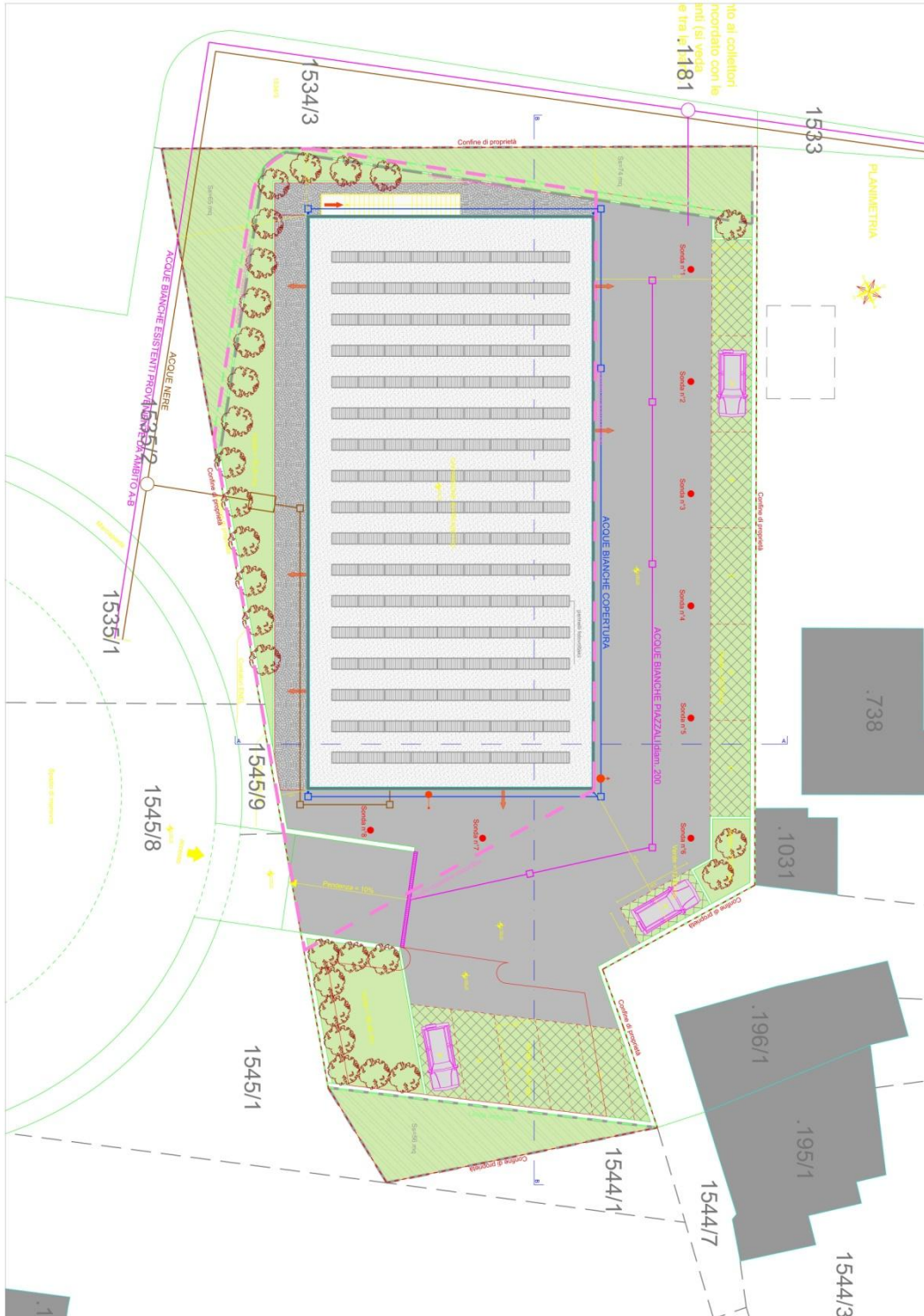
7.4 VHI-ILS script (Lodi TRT)

- *main* used to perform fit

```
% Load observed temperature e power time series
load -ascii DataLODI.txt

[min,n] = size(DataLODI);
t_in = 600;                 % initial time discarded [minutes]
m = (min - t_in);           % effective considered interval [minutes]
tau = zeros(m,1);           % sampling time [minutes]
Tfm_mis = zeros(m,1);       % measured mean fluid temperature [°C]
Q = zeros(m,1);             % heat injection rate [W]
L = 60;                     % borehole length [m]

% Create vector of time [minutes]
for i=1:m
    tau(i,1)= DataLODI(i+t_in,1);
end

% Create vector of measured temperature [°C]
for i=1:m
    Tfm_mis(i,1)= DataLODI(i+t_in,2);
end

% Create vector of step injection power [W]
for i=1:m
    Q(i,1)= DataLODI(i+t_in,3);
end

sp_power=zeros(14,1);
t=zeros(14,1);
dpower=zeros(13,1);

% initial values
i=1;
t(1,1)=0;
sp_power(1,1)=0;

% step specific power
for j=1:m-1
    if Q(j+1,1)== Q(j,1);
        sp_power(i+1,1)= Q(j,1)/L;
        t(i+1,1)= j+1;
    else
        i=i+1;
        sp_power(i,1)= Q(j,1)/L;
    end
end
```

```matlab
% step specific power variation
for i=1:13
    dpower(i,1)= sp_power(i+1,1)-sp_power(i,1);
end

%  Set initial values for Conductivity - Borehole Resistance
par = [ 2.0 ,   0.15] ;

% Calling function to create Tfluid from VHI LS theory
[RMSE,Tfm_LS] = Tfm_LS_fit(par,tau,t_in,Tfm_mis,dpower,sp_power,t);

[par,RMSE] =
fminsearch('Tfm_LS_fit',par,[],tau,scarto,Tfm_mis,dpower,sp_power,t)
;

% Comparison of temperature time series
figure
plot(DataLODI(:,1)/60,DataLODI(:,2),'b')
hold on
plot(tau/60,Tfm_LS,'r')
title 'T_m_e_a_s vs T_V_H_I_-_I_L_S'
xlabel 'Time [hours]'
ylabel 'T [°C]'

% Plot dpower input
m_dpower=zeros(numel(tau),13);

for i=1:13
    for j=t(i)+1:t(14)
        m_dpower(j,i)=dpower(i);
    end
end

figure
for i=1:13
    plot(tau/60,m_dpower(:,i))
    hold on
    title 'Step Specific Power Variation'
    xlabel 'Time [hours]'
    ylabel 'Specific Power [W/m]'
end
```

- – 'Tfm_LS_fit' VHI-ILS function

```
function [RMSE,Tfm_LS] =
Tfm_LS_fit(par,tau,scarto,Tfm_mis,dpower,sp_power,t)

% par = [lambda_0, R_bh_0];
% lambda_0 = effective thermal conductivity  [W/mK]
% tau = times vector [minutes]
% Tfm_mis = measured mean fluid temperature time series

T_0 = 17.4;          % undisturbed ground temperature [°C]

% effective volumetric thermal capacity[J/mc.K]
C_0 = 2400000;

r_bh = 0.0635;     % borehole radius [m]
a = par(1)/C_0;    % 1st try thermal diffusivity [m2/s]

f=zeros(numel(tau),numel(dpower));
Tfm_LS = zeros(numel(tau),1);
f(1)=0;

% VHI-ILS mean fluid temperature time series [°C]

 for i=1:numel(dpower)
    for j=t(i)+1:t(i+1)
        f(j+1,i+1)=f(j,i)+dpower(i)*(-0.5772+log(4*a*(tau(j)-
t(i))/(r_bh^2)))/(4*pi*par(1));
        Tfm_LS(j)= sp_power(i+1)*par(2)+T_0+f(j+1,i+1);
    end
 end

% RMSE [°C]
RMSE=(sum((Tfm_LS(scarto:1:numel(tau))-
Tfm_mis(scarto:1:numel(tau))).^2)/length(tau))^0.5;
```

```
function [RMSE,Tfm_LS] =
```

7.5 Stratigraphy of BHE1 (Lodi Case Study)

Franco Lý

Interpretation of Borehole Heat Exchangers Thermal Response Tests under groundwater influence: analysis of three case studies

COMMITTENTE: TETHYS s.r.l.	PIEZOMETRO: P1 NESTED (2 piezometri coassiali)	2/2
CANTIERE: via dell'Universita' - Lodi	PROFONDITA': P1A = 30 m ; P1B = 60 m	
PROGETTO: PROGETTO ECOZOO	DIAMETRO: P1A = 4" ; P1B = 1.5"	
DATA DI INIZIO: 03/02/2014	QUOTA B.P.= 78.74 m s.l.m.	
DATA ULTIMAZIONE: 10/02/2014	LIVELLO FALDA: -4.01 m da p.c. (P1A) / -5.54 m p.c. (P1B)	
DITTA ESECUTRICE: Geoprove s.n.c.	COORD. GB: E=1537117 m; N=5016896 m	

COMPLETAMENTO — **STRATIGRAFIA**

Labels (completamento): CEMENTAZIONE; CAMP. 2 33.0 / 33.3; CIECO 35.0; CIECO; FILTRO; DRENO; DRENO; FILTRO; depths 30.0, 39.0, 60.0; 1.5"

Stratigrafia descriptions:
- Sabbia fine debolmente limosa — 30.5
- Limo argilloso compatto plastico colore grigio — 33.0
- Sabbia grossolana con ghiaia e ciottoli colore grigio — 35.0
- Sabbia grossolana e ghiaia con molti ciottoli colore grigio — 36.5
- Sabbia grossolana con ghiaia e ciottoli colore grigio chiaro — 38.0
- Sabbia e ghiaia con frequenti ciottoli colore giallo-ocra — 40.0
- Sabbia media con ghiaia e ciottoli — 42.0
- Sabbia media pulita colore giallo-ocra — 43.0
- Sabbia medio-fine debolmente limosa con ghiaia e qualche ciottolo colore giallo-ocra — 44.0
- Sabbia grossolana a tratti debolmente limosa con ghiaia e qualche ciottolo — 45.5
- Sabbia media pulita color ocra — 52.5
- Sabbia medio-fine pulita colore giallo-ocra-grigiastra — 55.0
- Sabbia medio-fine da debolmente a mediamente limosa colore giallo-grigiastra — 56.3
- Sabbia medio-fine pulita colore grigio scuro — 60.0

Franco Lý

Interpretation of Borehole Heat Exchangers Thermal Response Tests
under groundwater influence: analysis of three case studies

7.6 Geothermal BHEs Field (Lodi case study)

Franco Lý

*Interpretation of Borehole Heat Exchangers Thermal Response Tests
under groundwater influence: analysis of three case studies*

Nomenclature

a	thermal diffusivity [m^2/s]
A	cross sectional area [m^2]
C	volumetric thermal capacity [J/(m^{3}K)]
COP	coefficient of performance [/]
c	specific heat [J/(°C·kg)]
c_f	specific heat of the heat carrier fluid [J/(°C·kg)]
D	thermal dispersion coefficient [m^2/s]
d	diameter [m]
E_1	exponential integral
h	convection heat transfer coefficient [W/m^2·K]
i	hydraulic gradient
L	overall BHE length [m]
k	hydraulic conductivity [m/s]
Nu	Nusselt Number [/]
Pe	Péclet Number [/]
Pr	Prandtl Number [/]
Q	fluid mass flow rate [kg/s]
q	heat transfer rate for unit length [W/m]
Re	Reynolds Number [/]

Franco Lý

*Interpretation of Borehole Heat Exchangers Thermal Response Tests
under groundwater influence: analysis of three case studies*

r	radius [m]
R_c	overall linear thermal resistance [m·K/W]
R_b	borehole thermal resistance [m·K/W]
S	surface [m^2]
T	temperature [°C]
T_{fm}	mean heat carrier fluid temperature [°C]
t	time [s]
U	internal energy [J]
u	integration variable
V	volume [m^3]
v	Darcy velocity [m/s] or [m/day]
v_{th}	heat transport velocity [m/s] or [m/day]
x, y	Cartesian coordinates [m]

Greek Symbols

α	dispersivity [m]
γ	Euler constant
η	efficiency [/]
ϑ	polar angle [rad]
λ	thermal conductivity [W/(m·K)]
μ	dynamic viscosity [N·s/m^2]
ν	kinematic viscosity or momentum diffusivity [m^2/s]

Franco Lý

Interpretation of Borehole Heat Exchangers Thermal Response Tests
under groundwater influence: analysis of three case studies

π	Pi, mathematical constant
ρ	density [kg/m^3]
ϕ	porosity [/]
Δ	variation/difference

Subscripts and Superscripts

0	initial or undisturbed value
b	borehole
bw	borehole wall
c	characteristic
eff	obtained effective property value
f	heat carrier fluid
in	inlet pipe
l	longitudinal
m	property of the ground
out	outlet pipe
s	solid
sub	property of the subsurface
t	transversal
w	water

Franco Lý

Interpretation of Borehole Heat Exchangers Thermal Response Tests under groundwater influence: analysis of three case studies

List of Acronyms

ASHRAE	*American Society of Heating, Refrigerating and Air-Conditioning Engineers*
BHE	*Borehole Heat Exchanger*
COP	*Coefficient of Performance*
GCHP	*Ground Coupled Heat Pump*
GHP	*Geothermal Heat Pump*
GSHP	*Ground Source Heat Pump*
GWHP	*Ground Water Heat Pump*
HDPE	*High Density Polyethylene*
HE	*Heat Engine*
HP	*Heat Pump*
IGA	*International Geothermal Association*
ILS	*Infinite Line Source*
MLS	*Moving Line Source*
PN	*Pressure Nominal*
SIA	*Swiss Society of Engineers and Architects* (*Schweizerischer Ingenieur- und Architektenverein*)
SWHP	*Surface Water Heat Pump*
TRT	*Thermal Response Test*
VDI	*Association of German Engineers* (*Verein Deutscher Ingenieure*)
VHI	*Variable Heat Injection*

Franco Lý

Interpretation of Borehole Heat Exchangers Thermal Response Tests
under groundwater influence: analysis of three case studies

List of References

Alberti, L. a. (2012). ow temperature geothermal energy: heat exchange simulation in aquifers through Modflow/MT3DMS codes. *AQUA MUNDI , 3* (1), 39-51.

Antelmi, M. a. (2010). *Geotermia a bassa entalpia: simulazione dello scambio termico in acquiferi mediante i codici Modflow e Trnsys.* Tesi di 2° livello , Politecnico di Milano.

ASHRAE. (2007). GEOTHERMAL ENERGY. In R. a. American Society of Heating, *ASHRAE Handbook: Heating, Ventilating, and Air-Conditioning Applications* (p. 32.1-32.30). Atlanta, Georgia, USA.

Bandos, T. a. (2011). Improving parameter estimates obtained from thermal response tests: Effect of ambient air temperature variations. *Geothermics , 40* (2), 136-143.

Banks, D. (2009). An introduction to 'thermogeology' and the exploitation of ground source heat. *Quarterly Journal of Engineering Geology and Hydrogeology , 42* (3), 283-293.

Basta, S. a. (2008). *Geotermia e pompe di calore: guida pratica agli impianti geotermici di climatizzazione.* Associazione Geotermia. Org.

Brassington, R. (1998). *Field Hydrogeology.* Chichester, West Sussex, UK: John Wiley & Sons Ltd.

Casasso, A. a. (2014). Efficiency of closed loop geothermal heat pumps: A sensitivity analysis. *Renewable Energy , 62* (0), 737-746.

Chiasson, A. D. (2000). *A preliminary assessment of the effects of groundwater flow on closed-loop ground source heat pump systems.* Technical report, Oklahoma State University, Oklahoma, Stillwater, OK (US).

CTI. (2012, 11). UNI 11466 Heat pump geothermal systems - Design and sizing requirements. Ente Nazionale Italiano di Unificazione.

Curtis, R. a. (2005). Ground source heat pumps--geothermal energy for anyone, anywhere: current worldwide activity. *World Geothermal Congress*, (p. 24-29). Antalya, Turkey.

Delmastro, R. a. (2011). *Manuale di geotermia a sonde verticali.* Ulrico Hoepli.

Diao, N. F. (2004). Heat transfer in ground heat exchangers with groundwater advection. *International Journal of Thermal Sciences , 43* (12), 1203-1211.

Franco Lý

*Interpretation of Borehole Heat Exchangers Thermal Response Tests
under groundwater influence: analysis of three case studies*

Fujii, H. a. (2009). An improved thermal response test for U-tube ground heat exchanger based on optical fiber thermometers. *Geothermics , 38* (4), 399-406.

Gehlin, S. a. (2003). Influence on thermal response test by groundwater flow in vertical fractures in hard rock. *Renewable energy , 28* (14), 2221-2238.

Gehlin, S. a. (2000). Recent Status of In-Situ Thermal Response Tests for BTES Applications in Sweden. *Proc. Terrastock 2000 ,* 159-164.

Gehlin, S. a. (2003). The influence of the thermosiphon effect on the thermal response test. *Renewable energy , 28* (14), 2239-2254.

Gehlin, S. a. (2002). Thermal Response test for BTES applications - State of the Art 2001. *Report IEA ECES Annex , 13*.

Gehlin, S. E. (2003). Determining undisturbed ground temperature for thermal response test. *TRANSACTIONS-AMERICAN SOCIETY OF HEATING REFRIGERATING AND AIR CONDITIONING ENGINEERS , 109* (1), 151-156.

Gehlin, S. (2002). *Thermal response test method development and evaluation.* Doctoral Thesis, Lulea University of Technology.

Harbaugh, A. W. (2000). *MODFLOW-2000, the US Geological Survey modular ground-water model: User guide to modularization concepts and the ground-water flow process.* VA, USA: US Geological Survey Reston.

Harbaugh, A. W. (2005). *MODFLOW-2005, the U.S. Geological Survey modular ground-water model - the Ground-Water Flow Process.* U.S. Geological Survey Techniques and Methods 6-A16.

Hecht-Méndez, J. a.-G. (2010). Evaluating MT3DMS for heat transport simulation of closed geothermal systems. *Groundwater , 48* (5), 741-756.

Hellstrom, G. (1991). *Ground heat storage: Thermal analyses of duct storage systems.* Doctoral Thesis, Lulea University of Technology.

Incropera, F. P. (2011). *Fundamentals of heat and mass transfer.* John Wiley & Sons.

Lagarias, J. C. (1998). Convergence properties of the Nelder--Mead simplex method in low dimensions. *SIAM Journal on optimization , 9* (1), 112-147.

Lamarche, L. a. (2010). A review of methods to evaluate borehole thermal resistances in geothermal heat-pump systems. *Geothermics , 39* (2), 187-200.

Franco Lý

Interpretation of Borehole Heat Exchangers Thermal Response Tests under groundwater influence: analysis of three case studies

Lombardia, R. (s.d.). Regolamento Regionale 15/02/10 n.7.

Marocchi, B. U. (2015). *L'influenza dei parametri idrogeologici e termodinamici di un acquifero eterogeneo: simulazione numerica dello scambio termico in falda di un impianto pilota geotermico a bassa entalpia.* Tesi magistrale, Politecnico di Milano, Dipartimento di Ingegneria Civile e Ambientale (DICA), Milano.

Molina-Giraldo, N. a. (2011). A moving finite line source model to simulate borehole heat exchangers with groundwater advection. *International Journal of Thermal Sciences , 50* (12), p. 2506-2513.

Molina-Giraldo, N. a. (2011). Evaluating the influence of thermal dispersion on temperature plumes from geothermal systems using analytical solutions. *International Journal of Thermal Sciences , 50* (7), 1223-1231.

Raymond, J. a. (2011). A review of thermal response test analysis using pumping test concepts. *Groundwater , 49* (6), 932-945.

Raymond, J. a. (2010). Borehole temperature evolution during thermal response tests. *Geothermics , 40* (1), 69-78.

RegolamentoRegionale15/02/10n.7. *Regione Lombardia.*

Rohner, E. a. (2005). A new, small, wireless instrument to determine ground thermal conductivity in-situ for borehole heat exchanger design. *Proceedings of the World Geothermal Congress.* Antalya, Turkey.

Roth, P. a. (2004). First in situ determination of ground and borehole thermal properties in Latin America. *Renewable energy , 29* (12), 1947-1963.

Saner, D. a. (2010). Is it only CO 2 that matters? A life cycle perspective on shallow geothermal systems. *Renewable and Sustainable Energy Reviews , 14* (7), 1798-1813.

Sanner, B. a. (2005). Thermal Response Test – Current Status and World-Wide Application. *World Geothermal Energy Congress* (p. 9). Antalya, Turkey: International Geothermal Association.

SIA384/6. (2010). Sonde geotermiche.

Signorelli, S. a. (2007). Numerical evaluation of thermal response tests. *Geothermics , 36* (2), 141-166.

Sutton, M. G. (2003). A ground resistance for vertical bore heat exchangers with groundwater flow. *Journal of Energy Resources Technology , 125* (3), 183-189.

Tinti, F. (2008). *Geotermia per la climatizzazione.* D. Flaccovio.

UNI11466. (2012, 11). Heat pump geothermal systems - Design and sizing requirements. Ente Nazionale Italiano di Unificazione.

VDI4640/part2. (s.d.). Thermal use of the Underground. *Part 2: Ground Source Heat Pumps* .

Wagner, V. a. (2013). Analytical approach to groundwater-influenced thermal response tests of grouted borehole heat exchangers. *Geothermics , 46*, 22-31.

Wagner, V. a. (2012). Numerical sensitivity study of thermal response tests. *Renewable Energy , 41*, 245-253.

Witte, H. a. (2006). Geothermal response tests using controlled multi-power level heating and cooling pulses (MPL-HCP): quantifying ground water effects on heat transport around a borehole heat exchanger. *Proc. Ecostock* .

Witte, H. (2001). Geothermal response tests with heat extraction and heat injection: examples of application in research and design of geothermal ground heat exchangers. *Europaischer Workshop uber Geothermische Response Tests* .